Mould powders for high speed continuous casting of steel

Jan Kromhout

Title: Mould powders for high speed continuous casting of steel
Author: J.A. Kromhout
ISBN: 978-90-805661-8-7
Copyright: Tata Steel Nederland Technology BV
Print: Gildeprint Drukkerijen

Mould powders for high speed continuous casting of steel

Proefschrift

ter verkrijging van de graad van doctor
aan de Technische Universiteit Delft,
op gezag van de Rector Magnificus prof.ir. K.C.A.M. Luyben,
voorzitter van het College voor Promoties,
in het openbaar te verdedigen op donderdag 27 januari 2011 om 15.00 uur

door

Jan Albert KROMHOUT

ingenieur chemische technologie
geboren te Leiden

Dit proefschrift is goedgekeurd door de promotoren:

Prof.dr. R. Boom
Prof.dr. K.C. Mills

Samenstelling promotiecommissie:

Rector Magnificus	Voorzitter
Prof.dr. R. Boom	Technische Universiteit Delft, promotor
Prof.dr. K.C. Mills	Imperial College London, promotor
Prof.dr. J.H.W. de Wit	Technische Universiteit Delft
Prof.dr. P.D. Lee	Imperial College London
Prof.dr.ir. J. Sietsma	Technische Universiteit Delft
Dr. M. Kawamoto	Sumitomo Metal Industries
Dr.ir. M.C.M. Cornelissen	Tata Steel Strip Products IJmuiden

This research was sponsored by Tata Steel Research, Development & Technology and carried out as part of the programme of the Materials innovation institute M2i under project number MC5.05225.

Contents

1 Introduction

1.1 Steelmaking and continuous casting

Steel is the alloy of choice for engineers, consisting mostly of iron with a carbon content between 0.2 and 2.1% by weight. When iron is smelted from its ore, it contains more carbon than is desirable. To become steel, it must be reprocessed to reduce the carbon to the correct amount. Carbon is the most cost-effective alloying material for iron, but various other alloying elements are used such as manganese, silicon, chromium, vanadium and niobium.
Though steel has been produced by various inefficient methods long before the Renaissance, its use became more common after the introduction of more efficient production methods in the 17th century. With the invention of the Bessemer process in the mid-19th century, completed by the Siemens-Martin process, steel became a relatively inexpensive mass-produced material. The introduction of the Linz-Donawitz process of basic oxygen steelmaking, developed in the 1950s, further lowered the cost of production while increasing the quality of the metal. An alternative process for steelmaking is the electrical arc furnace (EAF). With an annual production of 1500 Mt, steel is one of the most common man-made materials in the world and is a major component in buildings, infrastructure, tools, ships, trains and railroads, automobiles, machines and appliances.

The steelplant of Tata Steel in IJmuiden (The Netherlands), formerly Hoogovens IJmuiden, uses two blast furnaces with a production of 6.4 Mt/y liquid iron. An illustration of the process flow is given in Figure 1.1.

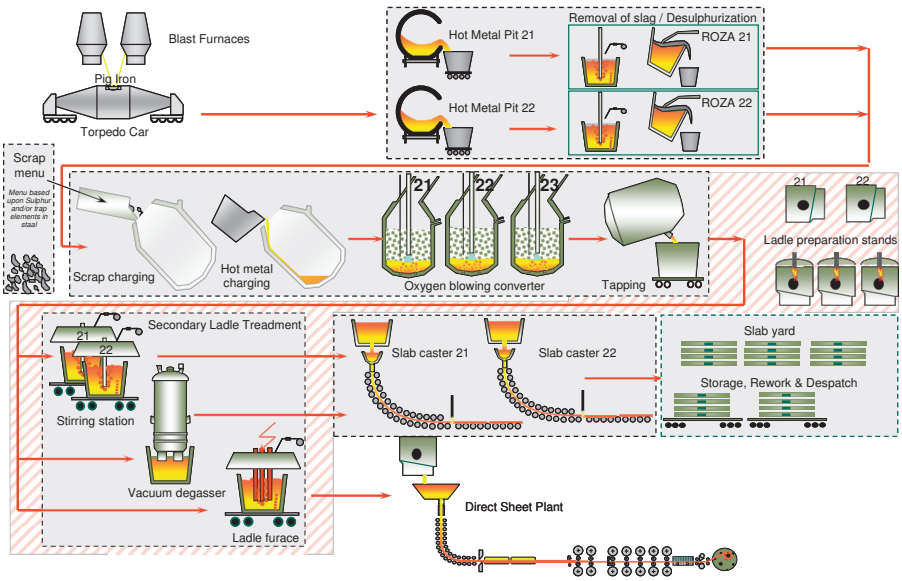

Figure 1.1: *Process and material flow at BOS No. 2, IJmuiden, The Netherlands (Courtesy of Tata Steel IJmuiden BV)*

After pre-treatment, the liquid iron is fed into one of the three converters in the Basic Oxygen Steelplant (BOS No. 2). The capacity of the converters is 325 tonnes each. Secondary ladle treatment in this plant consists of ladle stirring, vacuum degassing or treatment in the ladle furnace. The steel is then directed to one of the continuous casting machines where the steel solidifies as slabs.

Based on a patent application of 1886, the first continuous casting machine was constructed in the United States in 1901. This apparatus consisted of a tundish, a water cooled mould, a dummy bar and a pair of driven rolls. After significant pioneering work, especially in Europe and the United States, the industrial breakthrough of the continuous casting process was only around fifty years ago. A very important step in the development of continuous casting was the introduction of mould oscillation by Junghans in Germany, enabling one to reduce excessive mould friction and consequently sticking of the solidified shell. Subsequently, mould oscillation was optimised resulting in the introduction of negative strip, which is equivalent to moving the mould slightly faster than the strand during the downstroke of the oscillation cycle. This concept proved to be essential to minimise shell sticking. During the last fifty years, continuous casting of steel as an industrialized method of solidification processing, has made enormous advances. Important process developments have been reported from Japan as well. Nowadays, more than 90% of the world steel production is continuously cast [1].

In IJmuiden, continuous casting started in 1980 with the introduction of a two-strand continuous slab caster with slab thickness of 225 mm. Another two-strand slab caster followed in 1986 with the same thickness. Both casters were built using Japanese casting technology (NSC, Nippon Steel Cooperation) and German machine supply (MDM, Mannesmann Demag Metallurgy). In 1988 two six-strand billet casters (Concast) were commissioned in the other steelshop of Hoogovens, BOS No. 1. This plant is now closed and the casters have been dismantled and sold. Ingot casting stopped by the end of the 1980s and currently all steel is cast via the continuous casting process [2].

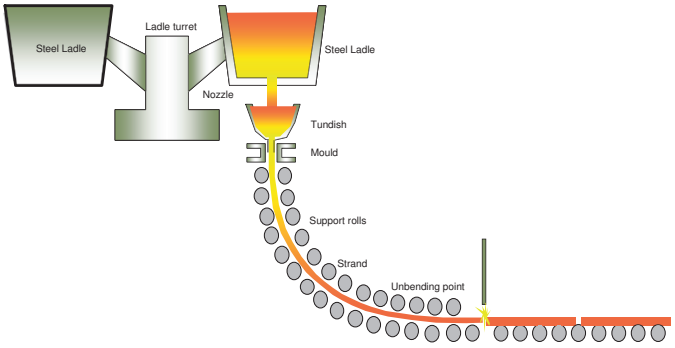

Figure 1.2: *Schematic illustration of a continuous caster (Courtesy of Tata Steel IJmuiden BV)*

The main parts of a continuous caster are a ladle turret, a tundish, a water cooled copper mould, a secondary cooling system with support rolls, driving units and a slab cutter, Figure 1.2.

Steel flows from the ladle to the tundish (a refractory coated vessel that distributes the liquid steel to the strands) and through a submerged entry nozzle (SEN) into the mould. At the start of casting, the bottom of the mould is blocked with a dummy bar. In the mould, the liquid steel solidifies to form a shell of steel and the dummy bar is withdrawn. Then, the shell is withdrawn at a constant velocity and having left the mould is further cooled by water sprays. After bending and final solidification, the steel is cut into slabs. During casting the mould oscillates. Sticking of the shell to the mould is prevented by both mould oscillation (negative strip) and the use of mould powders (or oil for some billet practices, however not for slab casting). Mould powders typically consist of CaO, SiO_2, Al_2O_3, $Na_2O/K_2O/Li_2O$, fluorine and carbon. Generally, the mould is equipped with one or more rows of thermocouples in order to monitor the casting process in more detail.
Over the years, the total production at IJmuiden BOS No. 2 has grown to approximately 7.3 Mt liquid steel in 2007; a quantity of 5.9 Mt steel being cast by the two continuous slab casters and 1.2 Mt steel cast at the thin slab caster.

1.2 Thin slab casting at Tata Steel IJmuiden

Thin slab casting (slab thickness <100 mm) started commercial operation in 1989. Since commissioning of the first commercial caster in Crawfordsville, USA, the quality level and the production capacity improved significantly. In 2010, almost 40 installations as well as ten plants under construction provide a worldwide production capacity of 83 Mt/y of steel. The need for further development of this young technology will remain high in the coming years [3].

The thin slab caster at Tata Steel IJmuiden (Direct Sheet Plant, DSP) started production in 2000. The liquid steel is produced in BOS No. 2 and is treated in a ladle furnace. The caster has one strand and is equipped with a funnel shaped mould, a specially designed submerged entry nozzle (SEN) and an adjustable multiple pole electromagnetic brake (EMBr) aiming to control mould fluid flow during casting [4]. The mould level is measured using a radiometric system. Liquid core reduction decreases the slab thickness from 90 mm to 70 mm. The designed production level is 1.3 Mt/y of coils. For mould oscillation, a hydraulic oscillation system is used. The layout of the Direct Sheet Plant is given in Figure 1.3 and the main specifications are summarised in Table 1.1.

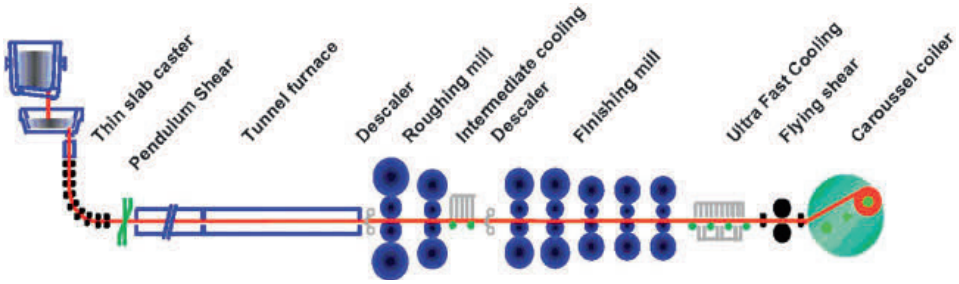

Figure 1.3: *Layout of Tata Steel IJmuiden Direct Sheet Plant*

Since commissioning, several technological developments have been implemented in order to improve the operational performance [5]. The maximum operational casting speed is 5.8 m/min and the average value is over 5.4 m/min. Steel grades produced at the thin slab

caster are mainly low carbon and high strength low alloy grades (HSLA). The maximum sequence length is ten ladles which is equivalent to more than 12 h uninterrupted casting.

Table 1.1: *Main specifications Direct Sheet Plant*

Steel grades	low carbon, HSLA [C] < 0.06 wt%
Casting speed (max)	6.0 m/min
Mould/slab thickness	90/70 mm
Strip thickness	0.7 – 2.5 mm
Strip width	1000 – 1560 mm
Capacity	1.3 Mt/y (coils)

It has been decided to increase the production of the DSP to a level of 1.8 Mt/y using one caster strand. By doing this, expansion with a second strand and a second tunnel furnace can be avoided. To meet this demand, the steel in mould time has to be increased to approximately 85% and the maximum casting speed to 8.0 m/min. A project was started to develop and implement the essential technologies to achieve this goal, with special attention being given to the design of mould powders for high speed casting [6].

1.3 Mould powders for high speed casting

Mould powders significantly affect the stability of the continuous casting process of steel at all casting speeds. The main functions of mould powder are to provide strand lubrication and to control the mould heat transfer in horizontal direction. At higher casting speeds associated with thin slab casting, the role of mould powder is even more important. An illustration of the mould of a continuous caster is given in Figure 1.4.

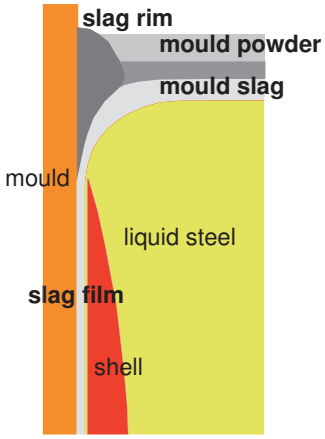

Figure 1.4: *Schematic representation of mould powder in the mould*

During casting, the powder melts on the steel surface, forming a layer of liquid mould slag. Subsequently, the mould slag infiltrates between the steel shell and the mould creating a

thin slag film which solidifies into glassy and crystalline phases. The properties of the slag film dictate the main functions of strand lubrication and mould heat transfer. The formation of crystals is favourable for a homogeneous and controlled (horizontal) heat transfer during casting, which is required in order to prevent the formation of surface cracks.
The transformation from powder to liquid slag and to a (partly) solidified slag as well as the relation to its physical properties and the metallurgical demands is not fully understood. Clarifying and identifying the coherence between these subjects is until now not satisfactorily resolved by the leading research institutes in this field.

Several authors have reviewed the composition, properties and operational experiences of mould powders for conventional slab casting [7,8]. Only some publications have been issued on the design of mould powders and the choice of mould powder raw materials i.e. the chemical and mineralogical constituents [9,10]. A few papers describe the mineralogical behaviour of mould powder and mould slag at high temperatures. Nevertheless, knowledge on the mineralogy and the high-temperature phase relations is considered essential to understand the mould powder behaviour and the mould powder functions strand lubrication and control of mould heat transfer [11,12]. This applies especially to high speed thin slab casting, where the process demands are more stringent compared with conventional casting techniques [13,14].

Mould powder developments are still mainly based on trial and error. A general approach is to relate the chemical composition of a mould powder to the operational behaviour during casting. Some physical properties like the melting point and the viscosity of mould slag are addressed as well, but this approach will not automatically result in a suitable mould powder or in-depth knowledge on powder design [15,16].

At Tata Steel IJmuiden, a project was started within the framework of the Materials innovation institute M2i - Delft University of Technology with the aim to develop mould powders suitable for high speed thin slab casting with a maximum casting speed up to 8 m/min. For this work, a fundamental understanding and quantification of the melting and solidification behaviour of mould slag as well as the mould powder functions are required. To obtain these, the chemical and mineralogical compositions of mould powders need to be related to the physical properties of mould slag and to the operational performance during casting.

1.4 Aim of the study

The aim of the study is:

> *the development of recipes for mould powders, allowing high speed casting of steel up to 8 m/min applying the thin slab casting technique.*

The study has to deliver a fundamental understanding and quantification of the melting and solidification behaviour of mould slag as well as of the functions of mould powders. As a result, windows of physical properties can be defined in order to design mould powders for high speed casting.

1.5 Research approach

Characterization of mould powder and mould slag focuses on the chemical composition, the mineralogy and the physical properties and is done at room temperature and at elevated temperatures. Main topics are chemical analyses, X-ray diffraction (XRD) including high-temperature XRD (HT-XRD) and Rietveld analysis (quantitative XRD), electron microscopy (SEM-EDS), optical microscopy, hot-stage microscopy and viscosity measurements. A next step is the evaluation of process data of the casting process such as slag formation, lubrication and mould heat transfer. This part of the project is completed by the characterization of mould slag, slag rims and slag films obtained from the casters.
Combination of the chemical and mineralogical composition, the physical properties and the operational performance during casting will lead to an understanding of the working and functions of mould powders at casting speeds up to approximately 6.0 m/min. As a next step, design proposals are made for mould powders suited for high speed casting. Mould powders are produced by an industrial partner. Subsequently, the mould powders are characterized and tested at lab-scale and pilot-scale before full-scale plant trials at the caster are done. This step also includes fine-tuning of the mould powders. A schematic illustration of the approach in this project is given in Figure 1.5.

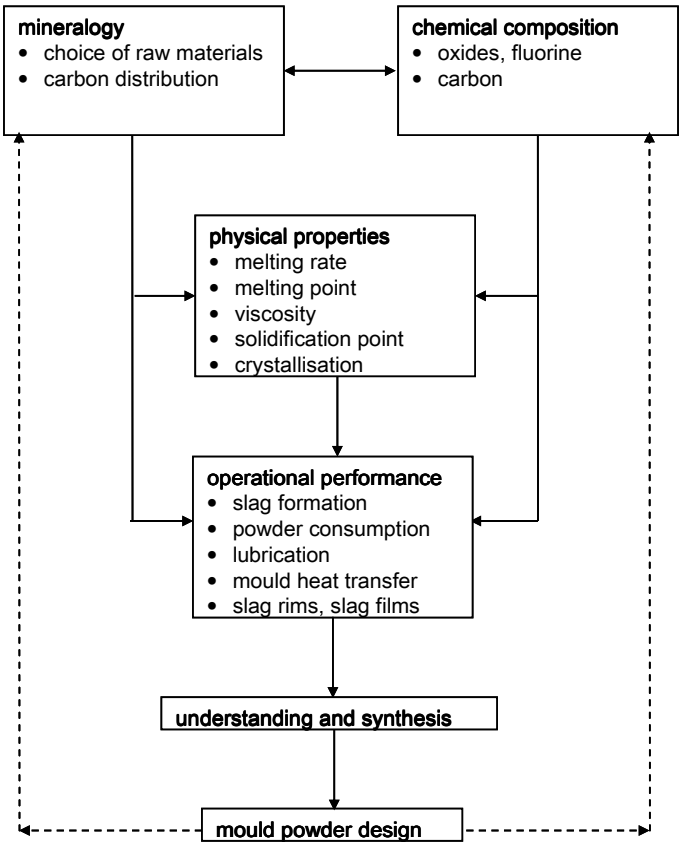

Figure 1.5: *Interrelations between the different topics in the study*

1.6 Thesis outline

Following this introduction, Chapter 2 provides a general overview of mould powders for continuous casting. Specific attention is given to the thin slab casting process and high speed casting. In Chapter 3, a standard mould powder for the DSP caster is described as well as the main characterisation methods applied in this study. Together with a comprehensive literature review, Chapter 4 concentrates on the melting process of mould powder under laboratory and production conditions. The same approach is used in Chapter 5, focussing on the solidification phenomena of mould slag with emphasis on the main subject slag crystallisation. Chapter 6 highlights mould powder requirements for increased casting speeds. In Chapter 7, the operational performance during thin slab casting is reviewed and related to the mould powder properties. Furthermore, recommendations are given for both thin slab casting and conventional slab casting. Chapter 8 presents the general conclusions of this research.

1.7 References

[1] M.M. Wolf in 'The making, shaping and treating of steel', 11th edition, Casting Volume, Historical aspects and key technologies, AISE Steel Foundation, Pittsburgh, USA, 2003.

[2] R. Boom, The impact of Japanese technology on iron and steelmaking – a view from the Netherlands. Proc. SANO Symposium, 2-3 October 2008, Tokyo, Japan, Institute of Industrial Science, The University of Tokyo, Japan, 2008, 12-19.

[3] T. Bolender, R. Fandrich, H-A. Jungblut, G. Kemper, R. Müller, H.P. Narzt, G. Ney und H. Schnitzer, Zum Entwicklungsstand der Stranggießtechnologie - State of the art in continuous casting technology. Stahl u. Eisen, 129 (2009) No.7, 22-39.

[4] M.C.M. Cornelissen and R. Boom, Flow control in the thin slab mould at the Corus Direct Sheet Plant. Steel Research Int., 74 (2003) 716-723.

[5] M.C.M. Cornelissen, J.A. Kromhout, A.A. Kamperman, M. Kick and F. Mensonides, High productivity and technological developments at Corus DSP thin slab caster. Ironmaking and Steelmaking, 33 (2006) 362-366.

[6] C.S.M. Stolwijk, J.G. Hekkema, J.J.M. Cornelissen and M.A.H. van Es, Development of Corus Direct Sheet Plant. Proc. 2006 Int. Symposium on Thin Slab Casting and Rolling (TSCR2006), 11-13 April 2006, Guangzhou, China, The Chinese Society for Metals, Beijing, China, 2006, 119-122.

[7] S. Ogibayashi, K. Yamaguchi, T. Mukai, T. Takahashi, Y. Mimura, K. Koyama, Y. Nagano and T. Nakano, Mold powder technology for continuous casting of low-carbon aluminum-killed steel. Nippon Steel Tech. Rep., 34 (1987) 1-10.

[8] K.C. Mills, A.B. Fox, Z. Li and R.P. Thackray, Performance and properties of mould fluxes. Ironmaking and Steelmaking, 32 (2005) 26-34.

[9] P.V. Riboud in 'Metallurgie des Stranggießens, Gießen und Erstarren von Stahl', (Herausgeber K. Schwerdtfeger), Eigenschaften und Aufgaben von Stranggießschlacken, Verlag Stahleisen mbH, Düsseldorf, Germany, 1992.

[10] H.J. Eitel, Entwicklung und Produktion von Gießpulvergranulat mittels Sprühtrocknungsverfahren sowie dessen Bedeutung für die Stahlindustrie, Dissertation, Rheinisch-Westfälische Technische Hochschule Aachen, Germany, 1990.

[11] A.W. Cramb, From liquid to solid: Key issues in the future of steel casting (2007 Howe Memorial Lecture). Iron & Steel Technology, 4 (2007) No.7, 59-75.
[12] K. Wünnenberg, Möglichkeiten und Grenzen der Wärmeübertragung in Stranggießkokillen. Stahl u. Eisen, 120 (2000) No.7, 29-35.
[13] M. Kawamoto, K. Nakajima, T. Kanazawa and K. Nakai, Design principles of mold powder for high speed continuous casting. ISIJ Int., 34 (1994) 593-598.
[14] D. Blevins, M. Ingold, A. Schaefer, J. Neal, F. Neumann and C. Sowa, Mold powder performance: Steel Dynamics' high speed thin slab casters. Ironmaking Steelmaking, 27 (2000) No.3, 85-88.
[15] M. Hanao, M. Kawamoto, T. Murakami and H. Kikuchi, Mold flux for high speed continuous casting of hypoperitectic steel slabs. Proc. 5th Eur. Continuous Casting Conf., 20-22 June 2005, Nice, France, La Rev. Métall., Paris, France, 2005, Volume 1, 48-55.
[16] J.A. Kromhout, A.A. Kamperman, M. Kick and J. Trouw, Mould powder selection for thin slab casting. Ironmaking and Steelmaking, 32 (2005) 127-132.

2 Mould powders for continuous casting

2.1 Introduction

Mould powders are essential for the stability of the continuous casting process of steel at all casting speeds. Almost all mould powders are mixtures of several mineralogical components and carbon. Mould powders typically contain SiO_2 and CaO (together minimum 60 wt%), Na_2O, Al_2O_3, F and C with minor amounts of metal oxides such as MgO, MnO, Li_2O and Fe_2O_3. The main functions of mould powders are to provide strand lubrication and to control the mould heat transfer in horizontal direction between the developing steel shell and the copper mould [1,2].
During casting, the powder melts on the steel surface, forming a layer of liquid mould slag. Subsequently, the mould slag infiltrates between the steel shell and the oscillating mould, creating a thin slag film which solidifies into glassy and crystalline phases [3]. The formation of cuspidine crystals ($Ca_4Si_2O_7F_2$ or $3CaO{\cdot}2SiO_2{\cdot}CaF_2$) is common for almost all mould powders. The properties of the slag film dictate the main functions of strand lubrication and mould heat transfer [4,5]. An illustration of the process is given in Figure 2.1.

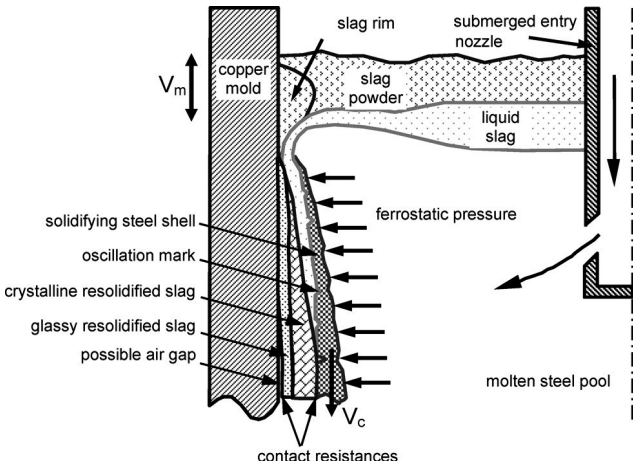

Figure 2.1: *Schematic representation of the mould during continuous casting [6]*

2.2 Mould powder functions

The functions of mould powders are fivefold:

- Protection of the steel from oxidation
- Thermal insulation of the steel meniscus
- Absorption of inclusions from the steel
- Lubrication of the steel shell (strand)
- Control of mould heat transfer between the steel shell and the mould.

The first three functions can be compared to the functions of tundish covering materials. The two main functions of strand lubrication and the control of mould heat transfer directly impact the stability of the casting process and the surface quality of the cast product. These two functions are conflicting and this compromise between lubrication and mould heat transfer is a characteristic of any mould powder. A more detailed description of the mould powder functions is given below.

Protection of the steel from oxidation
Protection of the steel from oxidation follows from the presence of a continuous, uninterrupted layer of (liquid) slag on the steel meniscus. An uninterrupted liquid layer can be obtained by proper powder melting and by stable process conditions in the mould; in particular the mould level fluctuations and the flow conditions in the meniscus area. Furthermore, the mould slag should contain a restricted amount of reducible oxides like Fe_2O_3 and MnO.
Important parameters to control powder melting are the melting rate of the mould powder and the heat transfer in vertical direction from the liquid steel to the meniscus area. A more detailed description of powder melting is given in Section 2.7.

Thermal insulation of the steel meniscus
Thermal insulation follows from the presence of a layer of solid particles or granules, which acts as a blanket. A sufficiently thick powder layer can be obtained by controlled powder melting which is influenced by the powder properties and by the process conditions in the mould. Special attention should be given to a controlled, constant supply of fresh mould powder to the mould surface.

Absorption of inclusions from the steel – reactions at the interface
Absorption of inclusions is made possible by the presence of a liquid slag layer on the steel meniscus. The main purpose of this liquid layer is to absorb Al_2O_3 inclusions (alumina). However, an increase of alumina will result in an increased slag viscosity and a change in solidification and crystallisation properties of the slag film which will affect both the casting process and the surface quality of the product [7,8]. There are two sources for alumina enrichment in mould slag: alumina particles coming from the steel and the reaction at the interface between dissolved aluminium [Al] from the steel and reducible oxides such as SiO_2 in mould slag, indicated by (SiO_2).

Alumina particles
The presence of alumina particles (solid inclusions) in steel is relevant for slab casting of Al-killed steel grades. Due to the difference in density, alumina particles float upwards to the steel–slag interface. After absorption, the particles will dissolve in the mould slag. Note that steel does not wet the particles ($\theta>90^\circ$) but the slag wets the particles ($\theta<90^\circ$). For casting processes like thin slab casting which make use of calcium treatment, the alumina is now present as liquid calcium aluminates. For this reason, the pick-up of alumina particles is not relevant.

Reaction at the interface
The reaction between [Al] (and for certain steel grades [Ti]) from the steel with (SiO_2) is another source for alumina enrichment in mould slag. This can be described by the reaction:

$$4[Al] + 3(SiO_2) \rightarrow 2(Al_2O_3) + 3[Si]$$

Based on conventional slab casting, a critical alumina level in mould slag is reported to be in the range between 15 and 20 wt% i.e. a total alumina enrichment of around 12 wt% (absorption and interface reaction). For slab casting of Al-killed steels under common process conditions, an increase is reported of maximum 4 wt% Al_2O_3 [9,10]. If required, unwanted effects of alumina enrichment can be compensated by changes in the chemical composition of the slag. In particular, the ratio between CaO and SiO_2 and the amount of F, Li_2O and Na_2O are applied.
Interfacial reactions result in convective flows in the boundary layers of mould slag due to disturbances of the interfacial tension. This was investigated and described for CrNi and Cr steels [11].

It can be stated that a stable casting process and in particular thin slab casting will not be influenced by increased alumina contents in the mould slag. An exception can be made for casting steel grades with an Al-content above 0.5 wt%, such as TRIP steels [12]. Details on this application are described in Section 2.10.

Lubrication of the steel shell (strand)
Strand lubrication is made possible by the presence of liquid slag in the slag film. Consequently, the ratio between the liquid and solid part in the slag film is important. The solidification point (or solidification temperature) of the mould slag and the mould heat transfer (as an effect of the casting speed) are the most important parameters for strand lubrication. The crystallisation properties of the mould slag are also relevant since glass will have better lubrication properties than the more rigid crystals. When solidification takes place, glass formation is preferred to crystallisation in relation to strand lubrication. Lack of lubrication will result in an increased friction between the strand and the mould, rupturing of the steel shell, sticking of the strand and break outs of the liquid steel at mould exit [13,14].

Control of mould heat transfer
Mould heat transfer during casting is principally determined by (i) the thickness of the slag film and (ii) the presence of crystals in the slag film. The crystallisation properties of the mould slag and the corresponding solidification temperature are important parameters to control mould heat transfer. These properties are influenced by the composition of the mould slag and by the process conditions (casting speed, mould heat transfer). Crystallisation of slag may result in voids or pores in the slag film as well as an increase of the surface roughness between the slag film and the mould. Together with the presence of crystals, these effects will have a positive contribution to control mould heat transfer during casting. As will be described in Section 2.15, the presence of transition metal oxides like MnO and Fe_2O_3 will have an effect on the control of mould heat transfer.
The underlying mechanisms for a controlled mould heat transfer will be described later; an important aspect is hindering of radiation during casting. A controlled mould heat transfer is essential for the surface quality of the product; in particular the formation of longitudinal facial cracks can be related to the amount and variation of local heat transfer.

From the above it is obvious that powder performance results from both the mould powder properties and the process conditions in the mould. Given the actual casting process, a balance has to be found between strand lubrication and the control of mould heat

transfer. The presence of a continuous slag film between the steel shell and the strand is essential for the two important functions. Consequently, proper powder melting and undisturbed infiltration of mould slag are key items for a stable casting practice [15,16].

2.3 Historical background

Mould powders for industrial continuous casting and ingot casting were introduced in the 1960s and were based on fly ash, mixed with soda ash (Na_2CO_3) as fluxing material. Major functions were lubrication and a controlled heat transfer. Initially, oil was used to provide both lubrication and a thermal barrier between the steel shell and the mould.
Fly ash mainly consists of SiO_2, Al_2O_3 and CaO and can fairly be described by the system CaO-Al_2O_3-SiO_2. Almost all fly ash sources were coming from coal-fired power stations. Consequently, fly ash contained significant amounts of carbon which proved to be very helpful to control the melting rate of mould powders and to create a reducing atmosphere above the meniscus.

Compared to the use of oil, the first mould powders showed very good insulating properties and generated a significant decrease in surface cracks. Mould powders proved to be superior in many applications and were widely introduced during the industrial growth of the continuous casting process. Nowadays, oil is only used for continuous casting of specific billet grades. Mould powders are used for the continuous casting process of slabs, billets and blooms.

With the restricted availability of fly ash from power stations and the increasing demands on a constant quality of fly ash as a raw material, synthetic mould powders were developed. Based on the "fly ash system" CaO-Al_2O_3-SiO_2, several minerals as raw material sources were introduced to obtain a specific chemical composition of mould powders with powder basicity (CaO/SiO_2) and slag viscosity being important variables. During this development, specific carbon sources like coke dust, graphite and carbon black had to be introduced. Carbon black proved to be very effective in the control of powder melting due to the very small particle size, for instance <1 µm.

Main raw materials in synthetic mould powders were wollastonite ($CaO{\cdot}SiO_2$) or Portland cement as sources for CaO and SiO_2 and feldspar (silicates) for Na_2O, Al_2O_3 and SiO_2. Furthermore, natrite or soda ash (Na_2CO_3), an important source of Na_2O, was used to reduce the melting point, the melting trajectory and the viscosity of the slag. A further decrease in viscosity of the slag was obtained by the use of F via fluorite or fluorspar (CaF_2). In later work, it is reported that the presence of fluorine plays a major role in the crystallisation of mould slag as well.

A next important development was the introduction of mould powder in a *granulated* form. This was developed to reduce dust formation and to improve the flowability to achieve more uniform powder addition. Spray drying was selected as the most suitable method for granulation of mould powder. Because this process is based on a water-based suspension, research was done on the mixing process of the mould powder raw materials and the selection of binders and additives like anti foam and surface active agents. Besides, controlling parameters for the spray drying process like nozzle design, gas flow rates and the temperature distribution within the spray tower had to be investigated as well. The spray drying process resulted in the production of hollow granules (hollow

spheres) of mould powder. This product showed a good performance at the steelplants with excellent flow behaviour of the granules, low dust formation during handling, good insulating properties of the meniscus, a constant chemical composition (raw material distribution within the granules) without any physically-bound water. The first spray drying towers for powder granulation were built in 1982. Nowadays, spray dried, granulated mould powders are widely applied in the continuous casting process, although the more "classical" and cheaper non-granulated mould powders are still used.
The flow behaviour of the granules enabled automatic powder feeding at the caster, a significant step to automatise the casting process. A well known system called Dapsol (Distribution Automatique de Poudre Sollac) was developed at Sollac, France, in 1982. Due to the use of mould powder and mould slag, the eddy current principle proved to be the most appropriate mould level detection system for continuous casting. The introduction of automatic powder feeding made the application of eddy current meniscus level control easier [17,18].

2.4 Chemical and mineralogical aspects

Traditionally, mould powders are described by the chemical composition and by the physical properties such as slag viscosity, melting point and solidification point and not by the raw materials. The chemical composition of a mould powder is a result of a specific choice of raw materials denoted as the mineralogical composition. A given chemical composition of a mould powder can be realised by various combinations of raw materials.
Frequently used raw materials are wollastonite, feldspar, natrite, fluorite and free carbon sources like carbon black and coke particles. An overview of common mould powder compositions for thin slab casting is given in Table 2.1.

Table 2.1: *Common composition of mould powder for thin slab casting*

Main components		
component	**amount (wt%)**	**raw materials**
SiO_2	25-36	wollastonite, quartz
CaO	27-34	wollastonite, calcite
Al_2O_3	2-6	feldspar,cryolite
Na_2O	10-17	natrite, feldspar, cryolite
F	6-9	fluorite, cryolite
C_{free}	1-7	carbon black, graphite, coke
Minor components		
component	**amount (wt%)**	**raw materials**
MgO	<4	periclase, forsterite
TiO_2	<1	*
Fe_2O_3	<2	*
MnO	<4	pyrolusite
K_2O	<1	*
Li_2O	<1	spodumene

*: by raw materials or steel slag interaction (TiO_2)

As will be described in this chapter, each component contributes to effects on the slag properties like the viscosity and the solidification point. This is illustrated in Table 2.2.

Table 2.2: *Effect of composition on viscosity, melting point and solidification point*

component	viscosity	melting point	solidification point
SiO_2	+	-	-
CaO	-	+	+
Al_2O_3	+	+	-
Na_2O	-	-	-
F	-	-	+
MgO	-	-	-
TiO_2	+/-	+	+
Fe_2O_3	-	-	-
MnO	-	-	-
K_2O	-	-	-
Li_2O	-	-	-

+: increase -: decrease

In particular, additions of sodium will result in a considerable decrease of the melting point of mould slag. For example, an addition of 1 wt% Na_2O results in a 16 °C decrease of the melting temperature. Additions of fluorine show a restricted effect (decrease) on the melting temperature [19].

The concept of *basicity* is widely used to characterize a mould powder or mould slag and to predict its performance. As will be explained in the next section, mould slag can be described as a silicate network. Basicity can be considered as a ratio between network-modifiers and network-formers in the mould slag. A definition of the basicity is the ratio CaO/SiO_2:

$$basicity = CaO / SiO_2 \qquad (2.1)$$

where CaO and SiO_2 are given in wt%.

For some applications, this definition is extended with Al_2O_3 and MgO:

$$basicity = (CaO + MgO) / (SiO_2 + Al_2O_3) \qquad (2.2)$$

all components given in wt%.

As a rule of thumb, low values of basicity ($CaO/SiO_2 < 1.0$ for thin slab casting) will result in the formation of a more glassy slag film and consequently, improved lubrication and increased mould heat transfer. Increased values of basicity ($CaO/SiO_2 > 1.0$ for thin slab casting) will generally result in a more crystalline and rigid slag film and consequently, decreased values for mould heat transfer and strand lubrication. A balance has to be found between strand lubrication (glassy slag) and the control of mould heat transfer (crystalline slag).

Probably the most fundamental physics-based expression of slag basicity is the *optical basicity*. The optical basicity of a slag can be calculated from knowledge of its composition by the use of either the Pauling electronegativities or the average electron densities of the elements. Optical basicity is described as:

$$\Lambda = \frac{\sum x_1 n_1 \Lambda_1 + x_2 n_2 \Lambda_2 + x_3 n_3 \Lambda_3 + \ldots}{\sum x_1 n_1 + x_2 n_2 + x_3 n_3 + \ldots} \qquad (2.3)$$

where x_i = mole fraction, n_i = number of oxygen atoms in the oxide and Λ_i = optical basicity of each oxide i as derived from Pauling electronegativity. The validity of the formula is restricted when transition metal oxides are present, in particular FeO and MnO and anions such as fluorine. For non-transition metal oxides, a correlation has been deduced between the Pauling electronegativity of the cation x and the optical basicity Λ:

$$\Lambda = \frac{0.75}{x^{-0.25}} \qquad (2.4)$$

The concept proves to be applicable to network systems such as silicates. Optical basicity can also be considered as a measure of basicity according to the Lewis approach i.e. donating negative charge [20,21]. It has been shown that fluorides like CaF_2 are less basic than oxides like CaO or SiO_2; this can be understood since there is an extra positive charge on the fluorine nucleus. However, it is noted that the role of the fluorides and even Na_2O in the silicate network is subject for further research. Although the optical basicity is not widely used, the concept provides a rational basis for describing and optimising the composition of slags and fluxes [22].

2.5 Network theory and ternary diagrams

Given the amount of silica, the structure of mould slag and silicate-based raw materials can be described as a network. Another description of mould slag is based on the use of quasi-ternary diagrams. As with basicity, these two descriptions are simplifications of the more complex slag compositions. However, valuable information on the performance of mould slag and the effects of specific elements can be obtained [23].

The basic building block of all silicates is the SiO_4 tetrahedron (SiO_4^{4-}); a structural unit with a silicon atom in the centre of four surrounding oxygen atoms. All four oxygen atoms simultaneously touch the silicon atom and their external coordinating partners. The role of silicon can be understood by considering the electronic configuration and the resulting bonding character. The electronic structure of silicon is:

Si: $1s^2 2s^2 2p^6 3s^2 3p^2$ (or [Ne]$3s^2 3p^2$).

Relatively little energy is required for the conversion of the ground state $3s^2 3p^2$ to four unpaired electrons $3s^1 3p^3$, a spherical s orbital and three extended p orbitals which are hybridized to four equivalent orbitals pointing toward the corners of a tetrahedron.

In the case of oxygen being the coordination partner, this leads to the stable structural element SiO_4^{4-} which has a tendency to polymerise and to form networks i.e. complex silicates or chains. An illustration of a SiO_4^{4-} tetrahedron and a silicate network is given in Figure 2.2.

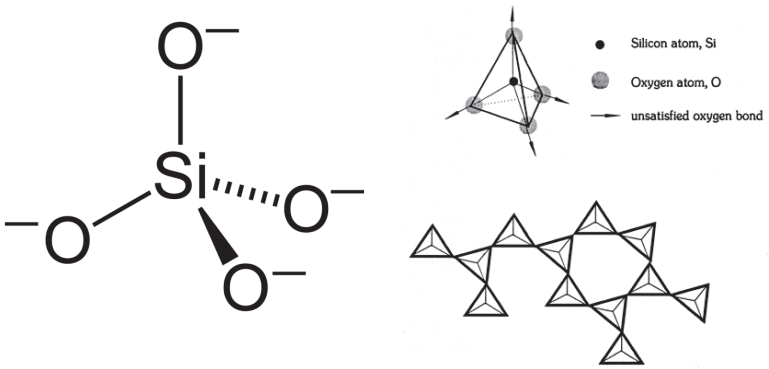

Figure 2.2: *Illustrations of the SiO_4^{4-} tetrahedron and a silicate network [24]*

The principle for the network formation is the complete saturation of oxygen atoms with electrons, with a preference for octet shells. This can be realised by either metals neutralizing the complex or by a connection between the SiO_4^{4-} tetrahedra themselves via oxygen bridges. In the latter case, each oxygen atom is shared by two tetrahedra so that the chemical formula of the silica network is $n(SiO_2)$, where n is a very large number. In general, silicates have a high melting point and in molten state, will show a very high viscosity.

As described by Vogel, Dietzel introduced the term field strength to characterise the effect of a single cation, assuming that the anion is oxygen [25]:

$$F = Z_c / a^2 \qquad (2.5)$$

where F = field strength ($1/Å^2$), Z_c = the valence of the cation and a = the ionic distance for oxides (Å), to be calculated by:

$$a = r_c + r_{O^{2-}} \qquad (2.6)$$

with r_c and r_{O2-} the radii (Å) of the cation and anion (oxygen).

Based on the network theory of Dietzel, cations can be classified as network-modifier, intermediate or network-former:

- network-modifiers: $F \approx 0.1 - 0.4$ $1/Å^2$
- network-formers: $F \approx 1.5 - 2.0$ $1/Å^2$
- intermediates: $F \approx 0.5 - 1.0$ $1/Å^2$.

This concept makes it possible to predict the effect of various cations on the silicate network. For instance, the presence of a network-modifier like Na with $F = 0.19$ $1/Å^2$ will result in breaking of the bridges in the network which will lead to an increased mobility within the slag and consequently a decreased viscosity and decreased melting point. Other

typical network-modifiers in silicates are the cations of K, Li, Ba, Sr, Ca and Fe^{2+}. Examples for network-formers are Si (F = 1.57 1/Å^2) and typical intermediates are Mg, Fe^{3+}, Al en Ti. Figure 2.3 illustrates the effect of sodium and calcium oxides on the network.

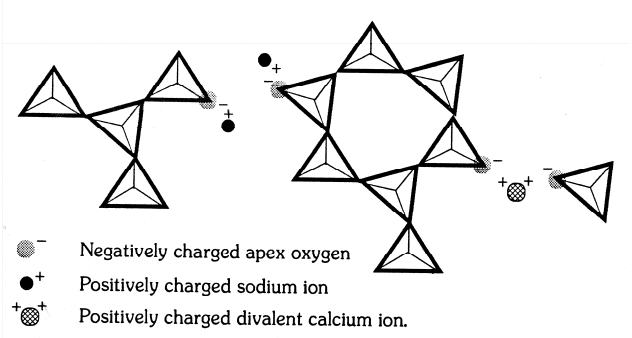

Figure 2.3: *Role of sodium and calcium oxides in modifying the silica network [24]*

Another network-former is B (F = 1.63 1/Å^2). However, the presence of B_2O_3 results in a dramatic reduction in viscosity, melting and solidification temperature of mould slag which is a complication for the network theory [23,26]. Mn^{2+} can act both as network-modifier and as an intermediate (dependent of the coordination number; ionic radius). The concept of basicity can be considered as a ratio between network-modifiers and network-formers in the mould slag.
Note that divalent ions like calcium and magnesium will break up the network but will link the tetrahedra via ionic bonds. These ionic bonds are less rigid than the Si-O-Si bonds in the network. As a consequence, Ca and Mg are less effective in lowering the viscosity and the melting point. Furthermore, Ca enhances the crystallisation tendency of mould slag [24,25].

It should be noted that alumina will form AlO_4^{5-} tetrahedra in almost all mould slags. Consequently, alumina acts as a network-former, resulting in an increased viscosity and a decreased solidification temperature. Although the role of alumina in mould slags is a subject for further research, the network forming capability is obvious and depends on the amount of alumina and the composition of the mould slag, in particular the presence of O^{2-} -ions (slag basicity) and divalent metal oxides [15,27].

The effect of fluorine in mould slag is another subject of research. A common description is that the single-valence fluorine ion will replace the oxygen in the silicate network, forming covalent Si-F bonds. As a consequence, no further bond is available. The network is broken up and the viscosity of the slag will be reduced. However, the role of fluorine in mould slags is much more complex. Another description is depolymerisation or breaking of the network for acidic silicate slags and no breaking of the silicate network in basic slags. In the latter case, the formation of CaF_2 or stable Ca-F clusters is mentioned which act as diluents. During solidification of mould slag, fluorine plays an important role in the crystallisation performance, where the crystal cuspidine is characteristic of many slag compositions [28].
Especially effects of sodium, calcium and fluorine in mould slag systems have thoroughly been investigated; this work includes phase relations and slag crystallisation studies as

well. Various aspects of these constituents in mould slag are still not fully understood [29,30]

Knowledge on the *structure* of the slag (silicate melts) is essential for a better understanding of the physical properties like viscosity, electrical conductivity and thermal conductivity. The structure of a silicate melt is affected by:

- the degree of depolymerisation of the slag
- the fitting of certain cations (e.g. Al^{3+}, Ti^{4+}) into the silicate network
- the nature of the network-breaking cations (e.g. Ca^{2+}, Mg^{2+}) present in the slag.

The degree of depolymerisation in the melt is the primary factor affecting most physical properties.

The number of non-bridging oxygen per tetrahedrally-coordinated atom can be used to represent the degree of depolymerisation of the melt. This is expressed in the NBO/T ratio. For mould slags, the NBO/T ratio can be calculated as:

$$NBO/T = \frac{2x_{CaO} + 2x_{BaO} + 2x_{CaF_2} + 2x_{Na_2O} - 2x_{Al_2O_3} + 6x_{Fe_2O_3} + (2x_{MgO} + 2x_{MnO})}{x_{SiO_2} + 2x_{Al_2O_3} + x_{TiO_2} + 2x_{B_2O_3} + (x_{MgO} + x_{MnO})} \qquad (2.7)$$

where x = mole fraction of the component in the mould flux. The bracket in the denominator/numerator means it will be included into the denominator if MgO is larger than 7% and/or MnO is larger than 4%, otherwise it will be included in the numerator.

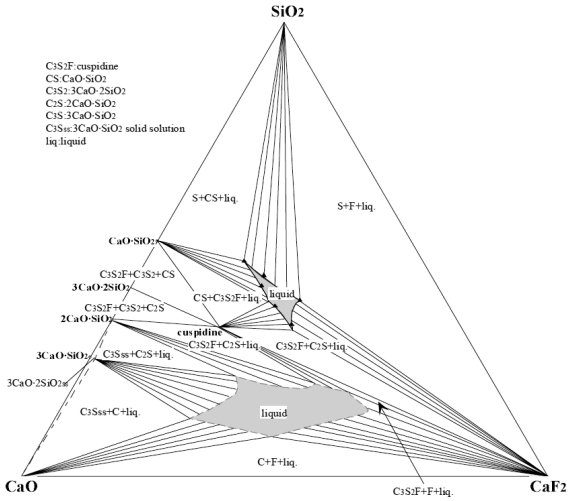

Figure 2.4: *Phase equilibria in the system CaO-SiO_2-CaF_2 at 1200°C [31]*

An alternative measure of the degree of depolymerisation is the optical basicity as described in the previous section. It is mentioned that the Field strength (F) is inversely proportional to the optical basicity of the oxides (Λ) [21,32].

In order to investigate the crystallisation properties of mould slag, in particular crystallisation of cuspidine, ternary diagrams have been developed. Typical systems are CaO-Al_2O_3-SiO_2, CaO-SiO_2-NaF and CaO-SiO_2-CaF_2, the last can be extended with Na_2O [33,34]. In Figure 2.4, an example is given of the system CaO-SiO_2-CaF_2.

2.6 Physical aspects

Common physical properties are the melting point or melting trajectory of mould powder and the viscosity and solidification point of mould slag. These properties are described below. Occasionally, laboratory tests are performed focussing on the interfacial properties and properties related to mould heat transfer. An excellent overview on physical properties of mould slags has been published by Cramb and co-workers [35].

The melting point and melting trajectory can be obtained by using a hot stage microscope. The melting trajectory is described by the softening temperature, the melting temperature and the fluidity temperature. The viscosity of mould slag depends on the chemical composition and the temperature. The viscosity is measured using a viscometer; main methods are a rotational viscometer and an oscillating plate viscometer. In both cases the viscosity is obtained as a function of the temperature at a given cooling rate [36]. The viscosity at 1300 °C is traditionally used as a characteristic value for mould slag. The temperature dependency of the viscosity of a given mould slag can be described by the Arrhenius equation:

$$\eta = A\exp(E/RT) \qquad (2.8)$$

Where η = viscosity in poise (1 poise = 0.1 Pa·s), A = Arrhenius constant (1/s), E = activation energy (kJ/mol), R = gas constant (8.3143 J/Kmol) and T = absolute temperature (K).

Clear relationships between the viscosity and the structure of the slag as indicated by the NBO/T ratio and the optical basicity Λ can be made. The activation energy is considered to be the energy required to break the bonds as is needed for viscous flow. Consequently, the activation energy could also be used to determine the relation between the structure of the slag and the physical properties.
The effect of the temperature on the viscosity is commonly illustrated in a graph where ln (η) is plotted against 1/T. The obtained curve consists of a linear part with slope (E/R) and a sharp transition to a nearly vertical curve. This transition, a sudden increase in viscosity with decreasing temperature, is considered as the start of solidification (or crystallisation). The corresponding temperature is used as the solidification temperature of a mould slag. The transition is defined as crystallisation point (crystallisation temperature) or break point, denoted as T_{break} [37,38].

Another approach to describe slag viscosity is based on the Weyman-Frenkel equation:

$$\eta = AT\exp(E/RT) \qquad (2.9)$$

Several relations have been developed to calculate the slag viscosity as a function of the temperature and the T_{break} or solidification temperature. The relations for the slag

viscosity as defined by Riboud and the Sridhar formula for T_{break} proved to be useful for various slag compositions and are given below [37-39]. The viscosity relationship is based on the Weyman-Frenkel equation and can be described as:

$$\eta = AT\exp(B/T) \tag{2.10}$$

$$A = \exp(-19.81 + 1.73(x_{CaO} + x_{MnO} + x_{MgO} + x_{FeO}) + 5.82(x_{CaF_2}) + 7.02(x_{Na_2O} + x_{K_2O}) - 35.76x_{Al_2O_3}$$

$$B = 31140 - 23896(x_{CaO} + x_{MnO} + x_{FeO}) - 46356x_{CaF_2} - 39159(x_{Na_2O} + x_{K_2O}) + 68833x_{Al_2O_3}$$

where η = viscosity (Pa·s), x = mole fraction and T = absolute temperature (K).

The break point can be calculated by:

$$T_{br} = 1120 - 8.43\%Al_2O_3 - 3.30\%SiO_2 + 8.65\%CaO - 13.86\%MgO - 18.40\%Fe_2O_3 - 3.21\%MnO - 9.22\%TiO_2 + 22.86\%K_2O - 3.20\%Na_2O - 6.46\%F \tag{2.11}$$

where the chemical composition of the mould slag is given in wt% and T_{br} is given in °C. This relation was developed for a cooling rate (slag) of 10 °C/min.

Together with the basicity, the viscosity, solidification temperature (or break point) and the melting point of mould slag are considered the most important parameters to describe mould powder performance.

2.7 Melting of mould powder

This section reviews main aspects associated with melting of mould powder.

After addition of mould powder to the steel surface, the powder melts and forms a layer of liquid slag. Powder melting is affected by the mould powder properties and by the heat flux in vertical direction from the steel to the mould, the *vertical* heat transfer. During melting, several layers are formed. A layer of unreacted mould powder on top, a layer of liquid mould slag all below and one or two intermediate layers: the sinter layer and half molten layer or mushy zone [40].

The thickness of the liquid slag layer or liquid pool depth is the result of the *dynamic equilibrium* or balance between powder melting and slag consumption. Increased powder melting will automatically result in a thicker slag layer, being the outcome of a new equilibrium. A thick slag layer can cause process instabilities and the formation of big slag rims. A thin slag layer can be the source of uneven infiltration of mould slag during casting, reoxidation and carbon pick-up of steel. A well balanced and stable slag layer is required for stable operation and good product quality.

The liquid pool depth is measured by dipping a steel wire or a combination of a steel wire and a copper wire into the mould. Occasionally, an aluminium wire is also added to the steel and copper wires. The melting points of Fe, Cu and Al come close to the temperatures of the steel, slag and sinter layers, respectively. When using a steel wire, the original end of the wire will melt in the steel and the liquid slag adheres to the surface of the wire. The length of the adhered slag indicates the liquid pool depth. When using a combination of wires (Fe-Cu or Fe-Cu-Al), the differences in lengths of the wires represent the thickness of the slag layer and sinter layer, respectively.
At Hoogovens IJmuiden (now Tata Steel IJmuiden), steel sheets were introduced to measure the liquid pool depth during casting. The thickness of the sheets is 0.3 mm and the sheets are immersed into the steel for 1 second. The width of the sheets is around 5 or 15 cm and wider sheets, up to around 30 cm can be used as well. The liquid slag adheres to the steel surface which indicates the liquid pool depth. An advantage of this method is that an indication of the meniscus stability and the thickness variations within the slag layer is obtained as well [41]. As a guideline, the liquid pool depth should be around 5 mm or more, for both conventional slab casting and thin slab casting [42,43]. Other workers suggest higher values for the slag pool depth for instance 10 mm or more [44].

Characteristic powder properties are the melting point (or melting trajectory) and the melting rate. The melting trajectory is determined by the inorganic mould powder components (especially the alkaline metals and fluorine). The presence of *free carbon* in the mould powder is the dominant factor for powder melting.

Free carbon is added to the mould powder in order to control the melting rate. The role of free carbon is to prevent the mould powder particles i.e. the slag droplets to agglomerate or coagulate during melting. Due to the high interfacial tension between carbon and the slag particles i.e. bad wetting performance, carbon will form a network or skeleton between the inorganic particles, acting as inert barrier that prevents the formation of a liquid slag [45,46]. A schematic illustration of this phenomenon is given in Figure 2.5.

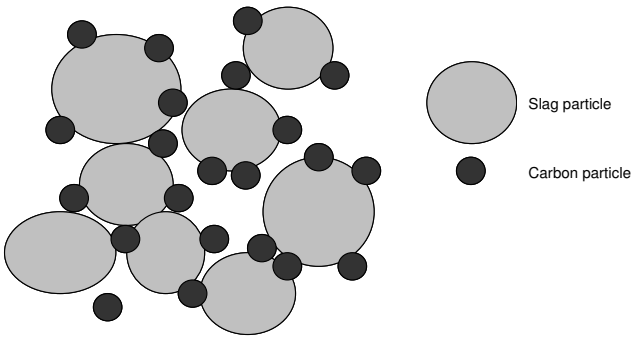

Figure 2.5: *Schematic illustration of slag particles separated by free carbon*

Complete melting is only possible after combustion (removal) of the free carbon in the mould powder. Consequently, the melting process and melting rate of mould powder can be described via the combustion of free carbon.

Main sources of free carbon are coke, graphite and carbon black. Due to the mechanism of powder melting, it is obvious that a fine grade of free carbon is more effective than a coarser grade. Up to now the properties and choice of free carbon in mould powder have rarely been described in literature; these aspects are mainly based on the tradition and experiences of the mould powder supplier. A selection criterion seems to be the particle size of the free carbon. However, a useful and characteristic property like the specific surface area of the carbon particles (m^2/g) is not commonly used. It has been shown that the melting rate is *independent* of the melting temperature; four nearly identical mould powders were tested with a melting point between 1110 and 1200 °C [47].

During heating and melting, the amounts of carbon and carbonates in the mould powder will vaporise as CO_2 and CO gas. In order to calculate the *slag* formed during powder melting, it is necessary to correct for the losses of carbon and carbonates due to combustion and dissociation. This can be done by a correction factor f:

$$f = \left[1 - \%C_{free} / 100 - \left(44/12 \times (\%C_{total} - \%C_{free}) / 100\right)\right] \quad (2.12)$$

where f = the fraction of the mould powder which produces liquid slag, $\%C_{free}$ and $\%C_{total}$ are the weight percentages of free and total carbon respectively [48].

During casting, slag rims are formed. Rims consist of mould powder, mould slag and sintered products and will adhere to the mould walls. Rims can melt, providing some mould slag. Although slag rims are small and hardly visible during casting, they play a role in the infiltration of mould slag. However, rims can grow and disturb the casting process by forming bridges or even hindering the process of slag infiltration. At least two mechanisms for the formation of big slag rims have been described. Both are related to powder melting and meniscus fluctuations:

- The formation of big rims is often associated with heavy slag formation and a thick slag layer (liquid pool), usually due to strong mould level fluctuations and surface waves.
- Other workers mention the presence of a sinter layer and a carbon enriched layer between the sinter layer and the mould slag as a cause of rim formation and rim growth.

For both mechanisms, proper powder melting is important as well as a controlled steel meniscus.

2.8 Infiltration of mould slag, powder consumption

Because the slag wets the strand ($\theta<90°$), infiltration of mould slag can be considered as drawing through the liquid slag by the moving shell. In general, slag infiltration is enhanced by oscillation of the mould; most workers report a positive effect during the period of negative strip during the oscillation cycle. This has been confirmed by experiments on laboratory scale and by mathematical modelling [49]. Furthermore, the presence of the slag rim is considered to enhance the infiltration process as well. Mould

powder consumption is applied as a direct measure of slag infiltration during casting. It has been reported that there is no wetting between the water cooled copper mould and the mould slag or the liquid steel [50].

In general, mould powder consumption is expressed in kg/tonne (steel) or kg/m^2 (slab surface). As a rule of thumb, values of powder consumption for continuous casting are between 0.4 and 0.6 kg/tonne (steel). The powder consumption measured in kg/tonne (steel) can be converted into the powder consumption per square meter strand surface via the relation:

$$Q_s = 7.6 Q_t / R \qquad (2.13)$$

where Q_s = powder consumption (kg/m^2), Q_t = powder consumption (kg/tonne) and R = the ratio of the surface area to the volume of the mould. R can be expressed by:

$$R = 2(w + t) / (w \times t) \qquad (2.14)$$

where R = surface-to-volume ratio (1/m), w = width (m) and t = thickness (m) of the mould.

In order to calculate the *slag* consumption during casting, it is necessary to correct for the losses of carbon and carbonates due to combustion and dissociation, see Equation 2.12.

The slag consumption can now be expressed by:

$$Q_s^{corr} = f Q_s = f 7.6 Q_t / R \qquad (2.15)$$

Where Q_s^{corr} = slag consumption (kg/m^2). As will be described at the end of this section, the consumption of slag can be related to the formation of the slag film.

Researchers at Nippon Steel Corporation found that the *uniformity* of slag infiltration varies with slag viscosity and casting speed [44]. Variations in the mould temperature, mould heat transfer and the powder film thickness at the bottom of the mould were found to be minimal in the (ηv_c) range of 1 to 3.5:

$$\eta v_c = 1 \sim 3.5 \qquad (2.16)$$

where η = viscosity at 1300 °C (poise) and v_c = casting speed (m/min). As a next step the relationship between the parameter *(ηv_c)* and the powder consumption rate was defined as:

$$Q_s = 0.6 / \eta v_c \qquad (2.17)$$

where Q_s = powder consumption in (kg/m^2).

Based on plant data, Wolf [51,52] proposed the relation:

$$Q_s = 0.7 / \eta^{0.5} v_c \qquad (2.18)$$

Later, the modified-Wolf formula was defined [48]; still using the casting speed and slag viscosity as main parameters:

$$Q_s = 0.55 / \eta^{0.5} v_c \qquad (2.19)$$

Over the years, various empirical relations on powder consumption were formulated, with variables both related to mould powder and the casting process (mould oscillation). Even very complex relations were suggested with variables like melting point, solidification point, slag viscosity, mould stroke, positive strip time, negative strip time, oscillation frequency and casting speed. An example, based on a large database of plant data of slabs, billets, blooms and some thin slabs is given below:

$$Q_s = \frac{1}{v_c \eta^{0.46}} \times \frac{1}{f^{0.49}} \times \frac{1}{s^{1.37}} \times \frac{1}{T_{br}^{3.48}} \times e^{28.81} \qquad (2.20)$$

where f = oscillation frequency (cycles/min), s = stroke length (mm) and T_{br} = break point (°C). Note that the indices of v_c and η have a similar ratio as proposed by Wolf [51,52].
It can be questioned if such complex formulas are appropriate for high speed thin slab casting processes which are characterised by relatively smooth slab surfaces and almost no oscillation marks [53]. Consequently, it is suggested for this project to use a more simple relation like the modified Wolf formula.

The powder consumption for thin slab casting was measured at a pilot caster of Sumitomo (Quality Strip Production Process or QSP process, see Section 2.14). It was found that the consumption was around 0.1 kg/m^2 at a casting speed of 5 m/min and between 0.09 and 0.05 kg/m^2 at a casting speed of 8 m/min. Inspection of the slab surface showed a regular pattern of uniform oscillation marks and no surface cracks (longitudinal facial cracks). Furthermore, no sticking was reported. It was concluded that a powder consumption lower than 0.1 kg/m^2 is sufficient when casting at 8 m/min [54]. As a next step, the powder consumption was investigated in detail in the range between 2 and 8 m/min. It was found that the consumption can fairly be described by an equation, based on a parallel flat plate model:

$$Q_s = \frac{\rho}{2} d + \frac{g \rho \Delta\rho}{12 \mu v_c} d^3 \qquad (2.21)$$

where Q_s = powder consumption per unit strand surface area (kg/m^2), ρ = density of mould powder (kg/m^3), d = thickness of powder film (m), g = gravitational acceleration (m/s^2), μ = viscosity of mould powder (Pa·s) and v_c = casting speed (m/s). In this relation, the term $(\rho/2)d$ relates to shear and $[(g\rho\Delta\rho)/(12\mu v_c)]d^3$ relates to gravity.

Furthermore, it was reported that if the shear force is negligibly small, the equation can be transformed to:

$$Q_o = \frac{g \rho \Delta\rho L}{12 \mu} d^3 \qquad (2.22)$$

where Q_o is the powder consumption per unit time (kg/min) and L is the perimeter of the mould (m). This relation agreed well with the observed values.

In this work, gravity is considered the main driving force for inflow of slag (consumption) between the mould and the strand. Increase in powder consumption can be realised by *increasing the gap* between the mould and the strand; this can be realised by mould oscillation and shrinkage of the steel shell (which also depends on the steel grade). Powder consumption is also influenced by the physical properties of the mould slag [2,55]. Recently, the effect of the gap or channel width on mould slag consumption has been investigated in detail using physical and numerical models [56].
In Figure 2.6 an illustration is given of the measured powder consumption during the trials at the pilot caster of Sumitomo.

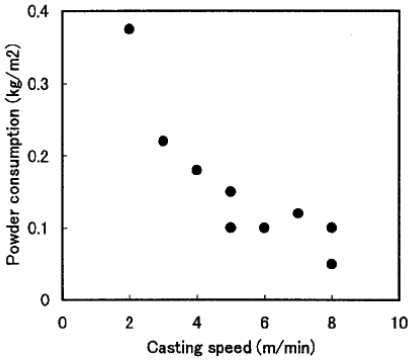

Figure 2.6: *Powder consumption between 2 and 8 m/min (QSP, pilot caster)[55]*

Plant data related to slab, billet and thin slab casting revealed that in general, the powder consumption expressed in kg/tonne (steel), changes only slightly with the casting speed and the dimensions of the mould [57]. The powder consumption for these processes is mainly between 0.4 and 0.6 kg/tonne. An exception is reported for slab casting at very low casting speeds i.e. 0.2 m/min showing maximal powder consumption around 1 kg/tonne.
The powder consumed in kg/m^2 *strand surface* was found to be more suitable to evaluate mould powder performance [57,58]. This is expressed via the surface-to-volume ratio:

$$R = 2(w + t) / (w \times t)$$

Typical values for the surface-to-volume ratio are around 10.5 for slabs, between 15 and 30 for billets and between 22 and 42 for thin slabs. The average powder consumption (kg/m^2) decreases dramatically with increasing surface-to-volume ratio. The following relation was found:

$$Q_s = 0.44 \exp(-0.04R) \qquad (2.23)$$

where Q_s = powder consumption per unit strand surface area and R = surface-to-volume ratio. Later, a comparable relation was defined:

$$Q_s = 2/(R-5) \qquad (2.24)$$

An illustration of the effect of surface-to-volume ratio on the mould powder consumption (Q_s) is given in Figure 2.7.

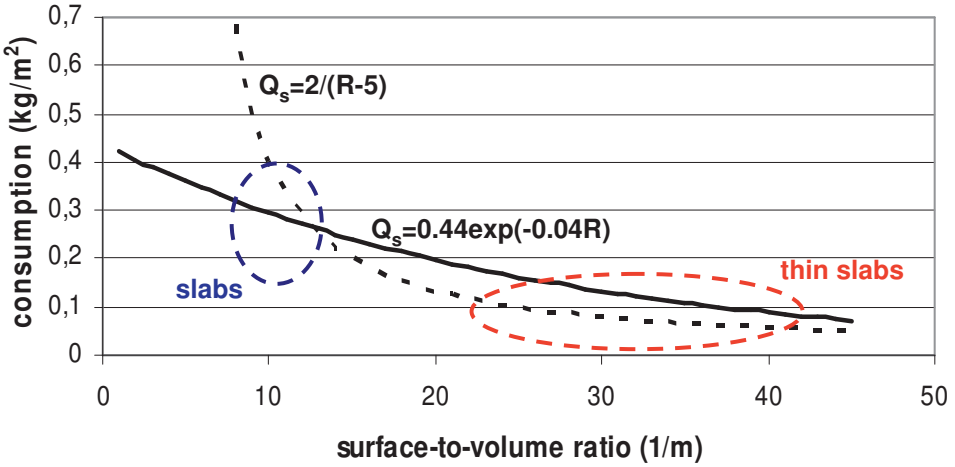

Figure 2.7: *Effect of surface-to-volume ratio on powder consumption (Q_s in kg/m^2) for various section sizes, according to equation (2.23) and (2.24)*

Powder consumption for round billet casting (Ø230 mm) with casting speeds between 1.2 and 1.75 m/min appeared to be low with minimum values around 0.05 kg/m^2. Another billet caster reported comparable low powder consumption with values between 0.05 and 0.1 kg/m^2 for sizes 150 and 180 mm^2. This proved to be sufficient and no operational problems have been reported [59,60].

Based on operational data, there seems to be *no* strictly defined minimum for powder consumption. It is noted that thick and rigid strand shells in the meniscus area show a bigger gap between the mould and the strand and consequently an increased slag consumption; such effects are only reported at very low casting speeds, for instance v_c = 0.2 m/min.

As a result of slag infiltration, a slag film between the solidifying steel shell and the copper mould is formed. Furthermore, slag can be trapped in the oscillation marks (if present). The amount of slag in the oscillation marks can vary as a result of changes in the interfacial tension between steel and slag and variations in oscillation parameters i.e. changes in the oscillation mark depth.

Given the powder consumption during casting, the average thickness of the resulting liquid slag film can be estimated by the equation:

$$d_l = fQ_s / \rho \approx Q_s^{corr} / 2600 \qquad (2.25)$$

where d_l = average thickness of the liquid film (m), f = fraction of the powder forming slag, Q_s = mould powder consumption (kg/m^2), ρ = density of the liquid flux (kg/m^3). In this approach, any mould slag present in the oscillation marks is neglected.
Undisturbed slag infiltration will result in a stable slag film which is essential to realise the two main mould powder functions.

2.9 Solidification of mould slag

Essentials on slag solidification and slag crystallisation are described in this section.

During infiltration, a slag film is formed which consists of a solid part located at the mould side and a liquid part at the strand side. The length of this liquid part (casting direction) depends on the solidification temperature (or T_{break}) of the mould slag. Since strand lubrication is realised by the liquid part of the slag film, excellent lubrication can be obtained by a complete (or nearly complete) liquid slag film contacting the steel shell [14]. The liquid part of the slag film moves together with the strand and is mainly accountable for slag consumption during casting. The solid slag moves very slowly or not at all; this part acts as a substantial thermal barrier which controls the horizontal heat transfer.

Given the local high cooling rate, glassy (or amorphous) solidification will take place at the surface of the water cooled copper mould. In principle, glass formation occurs when the cooling rate is high enough to prevent growth of any nuclei. Within time, crystallisation of the amorphous film or devitrification will start. Consequently, the solid part of the slag film consists of crystals in a glass matrix. Due to the very long residence times of the solid slag film, very dense crystals can develop, especially at the mould side. Given the composition of almost all mould fluxes, the primary crystalline component formed is cuspidine ($Ca_4Si_2O_7F_2$ or $3CaO{\cdot}2SiO_2{\cdot}CaF_2$) followed by smaller quantities of crystals like nepheline ($NaAlSiO_4$ or $Na_2O{\cdot}Al_2O_3{\cdot}2SiO_2$) and villiaumite (NaF). Slag crystallisation depends on the chemical composition, with basicity (CaO/SiO_2) and the presence and amount of components like fluorine and sodium as important variables. Next the cooling rate (horizontal heat transfer) and the presence of nucleation sites like bubbles, droplets and solids like carbon particles influences slag crystallisation substantially.

As a result of the difference in density between glass and crystals, slag crystallisation will result in the formation of cracks and voids located in the slag film and in a surface roughness at the mould side. Together with the crystals, these effects will act as additional thermal barriers [61,62].
The overall thermal resistance between the steel shell and the copper mould can be described as a series of resistances:

$$R_{total} = R_{Cu/sl} + (d/k)_{gl} + (d/k)_{crys} + (d/k)_{liq} \qquad (2.26)$$

where R_{total} = total thermal resistance (m^2.K/W), $R_{Cu/sl}$ = interfacial thermal resistance (m^2.K/W), d = thickness of the slag film part (m) and k = the corresponding heat transfer coefficient (W/m.K). The subscripts *gl*, *crys* and *liq* denote the glass, crystalline and liquid layers of the slag film, respectively.

An alternative description is given as:

$$R_{total} = R_{Cu/sl} + R_{film} = R_{Cu/sl} + \frac{d_{film}}{k_{eff}} \qquad (2.27)$$

where R_{film} = thermal resistance of the slag film, d_{film} = thickness of the slag film and k_{eff} = the heat transfer coefficient of the slag film.

Key parameters affecting the horizontal heat transfer are the solidification temperature and the crystallisation properties; crystalline slag films result in a decreased and more uniform horizontal heat transfer which is very favourable in order to control the formation of longitudinal facial cracks. The reduction of mould heat transfer is mainly based on a reduction of the radiative heat passing through the slag film due to scattering.

The NBO/T ratio as described in Section 2.5 (Equation 2.7) can be used to predict the crystallisation behaviour of mould slag.

The recommended equation to calculate the %crystallinity is:

$$\%crystallinity = 141.1(NBO/T) - 284.0 \qquad (2.28)$$

where *%crystallinity* is given in mole% [32].

The effect of the cooling rate on mould slag crystallisation has been demonstrated by Cramb and Scheller [63,64]. With increasing cooling rates, the start of crystallisation will move to lower temperatures. At very high cooling rates, solidification occurs as glass or partly crystalline. Given the effect of the cooling rate on slag crystallisation, it can be stated that there is not one solidification temperature, unless the cooling path is defined. Consequently, when the cooling rate is considered, the phase diagram is not necessarily useful in predicting the phases that will be formed.
Up to now, the concept of cooling rate (temperature and time) has hardly been used and investigations on slag crystallisation mainly focus on properties like the solidification temperature and the slag basicity (CaO/SiO_2).

2.10 Some operational aspects and developments

Fluorine emission
Fluorine in mould powder is essential during the complete process of powder melting, slag infiltration and crystallisation of the slag film. The presence of fluorine is closely related to the two main mould powder functions strand lubrication and the control of mould heat transfer. From the introduction of mould powders in continuous casting, all important developments related to the casting process and the quality of the as cast product are based on mould powder systems which include fluorine as a key component.
There are, however, some clear disadvantages on the use of fluorine in mould powder:

- Emission of volatile fluorine components like SiF_4 and NaF. These components are formed due to reactions within the mould slag.
- Reactions between fluorine components in the mould slag and moisture in the atmosphere and the cooling water of the caster (secondary cooling), leading to the formation of HF.

The disadvantages of fluorine in mould powder are the risks for plant personnel and severe corrosion of parts of the continuous caster. Up to now, these disadvantages are accepted.
During the years, attempts have been made to develop low-fluorine or even fluorine-free mould powders. A short introduction to fluorine in mould powder and alternatives is given in the appendix.

Reoxidation-free mould powders
In the 1990s, reoxidation-free mould powders were developed with the aim to suppress the interfacial reaction between [Al] or [Ti] and reducible oxides like (SiO_2). Reoxidation-free mould powders are based on relative stable oxides like BaO, Al_2O_3, MgO, SrO and CaO (ΔG^o < -700 kJ/mol O_2 in the temperature range between 1200 and 1600°C) and do not contain SiO_2.
Mould powders were developed based on the system CaO-Al_2O_3-SrO(-MgO) with additions of various fluorides and free carbon. Trials at the laboratory showed almost no oxidation of [Al]. Properties like melting trajectory, slag viscosity and glass formation proved to be comparable to a conventional mould powder containing around 35 wt% SiO_2 [65,66]. Unfortunately, plant trials resulted in serious operational problems related to strand lubrication and mould heat transfer and the developments were stopped [67]. Up to now, no new investigations have been reported

Al-TRIP steels
For TRIP steel grades with typical contents [Al] >0.5 wt%, the reaction at the interface will result in an increased slag viscosity and in different solidification and crystallisation properties:

$$4[Al] + 3(SiO_2) \rightarrow 2(Al_2O_3) + 3[Si]$$

In particular a lower solidification point, fewer and different crystals, formed at lower temperatures can be expected [68]. The most common crystal cuspidine ($Ca_4Si_2O_7F_2$) will partly be replaced by nepheline ($NaAlSiO_4$) and ghelenite ($Ca_2Al_2SiO_7$). These effects will influence the main functions strand lubrication and mould heat transfer which can lead to serious operational problems like severe rim formation, surface defects, sticking and break outs. The critical amount of alumina in mould slag is considered to be between 15-20 wt% Al_2O_3. A critical level in the steel of 0.5 wt% Al has been reported [69].

Casting TRIP steel at TKS (Germany), resulted in an amount of more than 30 wt% Al_2O_3 due to the reaction at the interface. Within 20–30 minutes casting, the alumina content increased by 25-30 wt% and the silica content decreased by approximately 20 wt%. Effects on strand lubrication and mould heat transfer were evident. For this reason, mould powders were used with the aim to maintain a significant amount of silica for lubrication purposes (network formation) in combination with a controlled increase of the viscosity of the slag. The mould powders are characterised by an increased amount of SiO_2, Na_2O and MnO; MnO with the aim to restrict the reaction between [Al] and (SiO_2). Other authors mention additions of Li_2O in order to decrease slag viscosity and to suppress the corresponding formation of rims. The basicity of these powders is between 0.6 and 0.8. [68,70]. When the role of MnO is included, the interfacial reaction can be described as:

$$6[Al] + 3(SiO_2) + 3(MnO) \rightarrow 3(Al_2O_3) + 3[Si] + 3[Mn]$$

Based on the reaction between [Al] and (SiO_2), effects on slag viscosity and slag crystallisation have been studied in more detail. During casting, the slag composition moves from a lime- and silica-based flux to a lime- and alumina-based flux. When cooling, the flux shows a sequence of crystal formation, starting with the formation of calcium fluoride (CaF_2) and followed by the formation of $Ca(Mn,Fe)Si_2O_6$ which transforms into $NaCaAlSi_2O_7$ with further increasing content of (Al). Finally, alumina (Al_2O_3) will be formed which will greatly increase the slag viscosity as well. As with conventional mould fluxes, it was found that crystallisation of mould slag is the primary factor that affects the radiation heat transfer in continuous casting [71].
The changes in slag viscosity have been described based on the molar ratio:

$$x_{Al_2O_3} / x_{SiO_2} \qquad (2.29)$$

The effect on the viscosity was investigated for the Al_2O_3/SiO_2 molar ratios between 0.06 and 2.14. The viscosity increased with increasing Al_2O_3/SiO_2 molar ratio and showed a sharp increase at the Al_2O_3/SiO_2 molar ratio of 0.57. This sharp increase can possibly be linked to the decomposition of the existing AlO_4^{5-} tetrahedron to (Si-O-Al) ions together with the formation of the AlO_6^{7-} octahedral.
Furthermore, effects of Li_2O and B_2O_3 have been explored. These components play a significant role in lowering the slag viscosity, despite the increased values of (Al_2O_3). In particular slag compositions with additions of both Li_2O and B_2O_3 proved to be suitable with respect to slag viscosity and the solidification point. The well known Riboud model for prediction the slag viscosity was successfully adapted for the high alumina containing fluxes [72,73].

Based on this study, it is strongly suggested to develop reoxidation-free mould powders for casting Al-TRIP steels.

Molten mould flux technology
Research at MEFOS and POSCO was done aiming to investigate the use of molten flux technology (pre-molten mould powder) in order to improve the casting process and product quality. Work at MEFOS concentrated on the start of casting. During this project various technical and operational problems with regard to powder melting had to be solved. Plant trials at a bloom caster showed serious difficulties related to powder melting and premature solidification of mould slag, which finally resulted in a bad surface quality of the cast material. However, the concept of feeding liquid mould slag showed some potential with respect to the stability i.e. steady-state during the start of casting. It was found that steady-state as documented by friction measurements and speed variations can be reached 5-10 minutes faster than in normal operations with mould powder [74].
Researchers at POSCO developed an alternative method of feeding molten mould powder i.e. liquid slag to the surface of the molten steel [75,76]. This work was done at a 10-tonne pilot caster which includes a powder melting furnace and feeding device. Referring to the conventional practice based on powder supply, the reported slag consumption was higher due to the absence of big slag rims. In the work of POSCO, it is assumed that molten mould powder, with the absence of free carbon, will result in less rim formation and no carbon pick-up whereas the usual feeding of mould powder will result in the formation of big slag rims which will hinder the infiltration of mould slag. As will be described in Chapter 4, the strict relation between the presence of free carbon and rim formation can be questioned. The increased consumption as found during the experiments resulted in increased

operational windows for slag viscosity and mould oscillation parameters. Although several mould slags are compared in this work, the differences in solidification and crystallisation properties, which significantly affect the results, are not mentioned. Furthermore, disadvantages related to the evaporation of fluorine and sodium are not addressed either. No (vertical) heat flux is needed for heating and melting the mould powder but a well designed insulation cover is required to control thermal radiation from the mould surface. Main advantages of this method are a direct observation of the surface of the molten steel and an easier access of designing mould flux by using raw materials.

Mould powder defects
During casting mould powder or mould slag can be entrapped in the steel. This will lead to non-metallic inclusions and finally surface defects in the product. Several mechanisms have been proposed which describe slag entrapment; all based on mould fluid flow in the meniscus area [41,77]. Slag can be sheared from the slag layer by a steel flow or vortex formation can occur resulting in entrapment of liquid slag. In particular for conventional slab casting, argon bubbles can cause disturbances in the meniscus area (metal–slag) which will lead to slag entrapment. All these mechanisms can be controlled by the casting parameters like metal flow velocity, SEN immersion depth and SEN design and argon flow rate.

Mould slag properties can be manipulated in order to reduce these effects. Effective parameters are the slag viscosity and the interfacial tension. An increase in these properties will suppress slag entrapment. However, it should be noted that an increased slag viscosity will result in less slag consumption during casting; an increased interfacial tension will lead to deeper oscillation marks (see Section 2.11).

Based on laboratory scale experiments, a quantitative relation on slag entrapment was developed [78]. This work focuses on vortex formation and describes effects of the slag viscosity and the interfacial tension:

$$m = 1.06 * 10^{7} \eta^{-0.255} \gamma_{ms}^{-2.18} \qquad (2.30)$$

where m = weight of entrapped mould slag (g/100g steel), η = viscosity of mould slag at 1300 °C (Pa·s) and γ_{ms} = interfacial tension between liquid steel and mould slag (mJ/m^2).

Mathematical modelling
Over the last thirty years, mathematical models have been developed which describe independently many of the phenomena occurring in the mould [79]. The current focus is to couple these different models to give reliable predictions of the performance and behaviour of the continuous casting process. Even though there remains a lack of reliable input data such as high temperature mechanical properties, advanced numerical models can give valuable insights into the process. These include meniscus phenomena, slag infiltration and the formation of oscillation marks [80,81].
The challenge for the future is to refine and adapt these models which were developed for conventional (slab and billet) casting processes, to high speed thin slab casting. This can only be achieved with reliable input data.

2.11 Initial solidification, oscillation marks and surface cracks

The most critical zone in the continuous casting process is in the upper part of the mould. At this location, the liquid metal forms a curved meniscus in contact with molten and solidified mould powder. The surface of the strand is created as the solidification of the metal begins. In general, the beginning of shell growth is determined by the local heat flow, the strength of the shell and the fluid dynamics. The most common defects on continuously cast material, the oscillation marks, are formed in the meniscus region. Other important casting defects formed during initial solidification are hot cracks (hot tears) and surface cracks.

Initial solidification and the formation of oscillation marks (or hook formation) has thoroughly been studied by Kurz, Frederiksson [82,83], Mizukami [84,85] and various other researchers [49]. Main parameters for hook formation are the heat flow and the surface (interfacial) tension balance at the meniscus. A decrease in surface tension and an increase in steel temperature will lead to more shallow marks. Oscillation marks and in particular deep marks will locally show a non uniform heat transfer; this can result in transverse surface cracks.

In general, two types of oscillation marks or hooks can be identified: overflow marks and folding marks. Considering the solidified shell which grows upwards and inwards, overflow marks are formed when liquid flows over this solidified shell. With folding marks, no overflow takes place but the front is bent backwards and grows towards the mould. Both types are repeated in a regular pattern and are affected by mould oscillation.
It has been clearly observed that in static casting, these marks (in particular folding marks) are formed as well.

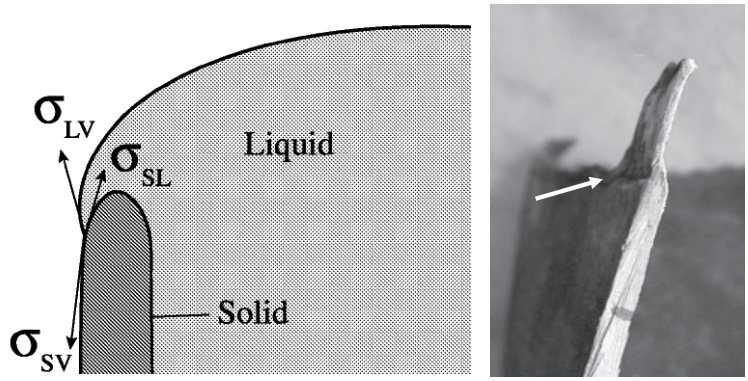

Figure 2.8: *Surface tension balance of top shell (left)and shell after a break out (right) [83]*

In Figure 2.8, an illustration is given of the surface (interfacial) tension balance at the top shell and a steel shell sampled after a break-out during continuous casting. Note that σ_{LV} in this illustration denotes the surface tension between the melt and the mould flux (or the vapour when not using casting powder). The white arrow most likely indicates the first oscillation mark of this shell; note that the thickness of the tip is less than 1 mm.

An almost classical illustration of the formation of oscillation marks is given in Figure 2.9. The liquid metal may overflow the solid shell or first the liquid overflows the shell and then the shell is remelted or the solid shell may be bent backward by ferrostatic pressure. Finally, solidification of the curved part results in hook formation [39,86].

2D-calculations were done in order to describe and understand phenomena in the meniscus region. This includes initial solidification of steel, the formation of oscillation marks, slag consumption and the width of the gap between the mould and the strand. Despite the lack of appropriate data on material properties, in particular of the thin solidified shell, promising results have been obtained [87]. Another example concerns calculations on temperature, stress and distortion of the steel shell during initial solidification. In this work the effect of (sudden) metal level fluctuations for different steel grades was investigated. It was demonstrated that level fluctuations increase (deepen) the depth of oscillation marks by increasing thermal distortion. Ultra-low carbon grades and peritectic steels show deeper oscillation marks and distort more during level fluctuations, comparing to low-carbon and high-carbon steels [88].

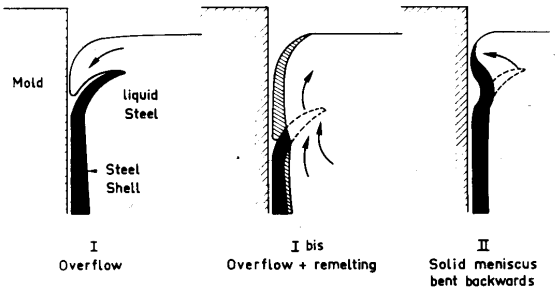

Figure 2.9: *First shell formation and mechanisms for oscillation marks [39]*

From an operational point of view, the depth of oscillation marks can be influenced by the oscillation parameters, the dimensions of the slag rim and the properties of the mould flux. An increased negative strip time, an increased stroke and a decreased frequency will result in deeper oscillation marks. It is generally accepted that big slag rims and a high viscous mould flux increase the depth of the oscillation marks as well [89].
Pioneering work at IRSID by Riboud and co-workers defined the shape of the meniscus in the continuous casting mould as a function of the interfacial tension and the specific mass of metal and slag [50]. An illustration is given in Figure 2.10 and the corresponding relations are given below. The radius of curvature r and the total height of the meniscus are given by:

$$r = \sqrt{\frac{\gamma_{ms}}{2(\rho_M - \rho_S)g}} \qquad (2.31)$$

$$h \approx 2r \qquad (2.32)$$

where r = the smallest radius of curvature in a vertical section (mm), γ_{ms} = interfacial tension (steel-slag) (mJ/m^2), ρ_M and ρ_S = density of metal (steel) and slag, respectively

(kg/m^3), g = gravity (9.81 m/s^2) and h = total height of the meniscus (mm). Increasing the interfacial tension (for instance from 1100 to 1400 mJ/m^2) will result in increased values for r and h and consequently in deeper and wider oscillation marks. These relations are comparable to the equations proposed by Frederiksson.

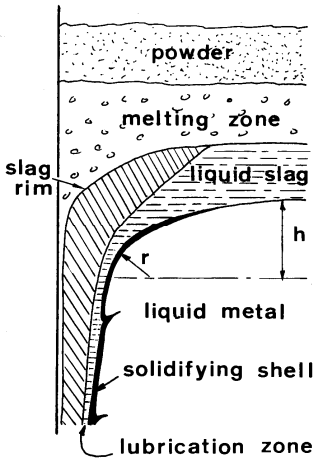

Figure 2.10: *Schematic illustration of the phases in the meniscus region [50]*

Early research on continuous casting suggested a positive effect of an increased interfacial tension and consequently an increased radius on slag consumption during casting [90]. However, any direct relation between the shape of the meniscus as an effect of changes in the interfacial tension, and slag consumption has not been identified yet. An increased gap, required for increased slag consumption, has never been reported.
It should be noted, however, that deeper oscillation marks, resulting from an increased interfacial tension, will contain more slag. Consequently, this can result in an increased powder consumption.

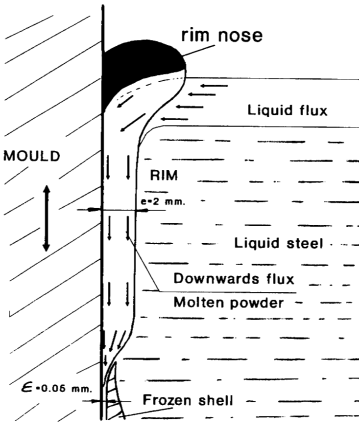

Figure 2.11: *ELV solidification model [91]*

Lainez suggested in his ELV concept (Extra Liquid Volume) that solidification does not start at the meniscus area but further down in the mould, at the lower part of the solid slag rim, around 50 mm under the steel meniscus [91]. These findings are based on experiments at billet casters which included extraction of the complete mould and strand, followed by longitudinal cutting of the mould. An illustration of this concept is given in Figure 2.11.

Longitudinal facial cracks

Surface defects, in particular longitudinal facial cracks are generated by an *uneven solidification* and consequently an uneven thickness of the solidified shell. If the shell has an uneven thickness, stress caused by shrinkage during solidification, δ-γ transformation or peritectic reaction is concentrated on the thinner, weaker parts of the shell. As a consequence, deformation and cracking can be initiated; this can finally result in surface defects. A variable local mould heat transfer during casting can be stated as a root cause of uneven solidification.

Uneven solidification of the shell can start in the meniscus area and is promoted by an increased casting speed, more precisely an increased mould heat transfer and an increased cooling rate. A reduced and controlled mould heat transfer, to be obtained by a proper choice of mould powder, is very effective in order to control uneven solidification during casting and to suppress the formation of longitudinal facial cracks. This has led to mould powders with mild cooling properties and the definition of critical local heat fluxes for low carbon and middle carbon steels [92].

Based on casting trials at Sumitomo with hypo-peritectic steel ([C] = 0.09 – 0.14 wt%) and a mild cooling mould powder (CaO/SiO_2 = 1.8 or 1.2 and T_{break} = 1235 °C), the growth of the solidified shell just under the meniscus was investigated. The trials were done at a pilot caster at casting speeds of up to 5 m/min [101,93]. It was found that there is a delaying period of solidification growth at the beginning, just below the meniscus, until the shell grows up to about 1 mm thick. In this first period, the solidification rate is proportional to solidification time. In the second period the solidification rate is proportional to the square root of solidification time:

$$d_{shell} = 69.7t \qquad 0<t\leq 0.005 \qquad (2.33)$$

$$d_{shell} = 30.0\sqrt{t} - 1.76 \qquad 0.005<t \qquad (2.34)$$

Where d_{shell} = thickness of solidified shell (mm) and t = solidification time (min).

Note that these relations are based on the specific operational data at the pilot caster. However, the principle of the relations proved to be very useful and can be seen as a logical extension of the well known solidification formula:

$$d_{shell} = k\sqrt{t} \qquad (2.35)$$

Where k = the solidification coefficient, ranging from approximately 20 to 30 mm/min$^{0.5}$.

Some similar findings have been reported for slab casting. For instance researchers at Bethlehem Steel Corporation reported that the solidification coefficient increases with

distance below the meniscus (solidification progresses), starting from zero near the meniscus up to around 20 mm/min$^{0.5}$ at mould exit [94].

It is noticed that the pioneering work at the pilot casters of Sumitomo and in particular Danieli reveals the need for *uniform initial solidification* during high speed thin slab casting, first of all to be realised by the stability of the meniscus. This will be described in more detail in Section 2.14.

2.12 Mould powders for slab casting at increased casting speeds

In the second half of the 1980s, Japanese researchers at NKK Fukuyama (now JFE Steel Corporation) developed mould powders for conventional slab casting at casting speeds up to 3.0 m/min. During these developments, slag infiltration and strand lubrication and in particular the prevention of sticker break outs was emphasized. Later, the need to control mould heat transfer, focussing on the temperature of the mould copper surface was addressed too. Typical properties of these powders are low values for powder basicity (CaO/SiO_2 = 0.9), the melting and crystallisation temperatures (around 950 °C) and the slag viscosity (0.09 Pa·s at 1300 °C) with around 8 wt% F and 15 wt% alkalines (Li_2O as an important component). Other important research themes for high speed slab casting were mould oscillation and meniscus stability [95].
American and Japanese mould suppliers reported comparable powder developments with low values for powder basicity, solidification temperature and slag viscosity [96].
In the late 1990s, NKK Fukuyama reported mould powder developments aiming to improve the surface quality of slabs. The reduction of surface cracks at medium carbon steels ([C] = 0.08-0.16 wt%), in particular longitudinal facial cracks, is highlighted. These mould powders are characterised by higher crystallisation temperatures (between 1125 and 1145 °C), low viscosities (between 0.05 and 0.06 Pa·s at 1300 °C) and high values of the basicity (CaO/SiO_2 = 1.4–1.5). Special attention is given to the *crystal growth* of the mould flux. Although the concept of crystal growth is not explained in this work, it is reported that a high crystal growth results in a higher thermal resistance which is favourable for the reduction of longitudinal facial cracks. As before, Li_2O plays an important role in these powders. Other research subjects are mould oscillation, electro magnetic steel flow control and secondary cooling control; all these themes enabled casting speeds of medium carbon steels up to 1.8 m/min [97].

2.13 Mould powders for thin slab casting

There are only a few publications on the design and performance of mould powders for thin slab casting [57,98]. Most of the information is based on technical discussions with mould powder suppliers and on surveys of mould powders, as done previously and within the framework of this study [99,100].

At the beginning in 1989, mould powders for thin slab casting were based on successful powders for (conventional) slab casting. In most cases, powder melting and slag infiltration were emphasised in order to maintain adequate strand lubrication. A main concept was that sufficient infiltration should be realised at increased casting speeds, as applied during thin slab casting, with strand lubrication being a prerequisite.

Compared to powders for conventional slab casting, mould powders for thin slab casting showed lower values for slag viscosity. Parallel to this development, some mould powders for casting crack sensitive steel grades (no peritectics) were developed as well. These powders showed increased values of the basicity and consequently an increased friction of the strand during casting. Up to now, these powders are not widely used. In the late 1990s, a leading mould powder supplier stated that for thin slab casting, sufficient slag infiltration is essential, to be realised by adequate powder melting and low values of slag viscosity.

In order to suppress the formation of slab surface cracks (in particular longitudinal facial cracks) and to combat the thermal wear of the mould copper plates as experienced at increased casting speeds, mould heat transfer became more and more an important requirement. As a consequence, the basicity and solidification point of the mould powders were slightly increased, whilst maintaining low slag viscosities.

Nowadays, the majority of mould powders for thin slab casting are characterised by low values of slag viscosity (around 0.1 Pa·s at 1300 °C or even lower), good powder melting properties and compared to sticker grade mould powders for conventional slab casting, increased values of the basicity (CaO/SiO_2 around 1.0) and a higher solidification point. As a rule of thumb, the solidification temperature of a thin slab casting mould powder is around 100 °C higher, compared to a corresponding powder for conventional slab casting. A minority of the mould powders focuses on either strand lubrication, with low values of slag basicity (CaO/SiO_2 around 0.8) or a controlled mould heat transfer, to be realised by increased values of the solidification point and the slag basicity (CaO/SiO_2 up to 1.3). For these applications, operational restrictions and risks (lower casting speeds, surface cracks, stickers etc.) are accepted.
It was only since around 2000 that the solidification point or T_{break} became widely used, being recognized as an important parameter for mould powder design [37,58].

In Table 2.3 a summary is given of a family of mould powders, as developed by a leading supplier. Powder I is a successful mould powder for conventional slab casting, powder II is a typical mould powder for thin slab casting during the 1990s with main emphasis on strand lubrication. Powder III is a further development, focussing on the control of mould heat transfer as well. Based on the concept of powder III, several versions have been developed aiming to improve slag infiltration, strand lubrication etc. Powder IV was designed with the aim to control mould heat transfer and to cast crack sensitive steel grades; this powder has been developed separately by the same supplier.

Table 2.3: *Development of mould powders for thin slab casting (supplier data)*

	I	II	III	IV
basicity (CaO/SiO_2)	0.83	0.86	0.98	1.15
melting point (°C)	1090	1060	1130	1130
crystallisation point or T_{break} (°C)	1102	1135	1167	1183
viscosity at 1300 °C (Pa·s)	0.16	0.14	0.13	0.09

Some operational results of powder III at a casting speed of 5 m/min are a liquid pool depth between 5 and 20 mm, powder consumption around 0.4 kg/tonne and an average mould heat transfer (wide faces) of 2.6 MW/m^2 [98].

Sumitomo developed mould powders for casting hypoperitectic steel slabs ([C] = 0.09-0.12 wt%) at casting speeds up to 5 m/min. These powders are characterised by a high basicity (CaO/SiO_2 up to 1.8) and solidification temperature (T_{sol} around 1230 °C), low viscosities (between 0.04 and 0.06 Pa·s at 1300 °C) and in particular specific amounts of sodium (Na_2O) and fluorine (F) [101]. The presence of sodium and fluorine promotes the crystallisation of mould slag (cuspidine) significantly, which results in a decreased mould heat transfer and no longitudinal surface cracks and depressions at the given casting speeds.

2.14 Thin slab casting technology and developments toward very high casting speeds

Bernard and co workers measured the *meniscus shell strength* of various steel grades under casting conditions, using a submerged split chill tensile test (SSCT) [102]. The meniscus shell strength was found to be in the range between 0.5 and 4.5 MPa. As a next step, they evaluated plant friction data. Friction shear stress (strand/mould) and friction coefficients under consideration of lubricant type (oil or mould slag) and mould oscillation mode at casting speeds of up to 11 m/min. In general, they found a friction shear stress mostly below 10 kPa, two to three orders of magnitude *lower* than the meniscus shell strength. Mould friction as it is (per se) cannot be the cause of shell tearing and sticking, as experienced during continuous casting. Shell tearing and sticking can only be understood in cases of irregular initial solidification, for example meniscus shell overflow, resulting in hook formation and potential non-uniform lubricant feeding. They concluded that the operational stability of high speed casting *entirely* rests on meniscus stability, with the necessary support of uniform lubrication.
In addition, evaluation of high speed casting plant data revealed that within the range of feasible mould lengths, a shell thickness at the mould exit of around 5 mm appears adequate for operation at casting speeds of up to 13–20 m/min. Up to now, operational casting speeds for industrial thin slab casting are substantially below these values with a maximum around 7 m/min.

Excellent overviews on thin slab casting–hot rolling in Europe with around four operational plants and Asia with more than 15 plants in operation can be found elsewhere [103,104]. Especially China adopted the thin slab casting technique with around 11 operational plants, commissioned during the last ten years and started various developments focussing on process and product developments [105].
The thin slab casting concepts of SMS Siemag (SMS), Danieli and Sumitomo will briefly be described. These concepts are characterised by a high yearly output with operational casting speeds mainly between 4 and 6 m/min and a wide variety of steel grades [106]. Both Danieli and Sumitomo demonstrated significant innovations and technologies for casting at *very high speeds*. Some additional remarks on the concept of Mannesmann Demag Hüttentechnik (MDH) will be given as well.

SMS
SMS Siemag (formerly SMS Demag) introduced the concept of Compact Stip Production (CSP) at Nucor Crawfordsville in 1989. This was the first industrial process capable of

casting, rolling and finishing a strip in one heat. The CSP concept is characterised by a vertical design with in-line bending, a funnel shaped mould, an especially designed SEN and a relative narrow mould thickness of around 60 mm. An illustration of a typical SMS mould is given in Figure 2.12.

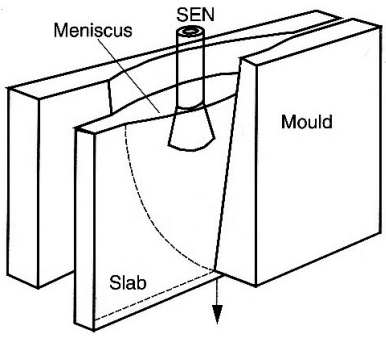

Figure 2.12: *CSP mould [107]*

Over the years, this concept became very successful with more than 25 plants worldwide. Initially, one strand casters with liquid steel coming from an Electrical Arc Furnace (EAF) were built, focussing on relatively simple steel grades. Later, the Basic Oxygen Furnace (BOF) route was introduced as well as two strand thin slab casters. Nowadays, a wide product range is cast, varying from low carbon steels to high strength low alloy grades and high carbon grades, electrical steels ([Si] up to >3 wt%), dual phase steels and various stainless grades. The casting speed is normally within the range between 4.5 and 6 m/min; some exceptions are heats cast up to 7 m/min. For years, thin slab casters supplied by SMS and mould powders produced by the supplier Metallurgica have made up a very successful combination. With developments focussing on casting various steel grades and extension of the product range, no serious developments have been reported with respect to high speed thin slab casting using casting speeds of 7 m/min and more [108,109].

Danieli

Based on developments at a pilot caster (ladle capacity 85 tonnes), Danieli demonstrated a thin slab casting concept which enables casting speeds up to 12 m/min. The mould dimensions are 62 mm*1200 mm and high values (up to 30 mm) of liquid core reduction can be used, resulting in a slab thickness of 36 mm (at a casting speed 10 m/min).

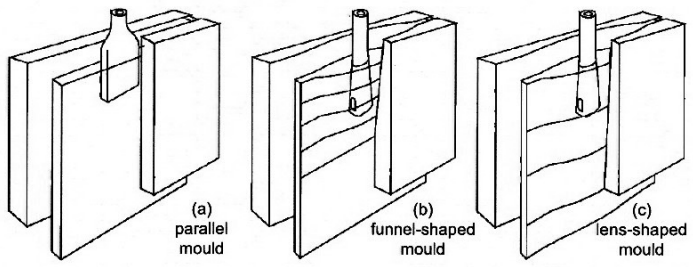

Figure 2.13: *Three types of a mould for thin slab casting [104]*

Key item of the concept is the *stability at the meniscus*, resulting in *uniform initial solidification* during casting. High thermal gradients in the solidified shell, due to non-uniform solidification must be avoided in order to avoid thermal discontinuities and consequently the formation of surface cracks. Uniform initial solidification is realised by a well defined mould fluid flow, an advanced meniscus control system using eddy current techniques, a lens-shaped mould (wide and long funnel, avoiding depressions and cracks) and a proper design of the taper. The caster is of a vertical curved type. A schematic illustration of several mould types for thin slab casting is given in Figure 2.13.

In order to guarantee adequate strand lubrication, powder melting (slag formation) is enhanced by increasing the *vertical heat flux* via the steel flow. For this purpose, a specific "hammer type" SEN is applied where a part of fresh liquid steel is directed in upward direction to the meniscus area. This SEN has four or even six ports, with two or four ports directing the steel flow upwardly. Mould powder consumption decreases at increased casting speeds and is reported to be 0.04 kg/m^2 at a casting speed of 12 m/min. It is clearly stated that it is impossible to optimise strand lubrication by working *only* on mould powder properties. The importance of an integral approach, containing developments of both mould powder and mould fluid flow is underlined.

The average (horizontal) heat flux at the wide and narrow faces is given by:

$$q_w = 5.70 t_d^{-0.30} \tag{2.36}$$

and

$$q_n = 3.83 t_d^{-0.27} \tag{2.37}$$

where q_w and q_n are the average heat fluxes (MW/m^2) at the wide and narrow faces respectively and t_d = dwell time (s).

The average heat flux at the narrow faces is reported to be around 70% of the heat flux at the wide faces. Based on the given equations, typical values of the average heat flux at 6 m/min (given a mould length of 1000 mm) are 2.86 and 2.06 MW/m^2 for the wide and narrow faces, respectively. Even at the very high casting speeds, no operational problems related to mould heat transfer and strand lubrication are reported, despite the reduced thickness of the solidified (initial) shell [110,111].

The thin slab casting concept of Danieli is applied at seven plants worldwide. Main casting requirements are high meniscus stability, a well defined fluid flow, stable powder melting and consequently undisturbed slag infiltration with a special focus on the control of mould heat transfer. Production lines are characterised by a high yearly output and the possibilities to cast a wide variety of steel grades such as ultra low carbon, micro alloyed low and medium carbon steels, high carbon and Corten grades. Silicon steel with [Si] up to 3 wt% has been cast at 4.1 m/min as well as peritectic steel grades [112]. Peritectic steels are cast with high basicity and low viscosity mould powders; a maximum average heat flux of 2.5 MW/m^2 is reported for this practice.

Sumitomo
Sumitomo Metal Industries developed the Quality Strip Production (QSP) process which focuses on high speed casting of low carbon and peritectic (crack-sensitive) steel grades. With a pilot caster (ladle capacity 100 tonnes), low carbon steels ([C] = 0.04–0.06 wt%) have been cast at a maximum speed of 8 m/min and peritectic steels ([C] = 0.09–0.12 wt%) up to 5 m/min and incidentally up to 10 m/min.

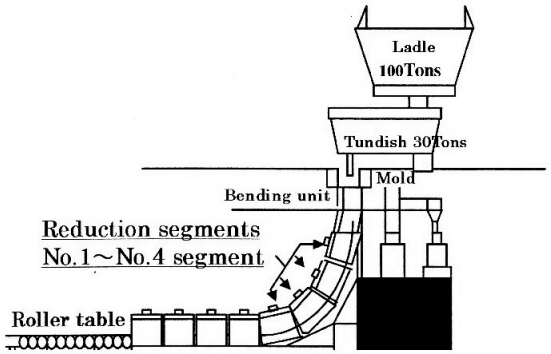

Figure 2.14: *Schematic illustration of the QSP pilot caster [54]*

The QSP process is characterised by a vertical bending type caster with a slab thickness of 90-100 mm, a parallel mould equipped with an EMBr (ruler type), a mould length of 900 mm, a "conventional" round shaped SEN and a well designed liquid core reduction (reduction of 40 mm or less). A sophisticated mould level control system based on eddy current techniques and especially designed mould powders complete this casting process.
Powder consumption is reported to be between 0.09 and 0.05 kg/m^2 at a casting speed of 8 m/min. No problems on lubrication, even at these high casting speeds, are mentioned. Operational windows were defined concerning powder basicity, slag viscosity and solidification temperature, meniscus velocity (steel), oscillation stroke and cooling intensity (secondary cooling). Note that the operational window for the meniscus velocity is between 20 and 50 cm/s with a maximum of 120 cm/s (horizontal direction). These values are above the operational window of 10 – 30 cm/s, applied at the Direct Sheet Plant of Tata Steel [113]. The QSP pilot caster is illustrated in Figure 2.14 [114,115].
The mould length of 900 mm is comparable to conventional slab casting (around 900 mm) and billet casting (around 800 mm); this length proved to be sufficient for casting at 8 m/min and consequently no need for a longer mould is reported. In particular for casting peritectic steel grades at very high casting speeds, mould powders with mild cooling properties were essential. Comparing to a funnel shaped mould, a parallel mould is advantageous for casting peritectic grades because there is less deformation of the initial shell [54,116].

Currently, operational casters do not practice the high casting speeds, as addressed above. However, adequate mould level control based on advanced eddy current techniques, mould powder design and a parallel sided mould, is considered to be essential for high speed casting. During the start up in the late 1990s of an operational caster, work was done on mould design (focussing on hot face temperatures and copper plate thickness),

mould cooling, mould powders and SEN life time. Nowadays, this caster reports a yearly production of more than 1.8 Mt coils, based on *one strand.* The thickness of the mould was increased from 90 to 100 mm in order to increase production and to stabilise mould fluid flow around the SEN, which is very advantageous for powder melting and initial solidification as well [117,118].

Mannesmann Demag (MDH), from ISP to ESP
The In-line Strip Production (ISP) process was jointly developed by Mannesmann Demag Hüttentechnik (MDH) from Germany and the Italian pipe and tube producer Arvedi. The first plant started production in 1992 at Arvedi, Cremona, Italy. Initially, the casting machine had a vertical bow-type mould design with parallel sides and a maximum casting speed (low carbon steel) of 6 m/min [104]. The concept of ISP was applied at three other plants (including Tata Steel DSP) and underwent various improvements, for instance with respect to the control of mould heat transfer during casting i.e. the occurrence of slab surface cracks [119].
The Arvedi plant, however, consequently improved stepwise over the years, leading to a stable production unit of high-quality hot-rolled strip. Based on the technology and experiences with Arvedi ISP, the Endless Strip Production (ESP) line was developed together with Siemens VAI, aiming at endless rolling of high-quality strip in a wide range of steel grades. The mould is of a funnel type and is equipped with an EMBr, hydraulic oscillation and a mould level control system using fast eddy current techniques (an additional radiometric system is stand-by and used during start of casting). A main casting subject within this concept is the control of initial slab solidification and shell formation in the upper area of the mould to be realised by optimisation of mould powders and the control of the temperature distribution and friction in the mould. The ESP-line is designed for a maximum casting speed of 6.0 m/min, first results after commissioning were reported in 2009 [120,121].

In conclusion, the innovations and relevance of the main subjects mould fluid flow (which includes design of mould, funnel and SEN), mould level control and mould powder can be summarised for the main thin slab casting concepts of SMS, Danieli and Sumitomo. See Table 2.4.

Table 2.4: *Summary of main subjects applied at the concepts of SMS, Danieli and Sumitomo*

	mould fluid flow	mould level control	mould powder
SMS	+++	+	-
Danieli	+++	+++	+
Sumitomo	++	+++	+++

2.15 Mould heat transfer and strand lubrication: an everlasting dilemma?

It is obvious that the presence of a continuous slag film between the steel shell and the strand is essential for the two important functions strand lubrication and the control of mould heat transfer. As these functions are conflicting, a well defined balance has to be found in order to guarantee a stable casting process. Over the years, additional

developments have been made in order to overcome this complexity of serving two masters. Work focussed on mould copper plates and mould powder additions.

Mould copper plates and coatings
Around 2004, the so called Advanced Funnel Mould was developed and used at several thin slab casters. With this mould, the mould heat transfer and especially the hot face temperatures are influenced by the use of improved mould materials, a reduced thickness of the wall, a non-uniform wall thickness and finally by water-sheet cooling. These developments resulted in an increased homogeneity of the hot face temperature and the mould heat transfer and consequently in longer mould life. Furthermore, an improved potential to cast crack-sensitive steel grades and to cast at increased casting speeds (> 5 m/min) is reported. It can be assumed that the slag film will be more uniform when using this advanced mould (film thickness and slag crystallinity). Future work concentrates on mould materials, mould cooling and on the development of appropriate coatings. Currently, coatings are not applied in this concept [122,123].

For conventional slab casting, nickel-based coatings are commonly used in order to increase the lifetime of the plates or to prevent crack formation (star-cracks) by minimising Cu pick-up. More recently, ceramic coatings and ceramic-metallic coatings have been developed and applied with the aim to increase the lifetime of the mould plates, focussing on the control of wear especially at the narrow faces [124]. As the development started with slab and bloom casters, thin slab casters are now equipped with this new technology as well. In all cases, an increased life time is reported for both narrow faces and full moulds [125].
In particular for thin slab casting, a more homogenous hot face temperature and mould heat transfer is reported, resulting in an improved product quality. These phenomena can be understood by the controlled wear and decreased crack formation of the coated mould plates. Furthermore, ceramic-metal coatings show *additional* thermal effects, which will also result in a controlled and more homogeneous mould heat transfer during casting. It is obvious that the developments for thin slab casting are concentrating on the meniscus area [125].

It can be assumed that the presence of a ceramic-metal coating on the copper mould will have an effect on the wetting properties of mould slag and probably on the performance of the slag film. Up to now, such effects have not been published.

Within the scope of this study, it has been discussed to develop ceramic coatings with the aim to further control mould heat transfer during casting and to reduce the hot face temperatures. Given the distribution of mould heat transfer, it was also suggested to use coatings with a non-uniform thickness, with emphasis on the meniscus area. Some promising developments were mentioned but no industrial applications of this type of insulating coatings have been reported yet. Mould coatings enabling to substitute the thermal resistance of the slag film, are still not available [126,127].

Up to now, the slag film is the biggest influence to control mould heat transfer and to reduce the hot face temperatures. If successful coatings with appropriate insulating properties become available, the two main mould powder functions can probably be separated. In this case, the emphasis for mould powder will be strand lubrication.

Mould powder additions – transition metal oxides
As described, the control of mould heat transfer by the slag film is based on the presence of crystals. In principle, the use of oxides of transition elements like Fe, Cr, Ni and Mn can have an effect on the control of mould heat transfer as well. Both the refractive index and the absorption coefficients of the slag film will increase with the addition of transition metal oxides. So far, some more fundamental work was done on this theme, resulting in insights into the possibilities of the use of transition metal oxides. Additions of transition metal oxides in Na_2O-SiO_2 and CaO-SiO_2-Al_2O_3 slags showed an increase in absorption coefficients and refractive indices [128]. Experiments during billet casting demonstrated the effect of 4 wt% Fe_2O_3 in mould slag on the control of mould heat transfer [129].
Around 2008, it was demonstrated that additions of 10 wt% MnO and 5 wt% Fe_2O_3 in mould flux reduce the radiation heat transfer by approximately 25%. Although the effect on the average mould heat transfer is relatively low, these additions can be effective on the control of local mould heat transfer, especially in the meniscus area. It should be noted that these additions lead to a fully glassy mould flux that loses transparency but remains as a glass [130]. Work with TiO_2 additions has been done as well, resulting in comparable findings [131,132].
Nothing has been reported yet on the lubrication properties of these mould slags. However, it can be assumed that the glassy slag films will result in improved strand lubrication, comparing to the more crystalline (and rigid) slag films. Further research is needed focussing on mould powder developments, slag characterisation and casting trials. The application of transition metal oxides might provide another possibility to separate the two mould powder functions.

2.16 Concluding remarks

It is striking that a mould powder can have many components or even a complex composition (chemical composition and raw material choice) where the motivation of such a composition is not always clear or is even absent. Mould powder compositions can be a result of tradition, previous adjustments and the wish to use cheaper raw materials. Over the years, the compositions can develop into complex ones. The more complex the powder composition, the more difficult it will be to predict or to evaluate the operational performance.
Within the operational windows of the casting process, a simplification of the chemical composition and raw material choice is desired. This can be illustrated by mould powders for thin slab casting. Only a few families of mould powders are widely used for this relatively new but more complex and very demanding casting process. Several mould powders for thin slab casting are universal for various plants. Traditional slab and bloom casting show an enormous variety of mould powders and various adaptations.
Another conclusion is to involve the metallurgical demands, the composition and the physical properties to a larger extent in the design of mould powders for all casting speeds; this approach is one of the motives for this study.

Crystallisation of mould slag is a function of the composition and the time i.e. the cooling rate. However, in common literature and reports, the cooling rate is rarely addressed and nearly all work on slag crystallisation is only based on the temperature and the slag composition. This can result in a lack of clarity on crystallisation and crystallisation kinetics, an overestimation of the use of phase diagrams (ternary systems) and finally in

wrong conclusions on the control of mould heat transfer, strand lubrication and mould powder design. It is recommended to include the cooling rate and crystallisation kinetics in all mould powder investigations.

The casting process itself is complex and depends on a multitude of variables. Processes in the mould are not fully understood and essential material properties of the solidifying steel are mostly unknown. It is difficult and sometimes nearly impossible to measure the process conditions in the mould and to characterise the various material properties at casting temperatures (i.e. up to roughly 1550 °C). As a consequence, essential data on the casting process and the material properties, especially at high temperatures are often lacking but are needed in order to evaluate the process and to develop more reliable models. In many cases the input variables of the models are assumptions or results of other models. It is very important to break out of this cycle.

Successful casting is a consequence of the choice of optimum casting conditions and mould powder properties. However, given the lack of knowledge, what is optimum?
During all the years mould powders have been expected to be *forgiving* or flexible in order to overcome (and repair) the fact that the casting conditions are sometimes not correct. This approach can finally result in a situation where no new developments can be started.

For all these reasons, fundamental research on mould powders and the casting process is essential in order to increase knowledge, to improve the casting process and to be able to cast novel steel grades. A close collaboration between the steel industry, the suppliers and the academic world is essential in order to make significant steps.

2.17 References

[1] K.C. Mills and A.B. Fox, The role of mould fluxes in continuous casting – so simple yet so complex. ISIJ Int., 43 (2003) 1479-1486.

[2] T. Emi, H. Nakato, Y. Iida, K. Emoto, R. Tachibana, T. Imai and H. Bada, Influence of physical and chemical properties of mold powders on the solidification and occurrence of surface defects of strand cast slabs. Proc. 61st National Open Hearth and Basic Oxygen Steel Conf., 16-20 April 1978, Chicago, USA, Iron and Steel Society, Warrendale, USA, 1978, 350-361.

[3] J. Sardemann and H. Schrewe, The influence of casting powder on the formation of cracks in continuous slab casting. Proc. 74th Steelmaking Conf., 14-17 April 1991, Washington, USA, Iron and Steel Society, Warrendale, USA, 1991, 719-728.

[4] J.A. Moore, R.J. Phillips and T.R. Gibbs, An overview for the requirements of continuous casting mould fluxes. Proc. 74th Steelmaking Conf., 14-17 April 1991, Washington, USA, Iron and Steel Society, Warrendale, USA, 1991, 615-621.

[5] G. Xia, J. Moertl, P. Narzt, M. Habert, E. Rockenschaub and P. Reisinger. Development and application of mould powders for steel slab continuous casting at Voestalpine Stahl. Proc. 5th Eur. Continuous Casting Conf., 20-22 June 2005, Nice, France, La Rev. Métall., Paris, France, 2005, Volume 1, 18-26.

[6] Y. Meng and B.G. Thomas, Simulation of microstructure and behaviour of interfacial mold slag layers in continuous casting of steel. ISIJ Int., 46 (2006) 660-669.

[7] L. Hering und H-W. Fenzke, On-line Überwachung der Wärmestromdichte beim Brammenstranggießen. Stahl u. Eisen, 112 (1992) No.7, 91-95.

[8] P.W. Johnston and G. Brooks, Effect of Al_2O_3 and TiO_2 additions on the lubrication characteristics of mould fluxes. Proc. 5th Int. Conf. on Molten Slags, Fluxes and Salts, 5-8 January 1997, Sydney, Australia, Iron and Steel Society, Warrendale, USA, 1997, 845-850.

[9] G.A. Bezuidenhout and P.C. Pistorius, Effect of alumina pickup on mould flux viscosity in continuous slab casting. Ironmaking and Steelmaking, 27 (2000) 387-391.

[10] G.A. Bezuidenhout and P.C. Pistorius, Alumina pick-up and mould flux crystallisation. Proc. 84th Steelmaking Conf., 25-28 March 2001, Baltimore, USA, Iron and Steel Society, Warrendale, 2001, USA, 369-376.

[11] P.R. Scheller, Interfacial phenomena between fluxes for continuous casting and liquid stainless steel. Ironmaking and Steelmaking, 29 (2002) 154-160.

[12] A.C. Münch, S. Petry, K. Schulz und D. Senk, Untersuchungen zur zeitlichen chemischen Veränderungen von Gießpulvern. Proc. 21. Aachener Stahlkolloquium, 14-15 September 2006, Aachen, Germany, Institut für Eisenhüttenkunde, Rheinisch-Westfälische Technische Hochschule, Aachen, Germany, 2006, 189-200.

[13] L. Hering, H-P. Heller und H-W. Fenzke, Untersuchungen zur Gießpulverauswahl beim Brammenstranggießen. Stahl u. Eisen, 112 (1992) No.8, 61-65.

[14] A.C. Münch, D. Senk and K. Schulz, Untersuchungen zur Messung von Reibkräften beim Strangguß im Labormaßstab. Proc. 21. Aachener Stahlkolloquium, 14-15 September 2006, Aachen, Germany, Institut für Eisenhüttenkunde, Rheinisch-Westfälische Technische Hochschule, Aachen, Germany, 2006, 181-187.

[15] R.V. Branion, Mold fluxes for continuous casting. Ironmaking Steelmaking, 13 (1986) No.9, 41-50.

[16] A.B. Fox, Mould fluxes: their properties and performance, Thesis, Imperial College London, United Kingdom, 2003.

[17] H.J. Eitel, Entwicklung und Produktion von Gießpulvergranulat mittels Sprühtrocknungsverfahren sowie dessen Bedeutung für die Stahlindustrie, Dissertation, Rheinisch-Westfälische Technische Hochschule Aachen, Germany, 1990.

[18] H.J. Eitel, Entwicklung und Produktion von Gießpulvergranulat mittels Sprühtrocknungsverfahren. Stahl u. Eisen, 111 (1991) No.6, 55-60.

[19] R. Scheel and W. Korte, Einfluß unterschiedlicher Gießpulverzusammensetzung auf Stranggießschlacken und Gießpraxis. Stahl u. Eisen, 107 (1987) No.17, 37-43.

[20] I.D. Sommerville and Y. Yang, Optical basicity for control of slags and fluxes. Steel Technology International (1994) 117-124.

[21] K.C. Mills, The influence of structure on the physico-chemical properties of slags. ISIJ Int., 33 (1993) 148-155.

[22] J.A. Duffy, Optical basicity of fluoride containing slags. Ironmaking and Steelmaking, 17 (1990) 410-413.

[23] K.C. Mills, Physical properties of casting powders: Part 1 Scheme to represent chemical composition of powders. Ironmaking and Steelmaking, 15 (1988) 175-180.

[24] A.W.D. Hills, The continuous casting mould, Hoogovens Groep BV, IJmuiden, The Netherlands, 1992.

[25] W. Vogel, Glass Chemistry, 2nd edition, Springer-Verlag, Berlin-Heidelberg, Germany, 1994.

[26] I.R. Lee, J.W. Kim, J. Choi, O.D. Kwon and Y.K. Shin, Development of mould powder for high speed continuous casting. Proc. Conference on Continuous Casting of Steel in Developing Countries, 14-18 September 1993, Beijing, China, The Chinese Society for Metals, Beijing, China, 1993, 814-822.

[27] F. Shahbazian, D. Sichen and S. Seetharaman, The effect of addition of Al_2O_3 on the viscosity of CaO-"FeO"-SiO_2-CaF_2 slags. ISIJ Int., 42 (2002) 155-162.
[28] M. Susa, S. Kubota, M. Hayashi and K.C. Mills, Thermal conductivity and structure of alkali silicate melts containing fluorides. Ironmaking and Steelmaking, 28 (2001) 390-395.
[29] T. Watanabe, M. Hayashi, S. Hayashi, F. Fukuyama and K. Nagata, Solid state ^{19}F NMR on CaO-SiO2-CaF_2 glasses. Proc. 7th Int. Conf. on Molten Slags, Fluxes and Salts, 25-28 January 2004, Cape Town, South Africa, The South African Institute of Mining and Metallurgy, Johannesburg, South Africa, 2004, 699-705.
[30] M. Hayashi, T. Watanabe, H. Nakada and K. Nagata, Effect of Na_2O on crystallization of mould fluxes for continuous casting of steel. ISIJ Int., 46 (2006) 1805-1809.
[31] H. Fukuyama, T. Watanabe and K. Nagata, Phase diagram $3CaO\text{-}2SiO_2\text{-}CaF_2$ around cuspidine – key to desirable mold fluxes. Proc. 6th Int. Conf. on Molten Slags, Fluxes and Salts, 12-17 June 2000, Stockholm/Helsinki, KTH, Stockholm, Sweden, 2000, pdf 21.
[32] Z. Li, R. Thackray and K.C. Mills, A test to determine crystallinity of mould fluxes. Proc. 7th Int. Conf. on Molten Slags, Fluxes and Salts, 25-28 January 2004, Cape Town, South Africa, The South African Institute of Mining and Metallurgy, Johannesburg, South Africa, 2004, 813-819.
[33] T. Watanabe, H. Fukuyama and K. Nagata, Stability of cuspidine ($3CaO\cdot 2SiO_2\cdot CaF_2$) and phase relations in the $CaO\text{-}2SiO_2\text{-}CaF_2$ system. ISIJ Int., 42 (2002) 489-497.
[34] M. Hanao, M. Kawamoto and T. Watanabe, Influence of Na_2O on phase relation between mold flux composition and cuspidine. ISIJ Int., 44 (2004) 827-835.
[35] S. Feldbauer, I. Jimbo, A. Sharan, K. Shimizu, W. King, J. Stepanek, J. Harman and A.W. Cramb, Physical properties of mold slags that are relevant to clean steel manufacture. Proc. 78th Steelmaking Conf., 2-5 April 1995, Nashville, USA, Iron and Steel Society, Warrendale, USA, 1995, 655-667.
[36] H.Y. Chang, T.F. Lee and T. Ejima, Effect of alkali-metal oxide and fluoride on mold flux viscosity. Trans ISIJ, 27 (1987) 797-804.
[37] S. Sukenaga, N. Saito, K. Kawakami and K. Nakashima, Viscosities of $CaO\text{-}SiO_2\text{-}Al_2O_3\text{-}(R_2O$ or RO) melts. ISIJ Int., 46 (2006) 352-358.
[38] S. Sridhar, K.C. Mills, O.D.C. Afrange, H.P. Lörz and R. Carli, Break temperatures of mould fluxes and their relevance to continuous casting. Ironmaking and Steelmaking, 27 (2000) 238-242.
[39] P.V. Riboud and M. Larrecq, Lubrication and heat transfer in a continuous casting mold. Proc. 62nd National Open Hearth and Basic Oxygen Steel Conf., 25-28 March 1979, Detroit, USA, Iron and Steel Society, Warrendale, USA, 1979, 78-92.
[40] K.C. Mills, A review of ECSC-funded research on mould powders, Synthesis report, EUR 13177 EN, ECSC, Luxembourg.1991.
[41] A.L. Spierings, W.H.L. Moonen, R. Boom, D.J. Scoones, S.G. Thornton and A.S. Normanton, Study of mould flux entrapment by monitoring casting parameters on Hoogovens and British Steel slab casters. Proc. METEC Congress 94, 2nd Eur. Continuous Casting Conf., 20-22 June 1994, Düsseldorf, Germany, Steel Institute VDEh, Düsseldorf, Germany, 1994, Volume 1, 86-94.
[42] J.A. Kromhout and D.W. van der Plas, The melting speed of mould powders, determination and application in casting practice. Ironmaking and Steelmaking, 29 (2002) 303-307
[43] J.A. Kromhout, A.A. Kamperman, M. Kick and J. Trouw, Mould powder selection for thin slab casting. Ironmaking and Steelmaking, 32 (2005) 127-132.

[44] K. Koyama, K. Nagano, Y. Nagano and T. Nakano, Design for chemical and physical properties of continuous casting powders. Nippon Steel Tech. Rep., 34 (1987) 41-47.
[45] H.J. Eitel and J. Eitel, Method of making a casting powder. US Patent, 4 127 407, 1978.
[46] T. Nakano, M. Fuji, K. Nagano, T. Matsuyama and N. Masuo, Model analyses of melting process of mold powder for continuous casting of steel. Nippon Steel Tech. Rep., (34) 1987 21-30.
[47] M. Kawamoto, K. Nakajima, T. Kanazawa and K. Nakai, Melting mechanism of mold powder for continuous casting. Proc. 75th Steelmaking Conf., 5-8 April 1992, Toronto, Canada, Iron and Steel Society, Warrendale, USA, 1992, 389-396.
[48] K.C. Mills, A.B. Fox, P.D. Lee and S. Sridhar, Modelling mould powder behaviour in the continuous casting mould. Proc. 2nd Int. Congress on the Science and Technology of Steelmaking (ICS 2001), 10-11 April 2001, Swansea, United Kingdom, IOM Communications Ltd., London, United Kingdom, 2001, Volume 1, 445-456.
[49] S. Nabeshima, Y. Itoh, H. Tozawa, H. Nakato and K. Sorimachi, Direct observation at early stage of solidification in continuous casting with copper alloy and mold powder. Proc. 4th Int. Conf. on Solidification Processing, 7-10 July 1997, Sheffield, United Kingdom, Department of Engineering Materials, University of Sheffield, United Kingdom, 1997, 10-13.
[50] P.V. Riboud, M. Olette, J. Leclerc and W. Pollak, Continuous casting slags: Theoretical analysis of their behaviour and industrial performances. Proc. 61st National Open Hearth and Basic Oxygen Steel Conf., 16-20 April 1978, Chicago, USA, Iron and Steel Society, Warrendale, USA, 1978, 411-417.
[51] M. Wolf, Mould powder consumption – a useful criterion? Proc. METEC Congress 94, 2nd Eur. Continuous Casting Conf., 20-22 June 1994, Düsseldorf, Germany, Steel Institute VDEh, Düsseldorf, Germany, 1994, Volume 1, 78-85.
[52] R. Saraswat, A.B. Fox, K.C. Mills, P.D. Lee and B. Deo, The factors affecting powder consumption of mould fluxes. Scandinavian Journal of Metallurgy, 33 (2004) 85-91.
[53] Y. Zhou, Z. Wei, R. Zhang, Y. Liu, D. Lu and T. Böcher, Development and application of non sinus oscillation curve in thin slab caster. Proc. 3rd Int. Conf. on Continuous Casting of Steel in Developing Countries (CCC'04), 14-17 September 2004, Beijing, China, The Chinese Society for Metals, Beijing, China, 2004, E059-11.
[54] H. Kikuchi, M. Hanao, M. Kawamoto, M. Ikeda, T. Murakami, M. Oka and K. Hanazaki, Continuous casting technologies of 8 m/min casting speed by Sumitomo's QSP process. Proc. 83rd Steelmaking Conf., 26-29 March 2000, Pittsburgh, USA, Iron and Steel Society, Warrendale, USA, 2000, 23-27.
[55] M. Kawamoto, T. Murakami, M. Hanao, H. Kikuchi and T. Watanabe, Mould powder consumption of continuous casting operations. Ironmaking and Steelmaking, 29 (2002) 199-202.
[56] T. Kajitani, K. Okazawa, W. Yamada and H. Yamamura, Experimental and numerical analysis on infiltration of mould flux in continuous casting of steel. Proc. 4th Int. Congress on the Science and Technology of Steelmaking (ICS2008), 6-8 October 2008, Gifu, Japan, The Iron and Steel Institute of Japan, Tokyo, Japan, 2008, 702-705.
[57] F. Neumann, J. Neal, M.A. Pedroza, A.H. Castillejos and F.A. Acosta, Mold fluxes in high speed thin slab casting. Proc. 79th Steelmaking Conf., 24-27 March 1996, Pittsburgh, USA, Iron and Steel Society, Warrendale, USA, 1996, 249-257.
[58] S. Sridhar, K.C. Mills and S.T. Mallaband, Powder consumption and melting rates of continuous casting fluxes. Ironmaking and Steelmaking, 29 (2002) 194-198.

[59] Stahlwerksausschuss, Unterausschuss Stranggießen, 4-5 September 2007, Eisenhüttenstadt, Germany, Stahlinstitut VDEh, Düsseldorf, Germany, 2007.
[60] P. Valentin, Saarstahl, Personal communication, 2006.
[61] B. Tarrant and G. Brooks, Solidification of industrial mold fluxes. Ironmaking Steelmaking, 30 (2003) No.5, 52-60.
[62] P. Hooli and L. Holappa, Layers in the film originating from the casting powder between steel shell and mould and associated phenomena in continuous casting of stainless steel. Proc. 6th Eur. Conf. on Continuous Casting, 3-6 June 2008, Riccione, Italy, Associazione Italiana di Metallurgia, Milano, Italy, 2008, 140.pdf.
[63] A.W. Cramb, From liquid to solid: Key issues in the future of steel casting (2007 Howe Memorial Lecture). Iron & Steel Technology, 4 (2007) No.7, 59-75.
[64] S. Lachmann and P.R. Scheller, Crystallization behaviour of synthetic mould slags. Proc. 6th Eur. Conf. on Continuous Casting, 3-6 June 2008, Riccione, Italy, Associazione Italiana di Metallurgia, Milano, Italy, 2008, 193.pdf.
[65] P. Hammerschmid and D. Janke, Untersuchungen zur Entwicklung reoxidationsfreier Gießpulver. Stahl u. Eisen, 111 (1991) No.9, 97-100.
[66] P. Hammerschmid and D. Janke, Experiments on the development of non-oxidizing fluxes for continuous steel casting. Steel Research Int., 62 (1991) 395-404.
[67] K. Schulz, Stollberg, Personal communication, 2010.
[68] A.C. Münch, Untersuchungen zur Veränderung der Eigenschaften und Wirkungen von Gießpulvern durch kinetische Vorgänge in der Gießschlacke, Dissertation, Rheinisch-Westfälische Technische Hochschule Aachen, Germany, 2007.
[69] F. Hücking, Stollberg, Personal communication, 2007.
[70] T. Omoto, T. Suzuki and H. Ogata, Development of "SIPS series" mold powder for high Al electromagnetic steel. Shinagawa Tech. Rep., 50 (2007) 57-62.
[71] W. Wang, K. Blazek and A.W. Cramb, A study of the crystallization behavior of a new mold flux used in the casting of transformation-induced-plasticity steels. Met. Trans. B., 39 (2008) 66-74.
[72] Z. Zhang, G. Wen, P. Tang and S. Sridhar, The influence of Al_2O_3/SiO_2 ratio on the viscosity of mold fluxes. ISIJ Int., 48 (2008) 739-746.
[73] X. Yu, G.H. Wen, P. Tang and H. Wang, Investigation on viscosity of mould fluxes during continuous casting of aluminum containing TRIP steels. Ironmaking and Steelmaking, 36 (2009) 623-630.
[74] L.E. From and R. Nyström, Optimisation of mould powder performance in casting long products. Final report EUR 19363, ECSC, Luxembourg, 2000.
[75] J-W. Cho, J-K. Park, K-H. Moon, S-H. Lee, G.H. Kim and H-S. Jeong, Characteristics of molten mold flux feeding technology. Proc. AISTech 2007, 7-10 May 2007, Indianapolis, USA, Iron and Steel Society, Warrendale, USA, 2007.
[76] J-K. Park, J-W. Cho, K-H. Moon, S-H. Lee, K.H. Kim and H-S. Jeong, Study on the initial solidification behaviour under the new process of molten mold flux feeding technology in the continuous casting mold. Proc. 7th Int. Conf. on Clean Steel, 4-6 June 2007, Balatonfüred, Hungary, Hungarian Mining and Metallurgical Society, Budapest, Hungary, 2007, 264-271.
[77] W.H. Emling, T.A. Waugaman, S.L. Feldbauer and A.W. Cramb, Subsurface mold slag entrainment in ultra low carbon steels. Proc. 77th Steelmaking Conf., 20-23 March 1994, Chicago, USA, Iron and Steel Society, Warrendale, USA, 1994, 371-379.
[78] K. Watanabe, K. Tsutsumi, M. Suzuki, M. Nakada and T. Shiomi, Effect of properties of mold powder entrapped into molten steel in a continuous casting process. ISIJ Int., 49 (2009) 1161-1166.

[79] M.B. Santillana, L.C. Hibbeler, B.G. Thomas, A. Hamoen, A.A. Kamperman and W. van der Knoop, Heat transfer in funnel-mould casting: effect of plate thickness. ISIJ Int., 48 (2008) 1380-1388.
[80] K.C. Mills, P.E. Ramirez-Lopez and P.D. Lee, Insights into the continuous casting process provided by mathematical modelling. Proc. SANO Symposium, 2-3 October 2008, Tokyo, Japan, Institute of Industrial Science, The University of Tokyo, Japan, 2008, 158-168.
[81] P.E. Ramirez-Lopez, P.D. Lee and K.C. Mills, Explicit modelling of slag infiltration and shell formation during mould oscillation in continuous casting, ISIJ Int., 50 (2010) 425-434.
[82] W. Kurz, About initial solidification in continuous casting of steel. La Metallurgia Italiana, 99 (2008) No 7/8, 56-64.
[83] H. Frederiksson and J. Elfsberg, Thoughts about the initial solidification process during continuous casting of steel. Scandinavian Journal of Metallurgy, 31 (2002) 292-297.
[84] H. Mizukami, S. Hiraki, M. Kawamoto and T.Watanabe, Initial solidification behaviour of ultra low, low and middle carbon steel. ISIJ Int., 39 (1999) 1262-1269.
[85] H. Mizukami and A. Yamanaka, Generation mechanism of unevennness of ultra low carbon steel at initial stage of solidification. ISIJ Int., 50 (2010) 435-444.
[86] J. Elfsberg, Oscillation mark formation in continuous casting processes, Dissertation, Royal Institute of Technology, Stockholm, Sweden, 2003.
[87] G. Zuba, P. Stadelmeyer and W. Freiseisen, Shell formation and behaviour studied by a two dimensional model of the meniscus region. Proc. 4th Eur. Continuous Casting Conf., 14 -16 October 2002, Birmingham, United Kingdom, IOM Communications Ltd., London, United Kingdom, 2002, Volume 1, 139-148.
[88] J. Sengupta, C. Ojeda and B.G. Thomas, Thermal-mechanical behaviour during initial solidification in continuous casting: steel grade effects. International Journal of Cast Metals Research, 22 (2009) 8-14.
[89] B.G. Thomas, M.S. Jenkins and R.B. Mahapatra, Investigation of strand surface defects using mould instrumentation and modelling. Ironmaking and Steelmaking, 31 (2004) 485-494.
[90] H. Litterscheidt in 'Gießen und Erstarren von Stahl III', Untersuchung des Verhaltens von Gießpulver beim Stranggießen, Abschlußbericht, EUR 8569, Forschungsvertrag Nr. 7210.CA/112, Verein Deutscher Eisenhüttenleute, Düsseldorf, Germany, 1984.
[91] E. Lainez and J.C. Busturia, The E.L.V solidification model in continuous casting billet moulds using casting powder. Proc. 1st Eur. Continuous Casting Conf., 23-25 September 1991, Florence, Italy, Associazione Italiana di Metallurgia, Milano, Italy, 1991, 1.621-1.631.
[92] S. Hiraki, K. Nakajima, T. Murakami and T. Kanazawa, Influence of mold heat fluxes on longitudinal surface cracks during high speed continuous casting of steel slab. Proc. 77th Steelmaking Conf., 20-23 March 1994, Chicago, USA, Iron and Steel Society, Warrendale, USA, 1994, 397-403.
[93] M. Hanao, M. Kawamoto and A. Yamanaka, Growth of solidified shell just below the meniscus in continuous casting mold. ISIJ Int., 49 (2009) 365-374.
[94] M.R. Ozgu and B. Kocatulum, Thermal analysis of the Burns Harbour No.2 slab caster mold. Ironmaking Steelmaking, 21 (1994) No.5, 77-84.
[95] T. Wada, M. Suzuki and T. Mori, High speed casting of 3 meters/minute on the NKK Fukuyama Works' No. 5 slab caster. Ironmaking Steelmaking, 14 (1987) No.9, 31-38.

[96] J.A. Moore, C. Camino, S. Diehl, R.J. Philips and D. Piwinsky, Mold flux developments for high speed slab casting. Proc. 79th Steelmaking Conf., 24-27 March 1996, Pittsburgh, USA, Iron and Steel Society, Warrendale, USA, 1996, 259-264.

[97] Y. Yamaoka, R. Nishimachi, M. Osame, K. Ozawa and H. Tanabe, Quality improvement of Nr. 6 caster slabs for plate mill at NKK Fukuyama Works. Proc. Int. ATS Steelmaking Days, 1-2 December 1998, Paris, France, La Rev. Métall., Paris, France, 1998, 172-173.

[98] D. Blevins, M. Ingold, A. Schaefer, J. Neal, F. Neumann and C. Sowa, Mold powder performance: Steel Dynamics' high speed thin slab casters. Ironmaking Steelmaking, 27 (2000) No.3, 85-88.

[99] J.A. Kromhout, V. Ludlow, S. McKay, A.S. Normanton, M. Thalhammer, F. Ors and T. Cimarelli, Physical properties of mould powders for slab casting. Ironmaking and Steelmaking, 29 (2002) 191-193.

[100] T. Cimarelli, A. Feretti, F. Hücking, K. Lerch and M. Vonderbank, Personal communication, 2006.

[101] M. Hanao, M. Kawamoto, T. Murakami and H. Kikuchi, Mold flux for high speed continuous casting of hypoperitectic steel slabs. La Rev. Métall.: 103 (2006) 82-88.

[102] C. Bernard, H. Hiebler and M.M. Wolf, How fast can we cast? Ironmaking and Steelmaking, 27 (2000) 450-454.

[103] D. Ameling, H.W. den Hartog and R. Steffen, Thin slab casting – hot rolling in the EU. Stahl u. Eisen, 121 (2001) No.12, 85-94.

[104] O. Kwon, Thin slab hot rolling process in Asia: installations, core technology and competitiveness. La Rev. Métall., 100 (2003) 25-33.

[105] R. Yin, Progress and prospect of thin slab casting and rolling process in China. Proc. 2006 Int. Symposium on Thin Slab Casting and Rolling (TSCR2006), 11-13 April 2006, Guangzhou, China, The Chinese Society for Metals, Beijing, China, 2006, 1-8.

[106] B. Mukhopadhyay and S. Roychoudhury, Past, present and future of thin slab casting and rolling. Proc. 2006 Int. Symposium on Thin Slab Casting and Rolling (TSCR2006), 11-13 April 2006, Guangzhou, China, The Chinese Society for Metals, Beijing, China, 2006, 351-355.

[107] B. Shen, S. Ye, R. Xu, Y. Li, H. Shen and B. Liu, Study on process parameters of level fluctuation in CSP mould for continuous thin slab casting. Proc. 2006 Int. Symposium on Thin Slab Casting and Rolling (TSCR2006), 11-13 April 2006, Guangzhou, China, The Chinese Society for Metals, Beijing, China, 2006, 314-317.

[108] D. Rosenthal and W. Hennig, CSP – The trend setting technology for more than 15 years. Proc. 2006 Int. Symposium on Thin Slab Casting and Rolling (TSCR2006), 11-13 April 2006, Guangzhou, China, The Chinese Society for Metals, Beijing, China, 2006, 9-17.

[109] C. Bilgen, T. Böcher, C-P. Reip and J. Schlüter, Erzeugung von Mehrphasen- und Röhrenstählen auf CSP-Analgen. Stahl u. Eisen, 127 (2007) No.12, 37-41.

[110] N. Kapaj, M. Antonelli, F. Vecchiet, L. Entesano and M. Pavlicevic, Thin slab casting – results with 10m/min speed. Iron and Steel Technology Conf. Proc. (AISTech 2004), 15-17 September 2004, Nashville, USA, Association for Iron and Steel Technology, Warrendale, USA, 2004, Volume 2, 1063-1073.

[111] N. Kapaj, F. Vecchiet, M. Pavlicevic, A. Poloni and M. Fornasier, Some technological aspects of the thin slab casting process at very high speeds. Iron & Steel Technology, 4 (2007) No.10, 81-88.

[112] C. Piemonte, M. Fornasier and A. Pigani, Thin slab casting and rolling. Millenium Steel (2007) 124-129.

[113] M.C.M. Cornelissen and R. Boom, Flow control in the thin slab mould at the Corus Direct Sheet Plant. Steel Research Int., 74 (2003) 716-723.
[114] A. Yamanaka, S. Kumakura, K. Okamura, T. Kanazawa, T. Murakami, M. Oka, I. Takeuchi and T. Watanabe, Thin slab casting with liquid core reduction. Ironmaking and Steelmaking, 26 (1999) 457-462.
[115] M. Kawamoto, M. Hanao, H. Kikuchi, T. Murakami and M. Oka, Method for continuous casting of steel. EP 1 059 132 B1, 2002.
[116] M. Hara, H. Kikuchi, M. Hanao, M. Kawamoto, T. Murakami and T. Watanabe, High speed continuous casting technologies of peritectic medium thickness steel slabs. La Rev. Métall., 99 (2002) 367-372.
[117] C.T. Miller, D. Onions, D. Kovach and D. Knights, North Star BHP Steel Ltd. issues at startup on the SMI/SHI caster. Proc. 83rd Steelmaking Conf., 26-29 March 2000, Pittsburgh, USA, Iron and Steel Society, Warrendale, USA, 2000, 3-8.
[118] T. Kanazawa and M. Kawamoto, Latest technology for QSP process. Proc. Int. Conf. on Continuous Casting - Past, Present & Future, 24-25 October 2005, Jamshedpur, India, The Indian Institute of Metals and TATA Steel Ltd., India, 2005, 227-230.
[119] S-C. Moon, T-H. Ha and Y-B. Kim, Improvement of product quality in POSCO minimil. Proc. 2006 Int. Symposium on Thin Slab Casting and Rolling (TSCR2006), 11-13 April 2006, Guangzhou, China, The Chinese Society for Metals, Beijing, China, 2006, 182-185.
[120] G. Arvedi, F. Mazzolari, A. Bianchi, G. Holleis, J. Siegl and A. Angerbauer, The Arvedi Endless Strip Production line (ESP), from liquid steel to hot-rolled coil in seven minutes. La Rev. Métall., 105 (2008) 398-407.
[121] A. Flick, A. Jungbauer, J. Watzinger and G. Eckerstorfer, Technology and plant design for Arvedi ESP. Stahl u. Eisen, 129 (2009) No.11, 91-101.
[122] H. Schnitzer, Th. Jegelka, M. Thomasky, H-G. Wobker, G. Hugenschuett, D. Kolbeck and I. Bakshi, Development of the Advanced Funnel Mould (AFM) concept and field tests. Proc. 5th Eur. Continuous Casting Conf., 20-22 June 2005, Nice, France, La Rev. Métall., Paris, France, 2005, Volume 1, 296-304.
[123] I. Bakshi, G. Hugenschuett, D. Kolbeck and H-G. Wobker, Moulds for thin slab casting. Proc. 2006 Int. Symposium on Thin Slab Casting and Rolling (TSCR2006), 11-13 April 2006, Guangzhou, China, The Chinese Society for Metals, Beijing, China, 2006, 385-391.
[124] B. Stalker, K. Goode, D. Preshaw, M. Pitchford, H.P. Hengeveld, B. Allcock and C.M. Kay, Pushing the boundaries of mould plate coatings. Iron and Steel Technology Conf. Proc. (AISTech 2006), 1-4 May 2006, Cleveland, USA, Association for Iron and Steel Technology, Warrendale, USA, 2006, Volume 1, 861-867.
[125] C.B. Donovan, W.H. Emling, M. Badger and J.B. Sears, Application of specialty mold coatings for conventional, medium and thin slab casting. Iron and Steel Technology Conf. Proc. (AISTech 2006), 1-4 May 2006, Cleveland, USA, Association for Iron and Steel Technology, Warrendale, USA, 2006, Volume 1, 851-859.
[126] G. Hugenschütt, H-D. Piwowar and N. Volkmann, KME, Personal communication, 2004 and 2008.
[127] J.K. Brower, K.D. Rapp and M.J. Powers, Advanced alternative coatings for mold copper liners. Iron and Steel Technology Conf. Proc. (AISTech 2005), 9-12 May 2005, Charlotte, USA, Association for Iron and Steel Technology, Warrendale, USA, 2005, Volume 2, 145-155.

[128] M. Susa, K. Nagata and K.C. Mills, Absorption coefficients and refractive indices of synthetic glassy slags containing transition metal oxides. Ironmaking and Steelmaking, 20 (1993) 372-378.
[129] A. López, Z. Idoyaga, F. Plazaola, S. Riaz and K.C. Mills, Factors affecting powder consumption and heat extraction in billet casting. Proc. 4th Eur. Continuous Casting Conf., 14-16 October 2002, Birmingham, United Kingdom, IOM Communications Ltd., London, United Kingdom, 2002, Volume 1, 360-370.
[130] W. Wang and A. W. Cramb, The effect of the transition metal oxide content of a mold flux on the radiation heat transfer rate. Steel Research Int., 79 (2008) 271-277.
[131] J. Diao, B. Xie and J.P. Xiao, Experimental investigation into radiative heat transfer characteristics for mould fluxes containing transition oxides. Ironmaking and Steelmaking, 36 (2009) 610-614.
[132] J. Diao, B. Xie, J. Xiao and C. Ji, Radiative heat transfer in transition metal oxides contained in mold fluxes. ISIJ Int., 49 (2009) 1710-1714.

3 Material and experimental techniques

3.1 Mould powders for thin slab casting and operational criteria

During the first year of operation, the Direct Sheet Plant (DSP) used different mould powders with both high (>1.15) and low (~1.0) basicity (CaO/SiO_2), produced by one of Tata Steel IJmuiden main mould powder suppliers. After approximately a year, a low basicity powder was selected as the standard for the thin slab caster (powder A). With this powder, the casting speed and sequence length have been successfully increased to 5.8 m/min and ten ladles. In Table 3.1, an overview is given of the chemical composition of the standard mould powder.
Simultaneously, trials with alternative mould powders have been done with the aim to increase process stability and product quality. However, the standard mould powder is still used for almost all steel grades at all operational casting speeds.

Table 3.1: *Chemical composition of standard mould powder (wt%)*

Mould powder constituents	Powder A
CaO/SiO_2	1.0
SiO_2	33.2
CaO	33.6
MgO	0.7
Al_2O_3	2.9
Na_2O	11.9
K_2O	0.4
MnO	0
Fe_2O_3	0.5
F	8.8
C_{free}	3.7
CO_2	9.4
C_{tot}	6.3

For mould powder evaluation at the DSP, several operational criteria have been defined. These criteria are related to:

- slag formation, which includes liquid pool depth and rim formation
- powder consumption
- mould heat transfer
- strand lubrication
- scale formation

Referring to slag formation, the minimum liquid pool depth during casting is 5 mm. The liquid pool depth is measured by immersing stainless steel and copper sheets into the mould. This method was significantly improved during this project. The formation of rims and powder lumps are monitored by the caster operators. Special attention is to be given to control the growth of slag rims i.e. to prevent excessive rim formation during casting. The maximum thickness of slag rims is approximately 10 mm and the formation of lumps is to be avoided.

The powder consumption should not be lower than the current average value of 0.05 kg/m^2 (kg powder/slab surface). The consumption is measured by monitoring continuously the weight of the powder bin on the tundish car.
Homogeneous and controlled heat transfer and controlled strand lubrication are desired, within the given operational window of the caster. The main targets for mould heat transfer are to prevent slab surface cracks (longitudinal facial cracks) and to protect the mould copper plates in the meniscus area, due to the (increased) heat load. Mould heat transfer is calculated using mould cooling water temperatures and flow; additional data can be obtained via the mould thermocouples. Strand friction is obtained from the mould hydraulic oscillating system. An illustration of the mould of the DSP is given in Figure 3.1, showing the red hot SEN and the flaming carbon components from the mould powder.

Figure 3.1: *DSP mould and SEN*

Scale formation at the slab surface (i.e. wustite, FeO_x), especially in the tunnel furnace area, should be independent of the mould powder type. Scale formation is observed by inspection of the rolls in the tunnel furnace.

3.2 Mould powder characterisation

A summary of characterisation methods is given in sections 3.3 to 3.6. These include: quantitative phase analysis, equilibrium phase relations, viscosity measurements and microscopic analyses. The last two methods are standard methods for mould powder characterisation [1,2]. Quantitative phase analysis and equilibrium phase relations were developed specifically within the framework of this study.

3.3 Quantitative phase analysis

The chemical composition as given in Table 3.1 does not provide information on the mineralogical composition i.e. the raw material choice. The mineralogy is an important theme in the current mould powder developments.
Phase proportions within mould powders have been determined by X-ray diffraction (XRD) and subsequent Rietveld analysis. Samples of mould powder were ground in a ball mill (tungsten carbide) under cyclohexane to make grain sizes appropriate for XRD analysis (<5 µm). Subsequently, an internal standard (10 wt% ZnO) was added which shows no peak overlap with main reflections of common phases present in mould powder. The XRD patterns were recorded in reflection mode in the range of 10 to 130° (2Θ) using a fully automated Bruker D4 diffractometer (CoK_{α}-radiation) equipped with a position sensitive detector. Quantitative determination of phase proportions was also performed by Rietveld analysis using the Bruker Topas software package for Rietveld refinement. By doing this, the raw material composition was determined.
The Rietveld method was first reported in 1966 and was introduced for X-ray powder diffraction in 1977. The Rietveld method was originally developed to reveal crystal structures by refining neutron diffraction patterns. The method is also suitable for deriving phase proportions by full-pattern fitting of XRD data. An application of this method is quantitative phase analyses, based on powder XRD [3,4]. Results of the analyses of the DSP standard mould powder (powder A) are given in Table 3.2.

XRD with subsequent Rietveld-analyes on mould powders were applied and optimised in 2005, as part of this study. To our knowledge, Rietveld-calculations i.e. quantitative phase analyses on mould powders have not been performed and reported elsewhere.

Table 3.2: *Mineralogical composition of the standard mould powder (Rietveld-XRD) (wt%)*

Mould powder composition	Powder A
Silicates	
wollastonite ($CaSiO_3$)	50 ± 5
quartz (SiO_2)	2 ± 1
diopside ($CaMgSi_2O_6$)	2 ± 1
albite ($NaAlSi_3O_8$)	14 ± 3
Fluorites	
fluorite (CaF_2)	17 ± 3
cryolite (Na_3AlF_6)	0
Carbonates	
natrite (Na_2CO_3)	13 ± 3
calcite ($CaCO_3$)	2 ± 1
Glass	0

In general, a mould powder contains silicates, fluorites and carbonates. Additionally, amorphous components (glass) can be present. In mould powder A, wollastonite, albite (feldspar), fluorite and natrite are used as main raw materials. As will be shown in this work, for each mould powder significant differences in the raw material composition are observed.

During the execution of Rietveld-calculations on mould powders, some problems occurred on data-fitting, associated with effects of preferred orientation of wollastonite ($CaSiO_3$). In addition, wollastonite occurs in three different crystallographic structures, which have almost similar and overlapping reflection positions and intensities. Therefore, the complexity of recorded XRD patterns affected the accuracy of derived quantitative results.

The GeoForschungsZentrum (Experimental Geochemistry and Mineral Physics) in Potsdam, Germany assisted by characterising two standard wollastonite sources, as used by the mould powder supplier, and the standard mould powder (powder A). The powder diffraction patterns of these materials were measured using a diffractometer (Stoe STADIP) in the 2Θ range between 5 and 125 degrees. In contrast to XRD equipment at Tata Steel RD&T, XRD patterns were obtained in *transmission* which obviously minimises the problem of strong preferred orientation. For this, the powder was diluted with glue and mounted on a circular foil. To minimise preferred orientation, the powder was stirred during drying. The foil was then placed into the sample holder and covered with a second empty foil [5]. Rietveld structure refinements have been performed for each sample (using the program suite GSAS). By doing this, the identification and refinement of different wollastonite polymorphs occurring in the raw materials used in different mould powders and powder A was improved. The information has been used to improve the accuracy of Rietveld calculations on all mould powders at the IJmuiden Technology Centre of Tata Steel.

3.4 Equilibrium phase relations

Initial mixtures of raw-materials of the mould powders are not in chemical equilibrium but the systems tend towards it during heating, which results in a series of reactions between the phases and finally formation of secondary phases. These reactions may include solid-state reactions or partial melting and solid-liquid interaction. The mineralogical composition will change continuously during heating until the mould powder melts completely. The sequences of reactions are thereby specific for each mould powder and controlled by the mineralogical and chemical bulk composition.
Changes in mineralogy of the major phases (>10 wt%) for mould powders have been observed *in situ* using high-temperature X-ray diffraction (HT-XRD) with additional powder X-ray diffraction (XRD) and microscopic techniques. A description of the principle and use of HT-XRD techniques is given in [6,7].

Mould powder samples were ground in a ball mill under cyclohexane to make grain sizes appropriate for XRD analysis (<5 µm) and to attain chemical equilibrium. Each sample powder was then analysed using a diffractometer (Bruker D4) at room temperature to identify all phases present in the delivered initial mould powders. For HT-XRD measurements, sample powders were mounted on a Fe-metal strip. The strip was used as a resistance heater on a heating stage (Anton Paar HTK2000 sample chamber) that was mounted on a diffractometer (Panalytical X'pert Pro). Temperature was measured and controlled by a type S thermocouple (Pt-Rh) directly attached to the metal strip below the sample; the temperature accuracy is ±15 °C. An illustration of the equipment is given in Figure 3.2.

HT-XRD patterns in the reflection were recorded using a (Raytech) 12° position sensitive detector (PSD). The radiation used was Co-K_α. The Co-radiation was filtered using thin Fe-foils (incident and diffracted beam) to decrease the amount of CoK_β-radiation. For the

incident beam a divergence slit of 1/4° was used. The goniometer was set up according to the parafocusing Bragg-Brentano geometry.

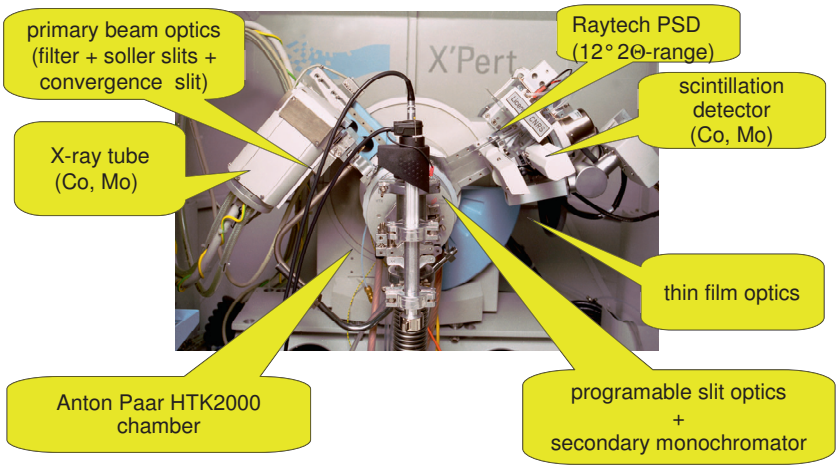

Figure 3.2 : *HT-XRD equipment*

XRD-patterns were collected in-situ in the 2Θ range from 20-60 degrees, while the temperature was raised from 500 °C to the liquidus temperature (between 1300-1375 °C) and then subsequently lowered to 500 °C. Heating and cooling rates were 200 °C/min between each measurement. Figure 3.3 shows a typical example of an XRD pattern (3D-plot) during heating of a mould powder.

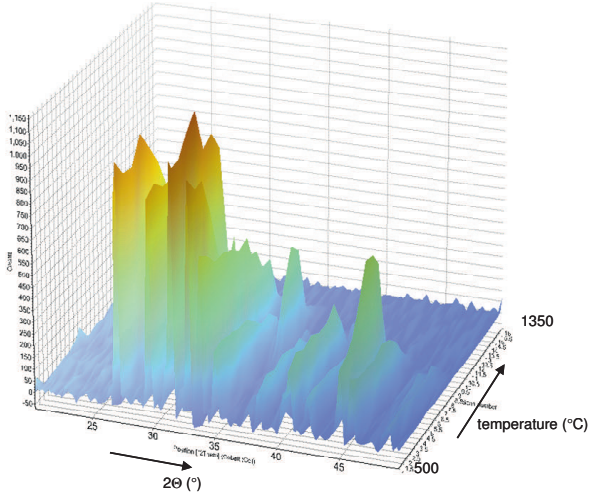

Figure 3.3: *3D-plot of XRD-pattern upon heating from 500-1350 °C*

XRD-patterns were taken with temperature increments of 50 °C. A second sequence of XRD-patterns was collected for each mould powder by heating with an offset of 25 °C compared to the first run (e.g. from 525-1325-525 °C) to obtain a higher resolution of phase stabilities as a function of temperature. It was not possible to perform a single experiment with steps of 25 °C, because the longer data acquisition times resulted in significant fluorine loss at temperatures above 1200 °C. In all cases diffraction patterns on the cooling paths showed relatively low intensities compared to heating paths. This is likely due to shrinking of the sample volume that occurs upon melting and to larger crystallites formed in the melt. Consequently, not enough crystallites contribute to the diffraction pattern resulting in very weak or absent reflections. Therefore, samples were reinvestigated with slower scan rates on the cooling path between 20-50 degrees 2Θ by directly heating to 1350 °C at 300 °C/min with subsequent cooling to 500 °C at 200 °C/min with increments of 50 °C. Phase relations and temperature stabilities were derived by combining all data sets. In Figure 3.4, a summary of the complete HT-XRD analysis of the standard mould powder (powder A) is given.

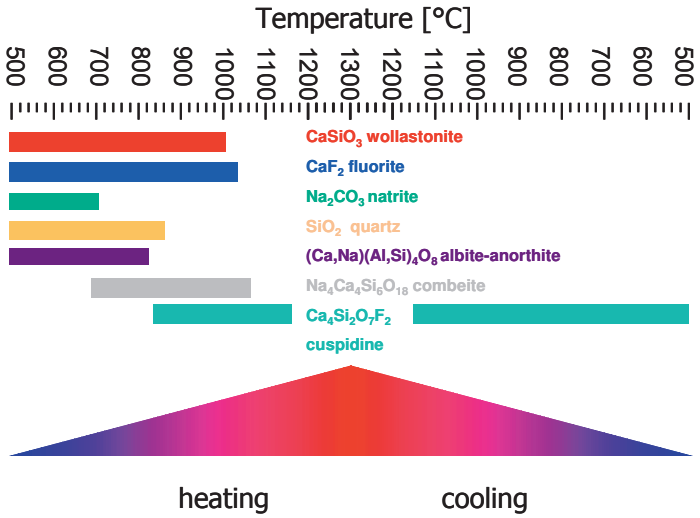

Figure 3.4: *Results of HT-XRD analysis of standard mould powder (powder A)*

After the experiments the samples were removed from the metal strips. Parts of the experimental products were then ground to a fine powder for a final room temperature XRD measurement for phase identification. To check for losses of the volatile components (Na, F) a fragment of the post-heated sample was embedded in epoxy resin, ground and polished for chemical analysis on a scanning electron microscope (SEM-EDS). Bulk chemical compositions were determined using a (Noran) EDS system in an area scan mode over several hundred μm^2 of the post-heated sample.
XRD-patterns of starting materials and of experimental products after high temperature measurements revealed amorphous material (glass). This implies that strictly speaking, the phase stabilities presented are valid only for the given heating and cooling rates, since the formation of nuclei, and thus crystallisation, may be kinetically hampered.

The analysis shows that during heating, first the carbonates (natrite) disappear, next some silicates, then the fluorites and wollastonite. In the meantime, the intermediate phases combeite and cuspidine are formed. Finally, the complete mould powder melts. During cooling, the mould slag (molten powder) forms cuspidine crystals ($3CaO{\cdot}2SiO_2{\cdot}CaF_2$ or $Ca_4Si_2O_7F_2$) directly from the melt. Crystallisation starts at temperatures between 1150 °C and 1100 °C. No other major phases were detected. For mould powder A the temperature of complete melting (stability during heating) is comparable to the temperature where the first crystallisation is detected.

It can be concluded that during heating, a mould powder shows a specific sequence of break-down of primary materials (raw materials) and formation of secondary phases, before melting takes place. During cooling, one or more crystalline phases can be formed. In Chapter 4 and 5, more information will be given on the high temperature phase relations of this mould powder and of various other powders. Subsequently, these findings will be related to the physical properties and the metallurgical behaviour.

As with the Rietveld analyses, *in situ* HT-XRD on mould powders during heating and cooling was applied and optimised from the beginning of this project. Based on our knowledge, this technique as applied to mould powders has rarely been reported elsewhere. One publication describes a heating experiment of a quenched powdered slag sample from the system CaO-SiO_2-CaF_2, using HT-XRD in the temperature range between 600 °C and 920 °C [8]. This work shows XRD-profiles of the slag at various temperatures within this range and is used additionally to a more comprehensive study which investigates the thermodynamic stability of cuspidine. In 2009, a mould powder supplier mentioned the use of HT-XRD techniques to investigate powder melting, especially with respect to raw materials like wollastonite and fluorite. Up to now, no significant results on powder properties have been reported and the work focuses only on heating experiments of a quenched mould slag, followed by some Rietveld calculations [9,10].
Other publications describing XRD-experiments on mould powders and mould slag are based on room temperature XRD; in some cases the slag samples are obtained by quench experiments.

3.5 Viscosity and melting trajectory

The viscosity of the mould powders and the corresponding break point (or solidification point) was measured by the supplier using a viscometer (rotating cylinder method) with a Pt crucible and cylinder and a cooling rate of 10 °C/min [11,12]. Results are given in Table 3.3. Occasionally, measurements were done at Tata Steel IJmuiden, using a rotating cylinder viscometer with a crucible and cylinder made from graphite.
The viscosity is considered a characteristic value of the mould slag and is related to slag infiltration i.e. mould powder consumption during casting. The break point or solidification point of a mould powder can be related to the mould heat transfer between the solidifying steel shell and the copper mould (horizontal heat transfer) and to mould friction during casting [13]. Usually, the viscosity of a mould slag is given at a temperature of 1300 °C.

Table 3.3: *Viscosity and break point, as measured by the supplier*

	Powder A
Viscosity at 1300 °C (Pa·s)	0.13
Break point (solidification point) (°C)	1167

The melting trajectories of the mould powders were measured at Tata Steel IJmuiden using a hot stage microscope (DIN 51730). The powder is pressed in the form a cylinder and the changes in the shape of the sample are monitored continuously. Shapes corresponding to softening, melting (hemispherical) and fluidity are specified and the corresponding temperatures are recorded. An illustration is given in Figure 3.5. Results of powder A are given in Table 3.4.

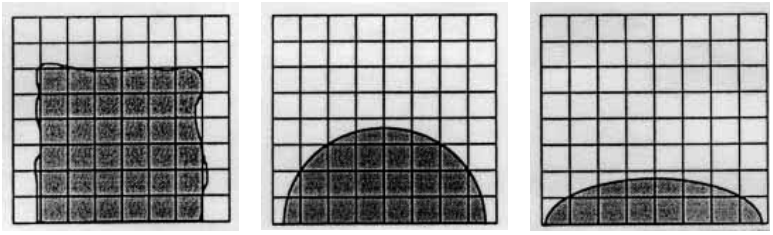

Figure 3.5: *Softening, melting and fluidity point (DIN 51730)*

Table 3.4: *Melting trajectory*

	Powder A
Softening temperature (°C)	1066
Melting temperature (°C)	1088
Fluidity temperature (°C)	1112

3.6 Microscopy and thermal analyses

Reflected light microscopy was applied to investigate mould powder granules, in particular the free carbon sources and other raw materials. Besides, optical microscopy was used for the analyses of slag rims and slag films. The analyses were completed by using scanning electron microscopy with energy dispersive X-ray spectroscopy (SEM/EDS; X-ray microanalysis). Occasionally, differential thermal analysis (DTA) was used to obtain additional information on the melting behaviour of mould powders and the solidification of mould slag [14]. Results were used supplementary to the data on high temperature phase relations and the viscosity measurements.

3.7 Concluding remarks

From the beginning of the project, characterisation of mould powder and mould slag played an important role to understand powder melting and slag solidification. In addition to conventional characterisation methods, mineralogical characterisation proved to be

essential for a further understanding of mould powder behaviour and mould powder functions.

Results of the techniques, in particular quantitative phase analyses (Rietveld-XRD) and high temperature phase relations (HT-XRD) together with the relevance with respect to continuous casting, have been presented during various seminars [15,16] and conferences [17,18]. Several of these contributions were published in international journals.
As a next step, the techniques have been used to support mould powder characterisation and mould powder design for all casting speeds. This includes round billet casting, conventional slab casting and high speed thin slab casting [19,20].

3.8 References

[1] K.C. Mills, A. Olusanya, R. Brooks, R. Morrell and S. Bagha, Physical properties of casting powders: Part 4 Physical properties relevant to fluid and thermal flow. Ironmaking and Steelmaking, 15 (1988) 257-264.

[2] R.V. Branion, D.A. Dukelow, G.D. Lawson, J. Schade, M. Schmidt and H.T. Tsai, Standardized testing of mold powder properties. Proc. 78th Steelmaking Conf., 2-5 April 1995, Nashville, USA, Iron and Steel Society, Warrendale, USA, 1995, 647-653.

[3] S.A. Howard and K.D. Preston in 'Modern Powder Diffraction; Reviews in Mineralogy Vol. 20.' (D.L. Bish and J.E. Post eds.), Profile fitting of powder diffraction patterns, The Mineralogical Society of America, Washington, USA, 1989, 217-272.

[4] A.F. Gualtieri, A. Guagliardi and A. Iseppi in 'Diffraction Analysis of the microstructure of materials' (E.J. Mittemeijer and P. Scardi eds.), The quantitative determination of the crystalline and the amorphous content by the Rietveld method: Application to glass ceramics with different absorption coefficients, Springer-Verlag, Berlin-Heidelberg, Germany, 2004, 147-163.

[5] S. Melzer, M. Gottschalk, M. Andrut and W. Heinrich, Crystal chemistry of K-richterite-richterite-tremolite solid solutions: a SEM, EMP, XRD, HRTEM and IR study, Eur. J. Mineral., 12 (2000) 273-291.

[6] N.V.Y. Scarlett, I.C. Madsen, M.I. Pownceby and A.N. Christensen, *In situ* X-ray diffraction analysis of iron ore sinter phases. J. Appl. Cryst., 37 (2004) 362-368.

[7] J.C. van Dyk, S. Melzer and A. Sobiecki, Mineral matter transformation during Sasol-Lurgi fixed bed dry bottom gasification – utilization of HT-XRD and FactSage modelling. Mineral Eng., 19 (2006) 1126-1135.

[8] K. Nagata and H. Fukuyama, Physicochemical properties of $3CaO\text{-}SiO_2\text{-}CaF_2$-NaF slag system as a mold flux of continuous casting. Steel Research Int., 74 (2003) 31-35.

[9] M. Dapiaggi, G. Artiolo, C. Righi and R. Carli, High temperature reactions in mold flux slags: Kinetic versus composition control. Journal of Non-Crystalline Solids, 353 (2007) 2852-2860.

[10] R. Carli, C. Righi and M. Dapiaggi, Melting process of mould fluxes: in situ investigation. Proc. 8th Int. Conf. on Molten Slags, Fluxes and Salts (MOLTEN2009), 18-21 January 2009, Santiago, Chile, GECAMIN Ltd., Santiago, Chile, 2009, 1121-1128.

[11] S. Seetharaman, K. Mukai and D. Sichen, Viscosities of slags – an overview. Steel Research Int., 76 (2005) 267-278.

[12] M. Persson, M. Görnerup and S. Seetharaman, Viscosity measurements of some mould flux slags. ISIJ Int., 47 (2007) 1533-1540.

[13] T. Watanabe, T. Matsushita and S. Seetharaman, “Break points” with respect to mold flux. Proc. 4th Int. Congress on the Science and Technology of Steelmaking (ICS 2008), 6-8 October 2008, Gifu, Japan, The Iron and Steel Institute of Japan, Tokyo, Japan, 2008, 710-713.

[14] R-H. Gronebaum und J. Pischke, Untersuchungen an Gießpulvern mittels der thermischen Analyse, Stahl u. Eisen, 127 (2007) No.11, 51-58.

[15] J.A. Kromhout, S. Melzer, E.W. Zinngrebe, A.A. Kamperman and R. Boom, Mould powder requirements for high-speed casting. Proc. 2006 Int. Symposium on Thin Slab Casting and Rolling (TSCR2006), 11-13 April 2006, Guangzhou, China, The Chinese Society for Metals, Beijing, China, 2006, 306-313.

[16] J.A. Kromhout, S. Melzer, D. Benne and R. Boom, Mould fluxes for thin slab casting at high speeds. Proc. 2nd CSM – VDEh – Seminar on Metallurgical Fundamentals, 18-19 June 2007, Düsseldorf, Germany, Stahlinstitut VDEh, Düsseldorf, Germany, 2007, 279-288.

[17] M.C.M Cornelissen, J.A. Kromhout, A.A. Kamperman, M. Kick and F. Mensonides, High productivity and technological developments at the Corus DSP thin slab caster. Proc. 5th Eur. Continuous Casting Conf., 20-22 June 2005, Nice, France, La Rev. Métall., Paris, France, 2005, Volume 1, 322-328.

[18] J.A. Kromhout, C. Liebske, S. Melzer, A.A. Kamperman and R. Boom, Mould powder investigations for high-speed casting. Proc. 6th Eur. Conf. on Continuous Casting, 3-6 June 2008, Riccione, Italy, Associazione Italiana di Metallurgia, Milano, Italy, 2008, 76.pdf.

[19] Y. Tsukaguchi, M. Hanao, M. Kawamoto, C. Liebske and J.A. Kromhout, Melilite Crystallization of High Basicity and High Viscosity Mold Flux. CAMP-ISIJ, 21 (2008) 826-829.

[20] J.A. Kromhout, M. Kawamoto, M. Hanao, Y. Tsukaguchi, E.R. Dekker and R. Boom, Development of mould flux for high speed thin slab casting. Proc. 13th VDEh – ISIJ – Seminar, 19-20 November 2008, Münster, Germany, Stahlinstitut VDEh, Düsseldorf, Germany, 2008, 203-210.

4 Melting of mould powders

4.1 Introduction

When mould powder is added to the surface of the liquid steel it melts and forms a slag layer. Powder melting is affected by both the powder properties and the heat transfer between the liquid steel and mould powder. This is also known as the vertical heat flux. An illustration of parameters affecting powder melting is given by Mills, Figure 4.1 [1].

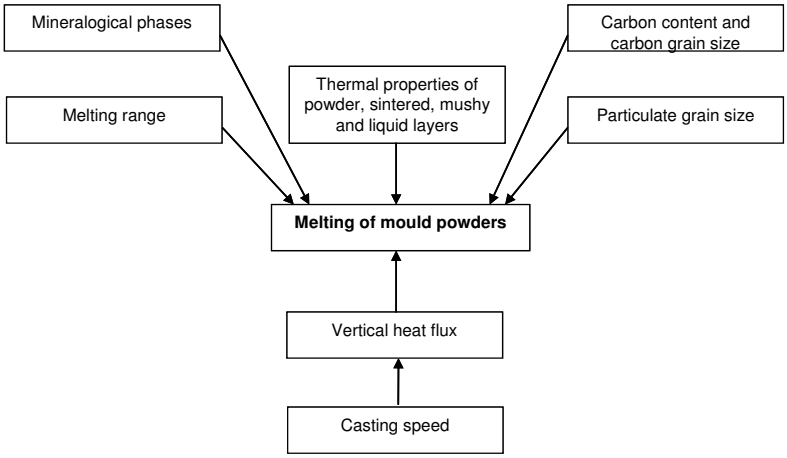

Figure 4.1: *Schematic illustration showing the factors affecting powder melting [1]*

In Section 4.2, a review is given on the mechanism and effects of powder melting. Experimental results are described in Sections 4.3 to 4.8, followed by concluding remarks in Section 4.9.

4.2 Mechanisms and effects of powder melting

4.2.1 Free carbon and carbonates

As described above, free carbon is used to control the melting rate of a mould powder. Complete melting is only possible after combustion of the free carbon particles [2].

CSM in Italy formulated a general relationship in which the melting rate of a mould powder is described as a function of the free carbon content [3]. The melting rate is given in milligrams powder melting per second at 1400 °C, using the same powder volume and without compacting:

$$M_r = 138.57(\%C_{free})^{-1.0669} \qquad (4.1)$$

where M_r = melting rate (mg/s) and C_{free} = amount of free carbon in the mould powder (wt%).

The equation is based on the results of approximately 70 mould powders for slab and billet casting, including some powders for thin slab casting. The obtained values are not absolute and the equation does not consider the several types of free carbon. However, a good indication of the effect of free carbon on mould powder melting rate can be obtained, Figure 4.2.

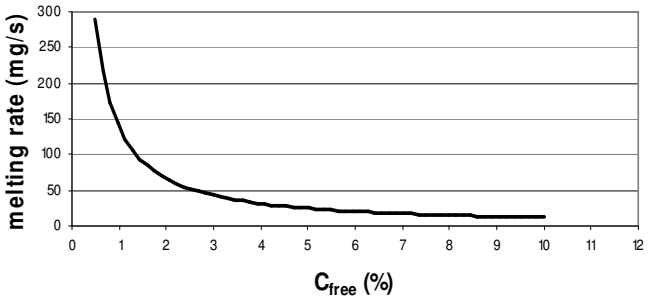

Figure 4.2: *Melting rate of mould powder as a function of the free carbon content [3]*

Work done by Kim et al. describes the effects of fine carbon particles (carbon black) and coarse particles (coke) on powder melting [4]. They found that a free carbon source has a minimum or critical content and a maximum content. Above the maximum content, there will be no effect on the melting rate. The effectiveness of free carbon is described in terms of the particle size, the combustion rate and the *covering intensity*. A high free carbon content or smaller carbon particles will result in lower melting rates due to the strong coverage of carbon on the solid powder and finally on the liquid slag droplets. The covering intensity of the free carbon is a dominant factor in powder melting.

Chinese researchers investigated the role of several free carbon sources like graphite and carbon black on the melting rate of mould powder. The effect of the fine carbon black is much higher than that of graphite [5]. During casting, a stable slag layer is required which is able to supply sufficient mould slag. More "flexible" powder melting is realised by using a mix of fine and coarse free carbon materials; this will result in a smoother combustion and increased flexibility. Furthermore, it was found that the presence of graphite enhances the formation of a multi layer structure (>2 layers) i.e. the presence of one or two intermediate layers. In contrast, the use of carbon black can result in the formation of only two layers; the slag layer and the powder layer. The presence of the intermediate layers is associated with the *formation of rims* during casting.
Recently, work was presented focussing on the effect of the relative amounts of *amorphous* and *crystalline* structures present in the free carbon sources. It was found that mould powders with a higher content of amorphous free carbon will show lower combustion activation energy and a higher melting rate, compared to mould powders with more crystalline carbon sources. This study was done using four types of graphite and two kinds of coke. In particular, coke contains a significant amount of amorphous carbon (approximately 20 wt% in this study). Unfortunately, no work was done on the amorphous carbon black which is widely used as a free carbon source [6].

An in depth study by Schürmann describes the formation of gaseous CO and CO_2 during melting of powders containing carbon black and graphite [7]. The presence of carbonates such as Na_2CO_3 in the mould powder will significantly increase the formation of CO_2 during heating. Furthermore, CO will be formed as described by the Boudouard reaction:

$$C + CO_2 \rightarrow 2CO$$

The gas atmosphere in the powder bed and the presence of carbon in the mould powder will result in the *reduction* of Fe^{3+} (i.e. Fe_2O_3, coming from the mould powder raw materials) to Fe. The reaction steps are described via the successive formation of Fe_3O_4, FeO and Fe. Given the use of Na_2CO_3 as raw material, Na_2O will be reduced too, resulting in the formation of *metallic* sodium. The last two findings are of special interest and like most of this work, are based on heating experiments and analyses of the *gaseous* components. No mould slag analyses after these experiments aiming to investigate the presence of Fe and Na components were carried out.

Schwerdtfeger continued this work using so-called isothermal heating experiments on commercial mould powders and five corresponding free carbon sources [8, 9]. The influence of carbonates on the carbon combustion and the effects of granulated materials were also investigated. The free carbon sources were two different grades of carbon black (particle sizes <1 µm and around 40 µm), coke dust (particle size around 90 µm), graphite (particle size around 40 µm) and fly ash (particle size around 120 µm). This is one of the few publications with detailed information on the relevance of the free carbon sources [9]. Two reactions mechanisms are described in this work:

- At lower temperatures (around 400 °C and lower), the combustion is controlled by the *chemical reactions*. The main overall reaction for the combustion is:

  $$C + O_2 \rightarrow CO_2$$

  The effect of the *type* of free carbon on the combustion rate is significant. The two grades of fine carbon black show a fast combustion rate, the fly ash shows a slower combustion and the coke dust and graphite a much lower rate. The reaction surface (specific surface) and the reaction rate constants (k) are important parameters in this temperature domain.
- At temperatures above 500 °C the combustion rate of free carbon is determined by the *gas transport* in the powder bed (pore diffusion) as well as the gas transport above the powder bed (gaseous diffusion). The combustion at these temperatures is the Boudouard reaction:

  $$C + CO_2 \rightarrow 2CO$$

  The resulting carbon monoxide diffuses upwards and reacts according to:

  $$2CO + O_2 \rightarrow 2CO_2$$

- Between the two temperature domains, the combustion kinetics are controlled both by chemical reactions and by mass transport (mixed control).

Starting around 500 °C the dissociation reactions of the carbonates (raw materials) will play an important role as well. Another effect is the granulation of mould powder.

Granulated material gives a higher reaction rate, possibly due to a better distribution of the carbonates within the granules and consequently more effective stirring of gas. All these findings show that melting of mould powder is a complex process with several simultaneous and subsequent reactions. Very interesting results are the reduction of Fe_2O_3 (from the mould powder raw materials) to FeO or Fe at temperatures ranging *between 600 °C and 700 °C*.

The distribution of the temperature and free carbon in the upper part of the flux layers was investigated experimentally, using a column (quartz tube) filled with powder and via calculations [10]. For the experiments, a so-called pre-molten mould powder was selected (i.e. containing no carbonates or other volatiles) and one grade of free carbon (5 mass% graphite). The quartz tube was filled with the mould powder and heated via the bottom to temperatures between 850 °C and 950 °C. The temperature at the surface of the upper part of the powder bed was between 100 °C and 200 °C.

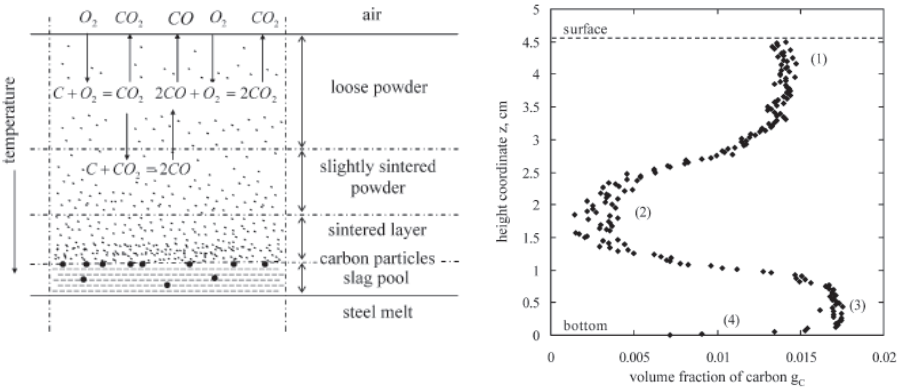

Figure 4.3: *Schematic illustration of mould powder layers and carbon combustion reactions in the mould (left); Carbon profile analysed by image analysis method (right) [10]*

Two reactions are proposed for the carbon combustion. At a depth where the temperature is high enough, carbon reacts with oxygen to form carbon dioxide. At deeper levels, all the oxygen will be consumed forming carbon dioxide. Some of the carbon dioxide diffuses towards the bottom layers where the temperature is high enough for the Boudouard reaction. The carbon monoxide diffuses upwards and partly combusts with oxygen. A mixture of carbon dioxide and carbon monoxide leaves the power bed.
As shown in Figure 4.3, two minima of carbon can be found: one in the region of moderate temperatures (~500 °C), caused by the combustion with oxygen and one in the region of the elevated temperatures (>750 °C) due to combustion with carbon dioxide. An important observation is that some residual carbon may still be present at the bottom of the bed and will enter into the slag pool. This may cause *carbon pick-up* by the steel and will be discussed later. A schematic illustration of the mould powder layers in the mould and the carbon combustion reactions as well as a measured carbon profile after an experiment are given in Figure 4.3.

Sumitomo describes the process of powder melting in terms of the melting point, the bulk density, the use of carbonates and the amount of free carbon [11]. An important

conclusion is that the melting rate of a mould powder increases as carbonate content increases. This is due to an increase in thermal conductivity of the powder bed, owing to stirring of gases formed through dissociation of carbonates:

$$M_xCO_3 + C \rightarrow M_xO + 2CO$$

$$M_xCO_3 \rightarrow M_xO + CO_2$$

With M = Li, Na, K, Mg, Ca, Ba. The use of $MgCO_3$ and Li_2CO_3 resulted in the highest melting rate, followed by $CaCO_3$, Na_2CO_3 and $BaCO_3$. Furthermore, the melting rate increases as the free carbon content or bulk density decreases with fine carbon black being more effective than coarse particles of coke. Based on this work, the melting rate of a mould powder can be expressed as:

$$M_r = 16.8\Sigma k^*(\%carbonate) - 0.00336C_v + 0.0477 \qquad (4.2)$$

where M_r = melting rate (mm/s), k^* = reaction rate constant based on carbonate content and C_v = carbon content per unit volume (kg/m^3). Note that it is assumed that there is no interaction between the carbonates and the mould slag.

4.2.2 Carbon pick-up

Steel grades with a very low carbon level such as ultra low carbon (ULC) grades are prone to carbon pick-up during the production route. There are several sources for recarburisation in the steelplant such as refractory materials, tundish covering materials and mould powders. Sources for carbon pick-up in the mould are mould powders and to a lesser degree the stopper and SEN [12]. The main mechanisms of carbon pick-up by mould powder are based on contact of steel with:

- the carbon enriched layer, located between the sinter layer and the molten slag
- the mould powder layer
- the slag rims, which can be enriched with carbon.

Carbon pick-up due to the presence of a carbon-enriched layer can result in a local zone of carbon-rich steel with a low melting point. This can even result in a sticker and a breakout during casting due to the different solidification behaviour of the steel [13,14].
Reduction of the amount of free carbon in the mould powder is an effective way to reduce carbon pick-up during casting [14,15,16]. ULC and IF-grades are cast with mould powders containing (very) low values of free carbon, mostly easily combustible grades like carbon black. Even the use of powders with no free carbon is reported but it should be noted that the use of a granulated material *automatically* results in a free carbon content of approximately 0.5 wt% due to the use of an organic binder.

Several authors report a carbon pick-up in the mould of 4 ppm or less, based on stable process operations and during casting the first ladle (at least after casting 30 - 35 meters) [16]. A further decrease in carbon pick-up can be realised with the use of alternatives for free carbon like nitrides such as Si_3N_4 or BN [17]. Most of these materials proved to be sensitive to sintering and to rim formation and are not widely used.
Other effective ways to reduce carbon pick-up in the mould are to minimise the mould level fluctuations and waves during casting and to maintain a sufficiently thick slag layer. The use of MnO as an extra oxygen source for carbon combustion in the several flux layers

is mentioned [15]. As will be discussed later, the presence of MnO may affect slag properties such as heat transfer.

4.2.3 Alternatives for free carbon

In order to decrease carbon pick-up (ULC grades), alternatives for free carbon have been investigated. In previous work, the possibilities of materials like BN are mentioned [7,15]. Significant work was done at Irsid and Sollac, supported by a mould powder supplier [17]. Based on melting and wetting experiments, the materials SiC, Si_3N_4 and BN were selected; BN was found too expensive and the research continued with SiC and Si_3N_4. Mould powders were developed and tested on laboratory scale, followed by plant trials at Sollac Dunkerque. The developed mould powder typically contained 0.6 wt% C_{free} (carbon black) and 0.35 wt% Si_3N_4; the reference material contained 1.8 wt% C_{free}. The developed powder proved to be equivalent to the standard mould powder with respect to powder melting, powder consumption and strand lubrication. The main advantage was a significant reduction of carbon pick-up during casting (approximately 5 ppm).

This work was continued by an American supplier of mould powder [18,19]. Several kinds of colour imparting materials (organic, organometallic and inorganic pigments, colorants and dyes) were suggested as alternatives for free carbon. The very small particle size of these materials made it possible to realise an effective cover. Furthermore, some of these colorants have a relatively high melting point or high decomposition temperature. This work resulted in so-called *colour coded mould powders*; where it is possible to select a specific colour for a mould powder.
During testing in the laboratory, the mould powder properties were largely comparable to the reference materials; although some differences in powder melting and heat transfer were reported. The developed powders were also tested on both conventional and thin slab casters. Results showed a reduction of carbon pick up during casting and a reduction of rim formation i.e. slag rims *associated* with free carbon and a carbon enriched layer. Note that this last point is due to a different sintering behaviour and more specifically, the absence of a carbon enriched layer. Up to now, these colour coded mould powders have not been widely used.

4.2.4 Inorganic components of mould powder

In particular, additions of sodium will result in a significant decrease of the melting point (and melting range) of the mould slag. Additions of fluorine hardly show a decrease of the melting point. Alumina (Al_2O_3) will give a significant increase (i.e. more than 10 °C per wt% Al_2O_3) of the melting point, especially with additions of 5 wt% or more [20].
Extensive work on the inorganic constituents has been done by Hiromoto and co-workers [21]. Based on raw materials like portland cement, natrite, fluorite and cryolite, several powders were prepared, each with a different chemical composition. Powder samples were heated for ten minutes at temperatures ranging from 500 °C to 1000 °C. Subsequently, the samples were quenched and characterised using room temperature X-ray diffraction. It was shown that the (crystalline) raw materials disappear during heating and that new crystalline constituents like cuspidine and combeite are formed, prior to melting. The work is based on batch experiments and only the relative increase or decrease of each mineral is given. However, this paper gives some insight into the reactions that take place during heating.
Grieveson et al describe the changes in phase compositions of mould powders during heating as well. The presence of secondary phases like cuspidine and combeite are reported; their occurrence is related to the annealing temperature and the powder

composition. Again, this work is based on batch experiments at fixed temperatures. Powder samples were annealed (sometimes for hours) and quenched, before XRD-analyses were performed [22].
Heating experiments at TU Clausthal, Germany investigated the effects of free carbon, carbonates and pre-fused raw materials on the melting behaviour of mould powders. Surprisingly, mould powders containing pre-fused materials showed *unstable* melting. Based on all the results, the authors suggest that during heating, several *unknown reactions* between the mould powder components could occur. Furthermore they concluded that due to the numerous process parameters, it will be very difficult to predict the performance of mould powders during casting [23].

Recently, the melting behaviour of some commercial mould powders was investigated using laboratory techniques like room-temperature XRD, optical microscopy, scanning electron microscopy and X-ray microanalysis. As before, the studies are based on quench experiments and describe the melting of the individual raw materials followed by the formation of intermediate phases like cuspidine and several silicates. Complete melting occurs between 1040 °C and 1270 °C. Two reactions are proposed for the formation of cuspidine: a solid-state reaction at lower temperatures (around 600 °C) and solid-liquid reactions at higher temperatures (900 °C -1200 °C) [24].

4.2.5 Rim formation

Rims composed of mould powder, mould slag and sintered products can adhere to the mould walls. Usually, slag rims are small (nearly visible during casting) and play a role in the infiltration of mould slag. However, rims can grow and disturb the casting process. In Chapter 2, two mechanisms for the formation of slag rims are addressed; both are associated with powder melting and meniscus fluctuations.

The painting mechanism as used to describe slag infiltration is also suggested as a mechanism for rim formation [25]. During the upward movement of the mould, the bottom part of the rim is coated by liquid and solid powder. During the downward motion, this layer will (partially) melt.
Rim samples were investigated in order to study this mechanism. However, almost all rims were obtained during or after casting steel grades with an increased [Mn], [Si] or [Al] content. Such casts show interfacial reactions and a significant change in the slag composition and slag viscosity, these have a considerable effect on the formation of rims [26]. Other experiences with casting high Al-steels (Al-TRIP) show that mould slag with an increased viscosity (due to interfacial reactions between steel and slag) will be very sensitive to the formation of rims [27].

An effect of the steel temperature (measured in the tundish) on rim formation is also suggested; a lower steel temperature could result in a bigger rim [28]. Furthermore, the powder supplier Kempro stated that a mould powder with a relatively *low melting point* is less sensitive to rim formation; the rim can melt again [29]. A low melting point is also mentioned by Emling in the overview on breakout prevention [30]. Based on experiences with stainless steel, it is suggested that the use of high basicity mould slags can result in more rim formation during casting [31].

There are only a few publications that describe slag rims and their effects during casting in more detail. Emi mentions that slag rims are not very well attached to the mould wall and can even float on the mould slag and/or molten steel. Slag rims can *obstruct* the

infiltration of mould slag during casting, which can cause breakouts [32]. Based on this work, the formation of rims is promoted by:

- inadequate melting behaviour of the mould powder
- a low surface temperature of the steel
- mould level fluctuations at the steel meniscus.

Mukai and Mills both suggest that carbonaceous agglomerates can block the flow of molten slag into the mould/strand gap. Furthermore, it is assumed that agglomerates arise from large amounts of Al_2O_3 or TiN which are not absorbed by the pool and collisions caused by metal flow turbulences causing agglomeration of these particles [13,14]. Big slag rims can also cause a notch and consequently a rupture in the solidified shell causing a weak spot in the shell [30].

Mahapatra and co-workers mention that the surface temperature of the mould copper plates in the meniscus region (hot face temperature) affects the formation of slag rims. A decreased hot face temperature, for instance due to thinner mould plates, was found to be more sensitive to rim formation. Furthermore, slag rims will act as an insulator and the presence of slag rims can have local effects on for example heat transfer, shell formation, the shape of the oscillation marks and the slag viscosity. The underlying mechanisms are very complex and are not fully understood [33]. Besides, it was concluded that a low melting point (melting trajectory) of the mould powder is preferred in order to reduce the formation of rims [34].
At the narrow face of the mould of a stainless steel caster, the temperatures in the meniscus region were measured using twelve thermocouples, placed in two rows. It was found that the presence of a slag rim results in lower thermocouple temperatures and in a decreased local mould heat transfer which will have an effect on the steel shell formation. For a controlled solidification process, the size of the slag rim should be as stable as possible [31].

4.2.6 Measurements on powder melting

There are several methods for measuring the melting rate of mould powders. The tests are generally based on laboratory scale; crucible and molten slag drip tests being commonly applied [1,6]. Tests involving melting of powder on a steel surface have also been reported [11]. The methods can give qualitative and reproducible data but they do not simulate the real casting process with a constant melting of mould powder and continuous consumption of mould slag. Although the melting rate of a mould powder is an important parameter, this property is not measured regularly and no standardised assessment method exists [35].

A general expression on powder melting and the corresponding slag layer thickness during casting is defined as:

$$d = 0.02 S_r / abv_c Q_t \qquad (4.3)$$

where d = liquid pool depth (mm), S_r = vitrification ratio (wt%), a and b = mould dimensions (m), v_c = casting speed (m/min) and Q_t = powder consumption (kg/tonne). The relation is based on slab and bloom casters with casting speeds between 0.7 and 1.8 m/min [36]. The powder melting rate is expressed as vitrification ratio, to be obtained from laboratory tests. It was found that the melting rate is the dominant parameter with respect to the slag layer thickness and that addition of free carbon determines powder melting (vitrification) considerably. Together with the well known expression:

$$Q_s = 0.6/\eta v_c$$

the relation on the liquid pool depth was proposed as an important guideline for undisturbed casting, in particular with respect to strand lubrication [36,37].

A new laboratory method for testing the melting rate of mould powders was developed at KIMAB, Sweden [38]. The mould powder is poured into a graphite crucible with a bottom temperature of 1500 °C. The slag flows through an opening in the bottom of the crucible and the mould powder consumption is recorded and given in kg/m^2. The method fairly resembles the actual casting process.

KTH in Sweden presented several characterisation methods for powder melting, based on two commercial mould powders [39,40]. Differential Scanning Calorimetry (DSC) showed the combustion (exothermic peaks) of free carbon sources of carbon black, probably coke dust and graphite at temperatures around 580 °C, 700 °C and 790 °C, respectively. The decomposition of some carbonates (endothermic peaks) was detected as well. Melting of both powders starts around 1100 °C. Furthermore, the use of laboratory equipment for simulating heating and melting of a mould powder is described.

The double hot thermocouple technique (DHTT) was used by Cramb and co-workers for investigating melting and solidification phenomena of transparent slags [41]. The solid sample consists of glassy and crystalline phases; melting experiments were done with a heating rate of approximately 16 °C/s. As the temperature reaches the solidus, crystals started to dissolve and the sample became transparent. Surprisingly, bubbles were observed which may originate from carbonates or hydrate contamination. Both Marangoni flow and natural convection cause the movement of the bubbles. The movement of the bubbles is high due to a low slag viscosity (1400 °C). Furthermore, it was observed that the (intercrystalline) glass melts first, followed by breaking of the crystals. Marangoni flow or natural convection transported crystalline particles within the liquid. It was stated that melting will be determined by the fraction of solid and the chemistry of the liquid between the crystals. Melting will start as soon as the interdendritic liquid reaches a temperature where viscosity is such that fluid flow will initiate. There is no discrete melting temperature, rather a melting range. Melting of mould slag is complex and is dependent on the heat flux and the fluid flow conditions, locally in the sample.

4.2.7 Casting conditions

The temperature distribution within the powder, sinter and slag layers was measured by Litterscheidt using thermocouples, fitted in small quartz tubes [42]. This excellent work was done in the mould of a continuous caster, see Figure 4.4.
The surface of the powder layer shows temperatures between 100 °C and 150 °C. The lower part of the slag layer shows a rapid increase in temperature; the slag temperature at the meniscus is equal to the steel temperature. It was also found that feeding fresh (relatively cold) mould powder to the surface results in a significant *decrease* in temperature; this effect can be observed even in the sinterlayer and slag layer.
The findings on the temperature distribution are largely confirmed by measurements done at Nippon Steel Corporation [2].

The slag pool thickness varies with its position in the mould, a thicker slag layer will be found around the SEN and the thickness decreases in the direction of the narrow faces. It has been reported that a higher casting speed will result in a thicker slag layer due to the higher heat flux (increased melting) [1]. However, it should be noted that these findings are related to conventional casting processes and not to high speed thin slab casting.

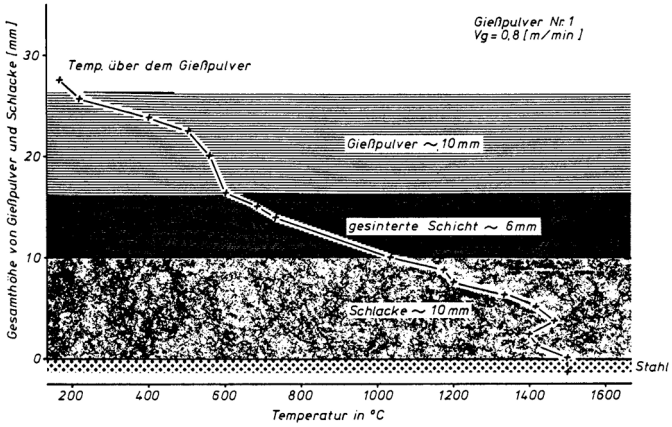

Figure 4.4: *Temperature distribution in powder layer, sinter layer and slag layer, measured in the mould of a caster [42]*

The melting process of mould powder was modelled using a heat balance [2]. It was found that the liquid pool depth stabilises at a certain value, some time after the addition of mould powder. During casting, mould powder melting is accelerated significantly by convection (steel) and molten steel surface oscillation in the mould. The liquid pool depth was calculated successfully with values ranging between 4 and 8 mm. Especially the conclusions regarding the effects of steel flow on powder melting and slag layer thicknesses were confirmed using extensive 3D-models and some plant trials at a slab caster [43]. It is also concluded that there is a recirculation of the (liquid) mould slag within the slag layer. The liquid steel will drag the slag towards the SEN and an opposing flow carries the upper layer of flux and powder in the opposite direction (to the narrow faces). A *coupled* 3D model, containing fluid flow and heat transfer phenomena was used to describe the formation of the powder and slag layers in a CSP mould at casting speeds of 4.5 and 6.0 m/min. Main findings are that the liquid pool depth is almost independent of the casting speed and that the liquid pool depth increases in the vicinity of the wide faces. These results were confirmed by plant measurements [44].

4.3 Effects of free carbon on powder melting

4.3.1 Operational experiences

During the first years of operation of the Direct Sheet Plant, several mould powders were used both with high and low basicity (CaO/SiO_2). Steel grades were mainly low carbon and HSLA. In Table 4.1 an overview is given of the chemical composition of the mould powders. Mould powders I and II have been used for prolonged periods as standard powders. The powders III to VI were only used for trial purposes. Mould powder VII is a conventional slab casting variant and serves as a reference material.
Mould powders III and IV are the same but originate from different batches and are closely related to mould powder I. Mould powder V is a further development of mould powder I with the aim to improve slag formation during casting. Finally, mould powder VI is designed to reduce the horizontal heat transfer especially in the meniscus area. With exception of mould powder II, all thin slab casting powders have a high basicity (CaO/SiO_2 > 1).

Table 4.1: *Chemical composition of mould powders for thin slab casting (I-VI) and reference material (VII) (wt%)*

	I standard	**II** standard	**III** trial	**IV** trial	**V** trial	**VI** trial	**VII** slab
CaO/SiO_2	1.3	1.0	1.3	1.3	1.3	1.2	0.8
SiO_2	25.3	33.4	27.2	26.7	26.0	30.3	32.8
CaO	33.1	32.7	34.4	34.0	34.3	34.7	26.5
MgO	3.7	0.4	3.7	3.4	3.6	3.7	1.2
Al_2O_3	3.9	3.2	3.8	3.7	3.9	2.9	5.1
Na_2O+K_2O	8.8	12.5	8.6	8.3	8.2	9.6	12.6
Li_2O	0.8	0	0.7	0.7	0.9	0.0	0.0
Fe_2O_3	0.6	0.5	0.3	0.3	0.4	0.8	1.6
F	9.9	7.7	10.5	10.0	11.5	5.9	9.1
C_{free}	6.7	4.0	5.9	5.6	5.4	5.0	4.4
CO_2	7.4	7.2	7.2	8.2	8.4	8.1	7.7
C_{total}	8.7	6.0	7.9	7.8	7.7	7.2	6.5
LOI (1000 °C)	*18.7*	*13.4*	*15.4*	*15.2*	*16.0*	*14.8*	*15.0*

The performance of each mould powder was evaluated using several operational criteria, including slag formation i.e. the liquid pool depth and rim and lump formation, uniformity and ratio of the heat transfer per side of the mould, friction and meniscus stability. The liquid pool depth was obtained by immersing a steel sheet into the mould. At the meniscus, the sheet melts and the liquid slag solidifies on the sheet. The operators observed the formation of rims and lumps. Friction of the strand was obtained by using the hydraulic oscillation system of the DSP. The meniscus stability was measured using a radiometric system. Mould heat transfer was calculated using mould cooling water temperatures.

In Table 4.2 an overview is given of the operational performance of the selected mould powders at the DSP. Casts with mould powder I were characterised by serious operational problems such as an unstable meniscus, a high mould friction, unstable heat transfer,

bridge formation and even breakouts. These problems were mainly initiated by insufficient powder melting/slag formation and infiltration i.e. too small liquid pool depth and excessive rim and lump formation. Minor changes were made (powder III) which successfully overcame these problems. For a longer trial, a new batch of this mould powder was ordered and tested at the DSP (powder IV). However, this time the powder behaved like mould powder I: excessive rim and lump formation causing serious operational problems and no slag formation. Differences between powder III and IV could not be explained using conventional tools (chemical analysis, viscosity and melting behaviour) and so *additional* characterisation methods based on optical microscopy were considered.
Mould powder V is a further improvement of powder I with the aim to improve slag formation during casting. This powder performed better than powders I and IV but still showed insufficient liquid pool depth. Furthermore, the colour of the mould slag was *black*, which indicates the presence of carbon in the liquid slag i.e. an insufficient combustion of the carbon particles during slag formation. Summarising, mould powders I and IV showed comparable operational problems that were closely related to insufficient powder melting and slag formation during casting. Mould powder V showed some improvements. Only powder III gave good operational results, but another batch of this powder (powder IV) did not show the required behaviour.

Table 4.2: *Mould powder performance at the DSP (mould powder I-VI)*

	I	**II**	**III**	**IV**	**V**	**VI**
CaO/SiO_2	*1.3*	*1.0*	*1.3*	*1.3*	*1.3*	*1.2*
C_{free} *(wt%)*	*6.7*	*4.0*	*5.9*	*5.6*	*5.4*	*5.0*
Liquid pool depth	1-2 mm	4-8 mm	6-8 mm	0 mm	2-5 mm* *black*	4-20 mm
Rim/lump formation	excessive	negligible	negligible	excessive	negligible	negligible
Meniscus stability	unstable	stable	stable	unstable	stable	stable
Friction	high	low	-	high	medium	medium
Heat transfer uniformity	bad	good	-	bad	good	good
Heat flux ratio**	70-80%	90-100%	-	70-80%	65-80%	90-100%

* liquid pool depth powder V: the slag was black coloured, indicating the presence of carbon i.e. insufficient carbon combustion and powder melting

** heat flux ratio: heat flux narrow face/average heat flux broad faces; the heat flux calculations are based on the increase of mould cooling water temperatures per side

On the other hand, mould powder II was successfully used over a very long period. In this period the average casting speed increased to 5.0 m/min, with an increasing casting time from 3 to 8 hours using the same refractory material of the submerged entry nozzle (SEN) and the same mould level control system. From these experiences it can be concluded that a liquid pool depth $\geq$5 mm is sufficient. However, occasionally lower values were measured during longer periods of casting without operational problems.

Mould powder VI is designed to reduce the horizontal heat transfer. The powder has been used supplementary to mould powder II. With mould powder VI several successful trials were performed and it is considered to be a good alternative for casting crack sensitive steel grades. However, all low alloyed steel grades can be cast with mould powder II and currently, there is no requirement for mould powder VI.

Based on the operational practice for casting low carbon and HSLA grades, slag samples showed no significant changes in composition (i.e. Al_2O_3, CaO and SiO_2 contents). During casts with various mould powders, it became clear that the mould slag basicity is not a key parameter in the observed in-mould behaviour.

No evidence has been found of strand bulging during all these experiments. As will be described in Chapter 7, powders with an increased basicity (CaO/SiO_2) show a redistribution of local mould heat transfer during casting; the total mould heat transfer and hence the shell thickness at mould exit being roughly the same [45]. Furthermore, it should be noted that mould powder VI having a basicity of 1.2, showed excellent casting performance. In a previous study, it has been demonstrated that mould powders with an increased basicity i.e. mild cooling behaviour will not affect the shell thickness at mould exit [46].

4.3.2 Mould powder characterisation

Physical characterisation plays an important role in the selection procedure and the operational evaluation. In general, the chemical composition, the viscosity including the start of solidification or break point and the melting behaviour are considered. This information proved insufficient to understand the slag formation process, which is critical in thin slab casting. Therefore, optical microscopy and X-ray diffraction were used as additional characterisation methods with the aim to focus on the composition and especially on the free carbon sources of the mould powders

Viscosity

The viscosity of a mould slag influences the infiltration of mould flux during casting. In general, infiltration increases with a decreased viscosity of the mould slag for the same operational conditions and this tendency is used for thin slab casting. Other demands like the control of slag entrapment also play an important role when defining the operational windows or required viscosity of a mould powder. The viscosity and break point of the two standard powders (I and II) and the reference material (VII) were determined using the rotating cylinder method with a *graphite* crucible and cylinder. Results are shown in Table 4.3.

Table 4.3: *Viscosity (Pa·s) and break point (°C) (mould powder I, II and VII*

t (°C)	I	II	VII
1350	0.09	0.15	0.18
1300	**0.11**	**0.17**	**0.21**
1250	0.12	0.22	0.27
1200	0.13	0.28	0.37
1150	0.17	0.38	0.51
1100	2.45	0.54	0.77
T_{break} (°C)	**1133**	**1106**	**1078**

The measured viscosity at 1300 °C and the break point are considered to be characteristic values.

Melting behaviour

The melting behaviour of a mould powder strongly influences both the liquid pool depth and the sensitivity towards rim and lump formation. The melting behaviour can be described by the melting trajectory and in particular by the melting rate. Additions of free carbon (C_{free}) are considered to be a principal factor [1,4]; the other main parameters for powder melting are the flow conditions in the mould. The liquid pool depth results from the balanced values of the feeding and the infiltration of the mould powder.

The melting trajectory of the mould powders was determined using a hot stage microscope. Results are given as values for the softening, the melting and the flow or fluidity temperature, Table 4.4. It is noted that the values of the break points roughly agree with the melting points (mould powders I, II and VII).

Table 4.4: *Melting trajectory (mould powder I-VII)*

	I	II	III	IV	V	VI	VII
Softening temperature (°C)	930	918	874	827	913	1068	1010
Melting temperature (°C)	1120	1110	1040	1005	1014	1169	1068
Fluidity temperature (°C)	1163	1126	1185	1134	1054	1169	1090

Melting rate

The melting rate of mould powders was determined using the so-called softening method. This method was developed at Hoogovens R&D, IJmuiden (now Tata Steel RD&T) in the late 1990s. With this method, the displacement of a prepressed cylinder of mould powder is measured as a function of time at a fixed temperature (1400 °C). A displacement of 20% is considered as a characteristic value [47]. The method yields qualitative results that can be related to the mould powder composition, in particular the free carbon content of a mould powder. Results of the various mould powders are given in Figure 4.5 and summarised in Table 4.5.

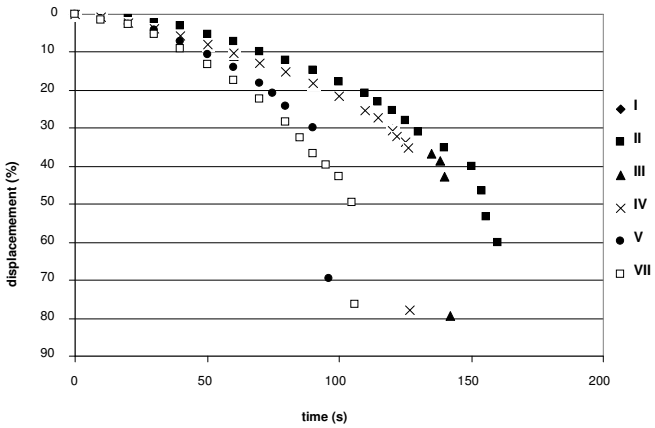

Figure 4.5: *Melting rate (displacement vs. time) (mould powder I-V and VII)*

Table 4.5: *Melting rate (displacement vs. time) (mould powder I-V and VII)*

Displacement (%)	I	II	III	IV	V	VII
10	-	70	57	60	49	41
20	-	117	95	95	74	65
40	-	150	139	126	85	95
60	-	160	141	127	90	105
C_{free} (wt%)	6.7	4.0	5.9	5.6	5.4	4.4

Mould powder I did not show any softening and melting during heating in the furnace i.e. hardly any slag was formed and no displacement was measured. Instead, the mould powder sintered and no results could be obtained. No results are available for mould powder VI. Note that mould powder VII, applied in conventional slab casting, shows a higher melting rate whereas almost all other (thin slab casting) mould powders show a lower melting rate. This confirms previous findings of the author where it was concluded that the melting rate of thin slab casting mould powders is generally between the melting rate for slab casting and billet casting powders [47].

Optical microscopy

Based on casting experience at the DSP and the subsequent characterisation of the mould powders using the conventional methods, the observed melting behaviour and the slag formation *could not* be explained. For these reasons other methods were needed which could give more insight into the mould powder composition. Main points of interest were the choice of carbon sources (free carbon) and the distribution of free carbon particles within the granules. The mould powders were investigated using reflected light microscopy, Table 4.6 and Table 4.7. A general review of carbon powders and graphite including some applications in mould powders can be found elsewhere [9,48].

Table 4.6: *Carbon sources (free carbon) in mould powder granules*

	I	II	III	IV	V	VI	VII
Graphite	+	0	+*	+*	0	0	0
Coke (fine)	+	0	+	+	+	+	+
Coke (metallurgical, recycled)	+	0	+	+	+	0	+
Carbon black (lumps)	+	0	+	+	0	0	0
Carbon black (fine)	+	+	+**	+**	+	+	+**

+: present +*: traces +**: probably present 0: not present

Table 4.7: *Distribution of carbon particles (free carbon) in mould powder granules*

	I	II	III	IV	V	VI	VII
Distribution	very poor	good	poor	very poor	poor	good	poor

The results were compared with the in-mould behaviour of each individual mould powder. To support the optical examinations, X-ray diffraction analysis of the mould powders was performed. The investigations revealed that for some mould powders up to five carbon sources are used and that in nearly all cases the distribution of the carbon particles within

the granules is poor or very poor. Only powders II and VI showed an even distribution of carbon particles based on carbon black, which in general combusts easier than graphite or coke. In mould powder VI, a minor supplement of one grade of fine coke is present. An illustration of two mould powders is given in Figure 4.6 and Figure 4.7.

Surprisingly, mould powders II and VI clearly showed stable slag formation during casting. With a poor carbon distribution the requirements for the in-mould behaviour could not be met. The relatively high combustion rate of carbon black also may enhance a uniform slag formation. It became clear that it is very difficult to achieve a uniform carbon distribution when two or more carbon sources are used. The application of *one fine grade of carbon black*, possibly supplemented with one grade of fine coke is therefore recommended.

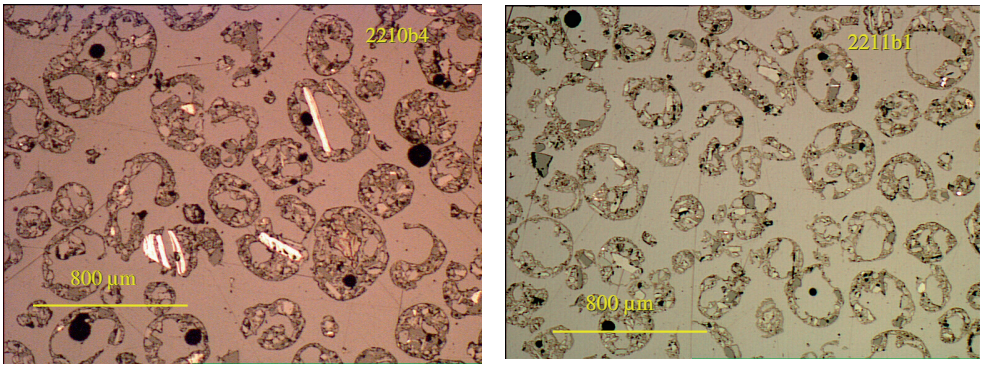

Figure 4.6: *Mould powder I (left) and II (right). Mould powder II showing a good carbon distribution*

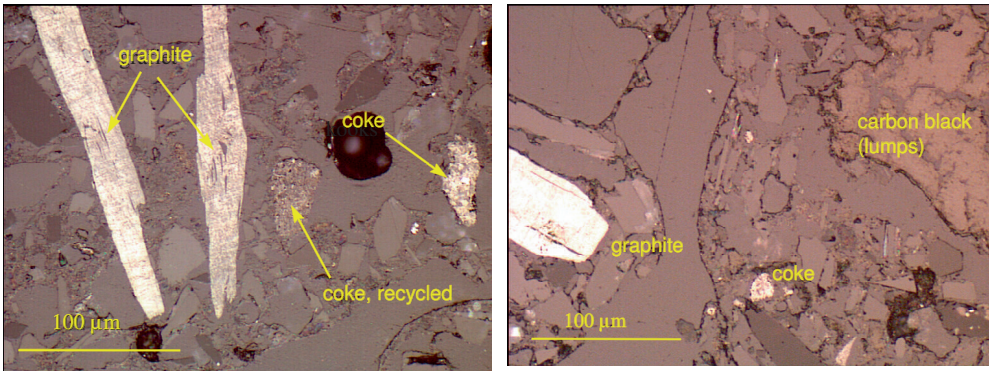

Figure 4.7: *Details of mould powder I, showing various free carbon sources and a poor carbon distribution within the granules*

X-ray diffraction

To support the optical examinations, X-ray diffraction (room temperature) was performed giving information about the choice of raw materials. Based on the intensities of the XRD-patterns, a quantitative indication of the phases present is obtained. A summary of the results is given in Table 4.8.

4.3.3 Discussion

All mould powders for thin slab casting were used with the same, or comparable, operational casting practices i.e. casting speed and width, oscillation and taper settings, SEN etc. Hence, all the operational experiences are fully comparable.

Conventional characterisation methods provided insufficient information to explain the observed in-mould behaviour. Especially, the slag formation required further investigations using mineralogical characterisation methods. As a result it was concluded that free carbon additions are very important in controlling the melting behaviour of a mould powder.

In addition to this, carbonates also affect the melting of mould powders. During casting, carbonates generate CO_2 and this increases the melting rate due to stirring the powder layer [11]. Considering an uneven distribution of carbon particles, the effect of carbonate probably does not promote the melting of these powders but enhances the formation of rims and lumps. This can be a further explanation for the bad performance of some of the mould powders.

Compared with mould powders for thin slab casting, the successful conventional slab casting powder showed a poorer distribution of free carbon. This indicates that slag formation at lower casting speeds (<1.9 m/min) and/or thicker slabs (225 mm) is less critical [49].

Table 4.8: *Mineralogical composition of mould powders (XRD)*

Mineral	I	II	III	IV	V	VI	VII
Silicates							
wollastonite ($CaSiO_3$)	++	++	++	++	++	++	++
quartz (SiO_2)		+				+	+
forsterite (Mg_2SiO_4)						+	
albite ($NaAlSi_3O_8$)		+					
spodumene ($LiAlSi_2O_6$)	+				+		
Fluorites							
fluorite (CaF_2)	++	++	++	++	++	++	++
cryolite (Na_3AlF_6)			+	+			
Carbonates							
natrite (Na_2CO_3)	+	+	+	+	+	+	+
calcite ($CaCO_3$)				?	?	+	+
magnesite ($MgCO_3$)	+		+	+	+		
Others							
glass	+	+	+	+	+		+
carbon	+	+	+	+	+	+	+

++: major phase +: phase present/minor phase

4.3.4 Status at the DSP

The caster output showed a continuous improvement from the moment of commissioning onward, which was accelerated by the introduction of mould powder II. During the years, the maximum casting speed was gradually increased to 5.8 m/min and occasionally to 6 m/min. Subsequently, the EMBr was introduced in order to control mould fluid flow. The sequence length was further increased to a maximum of 12 hours. Mould powder II proved to be suitable for casting low carbon steels and high strength low alloy grades (HSLA).

Mould powder II is denoted **powder A** in both Chapter 3 and in the next parts of this thesis. During this stage of the study, quantitative phase analyses (Rietveld-XRD) and high temperature phase relations (HT-XRD) became available for mould powder characterisation.

4.4 Effects of meniscus conditions on powder melting

After the introduction of the EMBr at the thin slab caster, it was found that the liquid pool depth was difficult or even impossible to measure when using the standard method, based on steel sheets. This was caused by the strong magnetic field in the mould area. The liquid pool depth appeared to be very *small* with values around 2 mm where values between 4 and 8 mm were expected. As a consequence, the liquid pool measurement method was adapted for casting practices in the presence of a strong electromagnetic field. Furthermore, the standard mould powder A and EMBr settings were adapted in order to generate more liquid slag during casting i.e. to increase the melting rate. Finally, all these steps resulted in decreased setting of the EMBr [50].

4.4.1 Liquid pool depth measurements

Initially, stainless steel sheets were introduced to measure the slag pool depth during casting in the presence of a strong electromagnetic field (EMBr). However, in most cases, the slag only adhered to the steel surface as a *liquid*. During cooling and solidification the slag cracked and came loose. Occasionally, some colour on the stainless sheet remained, indicating the presence of the slag pool. However, it proved difficult or sometimes even impossible to obtain reliable slag pool measurements using stainless steel sheets only. For this reason, a *combination* of a stainless sheet and a copper sheet was introduced. After immersing this combination, the slag adheres briefly to the stainless sheet but the difference in length between the stainless and copper sheets clearly indicates the liquid pool depth during casting.

Experiments in an induction furnace were done to develop this method in more detail. The diameter (surface) of the furnace is 180 mm, the standard mould powder of the DSP (powder A) and a standard low carbon steel grade were used. Based on measurements in the DSP mould, the steel temperature in the furnace was set at 1545 °C. Most experiments were performed using 400 g of mould powder which is equivalent to 5 mm liquid slag. During the experiments, the "old" method based on steel sheets with a thickness of 0.3 mm and an immersion time of 1 second was used as a reference.

Several experiments were done focussing on the optimum thickness of the stainless steel and copper sheets and the immersion time. It was found that:

- the required thickness of the stainless and copper sheets is 0.3 mm
- the immersion time is between 1 and 4 seconds and depends on the local flow conditions in the mould – an immersion time of 3 seconds was found to be best; an immersion time of 1 second resulted in insufficient melting of the steel sheet and skull formation at the steel surface
- during all experiments, the slag came loose from the surface of the stainless sheets during cooling and solidification, indicating different interfacial properties (steel – slag)
- there is no effect of a rough surface i.e. roughing of the stainless sheets on adhering of mould slag.

In all cases, a good impression of the stability of the liquid layer and the meniscus stability is obtained. For practical reasons, the optimum width of the sheets was found to be around 15 cm. When the meniscus stability is investigated, for instance during fluid flow measurements, stainless sheets without copper sheets are very useful.
The developed method based on a combination of a stainless sheet and a copper sheet is now standard practice for all casting experiments and plant trials.

4.4.2 Mould powder developments and vertical heat transfer

Given the small liquid pool depths after the introduction of the EMBr, mould powder A was adapted in order to generate more slag during casting. As a first step, it was decided to concentrate on the melting rate of the mould powder by decreasing the free carbon content.
Two mould powders with decreased free carbon contents of 2.5 and 1.5 wt%, respectively, were produced. Parameters such as the type and distribution of the free carbon particles, the inorganic slag composition (inorganic raw materials) and the main physical properties (slag viscosity, break point etc.) remained the same. As before, the carbon additions were entirely in the form of carbon black with a small particle size.

The melting rate of the mould powders was measured using the softening method; a displacement of 20% at 1400 °C is considered as a characteristic value [47]. The method was slightly adapted for these measurements. Characterisation was also carried out on a standard mould powder used for conventional slab casting. This reference powder is denoted as powder VII in Table 4.5. A summary of the results is given in Table 4.9 and Figure 4.8.

Table 4.9: *Standard mould powder (A) and variants (A1, A2)*

Mould powder	C_{free} (wt%)	time (s) 20% displacement	viscosity at 1300 °C (Pa·s)*	T_{break} (°C)*
A	3.5	78	0.13	1167
A1	2.5	60	0.13	1175
A2	1.5	48	0.11	1166
VII	*4.4*	*42*	*0.16*	*1102*

*: supplier data

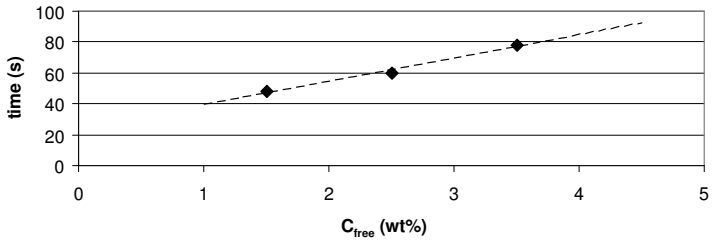

Figure 4.8: *Melting rate (time for 20% displacement) of mould powder A, A1 and A2*

Plant trials were also done using a standard EMBr current of 360 A. During these trials, slag pool depths were measured and the formation and occurrence of slag rims were carefully observed. Results are summarised in Table 4.10.

It was found that a decrease in free carbon content in the mould powders resulted in a limited increase in liquid pool depth during casting. Powder A2 (C_{free} = 1.5 wt%) was expected to give a significant increase in liquid pool depth but this was found not to be the case even though the carbon content was 50% less than the standard powder. Surprisingly, a significant formation of rims and bridges was observed; the liquid pool depth increased to the standard value of around 5 mm. Even freezing of steel at the meniscus was detected, Figure 4.9.

Table 4.10: *Liquid pool depth as a function of the free carbon content and EMBr-settings*

Mould powder	C_{free} (wt%)	Liquid pool depth (mm): EMBr=360 A	Liquid pool depth (mm): EMBr=210 A	Liquid pool depth (mm): EMBr=0 A
A	3.5	0-2	4-8	4-8
A1	2.5	2-4	no measurements	
A2	1.5	4-6 severe rim formation + freezing of steel	8-12	

The formation of rims and bridges and freezing of the steel may be a consequence of the loss of exothermic heat generated by carbon combustion. Furthermore, the EMBr has an effect on the vertical heat transfer which will also suppress slag formation. An illustration of the EMBr-poles and the mould is given in Figure 4.10.

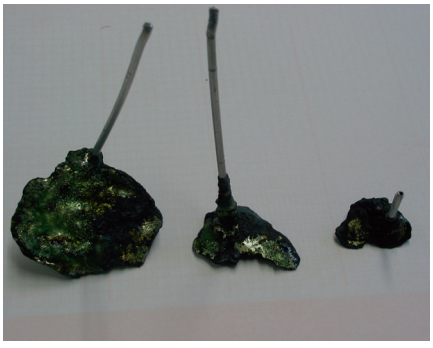

Figure 4.9: *Examples of freezing of the steel meniscus using powder A2 and EMBr setting of 360 A*

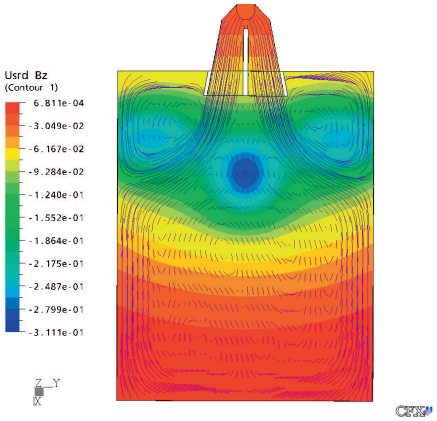

Figure 4.10: *Schematic illustration of EMBr-poles in the mould (left)*

Carbon content
Indicative calculations for the casting practice at the DSP showed that powder melting requires around 5.4 kJ/s. A decrease of 2 wt% C_{free} results in a decrease of exothermic heat of 1.6 kJ/s. This is more than 25% of the heat, needed for powder melting. In these calculations, it is assumed that all free carbon is combusted and that all heat generated is fully used for powder melting (no heat losses) [44].

EMBr settings
The effect of the EMBr settings on the vertical heat transfer in liquid steel layers was calculated using Computational Fluid Dynamics (CFD) simulations. The calculations showed that a 30% decrease in vertical heat transfer can be expected when applying the standard setting of 360 A. The use of the EMBr decreases the vertical heat transfer in the mould due to the reduction of turbulent metal flow velocities [51]. As a consequence, powder melting will be hampered and a thinner liquid pool will be formed.
As a next step, the EMBr setting was decreased from the standard 360 A to 210 A. The mould powder trials (especially with the low C powder A2) were repeated and resulted in a significant increase in liquid pool depth without any effect on rim formation and meniscus freezing for the standard powder and for the low carbon powder A2, Table 4.10.

The casting speed during the trials was between 5.0 and 5.2 m/min. The powder consumption remained the same during all trials, indicating that the increased liquid pool depth does not influence the mould powder consumption.
Plant experiments at the two strand thin slab caster (Danieli) of Tangshan, China showed that an *increased* vertical heat transfer and a more stable flow at the meniscus area resulted in improved powder melting and less formation (growth) of slag rims at the narrow faces. These results were obtained by adjusting the standard "hammer type" SEN, with a special focus on the upward steel flow during casting [52].

4.5 Phase analyses and phase relations

Trials with alternative mould powders have also been done with the aim to increase process stability and product quality (powder B and C). An alternative for the standard mould powder has been investigated as well (powder D). These powders are detailed in Table 4.11.
Mould powders A–D were investigated in more detail focussing on phase analyses and high temperature phase relations. The standard starter powder used at the DSP was investigated as well (powder F). Starter powder is only used during the start of casting with the aim to provide sufficient (liquid) lubrication. Slag formation is the most important requirement for starter powder. Starter powder has exothermic properties due to the presence of $CaSi_2$, $FeSi_2$ and Fe_2O_3. Note that starter powder is produced as *powder* and not as granulated material.

4.5.1 Powder composition
An overview of the chemical composition of the standard powder (A), three alternative materials (B, C and D) and starter powder (F) are given in Table 4.11. Mould powder B is an alternative powder for the standard material, especially for increased casting speeds with a maximum between 6.0 and 7.0 m/min. Mould powder C is used to increase mould heat transfer i.e. to increase strand solidification which will result in a thicker steel shell; this powder is applied for several specific steel grades. Mould powder D was tested as an

alternative to mould powder A. The powder performed well at the caster but resulted in excessive scale formation (wustite, FeO_x) in the first meters of the tunnel furnace which can be related to the interaction between the specific mould slag and the steel surface [53].

Table 4.11: *Chemical composition of mould powders for thin slab casting (A-D) and starter powder (F) (wt%)*

	A	B	C	D	F
CaO/SiO_2	1.0	0.9	0.8	1.0	0.8
SiO_2	33.2	32.4	35.3	32.4	41.8
CaO	33.6	29.3	27.0	32.5	34.3
MgO	0.7	1.3	1.3	2.3	0.4
Al_2O_3	2.9	2.7	2.7	3.9	3.3
Na_2O	11.9	14.2	16.6	10.7	8.7
K_2O	0.4	0.1	0.2	0.1	0.2
Li_2O	0	0	0	0.4	0
MnO	0	0	3.0	0	0.1
Fe_2O_3	0.5	0.3	0.4	0.3	15.7
F	8.8	7.0	8.4	7.7	11.0
C_{free}	3.7	5.7	0.6	4.8	0.6
CO_2	9.4	8.9	7.8	5.4	3.5
C_{tot}	6.3	8.1	2.7	6.3	1.6

Note the limited decrease in basicity (CaO/SiO_2) for mould powders A to C and the increase in sodium (Na_2O) for these powders. In all the mould powders, one source of free carbon is used. Mould powder C contains MnO and mould powder D is characterised by the presence of lithium (Li_2O) and an increased value of MgO.
Mould powder F is characterised by a low value of the basicity (CaO/SiO_2 = 0.8), increased amounts of F and in particular Fe_2O_3 and nearly no free carbon (C_{free}). The metallic components $CaSi_2$ and $FeSi_2$ in mould powder F are reported as oxides.

4.5.2 Phase analyses

As described in Chapter 3, the chemical composition does not give information on the mineralogical composition i.e. the raw material choice of the mould powders. Room-temperature X-ray diffraction measurements (XRD) with subsequent Rietveld-analyses were used to determine quantitatively the mineralogical phase composition of the mould powders. Results are given in Table 4.12.

In general, a mould powder can be divided into the silicates, the fluorites and the carbonates. Additionally, amorphous components (glass) can be present. Starter powder contains specific raw materials, providing an exothermic effect during powder melting.

As shown in Table 4.12, significant differences in the raw material composition can be observed. In mould powder A, albite (feldspar) is used. Furthermore, this mould powder has one source of fluorine. Mould powder B, C and D both have two sources of fluorine and do not contain albite. Mould powder C contains a significant amount of amorphous materials (glass) which is not present in the other two mould powders whereas powder D contains spodumene as a main phase.

Table 4.12: *Mineralogical composition of mould powders for thin slab casting (A-D) and front powder (F) (Rietveld-XRD) (wt%)*

	A	B	C	D	F
Silicates					
wollastonite ($CaSiO_3$)	50 ± 5	55 ± 5	49 ± 5	55 ± 5	32 ± 3
quartz (SiO_2)	2 ± 1	3 ± 1	2 ± 1	5 ± 1	1 ± 1
diopside ($CaMgSi_2O_6$)	2 ± 1	7 ± 2	2 ± 1	2 ± 1	4 ± 1
albite ($NaAlSi_3O_8$)	14 ± 3	0	0	0	4 ± 1
spodumene ($LiAl(SiO_3)_2$)				6 ± 1	
Fluorites					
fluorite (CaF_2)	17 ± 3	5 ± 1	7 ± 2	7 ± 2	13 ± 3
cryolite (Na_3AlF_6)	0	10 ± 2	8 ± 2	4 ± 1	9 ± 2
Carbonates					
natrite (Na_2CO_3)	13 ± 3	16 ± 3	14 ± 3	15 ± 3	6 ± 1
calcite ($CaCO_3$)	2 ± 1	4 ± 1	2 ± 1	5 ± 1	
Glass	0	0	16 ± 3		
Others					
periclase (MgO)				1 ± 1	
hematite (Fe_2O_3)					16 ± 3
$CaSi_2$					14 ± 3
$FeSi_2$					2 ± 1

Mould powder F basically contains the same raw materials as powder A. However, additions of Fe_2O_3, $CaSi_2$ and $FeSi_2$ are used as exothermic components in order to create the necessary heat during start of casting. The exothermic reaction is expected to occur via a redox-reaction where the silicides are reduced by oxidation of hematite.

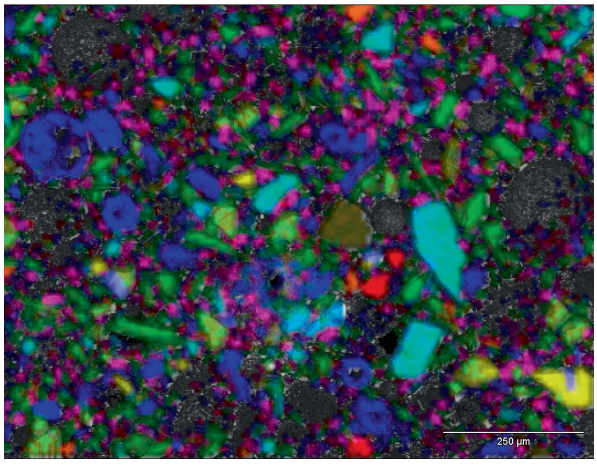

Figure 4.11: *Raw materials in powder F, indicated in a false-colour backscatter electron image: cyan (light blue) CaF_2, blue Fe_2O_3, yellow $CaSi_2$, green $CaSiO_3$, red Na_2CO_3, and pink Na_3AlF_6*

Cryolite is probably used in powder F to decrease the viscosity without changing the lubrication properties. Cryolite does not increase the CaO content but increases the Na_2O content. Consequently, the viscosity and crystallisation tendency will *decrease* whereas CaO (CaF_2 as raw material) increases the crystallisation tendency and decreases the lubrication. The various raw materials in powder F are illustrated in a false-colour backscatter image, Figure 4.11.

4.5.3 Equilibrium phase relations

Initial mixtures of the powder raw materials are not in chemical equilibrium but the systems tend towards it during heating, which results in a series of reactions between the phases and eventually, the formation of secondary phases. Changes in mineralogy of the major phases (>10 wt%) for the three powders during heating have been observed *in situ* using high-temperature X-ray diffraction (HT-XRD) with additional powder X-ray diffraction and microscopic techniques. Details of this method were given in Chapter 3.
The analyses of mould powder A-D showed a sequence whereby the primary phases (raw materials) disappear followed by the secondary phases and finally melting. A few minerals dominate this process; combeite ($Na_4Ca_4Si_6O_{18}$) and cuspidine ($Ca_4Si_2O_7F_2$). Each mould powder shows a specific melting sequence which depends on the raw material choice and consequently on the presence of primary and secondary phases. A summary of the melting sequence of the powders is given in Table 4.13.

Table 4.13: *Melting sequence of mould powders for thin slab casting (A-D) (HT-XRD) (°C)*

Primary phases (raw materials)	**A**	**B**	**C**	**D**	**Secondary phases**
calcite-out	nd	nd	nd	600	
cryolite-out			675	750	
natrite-out	700	1000	750	nd	
	675	900	750	700	combeite-in
albite-out	825				
spodumene-out				825	
	850	1000	800	900	cuspidine-in
fluorite-out	1025	975	950	1000	
wollastonite-out	1000	1050	950	1050	
	1050	1150	975	1050	combeite-out
melting	**1150**	**1200**	**1100**	**1150**	**cuspidine-out**

A brief summary on the phase relations during powder melting can be given as:

wollastonite + sodium → combeite

followed by:

combeite + fluorite → cuspidine

Note that sodium and fluorine have to be liberated from their raw materials in order to generate these phase relations. Corresponding results on slag solidification (mould powders A-D) and data of plant trials are described in Chapter 5.

4.5.4 Melting trajectory and slag viscosity

The melting trajectories of mould powders A-D were measured at Tata Steel IJmuiden using a hot stage microscope. The viscosity of the mould powders A-C and the corresponding break point (or solidification temperature) was measured by the supplier using a viscometer (rotating cylinder method) at a cooling rate of 10 °C/min. A summary of the analyses are given in Table 4.14 and Table 4.15.

Table 4.14: *Melting trajectory of mould powders for thin slab casting (A-D) (°C)*

	A	B	C	D
Softening temperature	1066	994	1012	1031
Melting temperature	1088	1026	1045	1055
Fluidity temperature	1112	1064	1070	1077

Table 4.15: *Viscosity and break point (powder A-C) (measured by the supplier)*

	A	B	C
Viscosity at 1300 °C (Pa·s)	0.13	0.09	0.10
Break point (solidification point) (°C)	1167	1110	1054

Based on powders A-D, there is no clear relationship between data on powder melting obtained with HT-XRD (complete melting, melting of cuspidine) and the melting trajectory, as observed with hot stage microscopy. Mould powder B shows a high melting temperature of cuspidine (HT-XRD) and a low melting trajectory (hot stage microscope) whereas the results of powder A, C and D show some similarity, Figure 4.12.

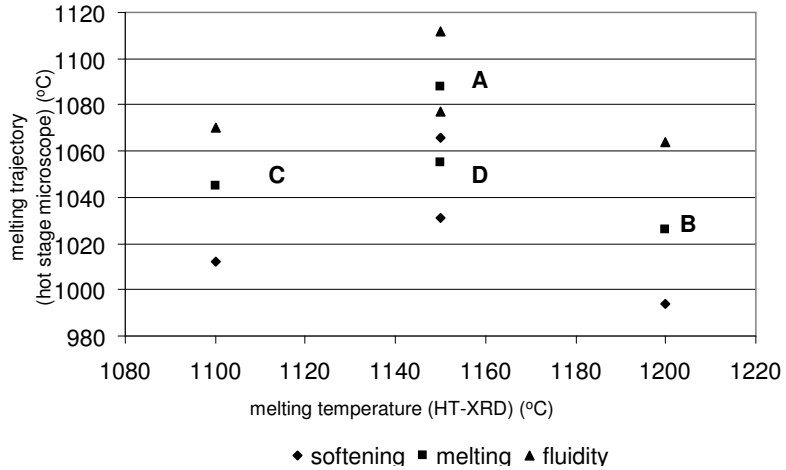

Figure 4.12: *Powder melting: melting trajectory (hot stage microscope) vs. melting temperature (HT-XRD) (°C)*

4.6 Rim formation

During casting, slag rims are formed which adhere to the mould walls close by the meniscus. Under stable casting conditions, slag rims are small but play a role during the infiltration of mould slag. However, rims can grow, disturb and even interrupt the casting process. Based on the experience of the DSP-caster, excessive rim formation should be avoided. The infiltration process (mould slag) can be hindered, parts of the rim can break and fall into the mould and bridges of very big rims can be formed, especially at the narrow faces or between the SEN and the mould wall. Owing to the mould dimensions (mould thickness) of a thin slab caster and the high casting speed, with increasing demands on meniscus stability, the control of rim formation and especially rim growth is very important. The formation and growth of rims can be affected by the properties of the mould powder and by the conditions at the meniscus.
In the previous section, it was shown that the rims and lumps can be formed due to insufficient powder melting (slag formation) which is caused by an excess of free carbon, a specific choice of free carbon sources or an inhomogeneous distribution of free carbon particles within the mould powder granules. An improper use of free carbon will be a source of rim formation during casting.

4.6.1 Standard mould powder

Typical rims have been characterised using optical microscopy and SEM/EDS techniques with special attention given to those from powder A.

Influence of mould powder

The rims show a *layered structure* of mould slag, intermediate phases and mould powder. Small Fe-droplets and carbon black particles (free carbon) were detected as well. The Fe droplets may originate from the steel (inclusions or interfacial reactions) or can be formed by reduction of FeO_x coming from the steel or from mould powder raw materials [7,54].

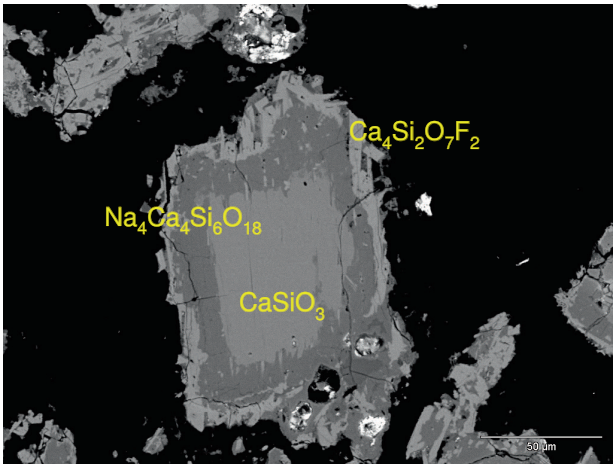

Figure 4.13: *Slag rim analysis showing a melting sequence wollastonite - combeite - cuspidine (powder A)*

It was shown that thin crystals of a condensed Na compound coat and cement the various layers. As a result the rims are dense, strong and will survive for relatively long periods of time during the casting process; the rims will not easily remelt. The dominant mechanism leading to the *formation* and *growth* of slag rims can be seen as a "painting" mechanism.
An excess of sodium, especially at lower temperatures possibly enhances the formation of these dense and strong rims. Note that mould powder A contains two Na-sources with relatively low melting temperatures: natrite and albite.
Analyses of the slag rims showed the melting sequence and phase relations, as detected by HT-XRD (powder melting). An illustration of this is given in Figure 4.13.

Surprisingly, *graphite crystals* (flakes) were detected in the rims, the graphite was formed from carbon black, being the only free carbon source in this mould powder.
Note that nearly all areas of mould slag in the rims show the bulk composition of the mould powder i.e. no changes in slag composition during casting (Al_2O_3, SiO_2) have been found.

Influence of process conditions
Rims sampled from the wide face of the mould showed some F-losses and differences in crystallisation behaviour, compared to rims sampled from the two narrow faces. This can be related to a higher heat load at the wide face.
Above all, the rims that have been investigated, especially the bigger ones, clearly show the effects *of mould meniscus fluctuations* i.e. turbulence at the meniscus area during casting. The "painting mechanism" will considerably be enhanced by these fluctuations. Stable casting conditions i.e. a stable mould meniscus will not result in excessive rim formation. Therefore, it can be argued that there is no direct need to adapt the mould powder composition and slag properties to control rim formation and rim growth and focus should remain on process stability.

4.6.2 Alternative mould powders

Mould powder D
Rims from mould powder D were investigated as well. As with mould powder A, these rims were initially *formed* by a "painting" mechanism. Thin layers of mould slag and mould powder adhere to the copper walls. However, the mechanism of *growth* is not the same.
Rims from powder D show a loose structure, containing a lot of small slag droplets, coarse particles of coke and a condensed tar binder. The slag droplets also contain secondary phases, comparable to the melting sequence (HT-XRD) and coke particles (free carbon source). The coke particles "survived" powder melting. It has been reported that combustion of coke (especially coarse particles) is relatively slow [9,49].

The slag droplets are sprayed and quenched and this "spraying" mechanism mainly causes the growth of the slag rims. Comparing to the rims of mould powder A, these rims are loose, seem to be formed in a shorter period and can be melted more easily. The spraying mechanism (slag droplets) is not fully understood. This can possibly be related to the presence and amount of carbonates i.e. the gas formation (CO_2) during casting. The rims from mould powder D did not contain Fe-droplets. It should be noted that powder D contains spodumene, whereas powder A makes use of albite.

Investigation into the free carbon sources in mould powder D revealed that the powder contains a significant amount of extremely fine grained carbon black, lining the surfaces of the mineral fragments, and a significant amount of coarse coke particles with grain sizes

comparable to the sizes of other mineral fragments (metallurgical coke). A part of the coke particles "survived" powder melting i.e. did not play a significant role in controlling the melting rate.
The formation of tar, which acts as a binder in the rim, can possibly be related to the abundance of the free carbon sources (fine carbon black and coarse coke particles).
As with mould powder A, graphite flakes were detected in the rims, the graphite was formed (grown) from the free carbon.

It had been stated that coke (as free carbon source) contains Al_2O_3 and SiO_2 and will show some wetting with the powder minerals during heating and melting. Consequently, sintering and rim formation can be promoted by the presence of coke. Carbon black does not contain inorganic materials and (if distributed well) will be very effective in controlling the melting rate of a mould powder (non wetting) without the formation of a sinter layer [55].

Mould powders B and C
Mould powder B showed comparable or sometimes less rim formation during casting, compared with mould power A. Mould powder C hardly showed any rim formation. Rims were not available for investigation purposes and it is not clear if the decreased rim formation can be related to the absence of albite or the lower melting temperatures of these two powders.

Figure 4.14 illustrates a standard rim (mould powder A) obtained from the DSP caster. An excessive rim, caused by severe mould level fluctuations is illustrated in Figure 4.15.

Figure 4.14: *Standard slag rim (DSP mould)*

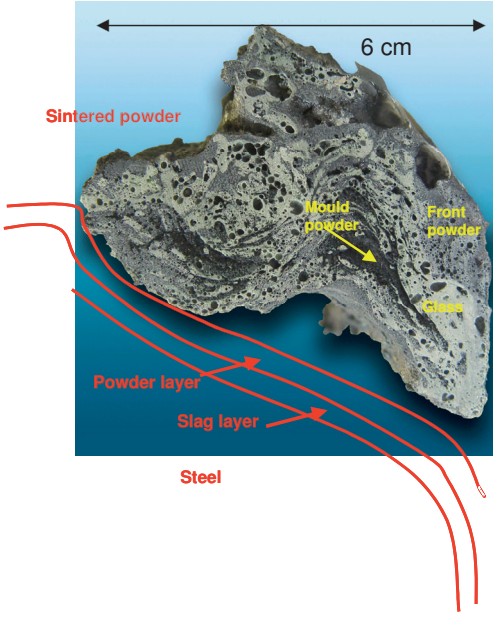

Figure 4.15: *Excessive rim, formed by severe meniscus fluctuations (DSP mould)*

4.7 Melting experiments

Several laboratory trials were done in order to investigate mechanisms on powder melting in more detail; all tests were done with mould powder A. In the first experiment, the mould powder was in contact with liquid steel and therefore, meniscus phenomena could be observed as well. In the other two experiments, the mould powder was not in contact with liquid steel.

Sampling technique

The sampling method, as described by Scheller (ThyssenKrupp Nirosta, now TU Freiberg) was slightly adapted for use at Tata Steel. The aim of this method is to obtain representative samples of the meniscus area in the continuous casting mould, which include steel, mould slag and mould powder. A measurement starts with the immersion of a steel plate fixed on to a bar, directly followed by a steel tube. After around two seconds, the whole sample is pulled out and quenched in water. The solidified content of the tube is sectioned for inspection purposes [56,57].

The dimensions of the sample holders are: steel plate 100 mm×100 mm, diameter of the bar 10 mm, diameter of the tube 45 mm. Sample holders, as used during the experiments are illustrated in Figure 4.16. A schematic illustration of the method is given in Figure 4.17.

Figure 4.16: *Holders for sampling mould powder layers*

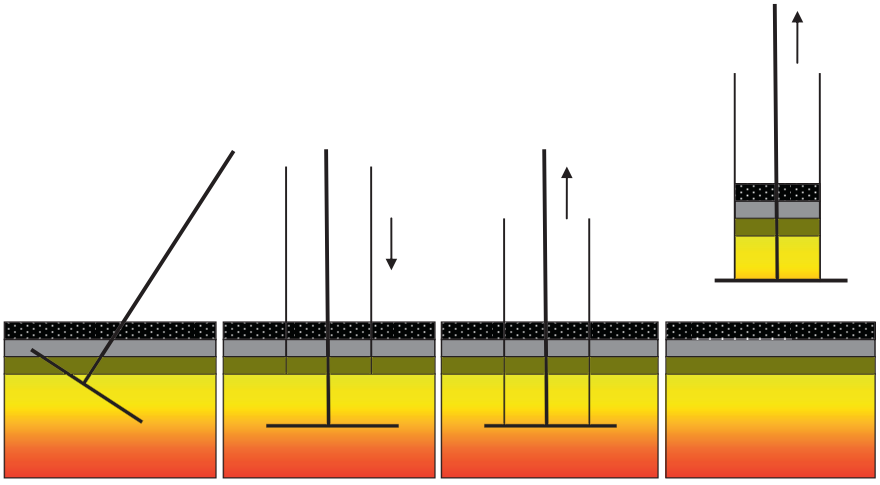

Figure 4.17: *Schematic illustration of sampling technique, applied at Tata Steel*

Trials were done in an induction furnace (surface diameter 290 mm) at a steel temperature of approximately 1545 °C. A standard LC steel grade ([C] = 0.06 wt%) and the standard thin slab casting mould powder (powder A) were used. For these experiments, around 200 g mould powder is required to obtain 1 mm mould slag. The mentioned

procedure was used and the samples were prepared for microscopic analyses. See Figure 4.18.

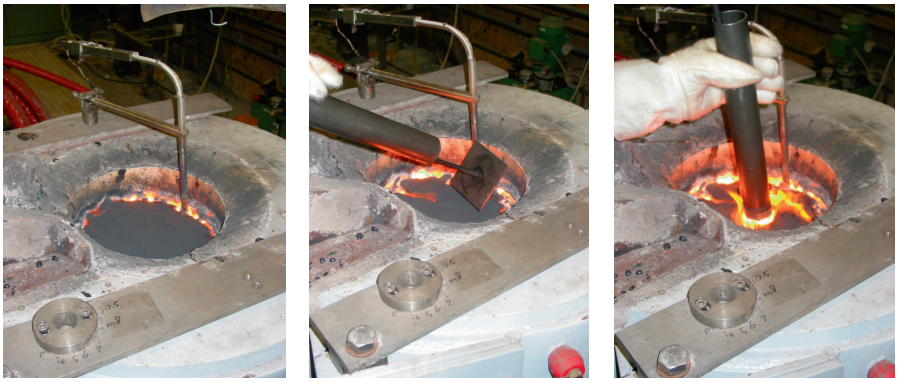

Figure 4.18: *Sampling of mould powder layers (induction furnace)*

Investigation focussed on the preserved layers and interfaces. First results show that there are three distinct layers and that the interface between the layers is sharp. See Figure 4.19.

A summary of the investigations is as follows:

- The interface between the slag and the liquid steel is sharp and does not give any indication of an interaction of the two phases. The slag in the molten pool is essentially of homogeneous composition and overlaps with that of the bulk composition of the mould powder. It does not show any modification of its composition close to the interface with the steel.

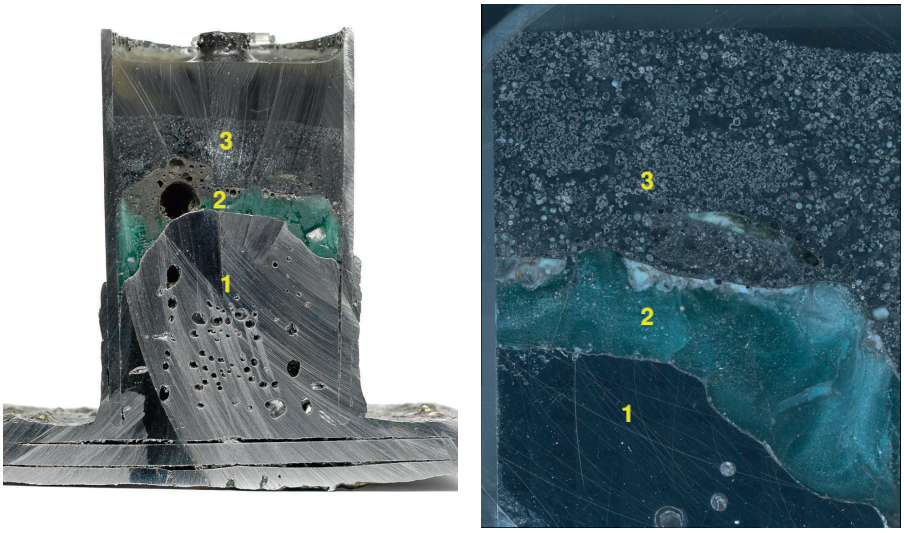

Figure 4.19: *Sample overview showing the steel layer (1), the slag pool (2) and the powder layer (3)*

- There is no clear evidence of carbon pickup in the liquid steel from the mould flux. The steel immediately in contact with the slag pool is still low-carbon type.
- Carbon black is completely absent from the main slag pool. However, the slag pool has a thin film of carbon black (~1–2 μm thick) that marks the *separation* of it from the overlying slag globules and variably recrystallised/partially molten particles. These are themselves always coated by carbon black.
- The top of the completely molten pool may roughly coincide with the critical temperature at which carbon black burns off. The globules above it are prevented from coagulating by their own carbon black coating and by the carbon black film at the top of the liquid pool. During melting, the globules immediately above the film will be assimilated into the main liquid pool. The role of free carbon in powder melting is shown in Figure 4.20. Free carbon controls the melting rate by preventing coagulation of slag droplets.

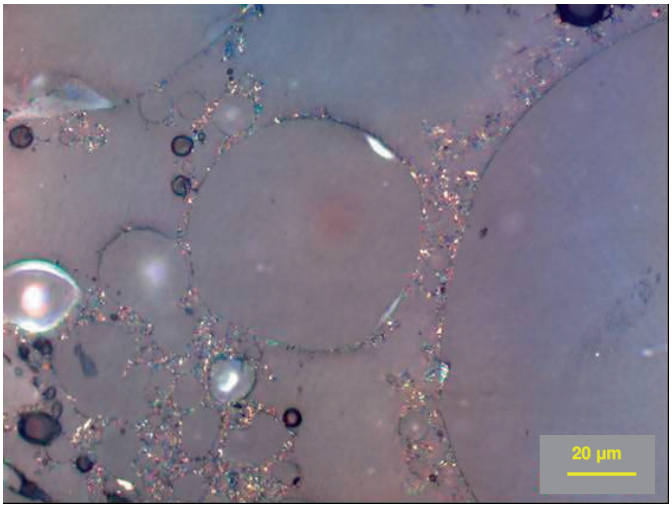

Figure 4.20: *High magnification reflected light micrograph showing slag globules surrounded by carbon black, which appear as bright multi-coloured flecks of <1 μm in size*

- The slag layer contains gas bubbles (~1 mm) and Fe-droplets. The vast majority of the Fe-droplets is small (~1–30 μm) and spherical and they are qualitatively different from the more irregularly shaped larger Fe-droplets (up to ~500 μm). Perhaps these larger droplets were formed by coagulation of smaller Fe-droplets.
- The Fe-droplets in the mould slag can be formed due to *internal reduction* of iron oxide by carbon, both present in the mould powder. There is a significant concentration of these metal droplets along the interface between the slag pool and the globularised powder layer. Furthermore, the high concentration of carbon blacks along this interface provides an obvious reduction agent and the high carbon content of the Fe-droplets at this interface (Fe + Fe_3C, cementite) suggests that indeed their formation is linked with the carbon blacks. An illustration is given in Figure 4.21.
- Although all stages of the melting sequence from powder to fully molten are represented by individual particles, their current distribution in the sample is not perfectly layered. The powder layer is not a perfectly layered bed, as widely assumed but shows some similarity with a fluidised bed.

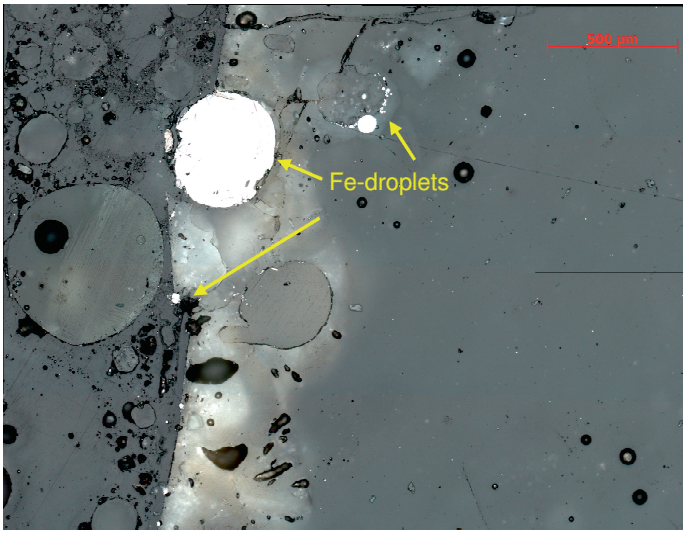

Figure 4.21: *Powder slag interface showing large and small Fe-droplets (bright coloured); the large Fe-droplet has a high carbon texture*

The test clearly showed the presence of graphite (lamella or flakes), formed during powder melting and in particular *during* the reduction of FeO_x, where carbon black acted as raw material, Figure 4.22. It should be noted that the formation and precipitation of all forms of graphite from a metallic solution, most likely by the initial formation of hexagonal layers of graphene sheets, is well known [58,59]. However, the formation of graphite or graphite flakes during powder melting and during continuous casting is not described elsewhere [48].

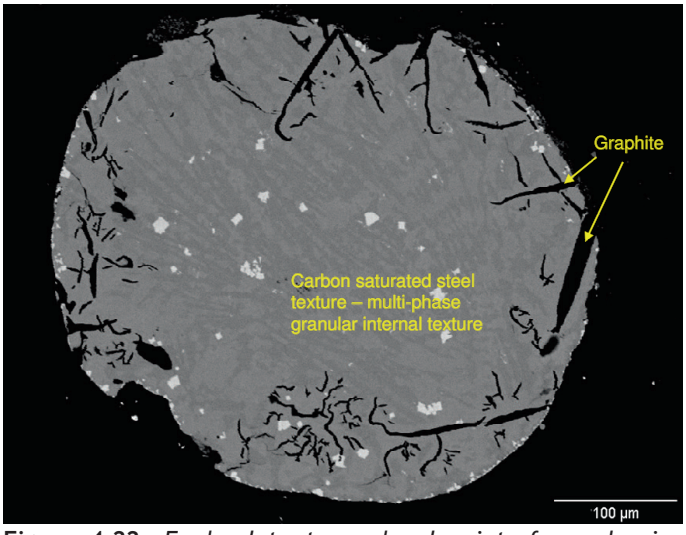

Figure 4.22: *Fe-droplet at powder-slag interface, showing high carbon texture (Fe_3C) and the presence of graphite lamella*

Two additional experiments were done focussing on phase relations during powder heating and on the presence of Fe-droplets in mould slag. In both experiments, the mould powder was not in contact with liquid steel.

Box test

In close collaboration with Sumitomo Metal Industries and the Japanese mould powder supplier Nippon Thermochemical, mould powder A was heated using a so called box test. Nippon Thermochemical uses this method to investigate the melting performance of mould powders. The box test is based on visual inspection and the experience of the investigator and proves to be useful in giving additional information on powder melting [55].
For this test, three steel containers ("boxes") are loaded with 150 g of mould powder each. The containers are heated in a furnace at 1300 °C for 1, 3 and 5 minutes. Subsequently, the sintered and molten powder samples are visually inspected. In particular droplets mould slag and the presence of a sinter layer and crusts indicate the melting properties of the mould powder. Based on the experience of Nippon Thermochemical, results of mould powder A were summarised as good fusion behaviour (less rims) and a low fusion speed (thin slag pool). An illustration is given in Figure 4.23.

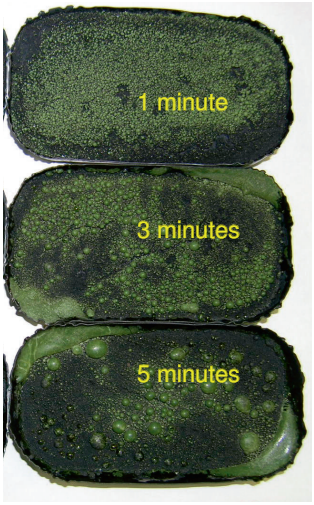

Figure 4.23: *Box test of mould powder A; heating at 1300 °C for 1, 3 and 5 minutes*

Within the framework of this study, remnants of mould powder A after heating at 1300 °C for 5 minutes were characterised using optical microscopy and SEM/EDS techniques. An illustration is given in Figure 4.24.

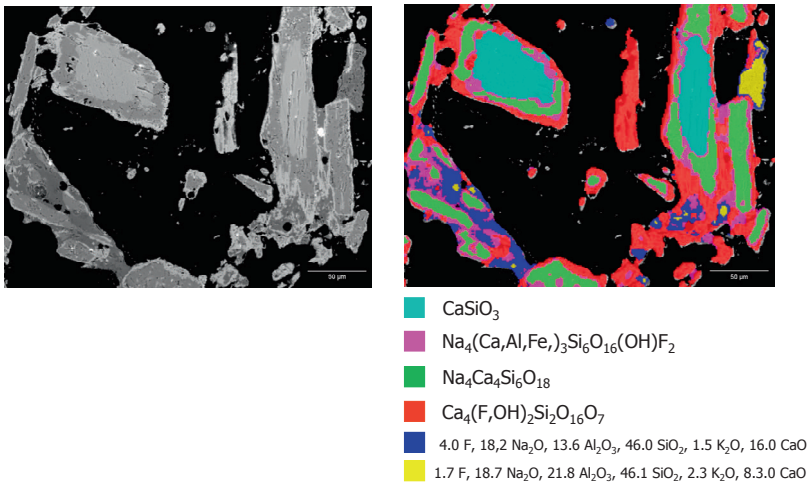

Figure 4.24: *Mould powder A after heating at 1300 °C for 5 minutes (box test)*

The mould powder shows primary phases (raw materials), secondary or intermediate phases and finally glass and cuspidine. The sequence of raw materials, secondary phases and glass/cuspidine indicates a slow melting process during this test which can be related to the relatively low test temperature of 1300 °C. However, the same mineral transformations were observed during HT-XRD experiments and the former experiment (sampling method). Consequently, phases observed from the box tests are not in equilibrium with each other. There is no clear evidence of the presence of metal droplets in the material. Probably, this can be understood by the relatively low test temperature during the experiment.

Graphite crucible

A graphite crucible (dimensions Ø75×160 mm) was filled with mould powder A and partially immersed in liquid steel using the same induction furnace as described above (temperature around 1550 °C). After 10 minutes, the sample was pulled out and prepared for microscopic investigations. The crucible was not broken or damaged during the experiment and there was no contact between the mould powder and liquid steel.

It was found that powder melting was not complete within the test period. As before, a powder layer and a slag layer were observed and showed all stages of powder melting and slag formation i.e. the melting sequence as found in HT-XRD analyses.

Although the mould powder was not in contact with any steel, almost *perfectly* analogous metal droplets were found. As in previous tests, a large concentration of these Fe-droplets was present along the interface between the slag pool and the powder layer, where a high concentration of free carbon (carbon black) acted as reducing agent. Several Fe-droplets showed textures that indicated relatively high carbon contents. Furthermore, the mould slag contained various small Fe-droplets. Note that this test also confirmed the formation of graphite lamella during powder melting (in situ) with carbon black as raw material source.

The *only* possible conclusion is that the Fe-droplets as observed in mould slag are derived from the mould powder itself via internal reduction of the Fe-components in the slag.

4.8 Powder consumption

Mould powder consumption effects both the lubrication and the horizontal heat transfer during casting. There are various empirical relations which describe the powder consumption as function of the casting speed, the slag viscosity and parameters like break point, mould stroke, oscillation frequency etc. This thesis focuses on high speed thin slab casting and consequently, smooth slab surfaces with very shallow oscillation marks. Initially, a simple and widely applied equation as proposed by Wolf was used to describe powder consumption:

$$Q_s = 0.55/\eta^{0.5} v_c \qquad (4.4)$$

where Q_s = powder consumption (kg/m^2), η = slag viscosity at 1300 °C (poise or dPa·s) and v_c = casting speed (m/min).

At the DSP, the powder consumption during casting is measured by continuously monitoring the weight of the powder bin. This method is considered to be more accurate than other methods like the counting of powder bags. Based on five months of casting operations with

casting speeds between 3.5 and 5.8 m/min, the powder consumption data was evaluated and plotted against the casting speed. An illustration is given in Figure 4.25 where the black line represents the measured powder consumption (kg/m^2). The modified-Wolf equation is plotted in this figure as well, represented by the blue dotted line.

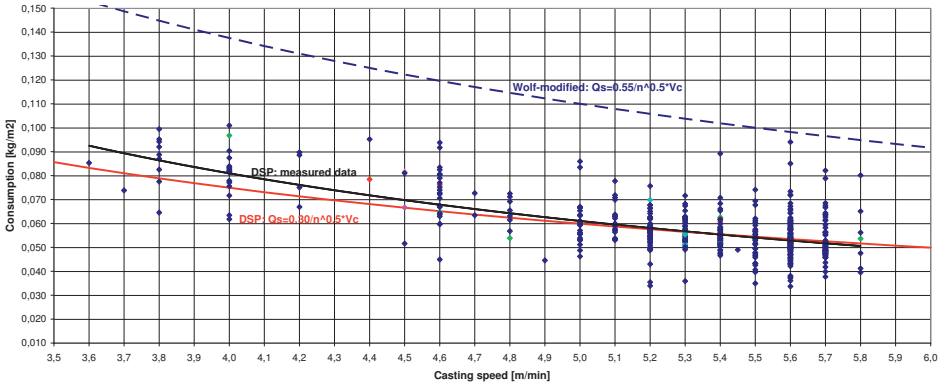

Figure 4.25: *Powder consumption at the DSP. Black line: measured (plant) data. Dotted blue line: modified Wolf equation. Red line: equation for DSP caster*

It can be seen that the measured values are about *half* of the predicted values using the modified-Wolf relation. A good fit can be obtained by the following equation:

$$Q_s = 0.30 / \eta^{0.5} v_c \qquad (4.5)$$

This relation is given by the red curve in Figure 4.25. Note that the indices of v_c and η are similar as those proposed by Wolf.

The view that the actual powder consumption is low is confirmed by some other thin slab casters which report values around 0.1 kg/m^2 at approximately 5 m/min and the QSP process of Sumitomo, reporting a consumption of 0.1 kg/m^2 at a casting speed of 5 m/min and between 0.09 and 0.05 kg/m^2 at a casting speed of 8 m/min.
It should be noted that the low consumption at the DSP caster does not cause any operational problem related to strand lubrication or mould heat transfer i.e. sticking of the shell and the occurrence of surface cracks. The low powder consumption at the DSP caster is not fully understood but the relatively small free meniscus surface, available for powder melting and slag formation may be a factor of influence.

Increased slag consumption is desired for reasons of high speed casting (>6 m/min) and operational stability. The powder consumption during casting can be increased by decreasing the slag viscosity. Furthermore, increasing the liquid pool depth (increasing the powder melting rate), changing the oscillation parameters and increasing the meniscus surface in order to enhance slag formation (changing the dimensions of the SEN and the mould) are alternatives.

As described in Section 4.4, an increased liquid pool depth did not result in any change in powder consumption during casting. A decreased slag viscosity and an increased free surface at the mould seem to be most relevant. A decreased slag viscosity has to be

realised by changing the composition of the mould powder and mould slag. Consequently, this will affect the main functions strand lubrication and mould heat transfer. A change in the dimensions of SEN and mould aiming to enlarge the mould surface and enhancing slag formation will impact the caster design and casting process.

4.9 Concluding remarks

The raw material choice of a mould powder and the material properties at increased temperatures are very important to understand the processes leading to powder melting i.e. the formation of a liquid pool and the growth of slag rims. However, the process conditions in the mould such as the steel flow in the meniscus area and the vertical heat transfer play an essential role as well. Powder melting can *only* be understood by considering the mould powder properties including the raw materials and the process conditions in the mould.

The free carbon source of a mould powder and an even carbon distribution within the granules are essential to guarantee stable slag formation without the formation of powder lumps and excessive slag rims. This can be obtained by using one grade of fine carbon black. A stable casting process and in particular, a well controlled steel meniscus and the vertical heat flux are other important conditions. Consequently, the physical properties of mould powders such as the melting point are not as important as widely assumed.

High temperature phase relations of the inorganic raw materials give insights into the processes during powder melting. These include the formation of intermediate phases such as combeite and cuspidine and the formation of phases like tar and sodium which act as a binder during rim growth and the formation of Fe-droplets together with graphite.

In addition to conventional characterisation methods, mineralogical characterisation proved to be essential for a further understanding of mould powder behaviour and mould powder functions. However, it is obvious that the interpretation of all the mineralogical findings can only be done in association with a good understanding of the casting process.

Neither a small liquid pool depth nor the very low powder consumption, as found during this work, affect the thin slab casting process and the product quality. However, for reasons of operational stability and flexibility as casting speeds increase, a minimum liquid pool of 5 mm is desired as well as a minimum powder consumption of 0.05 kg/m^2.

4.10 References

[1] K.C. Mills, A review of ECSC-funded research on mould powders. Synthesis report EUR 13177 EN, ECSC, Luxembourg, 1991.

[2] T. Nakano, M. Fuji, K. Nagano, T. Matsuyama and N. Masuo, Model analyses of melting process of mold powder for continuous casting of steel. Nippon Steel Tech. Rep., (34) 1987, 21-30.

[3] T. Cimarelli, Centro Sviluppo Materiali, Mould powders melting rate, Personal communication, 1997.

[4] J-W. Kim, S-K. Kim and Y-D Lee, Effects of carbon particle size and content on the melting rate of mold powder. Proc. 4th Eur. Continuous Casting Conf., 14-16 October

2002, Birmingham, United Kingdom, IOM Communications Ltd., London, United Kingdom, 2002, Volume1, 371-377.

[5] B. Xie, J. Wu and Y. Gan, Study on amount and scheme of carbon mixed in CC mold fluxes. Proc. 74th Steelmaking Conf., Washington, 14-17 April 1991, Washington, USA, Iron and Steel Society, Warrendale, USA, 1991, 647-651.

[6] D. Singh, P. Bhardwaj, Y. Dong, A. McClean, M. Hasegawa and M. Iwase, The influence of carbonaceous material on the melting behaviour of mold powder. Proc. 8th Int. Conf. on Molten Slags, Fluxes and Salts (MOLTEN2009), 18-21 January 2009, Santiago, Chile, GECAMIN Ltd., Santiago, Chile, 2009, 1073-1082.

[7] E. Schürmann, H. Steinhoff und H. Lachmund, Einfluß von Kohlenstoff und Eisenoxid in synthetischen Stranggießpulvern auf die Metall-, Schlacken- und Gasphase. Stahl u. Eisen, 110 (1990) No.9, 125-133.

[8] K. Schwerdtfeger and A. Jablonka. Kinetics of carbon combustion in packings of casting powder. Steel Research Int., 64 (1993) 77-86.

[9] K. Schwerdtfeger, J. Sardemann und H-J Grethe, Oxidation von Kohlenstoff und Zersetzung von Karbonat beim Erhitzen von Gießpulvern. Stahl u. Eisen, 114 (1994) No.2, 57-64.

[10] M. Supradist, A.W. Cramb and K. Schwerdtfeger, Combustion of carbon in casting powder in a temperature gradient. ISIJ Int., 44 (2004) 817-826.

[11] M. Kawamoto, K. Nakajima, T. Kanazawa and K. Nakai, Melting mechanism of mold powder for continuous casting. Proc. 75th Steelmaking Conf., 5-8 April 1992, Toronto, Canada, Iron and Steel Society, Warrendale, USA, 1992, 389-396.

[12] H. Lachmund, Metallurgical Measures for the achievement of ultra low carbon contents at Dillinger Hüttenwerke. Proc. 84th Steelmaking Conf., 25-28 March 2001, Baltimore, USA, Iron and Steel Society, Warrendale, USA, 2001, 613-623.

[13] K.C. Mills, T.J. Billany, A.S. Normanton, B. Walker and P. Grieveson, Causes of sticker breakout during continuous casting. Ironmaking and Steelmaking, 18 (1991) 253-265.

[14] T. Mukai, K. Yamaguchi and S. Ogibayashi, The mechanisms of breakout during continuous casting operation. Trans. ISIJ, 26 (1986) 163.

[15] S. Terada, S. Kaneko, T. Ishikawa and Y. Yoshida, Research of substitution for carbon (Development of mold fluxes for ultra-low carbon steel). Proc. 74th Steelmaking Conf., 14-17 April 1991, Washington, USA, Iron and Steel Society, Warrendale, USA, 1991, 635-638.

[16] S. Suresh, R.C. Sinha, J.B. Singh, A. Narayan and M.S. Sadhu, Carbon pick-up in IF steel. Tata Search, 2006, 291-294.

[17] C. Lefèbvre, J.P. Radot, J.N. Pontoire et Y. Roux, Développement d'une poudre de lingotière permettant de limiter la recarburation des aciers à ultra-bas carbone. La Rev. Métall., 94 (1997) 489-496.

[18] J.J. Macho, G. Hecko, B. Golimowsky and M. Frazee, The development and evaluation of a new generation of no free carbon continuous casting fluxes. Proc. 33rd McMaster Symposium on Iron and Steelmaking, 6-9 June 2005, Hamilton, Canada, Steel Research Centre, McMaster University, Hamilton, Canada, 2005, 131-146.

[19] J.J. Macho, M. McClymonds and D. Sturgill, Color coded powder for the continuous casting of steel. Proc. 5th Eur. Continuous Casting Conf., 20-22 June 2005, Nice, France, 2005, La Rev. Métall., Paris, France, 2005, Volume 2, 648-651.

[20] R. Scheel und W. Korte, Einfluß unterschiedlicher Gießpulverzusammensetzung auf Stranggießschlacken und Gießpraxis. Stahl u. Eisen, 107 (1987) No.17, 37-43

[21] T. Hiromoto, T. Shima and R. Sato, Development of fired mould fluxes for continuous casting. Proc. 62nd National Open Hearth and Basic Oxygen Steel Confer., 25-28 March 1979, Detroit, USA, Iron and Steel Society, Warrendale, USA, 1979, 40-47.
[22] P. Grieveson, S. Bagha, N. Machingawuta, K. Lidell and K.C. Mills, Physical properties of casting powders: Part 2 Mineralogical constitution of slags formed by powders. Ironmaking and Steelmaking, 15 (1988) 181-186.
[23] K-H. Spitzer, J-F. Holzhauser, F-U. Brückner, B. Siera, H-J. Grethe und K. Schwerdtfeger, Neuere Meßverfahren zur Beurteilung von Gießpulvern. Stahl u. Eisen, 108 (1988) No.9, 71-80.
[24] N. Kölbl, I. Marschall and H. Harmuth, Investigation of the melting behaviour of mould powders. Proc. 8th Int. Conf. on Molten Slags, Fluxes and Salts (MOLTEN2009), 18-21 January 2009, Santiago, Chile, GECAMIN Ltd., Santiago, Chile, 2009, 1031-1040.
[25] P.V. Riboud in 'Metallurgie des Stranggießens, Gießen und Erstarren von Stahl', (Herausgeber K. Schwerdtfeger), Eigenschaften und Aufgaben von Stranggießschlacken, Verlag Stahleisen mbH, Düsseldorf, Germany, 1992.
[26] C. Perrot, J.N. Pontoire, C. Marchionni, M.R. Ridolfi and L.F. Sancho, Several slag rims and lubrication behaviours in slab casting. Proc. 5th Eur. Continuous Casting Conf., 20-22 June 2005, Nice, France, 2005, La Rev. Métall., Paris, France, 2005, Volume 1, 36-46.
[27] K. Lerch and C. Sowa, Metallurgica, Personal communication, 2007.
[28] I. Marschall and H. Harmuth, Investigation of slag rim growth in the continuous casting process. Proc. 3rd Int. Conf. on Process Development in Iron and Steelmaking (SCANMET III), 8-11 June 2008, Luleå, Sweden, MEFOS AB, Luleå, Sweden, 2008, Volume 2, 419-426.
[29] A. Ferretti and T. Cimarelli, Kempro, Personal communication, 2005.
[30] W.H. Emling, Breakout prevention, part 2. Ironmaking Steelmaking, 21 (1994) No.6, 43-44.
[31] C-Å. Däcker, M. Glaes, S.P. Andersson, A. Salwén and C. Eggertson, Influence of slag rim formation on initial solidification of stainless steel. Proc. 6th Eur. Conf. on Continuous Casting, 3-6 June 2008, Riccione, Italy, Associazione Italiana di Metallurgia, Milano, Italy, 2008, 88.pdf.
[32] M. Emi, The mechanisms for sticking type break-outs and new developments in continuous casting mold fluxes. Proc. 74th Steelmaking Conf., 14-17 April 1991, Washington, USA, Iron and Steel Society, Warrendale, USA, 1991, 623-630.
[33] R.B. Mahapatra, J.K. Brimacombe and I.V. Samarasekera, Mold behavior and its influence on quality in the continuous casting of steel slabs: Part II. Mold heat transfer, mold flux behavior, formation of oscillation marks, longitudinal off-corner depressions, and subsurface cracks. Met. Trans. B, 22 (1991) 875-888.
[34] J.J. Kim, S.K. Kim, J.W. Kim, S.D. Shim and Y.D. Lee, Application of mold thermal monitoring system of improving slab surface quality at POSCO stainless steel works. Proc. 17h Process Technology Conf., 2000, Orlando, USA, Iron and Steel Society, Warrendale, USA, 2000, 1009-1018.
[35] R.V. Branion, D.A. Dukelow, G.D. Lawson, J. Schade, M. Schmidt and H.T. Tsai, Standardized testing of mold powder properties. Proc. 78th Steelmaking Conf., 2-5 April 1995, Nashville, USA, Iron and Steel Society, Warrendale, USA, 1995: 647-653.
[36] K. Koyama, K. Nagano, Y. Nagano and T. Nakano, Design for chemical and physical properties of continuous casting powders. Nippon Steel Tech. Rep., 34 (1987) 41-47.
[37] N. Pradhan, M. Ghosh, D.S. Basu and S. Mazumdar, Prediction of slag pool thickness in continuous casting mould. ISIJ Int., 39 (1999) 804-808.

[38] C-Å. Däcker, C. Eggertsson and J. Lönnqvist, Development of a laboratory method for characterisation of mould powder melting rate. Proc. 8th Int. Conf. on Molten Slags, Fluxes and Salts (MOLTEN2009), 18-21 January 2009, Santiago, Chile, GECAMIN Ltd.: Santiago, Chile, 2009, 1111-1120.
[39] M. Görnerup, M. Hayashi, C-Å. Dåcker and S. Seetharaman, Mold fluxes in continuous casting of steel – characterization and performance tuning. Proc. 7th Int. Conf. on Molten Slags, Fluxes and Salts, 25-28 January 2004, Cape Town, South Africa, The South African Institute of Mining and Metallurgy, Johannesburg, South Africa, 2004, 745-752.
[40] S. Basu, T. Matsushita, A.K. Lahiri and S. Seetharaman, Property measurement of slags and fluxes towards slag design in BOF and continuous casting. Proc. 16th IAS Steelmaking Conf., 6-8 November 2007, Rosario, Argentina, Instituto Argentino de Siderurgia, San Nicolas, Argentina, 2007, 233-242.
[41] C. Orrling, A.W. Cramb, A. Tilliander and Y. Kashiwaya, Observation of the melting and solidification behavior of mold slags. Ironmaking Steelmaking, 27 (2000) 53-63.
[42] H. Litterscheidt in 'Gießen und Erstarren von Stahl III', Untersuchung des Verhaltens von Gießpulver beim Stranggießen, Abschlußbericht, EUR 8569, Forschungsvertrag Nr. 7210.CA/112, Verein Deutscher Eisenhüttenleute, Düsseldorf, Germany, 1984.
[43] R.M. McDavid and B.G. Thomas, Flow and thermal behavior of the top surface flux/powder layers in continuous casting. Met. Trans. B, 27 (1996) 672-685.
[44] E. Macías, A.H. Castillejos, F.A. Acosta, M. Herrera and F. Neumann. Modelling molten flux layer thickness profiles in compact strip process moulds for continuous thin slab casting. Ironmaking and Steelmaking, 29 (2002) 347-358.
[45] J.A. Kromhout, M. Kawamoto, M. Hanao, Y. Tsukaguchi, E.R. Dekker and R. Boom, Development of mould flux for high speed thin slab casting. Steel Research Int., 80 (2009) 575-581.
[46] M. Kawamoto and M. Hanao, Sumitomo Metal Industries, Personal communication, 2006.
[47] J.A. Kromhout and D.W. van der Plas, The melting speed of mould powders, determination and application in casting practice. Ironmaking and Steelmaking, 29 (2002) 303-307.
[48] M. Wissler, Graphite and carbon powders for electrochemical applications. Journal of Power Sources, 156 (2006) 142-150.
[49] J.A. Kromhout, A.A. Kamperman, M. Kick and J. Trouw, Mould powder selection for thin slab casting. Ironmaking and Steelmaking, 32 (2005) 127-132.
[50] K.C. Mills, J.A. Kromhout, A. Hamoen and R. Boom, Selection of mould fluxes for thin slab casting. Proc. AdMet, 27-30 May 2007, Dnipropetrovsk, Ukraine, National Metallurgical Academy of Ukraine, Dnipropetrovsk, 2007, Volume 2, 174-181.
[51] S. Kenjereš and K. Hanjalić, Numerical simulation of magnetic control of heat transfer in thermal convection. Int. J. Heat and Fluid Flow, 25 (2004) 559-568.
[52] Y. Wang, Research on cold-rolling material production in ultra-thin hot rolling line. Proc. 2nd CSM - VDEh - Seminar on Metallurgical Fundamentals, 18-19 June 2007, Düsseldorf, Germany, Steel Institute VDEh, Düsseldorf, Germany, 2007, 342-353.
[53] J.A. Kromhout, S. Melzer, E.W. Zinngrebe, A.A. Kamperman and R. Boom, Mould powder requirements for high-speed casting. Steel Research Int., 79 (2008) 143-148.
[54] P.R. Scheller, Redox reactions in slags during continuous casting of stainless steel. Proc. Mills Symposium, 22-23 August 2002, London, United Kingdom, The Institute of Materials, London, United Kingdom, 2002, Volume 2, 487-493.
[55] M. Emi, Nippon Thermochemical Co., Personal communication, 2005.

[56] P.R. Scheller, TU Bergakademie Freiberg, Personal communication, 2006.
[57] J-F. Holzhauser, ThyssenKrupp Nirosta, Personal communication, 2006.
[58] D.D. Double and A. Hellawell, The nucleation and growth of graphite – the modification of cast iron. Acta metall. mater. 43 (1995) 2435-2442.
[59] B. Francis, Heterogeneous nuclei and graphite chemistry in flake and nodular cast irons. Met. Trans. A, 10 (1979) 21-31.

5 Solidification of mould slag

5.1 Introduction

During infiltration, a slag film is formed which consists of a solid part at the mould side and a liquid part at the strand side. A very large temperature gradient (approximately 1000 °C) exists across the slag film generating different regions: liquid in contact with the strand, amorphous and crystalline layers adjacent to the mould. Strand lubrication is realised by the liquid part of the slag film. This part moves together with the strand and is mainly accountable for slag consumption during casting. The solid slag does not move or moves very slowly; this part acts as a substantial thermal barrier which controls the horizontal heat transfer. An illustration of parameters affecting the formation of the slag film is given by Mills [1]. This illustration was slightly adapted for high speed thin slab casting, Figure 5.1.

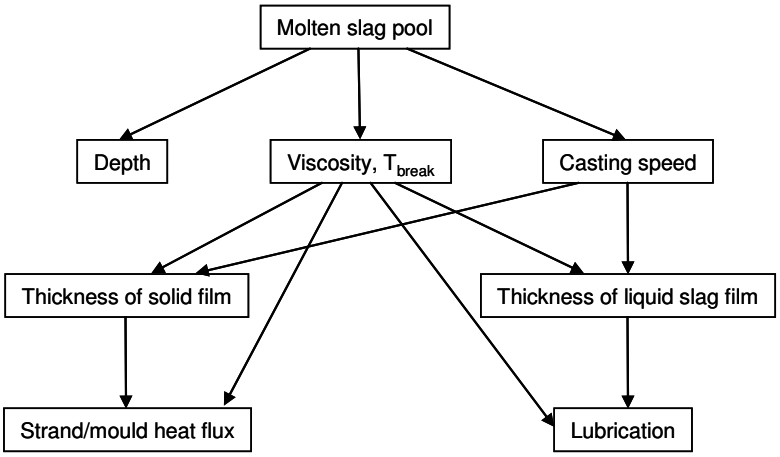

Figure 5.1: *Schematic representation of the factors affecting the formation of liquid and solid slag films [1]*

Section 5.2 reviews mechanisms of and effects on the solidification of mould slag. Investigations on slag solidification are described in Section 5.3, followed by effects of the cooling rate in Section 5.4. Characterisation of various slag films is described in Section 5.5, followed by remarks on the powder consumption in Section 5.6. Additional experiments focussing on the heat transfer through a slag film and slag crystallisation around the break temperature are described in Sections 5.7 and 5.8. An evaluation of the surface roughness of slag films can be found in Sections 5.9, concluding remarks are given in Section 5.10.

5.2 Mechanisms of and effects on slag solidification

5.2.1 Solidification and crystallisation of mould slag

As mentioned in Chapter 2, slag crystallisation depends on the chemical composition, the cooling rate and the presence of nucleation sites. Melting and in particular solidification

experiments on various slag compositions were done in order to identify the crystal phases formed in mould slag. It was found that cuspidine is always formed due to the presence of fluorine. Significant amounts of crystals such as combeite, nepheline and gehlenite can be present as well, depending on the chemical composition of the slag, in particular on the amounts of Na_2O and Al_2O_3 [2,3]. Furthermore, the presence of alkali oxides enhances cuspidine crystallisation, both by lowering the melting temperature and by increasing the mobility within the mould slag. It was found that the effectiveness of alkali oxides is in the order $Li_2O>Na_2O>K_2O$ [4]. Effects of Na_2O on cuspidine formation can also be described by considering phase relations in the mould slag.
A well known illustration, based on investigations of 30 slag samples with a CaO/SiO_2 ratio close to one is given in Figure 5.2. Note that cuspidine is excluded from this figure. A = Al_2O_3; C = CaO; Fl = CaF_2; N = Na_2O and S = SiO_2.

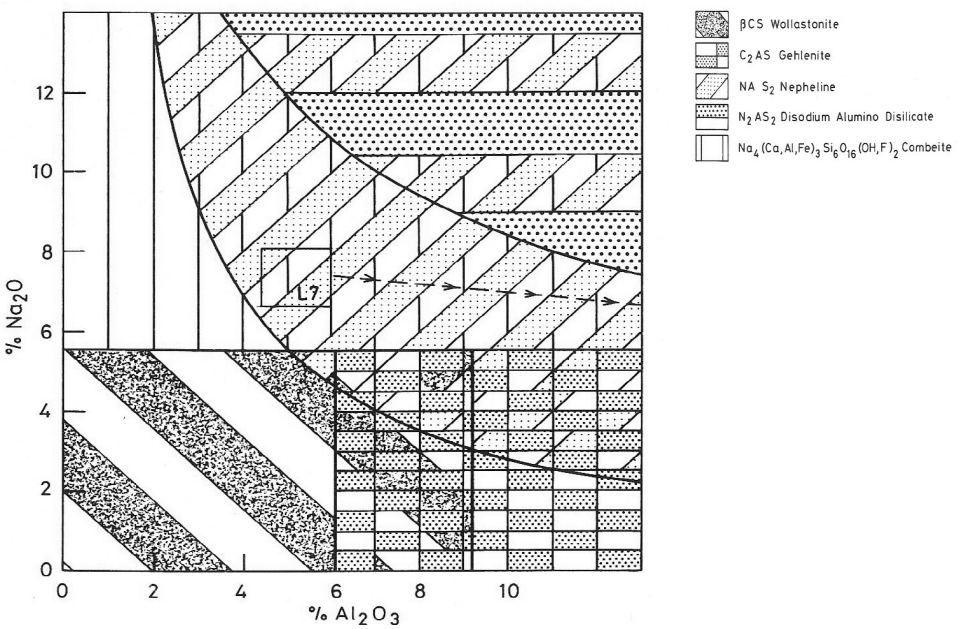

Figure 5.2: *Phases formed by mould powders on solidifying from melt; cuspidine has been excluded to improve clarity [2]*

The formation of cuspidine as well as the phase diagram has been investigated further during the past decade [5,6,7]. This has resulted in an increased understanding on slag crystallisation. However, several aspects of slag crystallisation are still unknown [8].

Thermodynamic calculations using the FactSage software tool were performed to evaluate the chemical interactions between a mould flux in contact with TRIP steel [9]. This work shows a nice similarity between calculated and experimental results and it is suggested that computational thermodynamics can be used to predict the chemical interactions of mould slag in contact with liquid steel. Up to now, reliable thermodynamic calculations on mould slag using FactSage are considered very difficult or even impossible due to the lack of essential thermodynamic data e.g. data on cuspidine and several other crystalline phases, mainly associated with fluorine and sodium.

In 2010, attempts were reported on thermodynamic *modelling* of CaF_2 oxide systems [10]. In this work, essential thermodynamic data and for instance the role of the F^- anion in the silicate system are obtained using *models* and calculations. As a next step, the FactSage software is used for calculations on the solidification and crystallisation of various slag systems. It should be noted that results on slag crystallisation can only be considered as a first step. Important thermodynamic properties are missing and this work – though perhaps not intentionally – underlines the need for reliable input data, obtained by experiments.

5.2.2 Effects of the cooling rate

At Carnegie Mellon University, Pittsburgh, USA, single and double hot thermocouple techniques (SHTT and DHTT) were developed for direct observation and measurement of mould slag crystallisation [11,12]. SHTT and DHTT techniques enable in situ observation and quantification of melting and solidification processes of transparent slags, applying high cooling rates (SHTT) and large temperature gradients (DHTT). This work was continued by researchers at TU Bergakademie Freiberg, Germany and IRSID, France where IRSID concentrated on quenching experiments of various oxide melts including mould slags [13,14]. In the work of TU Freiberg and Carnegie Mellon University, it is assumed that the cooling rates in continuous casting are in the range from less than 1 °C/s to 20 °C/s and even 100 °C/s. The techniques at both institutes roughly cover a major part of this range.

Effects of the cooling rate on several slags and a mould powder were studied. Results can be summarised in TTT-diagrams (time-temperature-transformation). A conclusion of this work is that crystallisation of mould slag can be described by *nucleation* and *growth* of individual crystals in an *undercooled* liquid. There is no specific crystallisation temperature for a mould flux but a range of temperatures, defined by experimental conditions i.e. cooling rates. The start of crystallisation will shift to lower temperatures with increasing cooling rate.

Each phase formation needs time for necessary diffusion of the components. If the time for diffusion decreases (i.e. suppressing diffusion), the undercooling must increase to make crystal formation thermodynamically favourable. At very high cooling rates, solidification occurs as glass or a partly crystalline phase. As the slag can undercool significantly below its equilibrium liquidus temperature, the phase diagram – if existing – will not necessarily be useful to determine the conditions under which crystallisation will occur.
Additionally, the results also show that nucleants like ZrO_2 can be used to modify the crystallisation behaviour. Furthermore, it was clearly demonstrated that an increased viscosity of the melt suppresses the diffusion.

An illustration of a TTT-diagram with the characteristic parabolically shaped curve (C-curve or nose curve) is given in Figure 5.3. Crystallisation (nucleation and growth) increases with decreasing temperature because the thermodynamic driving force increases. On further cooling, this influence is overcome by the kinetic hindrance due to the increased viscosity [15]. Note the nose temperature (T_{nose}) and nose time (t_{nose}); the nose time is the shortest time needed for growth, the corresponding temperature is called the nose temperature.

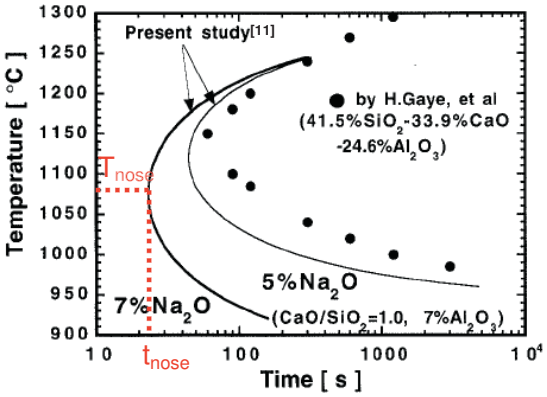

Figure 5.3: *TTT curve obtained by SHTT experiments [11]*

T_{nose} can be described as:

$$T_{nose} = 0.86T_{liq} \tag{5.1}$$

where T_{nose} = nose temperature (°C) and T_{liq} = liquidus temperature (°C) [14].

The critical cooling rate i.e. the rate of cooling to avoid crystallisation (more precisely to avoid a fraction of crystallised volume above 10^{-6}) can be estimated by:

$$r_c = \Delta T / t_{nose} = (T_{liq} - T_{nose}) / t_{nose} \tag{5.2}$$

where r_c = critical cooling rate (°C/s) and t_{nose} = nose time (s).

Basic mixtures of CaO and SiO_2 did not show a macroscopic precipitation of crystals. This might be due to the high viscosity of these slags or the transparent nature of the formed pseudo-wollastonite which makes it hard to detect. Additions of Al_2O_3 result in a lower crystallisation tendency whereas additions of CaF_2 promote crystallisation. The latter can be related to the formation of cuspidine (melting temperate = 1407 °C) and more important, to a decreased viscosity of the melt. It was also found that additions of Na_2O enhance crystallisation, most likely due to a decreased viscosity. Water vapour enhances slag crystallisation as well.
During several experiments, the formation of gas bubbles was observed. It is suggested that bubble formation is caused by evaporation of Na_2O and possibly F.

DHTT experiments with an applied temperature gradient typical for continuous casting showed that crystallisation starts at lower temperatures and proceeds to the hot side (strand). Industrial samples showed a similar layered structure, confirming the experimental findings [13].

In-depth studies on slag solidification and crystallisation were done using SHTT and DHTT techniques. The crystal morphology depends on the experimental temperatures and hence on the viscosity within the sample. Equiaxed crystals with a dendritic structure are

observed at higher temperatures followed by a mixture of equiaxed dendrites and columnar crystals at lower temperatures. Subsequently, columnar crystals are found, followed by facetted crystals and finally fine crystals at high undercooling. With a decreasing temperature, the viscosity increases and the fluid flow within the sample decreases which will result in slower mass diffusion during crystallisation [16].

5.2.3 The formation of slag films

In contrast with the great importance for continuous casting, only a few papers have been issued on sampling and characterisation of slag films. In general, slag films are obtained by lowering the steel level in the mould (for instance at the end of a sequence) and consequently at a decreased casting speed (slab casters). The films easily peel off from the mould walls and are sampled for investigation purposes. Many slag films show evidence of alumina pick-up (~2-3 wt%) due to the use of Al-killed steels (aluminium to deoxidise the steel). Due to the sampling method, the slag films and in particular the thickness of the glassy layer (strand side) will be modified by the decreased casting speed and by "painting" of the surface of the slag film (strand side) with extra liquid slag coming from the liquid pool. These two effects are not mentioned by most researchers.

One paper focuses on the thickness of various slag films [17]. Mould powders with an increased crystallisation tendency i.e. mould powders for crack-sensitive (peritectic) steel grades, result in a thicker slag film than mould powders with a more amorphous solidification as applied in casting low carbon steel grades. Furthermore, slag films coming from the wide faces of the mould show a thickness of up to 4 mm for medium carbon steels and up to 2.2 mm for low carbon steels. Slag films coming from the narrow faces show values around 2.7 mm and between 1.8 and 2 mm, respectively. It has been reported that increased crystallisation of the slag film will result in a reduction of radiative mould heat transfer during casting and in less or even poor strand lubrication. In all slag films, the main crystalline phase is cuspidine, complemented with minor crystalline amounts such as wollastonite, ghelenite and nepheline.
Comparable work on slab casters was done with special attention to the structure of the slag films [18]. All samples in this work originate from the wide faces of the mould. Sampling was applied on four mould powders and two steel grades (low carbon and medium carbon steel). The basicity (CaO/SiO_2) varies between 0.9 and 1.3, the casting speed between 0.7 and 1.3 m/min and the powder consumption rate between 0.6 and 0.7 kg/tonne (steel). The slag films always show one crystalline layer at the mould side and an amorphous layer at the strand side. The crystalline layer contains cuspidine as the main crystal; fluorite and nepheline can be detected additionally. The crystalline layer contains bubbles. In general, the crystalline layer appears to be thicker than the amorphous layer. The total film thickness varies between 1.5 and 2.5 mm and is found to *increase* with increasing basicity (CaO/SiO_2), due to the increased thickness of the crystalline layer. In contrast, the thickness of the amorphous phase is practically constant over the basicity range. No evidence of casting speed influence on the thickness of the slag film has been reported.

Slag films for casting medium carbon, low carbon and ultra low carbon steels were investigated. XRD analyses indicate a crystallinity of approximately 85%, 65% and 45%, respectively. The corresponding thickness is between 2 and 4.5 mm for medium carbon steel and between 1 and 2 mm for low and ultra low carbon steels. As before, two layers can be observed within the slag film: a (sometimes) dense crystalline layer with dendrites growing into an amorphous layer [19]. Information about the thickness of slag films,

sampled under the mould and the composition of some slag films is given; all films were obtained during/after slab casting [20]. The thickness roughly varies between 1 and 3.5 mm. In this overview, powders used for peritectic steels proved to have both the thinnest and thickest slag films! Furthermore, the sometimes heterogeneous composition of slag films is mentioned which may have an effect on the solidification of the strand. Some attention to slag films was given by Nippon Steel Corporation in the pioneering work on mould powders for continuous casting [21]. Effects of the casting speed on the film thickness are described. The thickness of slag films sampled *under the mould* proved to be between 0.3 and 0.5 mm. Evidence of long residence times of the slag film in the mould (>1 hour) was found.
It has been tried to determine the crystallinity of slag films using various techniques such as XRD, microscopy and thermal analyses. Although there is some reasonable agreement between the percentage glass obtained by various techniques, further developments are needed [22].

The thickness of the slag film was calculated using a mathematical model of mould flux infiltration and mould heat transfer [23]. Results confirm previous results of Sumitomo were it was found that the thickness of the slag film is directly related to the casting speed:

$$d = 0.9464 v_c^{-0.4895} \qquad (5.3)$$

where d = slag film thickness (mm) and v_c = casting speed (m/min) [24].

An illustration of this relation is given in Figure 5.4.

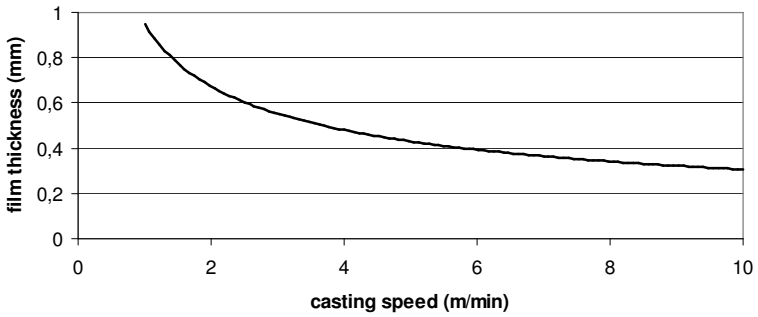

Figure 5.4: *Slag film thickness as a function of the casting speed [24]*

The equation is based on about 100 slag film samples, obtained from *under the mould* of a pilot caster (QSP), for casting speeds between 1 and 5 m/min. The basicity (CaO/SiO_2) of the mould powders varies between 0.95 and 1.6. The mould slags have low and very low viscosities with values between 0.01 and 0.07 Pa·s at 1300 °C.
It should be noted that the relationship between the slag basicity and the slag film thickness, as described for slab casting, was not found by the researchers of Sumitomo. This can be a result of the increased castings speeds and hence the thinner slag films as well as the crystallisation tendency of these mould powders. Due to the sampling method, the slag films will not show effects of additional “painting” (thicker layers).

Impressive work on slag films was done by Hooli at Outokumpu Tornio Works, Finland [25]. Slag film samples were taken from the mould at the end of casting sequences of stainless steel. A special tail-out practice was developed in order to get representative samples, knowing the original locations in the mould. Furthermore, the original thickness of the slag films was defined, considering the "painting" effects during sampling.
Slag film samples were investigated focussing on the structure and the composition. All samples contain a dominant cuspidine layer and an amorphous layer, the latter mainly formed during tail-out. The crystalline structure is formed during solidification or via devitrification. Furthermore, the crystals nepheline and NaF can be observed.
It was also found that the films can show very long residence times (several hours) on the mould wall. During this period, complex structures will develop, containing sub-layers, voids and pores. In particular the formation of a NaF layer and Na stuck to the mould wall is remarkable.
Variations in the surfaces of the slag film samples (mould side) are mentioned. These variations are explained by the fact that sometimes a thin layer remained on the mould wall during sampling. These remnants (mould wall) are rich in Na and it is suggested that Na acts as glue between the mould wall and the solid film. Furthermore, the rounded pores in the crystalline parts indicate the presence of Na and NaF (vapour) as well. Sublimation of gaseous NaF is found to be a cause of the presence of voids. During crystallisation and shrinkage, more voids are formed. The surface at the strand side proved to be very smooth. Furthermore, wave lines can be detected at the surface (mould side) of some samples, indicating oscillation marks and forced spreading (pumping) of the liquid slag on the (non-wetting) mould surface. Fractures and "bleed" are observed in some slag films. Fracturing of the slag films is discussed in Chapter 7.
Lainez (billet casting) reports waves at the mould-rim interface (slag film). The waves are perpendicular to the casting direction and are probably caused by the oscillation movement of the mould [26].

The results described by Hooli are largely confirmed by slag films, obtained from inside the mould of a conventional slab caster (casting speed between 0.8 and 1.0 m/min). It is noted that the surface of one of the slag films showed a folded appearance (mould side). Another slag film showed vertical stripes of crystalline material ("network") with stripes of glassy material in between. Breaking of the slag film, followed by refilling with liquid slag is also mentioned [27]. This work demonstrates first results of thermodynamic calculations on mould slag.

5.2.4 On the surface roughness of slag films

The interface between the slag and the mould is mentioned to be an important subject for further understanding of mould heat transfer during casting [28]. At TU Clausthal, Germany, experiments were done using a laboratory set-up which consists of a heated steel plate with a trough of 7 mm depth; the trough containing (liquid) mould slag [29,30]. The upper part of the apparatus is a heat flux probe made of copper. It was found that when immersing the cold probe into the slag melt, the upper part of the slag solidified very rapidly. Consequently, a rough mould flux interface (i.e. *wrinkles*) was formed causing a contact resistance or an interfacial thermal resistance during heat removal. It should be noted that the wrinkles are *only* formed due to chilling i.e. very rapid cooling of the liquid slag. Experiments with a pre-heated surface did not result in any formation of wrinkles. The wrinkle depth i.e. surface roughness was found to be up to approximately 100 μm and proved to be dependent on the thickness of the slag film within the range between 1.5 and 4 mm. The presence of wrinkles, acting as an interfacial thermal

resistance between the slag film and the copper, played a crucial role during these experiments.

The concept of *system conductivity* (k_{sys}) was introduced which consists of radiation and conduction properties of the mould slag (slag film) as well the contact resistance at the interface:

$$k_{film} = k_{rad} + k_{cond} \tag{5.4}$$

$$k_{sys} = k_{film} + k_{Cu/sl} = k_{rad} + k_{cond} + k_{Cu/sl} \tag{5.5}$$

where k = the heat transfer coefficient (W/mK). The subscripts *film*, *rad* and *cond* denote the slag film, radiation and conduction, respectively. Furthermore, the subscripts *sys* and *Cu*/*sl* denote the *total* slag film including the surface roughness at the interface between the copper and the slag film *Cu*/*sl*.

Later, it was stated that the upper part of the mould will show a *microscopic* gas gap due to the formation of wrinkles (quenching of slag on a cold surface) and that the lower part of the mould will show a *macroscopic* gas gap due to shrinkage of the steel shell and possibly breaking of the slag films. The microscopic gas gap was believed to play an important role during continuous casting [29].

Researchers at NKK Fukuyama (now JFE Steel Corporation) addressed additional effects of heat treatment (reheating) and crystallisation on the surface of the wrinkles and consequently on the interfacial thermal resistance. These experiments were based on a comparable laboratory set-up [31]. The importance of an interfacial thermal resistance, in particular for mould powders with an increased basicity (CaO/SiO2 = 1.1 and 1.6) was also underlined by researchers at Nippon Steel Corporation [32]. This work was mainly based on comparable laboratory scale experiments as mentioned above. Comparable findings obtained at Tohoku University, Japan have been reported previously [33].

Mould powder investigations using an alternative laboratory set-up revealed a surface roughness i.e. air gap at the slag – copper interface with a thickness between 20 and 50 µm. The surface roughness can be understood by considering the *solidification temperature* of the mould slag. It was found that an interfacial thermal resistance (air gap) will develop if the solidification temperature is higher than the temperature of the mould surface [34].

It should be noted that k_{sys} is dependent on the position and temperatures in the mould i.e. on the local values of k_{rad}, k_{cond} *and* $k_{Cu/sl}$. Furthermore, effects of the ferrostatic pressure (molten steel) during casting were not considered during these experiments. It can be assumed that the ferrostatic pressure, present during continuous casting, will reduce the surface roughness of the slag film and hence the interfacial thermal resistance during casting.

Tsutsumi et al. investigated the surface roughness of slag films with a confocal scanning laser microscope using cooling rates up to 30 °C/s [35]. They concluded that the surface roughness is mainly in the range between 10 and 30 µm and is caused by crystallisation of the mould slag. The surface roughness decreases with a higher cooling rate and increases

with an increase of the *critical cooling rate* of the mould slag. The size of the crystals at lower cooling rates appeared to be larger, resulting in an increased (larger) surface roughness.

As crystallisation not only depends on the actual cooling rate but also on the critical cooling rate, the *ratio* of the actual cooling rate and the critical cooling rate was defined as the *normalised* cooling rate r_n:

$$r_n = r_a / r_c \tag{5.6}$$

Where r = cooling rate, the subscripts n, a and c denote normalised, actual and critical, respectively.

No crystalline phases should precipitate when the normalised cooling rate r_n is greater than unity. The normalised cooling rate was used to investigate the relation with the surface roughness of various mould fluxes, Figure 5.5.

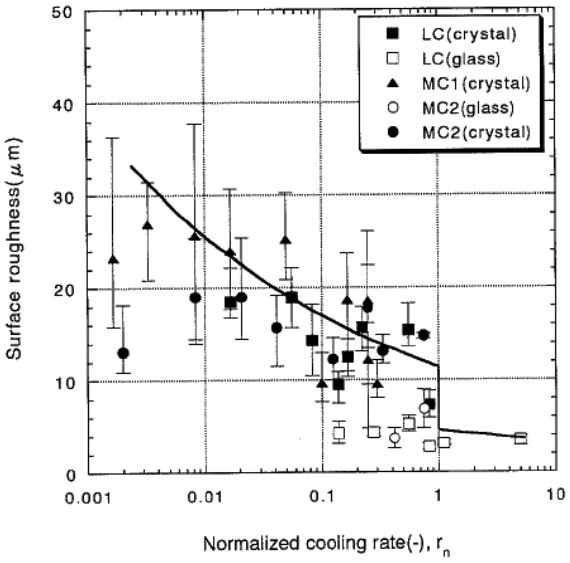

Figure 5.5: *Relation between normalised cooling rate (r_n) and surface roughness [35]*

Yamauchi et al. investigated mechanisms for mould heat transfer at the meniscus area, more precisely effects of slag crystallisation and the corresponding surface roughness [36]. Trials were done at a pilot caster with two mould powders having a basicity of 0.95 and 1.3 and corresponding solidification temperatures of 950 °C and 1190 °C, respectively. Slag films obtained from inside the mould of the caster proved to have a thickness between 200 and 450 µm for both mould powders. The surface roughness was around 5 µm for the mould powder with a medium basicity (CaO/SiO_2 = 0.95) and 12 µm for the high basicity mould powder (CaO/SiO_2 = 1.3).
Experiments using a laser scanning microscope with the same mould powders revealed for glassy samples a smooth surface and after annealing at 900 °C during 60 s, a surface

roughness of approximate 30 µm for *both* (crystalline) materials. It was concluded that the contact resistance or interfacial thermal resistance (mould - slag film) is essential to control mould heat transfer when using crystalline (high basicity) mould powders and that this resistance is highly affected by the solidification point (and hence crystallisation tendency) of the mould powder.

However, the significant differences between surface roughness values as measured on *slag films* obtained at a pilot caster and on samples measured under *laboratory conditions* should be noted. Up to now, this phenomenon is hardly or even not recognized.

Up to now it is generally accepted that the surface roughness, more specifically the interfacial thermal resistance $R_{Cu/sl}$ plays a major role in controlling the mould heat transfer (horizontal heat transfer) during casting. In this view, the surface roughness acts as an important barrier for mould heat transfer which can be described by:

$$R_{sys} = R_{film} + R_{Cu/sl} = \frac{d_{film}}{k_{film}} + \frac{d_{Cu/sl}}{k_{Cu/sl}} \qquad (5.7)$$

where R = thermal resistance (m^2K/W).

In 2008, it was demonstrated again that the effect of the interfacial thermal resistance and the corresponding surface roughness is not as large as widely assumed. This work is based on *slag films*, sampled from the mould of a pilot caster and on corresponding one-dimensional heat transfer calculations. As a result, a surface roughness up to 10 µm is suggested. The relatively low value of the surface roughness is assumed to be caused by the static pressure of steel during casting [37].

Calculations on the surface roughness were carried out by addressing both the *thermal* stress due to shrinkage of the slag film during solidification and *mechanical* stress due to the static pressure from molten steel, molten slag and the shear stress of molten slag. The surface roughness was found to be around 10 µm at a position of 8 mm under the steel meniscus; the thickness of the corresponding slag film varied between 800 and 950 µm [38].

5.2.5 Some developments in controlling mould heat transfer

Research done by Nakada and Hayashi in 2009 and before confirmed that slag crystallisation reduces the heat transfer (horizontal heat transfer). They found that *reflection* of radiation due to the presence of crystals is an important mechanism for this reduction [39,40]. The reflection can occur at the interface between the liquid slag and the crystalline slag layer and at the crystal grain boundaries. Increasing reflectivity by crystallisation will lead to more scattering of radiation and hence in a reduced mould heat transfer i.e. mild cooling, Figure 5.6.

However, it was also found that the reflection of radiation at the *interface* between the liquid and the crystalline slag layer is the dominant factor to control mould heat transfer and that reflection within the slag film, i.e. reflection at the crystal grain boundaries, is of less importance or even does not affect the total heat flux. Consequently, the thickness of the slag film and the surface roughness may be less important than usually assumed. Crystals showing a larger width of dendrites at the slag interface proved to be most effective in controlling mould heat transfer (reflection of radiation). From a theoretical

point of view, this will result in a required *cooling rate* for a given mould flux. No radiation from the shell will be transported to the mould if the crystallised mould flux acts as a perfect *reflector*.

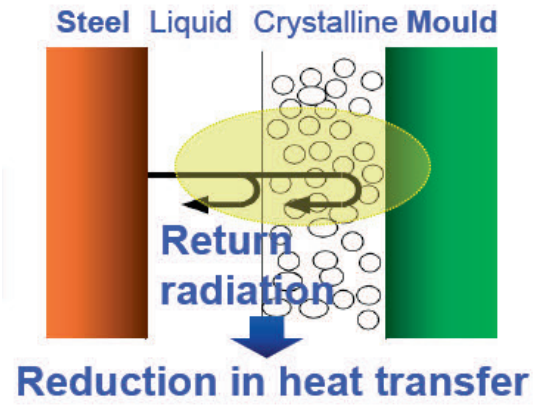

Figure 5.6: *Mechanism of the reduction of mould heat transfer, due to crystallisation [40,41]*

A description of the optical process where light interacts with the crystallised mould flux can be based on reflection (R), absorption (A) and transmission (T). Some light will be transmitted through the slag film and the remainder will be absorbed or reflected:

$$R = 1 - A - T \tag{5.8}$$

To increase the value of R, it is required to decrease the values of A and T. This can be realised by decreasing the amount of absorbing metal oxides like iron oxides (decrease of A) and the introduction of less translucent materials (decrease of T).

Effects of slag crystallisation and the presence of iron oxides on radiative heat transfer in mould fluxes were investigated by Susa et al. using a spectrophotometer with an integrated sphere covering the wavelength range between 300 and 2600 nm [42]. Measurements focussed on the investigation of the apparent reflectivity and transmissivity of various slags. Usually, the presence of scattered light is a serious problem in reflectivity and transmissivity measurements on polycrystalline samples. In this work, however, the installation of an integrating sphere enabled all scattered light to be collected and detected.

In this work, an evaluation method for radiative heat transfer of mould fluxes is proposed which is based on the ratio:

$$I_{Total} / I_s \tag{5.9}$$

where I_{Total} = the total energy which may reach the mould and I_s = the energy radiated from the shell. Smaller values of I_{Total}/I_s mean that the radiative heat transfer is smaller, resulting in mild cooling. It was found that the ratio I_{Total}/I_s can be expressed by the equation:

$$I_{Total} / I_s = \left[T_a + (1-R_a-T_a)(1-T_f^4 / T_s^4)\right] \times \left[1-(1-\varepsilon_s)R_a\right]^{-1} \qquad (5.10)$$

where R_a = apparent reflectivity and T_a = apparent transmissivity; T_f and T_s are the temperatures of the solid flux and the shell, respectively (K), and ε_s = emissivity of the shell. Smaller ratios of I_{Total}/I_s, i.e. mild cooling, can be obtained by increasing R_a and decreasing T_a.

The reflection and transmission of several mould fluxes were measured in air at room temperature as a function of the degree of crystallinity (0~60%) and the concentration of iron oxides (0~2%). The evaluation of results concentrated on a wavelength of 1600 nm which can be related to a temperature of 1536 °C i.e. the melting point of iron where the radiation will be maximum.
It was found that crystallisation of mould slag increases the reflectivity and decreases transmission; this is the mechanism for mild cooling behaviour of mould slags [38]. Additions of iron oxides increase absorption and consequently decrease reflection. A reduction of iron oxides in the mould powder will result in improved mild cooling properties i.e. a further reduction of horizontal heat transfer.

It should be noted that the heat transfer across the slag film is dominated by thermal conduction; the contribution from radiation is 20% or less of the total heat flux in the molten and crystalline slag layers [38]. In some cases, increasing the crystallinity of mould flux may lead to an increased conductive heat transfer, due to an improved contact between the crystals [43]. However, it can be clearly stated that reflection due to crystallisation is a very effective factor for a further reduction of the horizontal heat transfer.

5.3 Investigations on slag solidification

5.3.1 Equilibrium phase relations

Chapter 4 describes equilibrium phase relations of mould powders A to D, observed during heating. These findings are based on high-temperature X-ray diffraction techniques (HT-XRD), supplemented with high temperature properties like the melting trajectory and the viscosity. Details of the mould powders are given in Table 4.11 – 4.15.
As a continuation, phase relations of these powders were investigated *in situ* during cooling of the mould slag. This part of the work concentrates on the crystallisation properties in order to obtain a better understanding of the main mould powder functions. The basic principles of the HT-XRD techniques are described in Chapter 3 and 4.

During cooling mould powder A shows crystallisation of cuspidine ($3CaO{\cdot}2SiO_2{\cdot}CaF_2$ or $Ca_4Si_2O_7F_2$) at a temperature between 1150 °C and 1100 °C. No other major phases were detected using HT-XRD. Mould powder B shows the formation of three phases, all at the same temperature. Crystallisation starts around 1100 °C, i.e. at a temperature comparable to mould powder A. Together with cuspidine, the phases combeite ($2Na_2O{\cdot}4CaO{\cdot}6SiO_2$ or $Na_4Ca_4Si_6O_{18}$) and villiaumite (NaF) are formed. For mould powder A and B the temperature range of complete melting (stability during heating) is comparable to the temperature where the initiation of crystallisation is detected.

Mould powder C shows crystallisation of cuspidine at a temperature around 950 °C, followed by crystallisation of villiaumite at a temperature around 700 °C. Note that the crystallisation of cuspidine in powder C starts at a temperature approximately 100 °C to 150 °C *lower* than the observed stability during heating and also 100 °C to 150 °C lower than the crystallisation of cuspidine in mould powders A or B. For the cooling rates applied during the experiments, crystallisation in mould powder C is *suppressed* (undercooling) compared with A and B; which is probably an effect of the chemical composition and is controlled by nucleation rates of the glass-forming liquids. This effect is not yet fully understood.
Mould powder D clearly shows crystallisation of cuspidine starting around 1200 °C. No other major phases were detected using the HT-XRD techniques. The temperature where the crystallisation starts is somewhat higher than the range of complete melting.

A summary of the cooling experiments is given in Table 5.1 and a complete overview of the phase relations during heating and cooling is given in Figure 5.7. Note that the stabilities may be dependent on actual heating and cooling rates and are strictly valid only for the given experimental conditions.

Table 5.1: *Crystallisation of mould powders for thin slab casting (A-D) (HT-XRD) (°C)*

Crystalline phases	A	B	C	D
cuspidine-in	1150	1100	950	1200
combeite-in		1100		
villiaumite-in		1100	700	

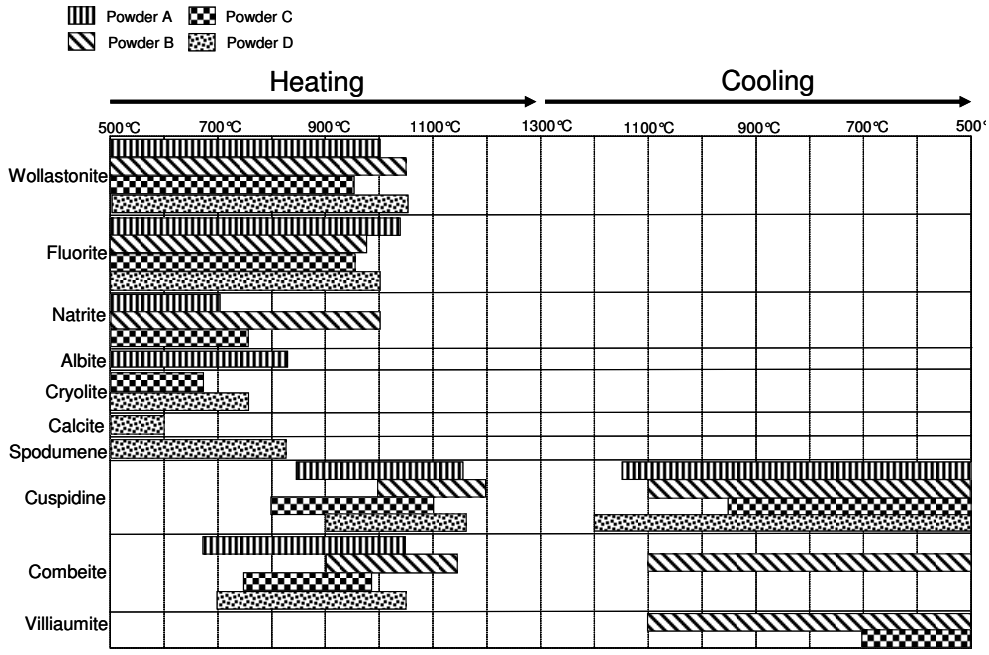

Figure 5.7: *Results of HT-XRD analyses and indications of phase stabilities of major phases, within the four mould powders (heating and cooling)*

After HT-XRD measurements, the remaining mould slags of powder A – C were analysed using XRD-measurements at room temperature. Mould powder A showed cuspidine as the major phase with some minor amounts of combeite and a sodium-aluminium silicate (e.g. nepheline). Mould powder B showed the three phases cuspidine, combeite and villiaumite with some minor amounts of nepheline. Mould powder C showed the two detected phases cuspidine and villiaumite and no additional (minor) crystalline components. Based on the intensities of the XRD-patterns obtained after high-temperature runs, the abundance of crystalline phases can be estimated qualitatively. Note that the samples contain significant proportions of glass, which is not considered in these analyses. A summary of the crystalline phases in mould powder A - C after HT-XRD measurements is given in Table 5.2. No data are available from mould powder D.

Table 5.2: *Estimation of the relative amounts of crystalline phases in mould slag after HT-XRD-measurements*

	A	B	C
Main phases			
cuspidine	+++	++	++
combeite		++	
villiaumite		++	+
Minor phases			
combeite	+		
nepheline	+	+	

+++: major/dominating phase ++: phase present +: minor phase

In general, cuspidine is predominantly formed as a crystalline phase during solidification of mould slag. Especially, the observation of the formation of villiaumite and the presence of only two phases in mould powder C differs from the observations of previous work. The presence of more than one crystalline phase, as in mould powder B, is not described and possible effects on mould heat transfer are not known.

5.3.2 Some calculations on mould slag

In order to obtain an indication of the behaviour of the mould powders during casting, some calculations have been made. The calculations are based on the chemical composition and are focussed on the crystallinity and on the break point or solidification point.

As described in Chapter 2, the crystallinity of mould slag or the crystallisation tendency can be calculated using the NBO/T-ratio: the number of non-bridging oxygen atoms per tetrahedrally-coordinated atom. See Equations 2.7 and 2.28. The crystallinity is expressed by:

$$\%crystallinity = 141.1(NBO/T) - 284.0$$

A relation between the chemical composition and the break point has been given by Sridhar, see Equation 2.11. Based on the chemical composition of the three mould powders, the crystallisation tendency and the break point were calculated. Results are given in Table 5.3.

Table 5.3: *Slag calculations*

	A	B	C	D
Crystallinity (NBO/T) (mole%)	81	79	71	72
Break point (Sridhar) (°C)	1182	1135	1072	1145

Compared with mould powders A and B, a lower crystallinity was calculated for mould powder C. The calculated break point decreased significantly from mould powder A via B to C. This can possibly be related to the increase in Na and the decreased value of basicity for powder C. Like powder C, mould powder D shows a decreased crystallisation tendency but a break point within the range of mould powders A and B.

5.3.3 Summary of data

An overview of the data obtained on slag properties is given in Table 5.4. It is clear that the data on measured and calculated break points for mould powders A, B and C show a similar trend. This trend can be recognized via the (measured) melting temperature and start of crystallisation, as measured using high-temperature XRD. There is a similarity between the melting point, the break point and the start of crystallisation, as measured with HT-XRD. Note that mould powder C shows less crystallisation starting at a lower temperature. Results of mould powder D confirm these trends with the exception of the crystallisation tendency, showing lower values.

Table 5.4: *Comparison of several slag properties*

	A	B	C	D
Melting temperature (measured) (°C)	1088	1026	1045	1055
Break point (measured) (°C)	1167	1110	1054	n/a
Break point (calculated - Sridhar) (°C)	1182	1135	1072	1145
Start of crystallisation (HT-XRD) (°C)*	~1150	~1100	~950	~1200
Number of crystalline phases (HT-XRD)*	1	3	2	1
Crystallinity (NBO/T) (mole%)	81	79	71	72
Basicity (CaO/SiO_2) (-)	1.0	0.9	0.8	1.0

5.3.4 Operational experiences

A general overview of the operational performance of mould powder A - C at a casting speed of 5.4 m/min is given in Table 5.5. Detailed plant data of mould powder D is not available for these analyses. However, it was noticed by the operators that comparing to the standard powder (A), mould powder D showed some improved strand lubrication (friction measurements) and comparable or less rim formation. Excessive scale formation in the first meters of the tunnel furnace impeded a further application of this mould powder.

It should be noted that the liquid pool depth as measured during trials with mould powders A – C showed the same values i.e. between 2 and 4 mm. No significant effect of the amount of free carbon (C_{free}) within these powders was observed. This indicates that the vertical heat transfer (or the lack of vertical heat transfer) dominates powder melting and slag formation. Most likely, this can be related to the EMBr practice at the DSP caster; more specifically the EMBr settings during casting. As demonstrated in Chapter 4, electromagnetic breaking will affect the (vertical) heat transfer in the mould due to the

reduction of turbulent metal flow velocities. The EMBr practice at the DSP caster i.e. the vertical heat transfer mainly determines powder melting and slag formation.

Table 5.5: *Mould powder performance at DSP-caster (v_c=5.4 m/min)*

	A	B	C
Liquid pool depth (mm)*	2-4	2-4	2-4
Rim/lump formation*	some rims, <10 mm	some rims, <10 mm	no rims
Powder consumption (kg/m^2)	0.055	0.065	0.080
Average mould heat transfer (MW/m^2)			
• wide face	2.9	3.0	3.4
• narrow face	2.4	2.4	2,1
Scale formation	no	no	no

* liquid pool depth and rim formation behaviour as measured during stable casting conditions (stable mould meniscus)

Furthermore, it was again observed that rim formation at the DSP is mainly affected by the conditions at the mould meniscus and to a lesser degree by the mould powder properties like the melting point. Mould powder C, with decreased values for the solidification temperatures, almost showed no rim formation.

5.3.5 Thermodynamic calculations

Within the framework of this study an attempt was made to predict crystallisation of mould slag applying the thermodynamic package MTDATA; this software package contains the essential components cuspidine as well as combeite. In 2009, a comparable approach with nice results has been described in a publication on slag films [27].
Calculations focussed on solidification and crystallisation of mould powders A – C. The equilibrium distribution was calculated at 5 degree intervals between 500 and 1300 °C. The outcome of the calculations was compared with results, obtained with HT-XRD experiments. Results of the calculations are summarised in Table 5.6.

Table 5.6: *Calculated crystallisation temperatures of mould powders for thin slab casting (A-C) using MTDATA (°C)*

Crystalline phases	A	B	C
cuspidine	1200	1185	1120
combeite	1105	1130	1105
calcium fluoride	1050	1040	1035

There appears to be a reasonable qualitative agreement between the calculated equilibrium and reported HT-XRD cooling results with respect to the major precipitates appearing upon crystallisation of the slags in that both cuspidine and combeite are predicted to be present.

It should be noted that sodium fluoride is not contained in the MTDATA database. Hence the fluorine in the solid state, other than that associated with cuspidine, is predicted to

exist as calcium fluoride (CaF_2). Factsage does not contain data on the main crystals cuspidine and combeite.
It is obvious that there is a need for reliable thermodynamic input data on mould fluxes, in particular with respect to components based on sodium and fluorine. Up to now, some first and promising results have been reported by Japanese researchers [5,44].

5.4 Effects of the cooling rate

In order to investigate the effect of the cooling rate on slag crystallisation in more detail, measurements were done at TU Bergakademie Freiberg using the single hot thermocouple method (SHTT). The measurements started with the standard mould powder for thin slab casting (mould powder A), followed by a mould powder as developed for high speed thin slab casting. The development of this powder and the characterisation will be described in Chapter 7.
For the measurements, a mould powder was heated at 600 °C for four hours. After crushing in a mortar, the material was heated at 1500 °C for one minute to obtain a homogeneous sample. Then, the sample was cooled with cooling rates of 5, 10, 20, 50, 100, 200 and 500 °C/min. During the measurements, the beginning of crystallisation was observed as well as the time at halfway crystallisation (50%) and the end of crystallisation. These measurements were repeated twice. Slag crystallisation appeared in all samples i.e. at all cooling rates with the exception of a cooling rate of 500 °C/min.

Based on the measurements, a TTT curve (time-temperature-transformation) was constructed followed by an estimation of the nose temperature (T_{nose}) and nose time (t_{nose}). Results are illustrated in Figure 5.8.

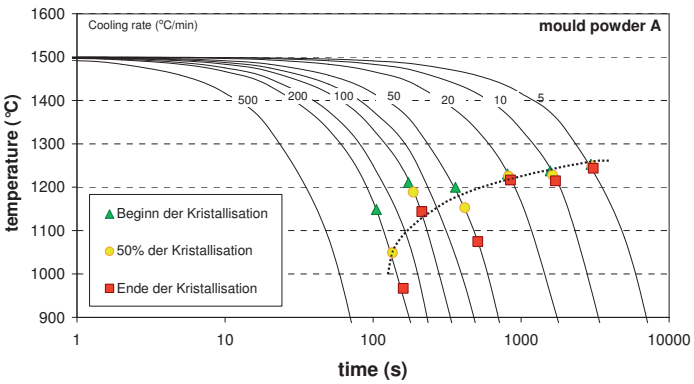

Figure 5.8: *Time-temperature-transformation diagram of a standard mould powder) - Mould powder A*

From these results the nose temperature (T_{nose}) of mould powder A is estimated to be around 1000 °C or lower and the corresponding nose time to be approximately 100 s.

Based on Equations 5.1 and 5.2 and the melting point of mould powder A (1088 °C) as given in Chapter 3, the nose temperature and the critical cooling rate for mould powder A can be estimated:

nose temperature: $T_{nose} = 0.86T_{liq} \approx 936\ ^{\circ}C$

critical cooling rate: $R_c = \Delta T / t_{nose} \approx 1.5\ ^{\circ}C/s$

Direct crystallisation of mould powder A during casting will not occur when the cooling rate exceeds the critical rate.

An estimation of the cooling rate of mould slag in the longitudinal (casting) direction at the DSP is between approximately 35 and 40 °C/s. The local cooling rate, especially near the meniscus, will be considerably higher. Based on these results, it can be concluded that especially at the start of casting, mould powder A will quench, followed by crystallisation (devitrification).

5.5 Slag films

The slag film realises the main powder functions mould heat transfer and strand lubrication and for this reason slag films can be considered as a key for a further understanding of the mould powder functions and to guide mould powder design. Sampling and characterisation of slag film structure and properties is strongly required, but for reasons of process stability and safety, very difficult.
At the thin slab caster, slag film sampling was tried at three locations:

- at the meniscus area
- from inside the mould
- under the mould

Extensive characterisation was done on various samples, in particular on samples coming from inside the mould. All samples are taken from the standard mould powder (mould powder A).

5.5.1 Meniscus area

Slag films adhering to the slag rim (meniscus area) show a dense, slow-growth layer of cuspidine crystals at the mould side (Cu) and an amorphous layer with incidentally some rapid-growth cuspidine crystals at the strand side (Fe). The crystals at the mould side show evidence of recrystallization and a long residence time. Mould powder particles and mould powder raw materials adhere to the strand side of the slag film. Furthermore, bubbles and small metal droplets can be observed in the slag films. The total thickness of the films is between 1 and 1.5 mm and in general, both sides (mould side and strand side) show a smooth surface. An illustration is given in Figure 5.9 (left).
Other samples, obtained after more than 12 hours of casting showed several layers within the film. At the mould side, a porous layer containing cuspidine, Na-Al silicate, NaF, glass and copper particles can be found. Remnants of unreacted and partially reacted starter powder are present as well. The surface is rough and porous and indicates fracturing and damaging after sampling. This first layer is followed by a massive and dense cuspidine layer. Subsequently, *one or more* layers of cuspidine crystals can be observed, followed by an amorphous layer with some rapid-growth (quench) cuspidine crystals. Mould powder remnants adhere to the surface of the film (strand side). The various fronts of dendritic crystals (layers) can probably be related to severe mould level fluctuations during casting. Stirring in the mould by the operators can also have an effect on these slag films.

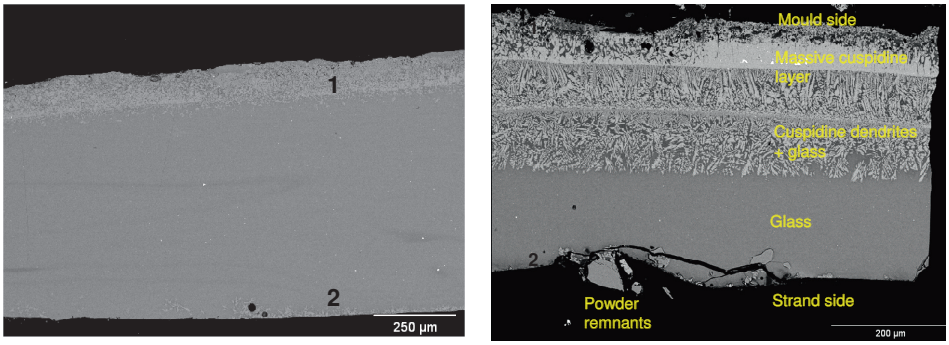

Figure 5.9: *Slag films, sampled from inside the mould (meniscus area), showing glass and cuspidine crystals (left) and extra layers of cuspidine crystals, NaF, pores and bubbles (right). Mould side = 1, strand side = 2 - Mould powder A*

The thickness of the samples varies between approximately 1.5 (upper part, rim) and 0.5 mm. All films show the presence of Fe-droplets, most droplets are smaller than 5 µm but several larger droplets of up to 100 µm can be observed as well.
It can be stated that these slag film samples reflect process instabilities during casting and in particular during the start of casting. Analyses of mould data during the first ladle of the casting sequence shows that the casting speed varied around 4.6 m/min and that different taper settings were applied. After the first ladle, the sequence appears to be more stable with a casting speed between 5.1 and 5.2 m/min and less mould taper variations. An illustration is given in Figure 5.9 (right).

5.5.2 Inside the mould

Slag films from inside the mould were sampled, with great difficulty, immediately after casting. Surprisingly, in addition to slag films, small slag fragments of mould slag were detected and obtained.

Slag fragments, droplets

After casting, remnants of mould slag were present in the funnel area of both wide faces at approximately half depth (~50 cm) of the mould; the fragments adhered to the mould surface. The remnants were subsequently scraped from the mould and collected using a wooden tray. Several slag film fragments were prepared and analysed using SEM/EDS techniques. Slag films, covering the entire mould surface or at least the main parts, as commonly observed at conventional slab casters, were not found during these attempts.

The shape of the slag film fragments proved to be somewhat similar to *droplets* of mould slag. The fragments or "droplets" were between 6 and 20 mm long with a thickness between 0.6 and 2.3 mm. The surface, corresponding to the side in contact with the mould (Cu) sometimes proved to be coarse and "crumbly" which can probably be related to damage of the fragments during sampling (scraping) due to the "sticky" nature. Several fragments are illustrated in Figure 5.10.
The mechanism of formation of these "droplets" is not fully understood. *Contraction* of (remnants of) the thin slag film on the surface of the non-wetting copper mould during emptying the mould seems to be the most reasonable explanation.
The occurrence of both slag droplets and slag film fragments was earlier reported by Lainez after experiments at a billet caster [26]. A mould slag with an increased viscosity

and hence a low slag consumption and slag film thickness showed smaller slag remnants and droplets. Both Hooli and Riboud mention non-wetting behaviour of mould slag to the copper mould. However, detailed information on this surface phenomenon is not given [25,45].

Figure 5.10: *Slag fragments, "droplets", sampled from inside the mould (approx. 50 cm depth) - Mould powder A*

Microscopic analyses of the droplets showed cuspidine crystals and a glass phase. The local amounts of crystals and glass differ within the several droplets. In some samples, the side in contact with the mould (Cu) showed significantly more crystals than the upper part of the droplets. At the mould side, large and dense cuspidine crystals embedded in a glass matrix can be detected, suggesting slow-growth formation during the casting process. In some samples, ZrO_2 acted as nucleation sites (seed) during the slow growth of these crystals. ZrO_2 enhanced crystal formation. Most likely, the ZrO_2-particles originate from the SEN. An illustration of a "droplet" is given in Figure 5.11.
On the slow-growth layer, a second glassy layer can be found, together with some cuspidine crystals which show a rapid-growth i.e. small, long cuspidine needles formed during rapid cooling (quench). These crystals are probably formed directly *after* the casting process. The glass composition was measured on several points per sample; it was found that the composition of the amorphous phase was nearly constant at all positions.
As with slag films, the samples show the presence of gas bubbles, sometimes present as a line of bubbles and small metal droplets. Furthermore, the mould powder components (raw materials) wollastonite ($CaSiO_3$) and albite ($NaAlSi_3O_8$) can be observed together with cuspidine, confirming high temperature phase relations and the melting sequence as described in Chapter 4.

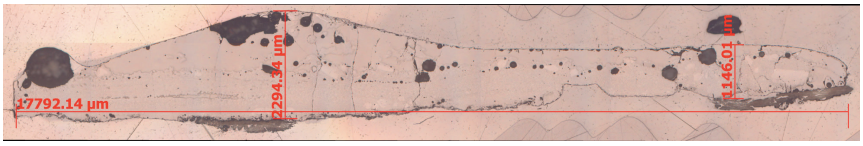

Figure 5.11: *Slag fragment, "droplet", showing glass, cuspidine crystals and bubbles*

Slag films (50 cm depth)
Thin pieces of slag film were obtained directly after casting at approximately half depth of the mould. An illustration is given in Figure 5.12.

The thickness of the slag films is between 0.2 and 0.3 mm. Microscopic analyses showed slow growth cuspidine crystals in a glass matrix; these predominant crystals can be observed in the *middle* of the slag films and at the *mould side* (Cu). No other crystals have been detected. Crystals present in the middle of the slag film are sandwiched between

glass layers on either side which may indicate fracturing of the slag film during casting, followed by refilling with liquid slag. Chapter 7 describes this phenomenon in more detail. The strand side of the films shows glass with some rapid-growth cuspidine crystals and occasionally mould powder particles, adhering to this side. These crystals and powder particles are probably formed directly after emptying the mould i.e. after casting. Furthermore, gas bubbles and small steel droplets can be found in the slag films. Incidentally, small ZrO_2-particles, most likely originating from the SEN are detected. These particles act as nucleation site for cuspidine crystals. Some samples showed evidence of *enrichment* of sodium (Na) and fluorine (F) at the mould side (Cu). Possibly, this indicates thermal diffusion in the slag film during casting; a Sorret effect [46].

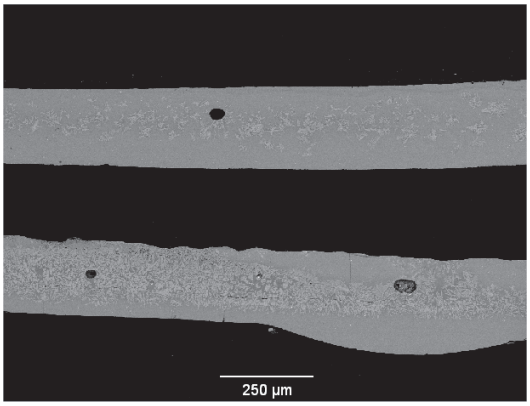

Figure 5.12: *Slag films, sampled from inside the mould (approx. 50 cm depth), showing glass and cuspidine crystals and to a lesser degree bubbles and small steel droplets*

Several slag film samples showed a very dense, compact layer of cuspidine crystals, surrounded by a less dense crystal layer at the mould side and a glass layer at the strand side. An example is given in Figure 5.13.

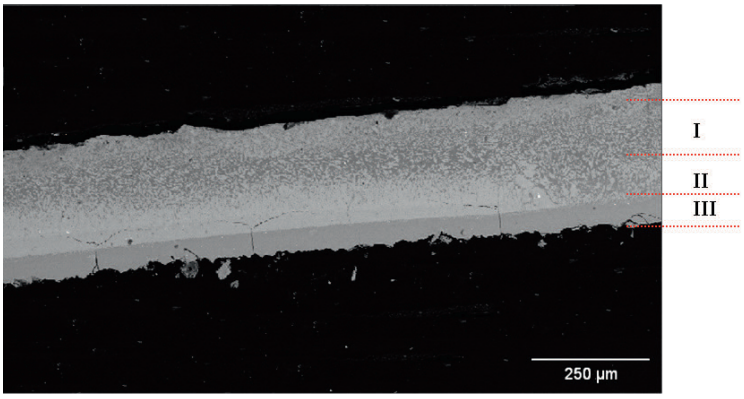

Figure 5.13: *Slag film showing a very dense, massive cuspidine layer (II), surrounded by glass (III) and cuspidine crystals (I)*

Recrystallization i.e. crystal growth is a mechanism for the formation of the very dense crystal layer. As a consequence, these slag films have a long residence time.
Like the slag droplets, some samples showed evidence of damage at the surface (mould side) due to sampling and partially sticking to the mould surface. In general, however, the slag films did not completely stick to the mould surface. Both the mould side and the strand side of the slag films showed a smooth surface.

Special attention has been given to the *surface roughness* of the slag films at the mould side. It is generally accepted that the surface roughness plays an important role in controlling the mould heat transfer during casting. Up to now, the surface roughness of slag films originating from inside the mould of a thin slab caster has not been investigated.

Results of the sampled slag films showed a very smooth surface with a surface roughness at the mould side of approximately 2 µm, Figure 5.14. The other side of the slag film, the strand side with a surface of glass, showed a very smooth surface with almost no surface roughness. These findings indicate that the control of mould heat transfer during thin slab casting is mainly achieved by the slag film and by the slag film properties. The interface at the mould side plays a less dominant role.

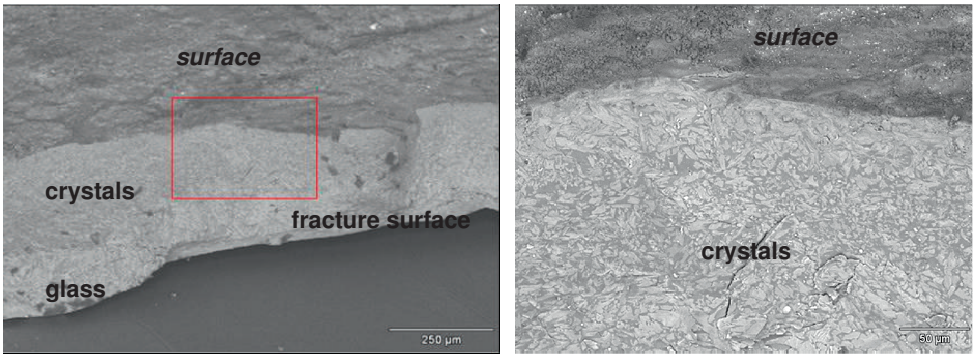

Figure 5.14: *Surface of slag film (mould side), sampled from inside the mould (left); Detail showing the surface of slag film and cuspidine crystals at the fractured surface (right) - Mould powder A*

Slag films (10 cm depth)
Additionally, slag films from approximately 10 cm under the steel meniscus were sampled and characterised. The thickness of these films is around 0.3 mm. As reported before, the slag films show an amorphous layer at the strand side and a layer of cuspidine crystals at the mould side. In some cases, the cuspidine layer is divided into some sub-layers: a layer containing cuspidine, glass and NaF at the mould side followed by a massive cuspidine layer. The crystalline layer shows evidence of detachment and movement along the film, most likely due to fracturing. Furthermore, some samples show a regular pattern of surface roughness at the strand side, resembling a *mechanical* damage like folding or wrinkling. The samples do not show remnants of starter powder.

5.5.3 Under the mould
Pieces of slag films were collected by means of a steel plate which is mounted between the mould and the first segment of the caster. After a maintenance stop, this plate is removed from the caster. Due to the local intense water-cooling, the slag film pieces are

possibly quenched and crumbled after leaving the mould and distributed under the mould area. A lot of small pieces were collected and several samples were prepared for characterisation. Note that the pieces are related to different sequences of casting (powder A). For reasons of possibly quenching and crumbling, the samples may only give an impression of the slag film in the mould.

Microscopic analysis was done using optical microscopy and SEM/EDS-techniques. Most slag film particles show a face, which has been in contact with either Fe-metal (strand) or Cu-metal (mould). It appeared that nearly all samples are split in transverse and longitudinal (casting) directions. As a consequence, all samples show a flat surface and a curved surface. The side opposing the flat face consists of curved, wavy surfaces, apparently derived from breaking along a line of bubbles, especially in the longitudinal direction. Hence, the observed film pieces are mainly fragments of the slag film. See Figure 5.15. The thickness of the fragments varies between 50 µm and even 500 µm; oscillation marks were not visible. Films in contact with the strand (Fe) show large and fine cuspidine crystals in an Al_2O_3 and SiO_2 enriched glass matrix. FeO_x-scales are sometimes attached to these films. Films in contact with the mould (Cu) show predominantly fine quenched crystals (cuspidine) in a glass matrix, enriched in Na_2O and F. Furthermore, the films contain small droplets of Fe (comparable with those observed in the slag rims), fragments of Cu, some mould powder granules and even carbon black particles, originating from the mould powder. The granules showed evidence of the melting sequence, as described in Chapter 4. An illustration of a slag film fragment showing a flat side, opposed by a curved surface is given in Figure 5.15.

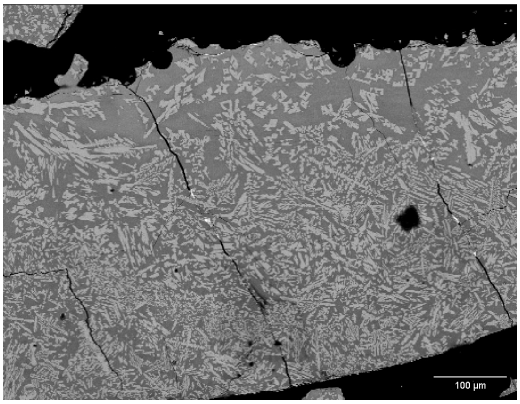

Figure 5.15: *Slag film fragment showing cuspidine crystals in a glass matrix; note the flat side, opposed by a curved surface - Mould powder A*

As mentioned above, a gradient in fluorine (F) and sodium (Na) components between the strand and mould side can be observed; the mould side showing the highest F and Na-concentrations. It has been suggested that this gradient is caused by thermal diffusion; a Sorret effect [46]. Based on the local compositions, it is proposed that the bubbles are probably formed by NaF components in the melt.

The enrichment of F and Na at the mould side has only been found in the samples from under the mould and in some samples originating from inside the mould.

5.6 Slag film thickness and powder consumption

As described in Equation 2.25, the average thickness of the liquid film can be calculated from the powder consumption during casting and the density of the mould slag:

$$d_l = fQ_s / \rho \approx Q_s^{corr} / 2600$$

where d_l = average thickness of the liquid film (m), f = fraction of the powder forming slag, Q_s = mould powder consumption (kg/m^2) and ρ = density of the liquid flux (kg/m^3).

Assuming an actual slag consumption of 0.05 kg/m^2 (powder A) and a slag density of 2600 kg/m^3, the liquid film thickness is approximately 0.0192 mm. As a rule of thumb, the average liquid film thickness is at least a tenth of the total film thickness [1]. This indicates an average film thickness of approximately 0.2 mm or more.

5.7 Reflection and transmission measurements on mould slag

Based on the work and procedures published by Susa in 2009 [42], the apparent reflectivity (R_a) and transmissivity (T_a) of three mould powders used for thin slab casting were measured at Tokyo Institute of Technology, Japan. The powders span a basicity range (CaO/SiO_2) from 0.8 to 1.2 and are denoted as powder 1, 2 and 3 respectively. Mould powder 1 (CaO/SiO_2 = 0.8) is applied to obtain increased mould heat transfer, mould powder 2 (CaO/SiO_2 = 1.0) is the standard mould powder at the thin slab caster and mould powder 3 (CaO/SiO_2 = 1.2) is a mould powder with mild cooling properties. Note that mould powders 1 and 2 are denoted mould powder C and A in this study and that mould powder 3 will be described subsequently in Chapter 7 as mould powder P. All mould powders contain transition metal oxides like MnO and Fe_2O_3.
Furthermore, a reference mould flux (R) was measured as well. This material has a basicity of 1.0 and contains no transition metal oxides. An overview is given in Table 5.7.

Table 5.7: *Mould powders for measurements on R_a and T_a*

Mould powder	Basicity (CaO/SiO_2)	Fe_2O_3 (wt%)	MnO (wt%)	Remarks
1	0.8	0.4	3.0	powder C, chapter 4,5
2	1.0	0.5	0	powder A, chapter 4,5
3	1.2	1.2	0	powder P, chapter 7
R	1.0	0	0	reference material

Measurements were done in air at room temperature using a spectrophotometer with an integrated sphere covering wavelengths between 300 and 2600 nm. The degree of crystallinity of the fluxes was determined by an internal standard method using XRD-analyses.

Glassy and crystalline samples of the three mould fluxes were obtained by melting at 1400 °C followed by quenching at room temperature and reheating at 660 °C for 30 minutes to obtain crystallisation. XRD analyses indicated that the crystallised samples only contained cuspidine as crystalline material. Table 5.8 shows the measured degree of crystallinity of the three mould powders.

Table 5.8: *Degree of crystallinity*

Mould powder	Basicity (CaO/SiO_2)	Crystallinity measured (wt%)
1	0.8	37 (cuspidine)
2	1.0	56 (cuspidine)
3	1.2	61 (cuspidine)

The apparent reflectivity and transmissivity of the glassy and crystallised samples of mould powders 1, 2 and 3 were measured. Subsequently, the ratios I_{Total}/I_s were calculated according to the procedures and conditions as described [42]: T_s = 1809 K (1536 °C, the melting point of iron), T_f = 1400 K (1127 °C, an approximate temperature at the solid/liquid interface in the mould flux) and ε = 0.3 (an approximate emissivity value for solid iron at the melting point). The results have also been compared to data from the reference material
The ratio I_{Total}/I_s ranges between 0.6 and 0.9 for glassy fluxes and between 0.2 and 0.6 for crystallised fluxes. This confirms the importance of crystalline mould slag to achieve mild cooling during casting. Focussing on the I_{Total}/I_s ratios only for the crystallised fluxes, it can be concluded that the control of mould heat transfer (mild cooling) improves from mould powder 1 to 3 i.e.

"mould powder 3 > mould powder 2 > mould powder 1"

This hierarchy corresponds to the degree of crystallisation as shown in Table 5.8.

Mould powder 1 shows strong absorptions, in particular below 1000 nm which is mainly due to the presence of Fe^{3+} and Mn^{2+} ions. Mould powders 2 and 3 also show absorption due to the presence of Fe^{2+} and Fe^{3+} ions. It was also found that the absorption shifts to higher wavelengths as the basicity increases. Furthermore, the ratio Fe^{2+}/Fe^{3+} decreases with increasing basicity. As a consequence, the absorption characteristics of mould powder 2 (amorphous) are more affected by the presence of Fe^{2+} ions.
In addition, the reference material contains no transition metal oxides and shows smaller absorptions over a wide range of wavelengths. This leads to higher reflectivities of the flux and hence to smaller I_{Total}/I_s ratios.

The presence of Fe_2O_3 and MnO in the three mould powders increases absorption and consequently decreases the reflection. Mild cooling properties of the mould powders, in particular with respect to mould powders 2 and 3, can be improved by reducing or even leaving out these components, assuming that there are no special reasons for the presence of these oxides.

5.8 Crystallisation at the break temperature of mould slag

5.8.1 Introduction

The break point or break temperature (T_{break}) measured by rotational viscometry is often used as a criterion to estimate the start of crystallisation of liquid mould slag and as a measure of mould powder properties [47]. Although there are several empirical models to predict break temperatures as a function of chemical compositions, the physical meaning of T_{break} has so far not been investigated in detail. The measured increase in viscosity is assumed to occur as a consequence of crystallisation but it is not precisely known at which crystal fraction this behaviour initiates and whether it is dependent on absolute temperature or the chemical composition of the mould powder. Furthermore, effects of the measuring device (material and dimensions of spindle and crucible) and measuring method are sometimes mentioned in literature, but details are rare.

5.8.2 Experiments

Equilibrium crystallisation experiments on four different mould powders were carried out at their break temperature. The aim of this work is to determine the crystal fraction in the products and to relate T_{break} to a defined crystal fraction. All mould powders have been applied at the DSP caster under operational conditions. As before, the powders span a basicity range from 0.8 to 1.2 (CaO/SiO_2) and break temperatures (T_{break}) between 1054 °C and 1190 °C. The break temperatures were determined by the supplier according to the standard specifications i.e. rotational viscometry with a Pt crucible and cylinder and a cooling rate of 10 °C/min. An overview of the mould powders is given in Table 5.9. Note that mould powders 1 and 2 are denoted powder C and A in Chapter 4 and 5 and that mould powders 3 and 4 will be described in Chapter 7.

Table 5.9: *Mould powders for T_{break} experiments*

Mould powder	Basicity (CaO/SiO_2)	Break point, T_{break} (°C) (measured)	Remarks
1	0.8	1054	powder C, chapter 4,5
2	1.0	1167	powder A, chapter 4,5
3	1.2	1153	powder P, chapter 7
4	1.2	1190	powder O, chapter 7

Equilibrium experiments were performed as closed capsule experiments. The sample powder was encapsuled in a Pt-tube (~4 mm inner diameter, 12-15 mm length) which was sealed by arc-welding both ends. The capsule was then inserted into a vertical tube furnace and equilibrated for up to 6h at the break temperature. Temperature values are accurate to within ± 5 °C. At the end of the experiment the sample was drop-quenched into water. By measuring the capsule weight before and after the experiment, potential leakage of the capsules could be determined. Heating of normal carbon- and CO_2-bearing mould powders will result in an overpressure in the capsule and possibly an explosion. Therefore, the starting powder was decarbonised and decarbonated for ~7h at 650 °C. After the experiment the Pt-capsule was cut open and the mould slag was removed from the capsule. The recovered material was embedded in epoxy-resin and prepared as polished section for electron microscopy. Chemical compositions of the phases were

determined by SEM-EDS. Each observed phase within one sample was analysed multiple times across different locations of the sample.

Phase proportions were calculated from a mass balance using a numerical method implemented in the software package IGOR Pro. This method finds the solution vector to a non-square phase composition matrix (number of phases ≠ number of components) and the bulk composition. Errors on mass proportions were calculated on the basis of measured standard deviations (2 sigma errors) from repetitive SEM analysis of phases. Mass-balance calculations were performed 500 times by randomly varying the phase compositions within their absolute range of uncertainty. For example, assuming that CaO in a phase was measured to within a precision of 34.5 ± 0.5 wt%, input values for repetitive mass balance calculation were varied randomly between 34.0 and 35.0 wt%. Reported mass proportions are average values and standard deviations on the 2-sigma level of those 500 mass balance solutions.

5.8.3 Results

For most mould powders two experiments were performed to check for the reproducibility of results. A time series was performed on mould powder 1, such that capsules were equilibrated at T_{break} for 1 and 6h, respectively. In another consistency check, two experiments were performed on mould powder 2 at 1167 °C, but different approaches to reach equilibrium and different run times were chosen. The capsule in the first run (c) was inserted at a temperature of 1250 °C to ensure total melting and homogenisation of the liquid and after 15 min cooled to 1167 °C (T_{break}). This temperature was then maintained for 2h. The capsule for the second run (d) was directly inserted at a temperature of 1167 °C, where it was kept for 2.5 h. An example of a SEM image is given in Figure 5.16 (mould powder 4). An overview of the experiments is given in Table 5.10.

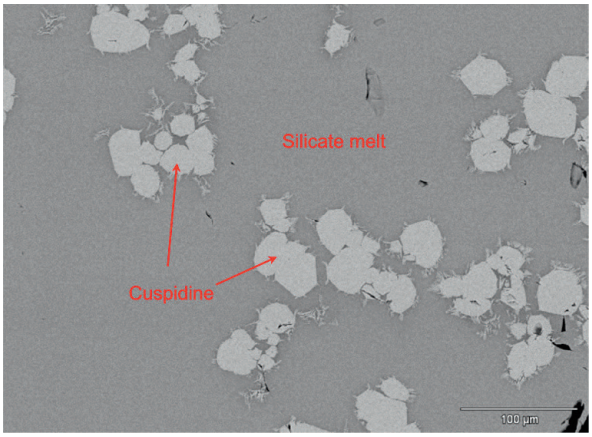

Figure 5.16: *SEM image, experiment f, quenched from 1190 °C: cuspidine phenocrysts can be found in a homogeneous glass matrix (silicate melt) - mould powder 4*

Table 5.10: *Summary of experimental results*

Mould powder	Experiment	Run time (h)	Basicity (CaO/SiO_2)	T_{break} (°C) (measured)	Melt (wt%)	Cuspidine (wt%)
1	a	1	0.8	1054	87 ± 5	13 ± 4
	b	6			89 ± 6	11 ± 4
2	c	2	1.0	1167	92 ± 2	8 ± 2
	d	2.5			89 ± 2	11 ± 2
3	e	2	1.2	1153	86 ± 3	14 ± 3
4	f	3	1.2	1190	75 ± 2	25 ± 2
	g	2			83 ± 2	17 ± 2

Experiments performed on mould powders 1 and 2 show weight proportions of cuspidine which are consistent within experimental uncertainties. The two experiments performed on powder 4, however, give inconsistent results showing ~25 ± 2 wt% crystallisation in experiment f which compares to 17 ± 2 wt% for experiment g. The source of inconsistency is not known but it may be related to inaccurate thermocouple readings in run f; the actual run temperature was slightly lower than reported here which could explain the higher crystal fraction.

Figure 5.17 shows the calculated weight proportion of cuspidine as a function of the break temperature and the basicity. If experiment f with ~25 wt% crystallisation is ignored, then the break temperature seems to be *independent* of absolute temperature and chemical composition (or basicity) but is related to an average crystal fraction of 12 ± 3 wt%.

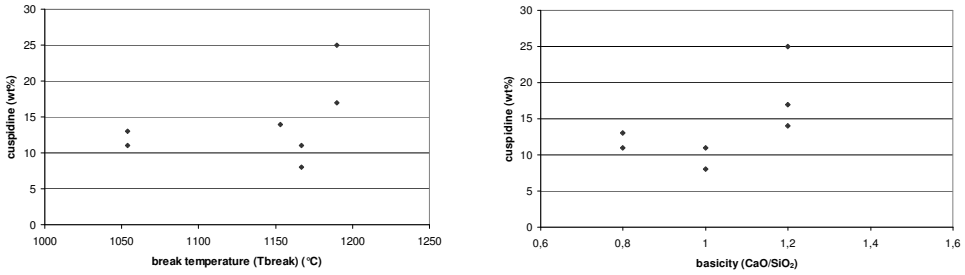

Figure 5.17: *Cuspidine (wt%) as a function of break temperature (left) and basicity (right)*

5.9 Afterthoughts on the surface roughness of slag films

It is generally accepted that slag films have a surface roughness at the mould side which acts as an important interfacial thermal resistance ($R_{Cu/sl}$). It should be noted, however, that a significant part of the samples and experimental work on this subject is based on experiments under laboratory conditions. Samples from the mould are essential for comparison and characterisation purposes but for reasons of process stability and safety difficult to obtain.

The samples obtained during laboratory experiments showed the presence of wrinkles with a surface roughness of up to 100 µm and effects of crystallisation (devitrification) due to reheating. However, crystallisation i.e. devitrification of glassy mould slag is widely

considered as a very important mechanism where at least various other types and mechanisms of surface roughness can be defined.

Based on literature data and findings within this project, several other mechanisms were reviewed. A summary is given below where a classification is made into chemical (thermodynamical) effects and mechanical effects of surface roughness of slag films.

Chemical composition and cooling rate

- Surface roughness resulting from the gradual crystallisation and corresponding shrinkage of the glassy solid slag film formed during casting. This mechanism depends on the composition of the mould slag, the presence of nucleation sites and the local cooling rates and is generally considered as the most important mechanism to generate surface roughness.
- Surface roughness due to the presence of bubbles in the slag film (most likely NaF), in particular in the upper part of the mould i.e. locations with the highest temperatures.

Mechanical causes, wetting and adhering

- Surface roughness due to mechanical effects and interfacial effects: pumping, forced spreading of liquid slag to the non-wetting copper surface which can result in folds or wave lines.
- Surface roughness due to the formation of wrinkles, ripples are most likely caused by quenching and subsequent crystallisation (reheating) of mould slag. It is this type of surface roughness that has been found during lab-scale experiments.
- Surface roughness as a result of breaking of the solid slag film, followed by refilling with liquid slag.
- Surface roughness resulting from damaging during sampling. The samples may stick to the mould wall which is most likely enhanced by the formation and presence of Na and NaF.
- Surface roughness resulting from sample preparation. The sodium bearing components (if present) in the slag film and in particular at the interface will flush out during sample preparation (using water) which will result in the formation of pores and holes.

In order to obtain a clear view on the relevance of the interfacial thermal resistance caused by the surface roughness of the slag film, it is recommended to define the *type* of the actual surface roughness followed by the proposed *mechanism* and the corresponding *location* in the mould (meniscus area, halfway the mould etc.).
In all cases, the effects of the ferrostatic pressure on the slag film and the surface roughness should be considered. This may become even more important for very thin slag films (for instance 200 µm), typical for a thin slab caster.

Although slag film samples are needed for investigation purposes, it should be realised that conclusions are based on what is observed *after* sampling which may not be the situation *during* actual casting.

5.10 Concluding remarks

This study emphasises the need for slag crystallisation in order to control mould heat transfer during casting. Although the need for a crystalline slag film (i.e. cuspidine in a glass matrix) is obvious, the mechanism to control mould heat transfer is, as yet, not fully understood. Given the thin slag films (approximately 200 µm) as obtained at the thin slab caster and the very low values of the surface roughness, *reflection* of radiation at the interface of the crystalline layer seems to be a plausible mechanism. The control of mould heat transfer is realised by the slag film properties themselves; the interfacial thermal resistance playing a less dominant role.

The thin slag film layer can be explained by the low values of slag consumption during casting. The very low surface roughness can most likely be related to the relatively low value for the critical cooling rate r_c and hence the relatively high value (>>1) of the normalised cooling rate r_n as well as the ferrostatic pressure during casting. A further improvement of the reflective properties of the slag film i.e. mild cooling performance can be obtained by reducing or even leaving out transition metal oxides such as Fe_2O_3.

The break point or break temperature is widely used as an important parameter in mould powder design. Equilibrium melting experiments on four mould powders revealed that the break point (T_{break}) corresponds to the temperature at which 12 ± 3 wt% crystallisation occurs. This value has been found to be independent of its absolute temperature and of the chemical composition of the mould powder.

Mineralogical characterisation can provide essential information on the processes leading to solidification and crystallisation of mould slag. However, interpretation of these data can only be done in close association with a good understanding of the casting process.

Reliable input data are essential for the successful development and application of thermodynamic models for mould slag. Up to now, important material properties and knowledge on the interactions of various components within the slag, for instance the role of fluorine and sodium at high temperatures, are not or only partially available. Experimental work is crucial for a further understanding of these slag systems as well as for reliable calculations [5,44].

5.11 References

[1] K.C. Mills, A review of ECSC-funded research on mould powders. Synthesis report EUR 13177 EN, ECSC, Luxembourg, 1991.

[2] P. Grieveson, S. Bagha, N. Machingawuta, K. Lidell and K.C. Mills, Physical properties of casting powders: Part 2 Mineralogical constitution of slags formed by powders. Ironmaking and Steelmaking, 15 (1988) 181-186.

[3] L. Hering, H-P. Heller und H-W. Fenzke, Untersuchungen zur Gießpulverauswahl beim Brammenstranggießen. Stahl u. Eisen, 112 (1992) No.8, 61-65.

[4] T. Watanabe, H. Hashimoto, M. Hayashi and K. Nagata, Effect of alkali oxides on crystallization in CaO-SiO_2-CaF_2 glasses. ISIJ Int., 48 (2008) 925-933.

[5] H. Nakada, H. Fukuyama and K. Nagata, Effect of NaF addition to mold flux on cuspidine primary field. ISIJ Int., 46 (2006,) 1660-1667.

[6] M. Hayashi, T. Watanabe, H. Nakada and K. Nagata, Effect of Na_2O on crystallization of mould fluxes for continuous casting of steel. ISIJ Int., 46 (2006) 1805-1809.
[7] T. Watanabe, H. Fukuyama, M. Susa and K. Nagata, Phase diagram cuspidine ($3CaO{\cdot}2SiO_2{\cdot}CaF_2$)-$CaF_2$. Met. Trans. B, 31 (2000) 1273-1281.
[8] R.G. Hill, N. Da Costa and R.V. Law, Characterization of a mould flux glass. Journal of Non-Crystalline Solids, 351 (2005) 69-74.
[9] J. Klug, N. Heck and A. Faria, Investigation of mold flux properties used in the continuous casting of steels. Proc. 8th Int. Conf. on Molten Slags, Fluxes and Salts (MOLTEN2009), 18-21 January 2009, Santiago, Chile, GECAMIN Ltd., Santiago, Chile, 2009, 1053-1059.
[10] I-H. Jung, Thermodynamic modeling of the CaF_2 containing slags and its applications to steelmaking process. Proc. AISTech 2010, 3-6 May 2010, Pittsburgh, USA, Iron and Steel Society, Warrendale, USA, Volume 1, 1211-1220.
[11] Y. Kashiwaya, C.E. Cicutti, A.W. Cramb and K. Ishii, Development of double and single hot thermocouple technique for in situ observation and measurement of mold slag crystallization. ISIJ Int., 38 (1998) 348-356.
[12] Y. Kashiwaya, C.E. Cicutti and A.W. Cramb, An investigation of the crystallization of a continuous casting mold slag using the single hot thermocouple technique. ISIJ Int., 38 (1998) 357-365.
[13] S. Lachmann and P.R. Scheller, Effect of Al_2O_3 and CaF_2 on the solidification of mould slags and the heat transfer through slag films. Proc. 8th Int. Conf. on Molten Slags, Fluxes and Salts (MOLTEN2009), 18-21 January 2009, Santiago, Chile, GECAMIN Ltd., Santiago, Chile, 2009, 1101-1110.
[14] P. Rocabois, J.N. Pontoire, J. Lehmann and H. Gaye, Crystallisation kinetics of Al_2O_3-CaO-SiO_2 based oxide inclusions. Journal of Non-Crystalline Solids, 282 (2001) 98-109.
[15] W. Vogel, Glass Chemistry, 2nd edition, Springer-Verlag, Berlin-Heidelberg, Germany, 1994, 22-56.
[16] C. Orrling, A.W. Cramb, A. Tilliander and Y. Kashiwaya, Observation of the melting and solidification behavior of mold slags. Ironmaking Steelmaking, 27 (2000) No.1, 53-63.
[17] M.V. de A. Fonseca, O.D.C Afrange, A. de O. Lavinas, A.A. Ramos and C.A.G. Valadares, Evaluation of solidified slag films from mould powders used in C.C., taken from plate/mold interface. Proc. 5th Int. Conf. on Molten Slags, Fluxes and Salts, 5-8 January 1997, Sydney, Australia, Iron and Steel Society, Warrendale, USA, 1997, 851-858.
[18] M.C.C. Bezerra, O.D.C. Afrange and C.A.G. Valadares, Evaluation of solidified slag films of mould fluxes used in continuous casting of steel, taken from slab mould interface. Proc. Mills Symposium, 22-23 August 2002, London, United Kingdom, The Institute of Materials, London, 2002, Volume 1, 293-304.
[19] B. Tarrant and G. Brooks, Solidification of industrial mold fluxes. Ironmaking Steelmaking, 30 (2003) No.5, 52-60.
[20] V. Ludlow, B. Harris, S. Riaz and A. Normanton, Continuous casting mould powder and casting process interaction: why mould powders do not always work as expected. Ironmaking and Steelmaking, 32 (2005) 120-126.
[21] S. Ogibayashi, K. Yamaguchi, T. Mukai, T. Takahashi, Y. Mimura, K. Koyama, Y. Nagano and T. Nakano, Mold powder technology for continuous casting of low-carbon aluminum-killed steel. Nippon Steel Tech. Rep., 34 (1987) 1-10.

[22] L. Courtney, S. Nuortie-Perkkiö, C.A.G. Valadares, M.J. Richardson and K.C. Mills, Crystallisation of slag films formed in continuous casting. Ironmaking and Steelmaking, 28 (2001) 412-417.
[23] A. Yamauchi, T. Emi and S. Seetharaman, A mathematical model for prediction of thickness of mould flux film in continuous casting mould. ISIJ Int. 42 (2002) 1084-1093.
[24] S. Hiraki, K. Nakajima, T. Murakami and T. Kanazawa, Influence of mold heat fluxes on longitudinal surface cracks during high speed continuous casting of steel slab. Proc. 77th Steelmaking Conf., 20-23 March 1994, Chicago, USA, Iron and Steel Society, Warrendale, USA, 1994, 397-403.
[25] P. Hooli, Study on the layers in the film originating from the casting powder between steel shell and mould and associated phenomena in continuous casting of stainless steel, Doctoral Thesis, Helsinki University of Technology, Helsinki, Finland, 2007.
[26] E. Lainez and J.C. Busturia, The E.L.V. Solidification model in continuous casting billet moulds using casting powders. Summary of the research performed under ECSC 7210-CA/932 and 7210-CA/935 Projects, 1994, Sidenor I+D, Basauri, Spain.
[27] B. Stewart, N. Jones, K. Bain, M. McDonald, R. Burniston, M. Bugdol and V.Ludlow, Development of the mould slag film and its impact on the surface quality of continuously cast semis. Proc. 8th Int. Conf. on Molten Slags, Fluxes and Salts (MOLTEN2009), 18-21 January 2009, Santiago, Chile, GECAMIN Ltd., Santiago, Chile, 2009, 1061-1071.
[28] R. Taylor and K.C. Mills, Physical properties of casting powders: Part 3 Thermal conductivities of casting powders. Ironmaking and Steelmaking, 15 (1988) 187-194.
[29] K. Schwerdtfeger, Heat withdrawal in the mold in continuous casting of steel. Review and Analysis. Steel Research Int., 77 (2006) 911-920.
[30] J-F. Holzhauser, K-H. Spitzer and K. Schwerdtfeger, Study of heat transfer through layers of casting flux: experiments with a laboratory set-up simulating the conditions in continuous casting. Steel Research Int., 70 (1999) 252-258.
[31] K. Watanabe, M. Suzuki, K. Murakami, H. Kondo, A. Miyamoto and T. Shiomi, The effect of crystallization of mold powder on the heat transfer in continuous casting mold. Tetsu-to-Hagané, 83 (1997) 115-120.
[32] S. Mineta, T. Kajitani and H. Yamamura, Experimental study on heat transfer behaviour through the mold flux film between the solidifying shell and mold. Proc. AISTech 2010, 3-6 May 2010, Pittsburgh, USA, Iron and Steel Society, Warrendale, USA, Volume 2, 71 - 80.
[33] H. Shibata, K. Kondo, M. Suzuki and T. Emi, Thermal resistance between solidifying steel shell and continuous casting mold with intervening flux film. ISIJ Int., 36 (1996) S179-S182.
[34] A. Yamauchi, K. Sorimachi, T. Sakuraya and T. Fuji, Heat transfer between mold and strand through mold flux film in continuous casting of steel. ISIJ Int., 33 (1993) 140-147.
[35] K. Tsutsumi, T. Nagasaka and M. Hino, Surface roughness of solidified mold flux in continuous casting process. ISIJ Int., 39 (1999) 1150-1159.
[36] A. Yamauchi, K. Sorimachi and T. Yamauchi, Effect of solidus temperature and crystalline phase of mould flux on heat transfer in continuous casting mould. Ironmaking and Steelmaking, 29 (2002) 203-207.
[37] M. Hanao and M. Kawamoto, Flux film in the mold of high speed continuous casting. ISIJ Int., 48 (2008) 180-185.

[38] H. Nakada, M. Susa, Y. Seko, M. Hayashi and K. Nagata, Mechanism of heat transfer reduction by crystallization of mold flux for continuous casting. ISIJ Int., 48 (2008) 446-453.

[39] K. Nagata and H. Nakada, Designing of mold flux for continuous casting of steel. Proc. AdMet, 27-30 May 2007, Dnipropetrovsk, Ukraine, National Metallurgical Academy of Ukraine, Dnipropetrovsk, Volume 2, 182-186.

[40] M. Hayashi, K. Matsuo, K. Nagata and H. Nakada, Effect of crystalline morphology on heat transfer through mould flux. Proc. 8th Int. Conf. on Molten Slags, Fluxes and Salts (MOLTEN2009), 18-21 January 2009, Santiago, Chile, GECAMIN Ltd., Santiago, Chile, 2009, 1091-1100.

[41] H. Nakada and M. Hayashi, Tokyo Institute of Technology, Personal communication, 2007 and 2009,

[42] M. Susa, A. Kushimoto, H. Toyota, M. Hayashi, R. Endo and Y. Kobayashi, Effects of both crystallisation and iron oxides on the radiative heat transfer in mould fluxes. ISIJ Int., 49 (2009) 1722-1729.

[43] S. Ozawa, M. Susa, T. Goto, R. Endo and K.C. Mills, Lattice and radiation conductivities for mould fluxes from the perspective of degree of crystallinity. ISIJ Int., 46 (2006) 413-419.

[44] H. Fukuyama, H. Tabata, T. Oshima and K. Nagata, Determination of Gibbs energy of formation of cuspidine ($3CaO{\cdot}2SiO_2{\cdot}CaF_2$) by transpiration method. ISIJ Int., 44 (2004) 1488-1493.

[45] P.V. Riboud, M. Olette, J. Leclerc and W. Pollak, Continuous casting slags: Theoretical analysis of their behaviour and industrial performances. Proc. 61st National Open Hearth and Basic Oxygen Steel Conf., 16-20 April 1978, Chicago, USA, Iron and Steel Society, Warrendale, USA, 1978, 411-417.

[46] C.E. Lesher and D. Walker, Solution properties of silicate liquids from thermal diffusion experiments. Geochimica et Cosmochimica 50 (1986) 1397-1411.

[47] S. Sridhar, K.C. Mills, O.D.C. Afrange, H.P. Lörz and R. Carli, Break temperatures of mould fluxes and their relevance to continuous casting. Ironmaking and Steelmaking, 27 (2000) 238-242.

6 Toward high speed casting

6.1 Introduction

As mentioned in Chapter 1, it has been decided to increase the production of the DSP caster in IJmuiden from the designed production level of 1.3 Mt/y (coils) to a level of 1.8 Mt/y (coils) using one caster strand. In order to meet this demand, the steel in mould time has to be increased to approximately 85% and the maximum casting speed to 8 m/min. A project was started to develop and implement the essential technologies to achieve this goal, with special attention being given to the design of mould powders for high speed casting.

A collaborative project between Sumitomo Metal Industries (SMI) and Tata Steel IJmuiden was initiated to develop mould powders which facilitate casting speeds up to 8 m/min. Main subjects of this project are:

- mould powder design which includes the chemical and mineralogical composition and the physical properties
- characterisation of mould powder and mould slag
- trials at the Sumitomo pilot caster
- full scale plant trials at the Tata Steel thin slab caster.

Evaluation of the trials will be based on the in-mould behaviour of the mould powder with respect to slag formation (which includes slag pool depth and the formation and growth of slag rims), mould heat transfer and strand lubrication followed by inspection of the slab surface. A special point of attention is the condition to use mould powder as a *granulated* material at the thin slab caster of Tata Steel. As a consequence, the characterisation work focuses on the choice of raw materials and on the corresponding specific phase relations at elevated temperatures i.e. during heating of mould powder and cooling of mould slag [1].

6.2 Mould powder design

Mould powder design for this project was initially based on Sumitomo's experience with high speed casting in the Quality Strip Production (QSP) process [2]. Sumitomo developed this casting process (mould dimensions 90 mm×1000 mm) as well as suitable mould powders focussing on low carbon steel grades with a maximum casting speed of 8 m/min and peritectic steel grades with a casting speed up to 5 m/min and even up to 10 m/min [3,4]. As described in Chapter 2, the QSP process is characterised by a vertical bending type caster, a parallel mould with a round shaped SEN, a well designed liquid core reduction and an advanced mould level control system, using eddy current techniques.

Based on their experiences with high speed casting of low carbon steel grades, Sumitomo selected a mould powder for *first* trials at the pilot caster and at the thin slab caster of Tata Steel. It is common for the casters at Tata Steel IJmuiden to use mould powder as a *granulated* material; this in contrast with the practice at Sumitomo. So, the initial mould powder had to be adapted for use as a granulated flux. Based on the same chemical composition, the raw material choice of the original powder was partly changed in order to manufacture a granulated mould powder.

The development project on mould powders was started in the light of the differences between the thin slab casting processes of Sumitomo (QSP) and Tata Steel (DSP) and the condition to use granulated materials at the Tata Steel thin slab caster. An overview of main steps in this project is given below.

A summary of the chemical composition of the mould powders is given in Table 6.1. Powder L is the initial mould powder, selected by Sumitomo and powder M is the granulated version of this material. The granulation was done by the Japanese mould powder supplier of Sumitomo. For reasons of logistics however, it was decided to have future mould powders granulated by a European supplier, based on the composition as formulated by Sumitomo and Tata Steel. Mould powder A is the standard powder, used at the thin slab caster of Tata Steel and described in the previous chapters; powder A can be considered as a reference material [5]. Mould powders M and A have been tested at the pilot caster of Sumitomo. A next step was a full scale plant trial of powder M at the thin slab caster of Tata Steel.

Table 6.1: *Chemical composition of mould powders (wt%)*

	L	M*	*A**
CaO/SiO_2	1.2	1.2	*1.0*
$MgO + Al_2O_3$	11.7	12.3	*3.6*
$Na_2O + F$	17.0	16.2	*20.7*

* mould powder as a granulated material

Based on the casting experiences with mould powders M and A, the design of mould powders for high speed casting was adapted. The criteria are given in Table 6.2 and Table 6.3 and are illustrated in Figure 6.1. The experiences are described in more detail below.

Table 6.2: *Mould powder design for high speed casting*

basicity (CaO/SiO_2)	1.2
solidification point or T_{break} (°C)	1150
crystallisation of mould slag	cuspidine

The mould powder is designed for a basicity (CaO/SiO_2) of 1.2, a solidification point or T_{break} of 1150 °C (to be measured during viscosity measurements) and a preferred crystallisation (mould slag) of cuspidine ($3CaO{\cdot}2SiO_2{\cdot}CaF_2$ or $Ca_4Si_2O_7F_2$) [6,7]. The corresponding chemical composition as designed is given in Table 6.3.

Table 6.3: *Mould powder for high speed casting, chemical composition (wt%)*

CaO/SiO_2	$MgO + Al_2O_3$	$Na_2O + F$
1.2	8.5	20

These criteria will result in “mild cooling” properties, aiming to control the heat transfer between the solidifying steel shell and the mould copper plates (horizontal heat transfer). Mild cooling properties are required in order to prevent the formation of slab surface cracks (especially longitudinal surface cracks) during casting and to protect the mould copper plates with respect to the increased heat load, resulting from high casting speeds

[8,9]. Furthermore, special attention was given to control the formation and growth of slag rims during casting at the DSP.

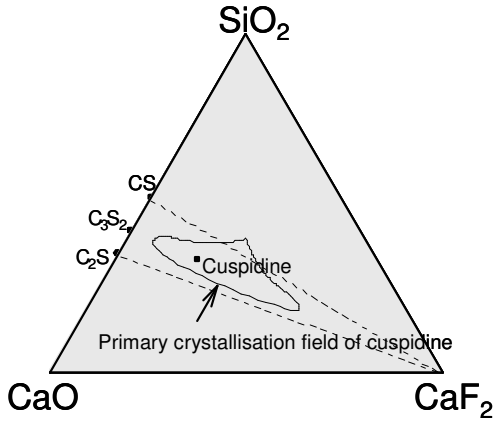

Figure 6.1: *Mould powder for high speed casting – crystallisation of cuspidine*

Mould powders N, O and P are based on these design criteria, given in Table 6.4. Mould powder N is a *powder*, as formulated by SMI. Mould powders O and P are *granulated* materials with an almost identical chemical composition. The granulation (and production) of these materials was done by a European mould powder supplier. Mould powders N and O have been tested at the pilot caster of Sumitomo, followed by some plant trials (DSP) with mould powder O.

Table 6.4: *Chemical composition of mould powders (wt%)*

	N	**O***	**P***	***A****
CaO/SiO_2	1.2	1.2	1.2	*1.0*
$MgO + Al_2O_3$	8.3	7.7	8.8	*3.6*
$Na_2O + F$	17.8	16.7	21.0	*20.7*

* mould powder as a granulated material

Mould powder P is a further development, based on mould powder O. Modifications were introduced with respect to the composition of this powder, aiming to reflect the designed properties (in particular the solidification point) as defined in Table 6.2 more accurately. Special attention was given to the amount of sodium which has significant effects on the solidification point of mould slag, denoted as T_{break} and on the viscous flow behaviour [5,10]. Both effects can be understood by considering the role of sodium on both the solidification and crystallisation properties and on the depolymerisation of the alumino-silicate network, respectively [11].
After characterisation, mould powder P has frequently been tested at the thin slab caster of Tata Steel.

6.3 Mould powder characterisation and phase relations

6.3.1 Characterisation

Room-temperature X-ray diffraction (XRD) was used to determine the mineralogical composition i.e. the raw materials selection of the mould powders. As concluded before, the mould powders are generally composed of silicates, fluorites and carbonates. Additionally, amorphous components (glass) can be present as well as smaller amounts of raw materials. Each mould powder can show significant differences in raw material composition.
The two powders L and M are characterised by the use of Portland Cement as a main raw material (silicates) and by a significant amount of periclase (MgO). Furthermore, mould powder L contains two other sources of silica: quartz and cristobalite (SiO_2). Powder L also uses natrite (Na_2CO_3), whereas mould powder (granulate) M contains a considerable amount of amorphous material (glass).

Main differences between mould powders N and O are the use of Portland Cement and quartz (SiO_2) in mould powder N. For the granulated version powder O, wollastonite ($CaSiO_3$) is applied as a major raw material with a minor amount of quartz. Furthermore, mould powder N contains periclase (MgO) as a magnesium-source and mould powder O forsterite (Mg_2SiO_4). Mould powder P is nearly identical with powder O. Some small modifications were introduced, especially with respect to the amount of sodium.
Note that the standard mould powder A corresponds roughly to mould powders O and P. Exceptions are the use of albite ($NaAlSi_3O_8$) as major raw material in powder A and the use of forsterite (Mg_2SiO_4) and corundum (Al_2O_3) in powders O and P. All the mould powders use fluorite (CaF_2) as the single source of fluorine.

Based on the mould powder characterisation and on supplier information, mould powders L, M and N use two free carbon sources in order to control the melting rate during casting. Mould powders O and P only contain *one source* of free carbon i.e. carbon black which is fully comparable with mould powder A. As described previously, the choice, amount and distribution of free carbon particles is an *essential* condition for a demanding casting process like thin slab casting, especially with respect to slag formation [12].

The viscosity of the mould powders L – O and the corresponding solidification point or T_{break} were measured. Results obtained at Sumitomo are summarised in Table 6.5 and are based on an oscillating plate method with a cooling rate of 2 °C/min. Note that powder O does not show the required solidification point of 1150 °C. Additionally, the granulated materials O en P were characterised by the European mould powder supplier, using a rotating cylinder viscometer and a cooling rate of 10 °C/min, Table 6.6.

Table 6.5: *Viscosity and solidification point, as measured at Sumitomo*

	L	M	N	O
Viscosity at 1300 °C (Pa·s)	0.09	0.08	0.09	0.08
Solidification point (T_{break}) (°C)	1101	1115	1161	1187

Table 6.6: *Viscosity and solidification point, as measured by the powder supplier*

	O	P
Viscosity at 1300 °C (Pa·s)	0.09	0.06
Solidification point (T_{break}) (°C)	1190	1153

6.3.2 Phase relations

The mineralogy of the major phases for the powders has been observed *in situ* using high-temperature X-ray diffraction (HT-XRD) with additional powder X-ray diffraction and microscopic techniques. The XRD-patterns can be summarised as a 3D-plot, see Figure 6.2. XRD-patterns were collected in the 2Θ range from 20 to 60 degrees, while the temperature was raised from 500 °C to 1350 °C and subsequently lowered to 500 °C. Heating and cooling rates were 200 °C/min. XRD-patterns were taken in temperature increments of 50 °C. A second sequence of XRD-patterns was collected by heating with a shift of 25 °C compared to the first run to obtain a higher resolution of phase stabilities. The crystallisation path was investigated additionally by heating directly to 1250 °C at 300 °C/min, followed by cooling to 500 °C and by using a lower scan rate. Phase relations and temperature stabilities were derived by combining all three data sets. A summary of the results of powders M, N, O and P is given in Figure 6.3.

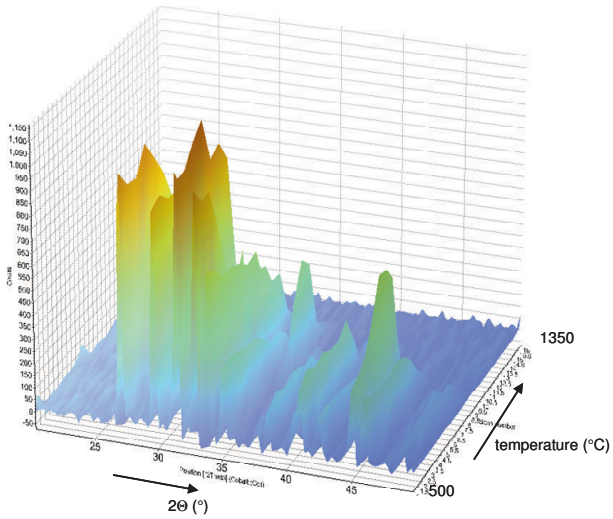

Figure 6.2: *3D-plot of XRD-pattern upon heating from 500-1350 °C - Powder N*

The data on powder melting (heating) gives information on the processes leading to slag formation and the formation of rims. Results on slag solidification (cooling) are essential for a better understanding of slag crystallisation and the control of mould heat transfer during casting.

During heating, each mould powder shows a specific melting sequence i.e. disappearance of original raw materials and appearance of intermediate (secondary) phases, before melting takes place. Melting is complete around a temperature of 1250 °C. During cooling, one or more crystalline phases can be formed.
Cooling of powder M shows two major crystalline phases: cuspidine ($Ca_4Si_2O_7F_2$) and melilite $(Ca,Na)_2(Al,Mg)(Si,Al)_2O_7$. Both phases show a strong peak-overlapping, which makes the exact temperature at which melilite becomes visible difficult to determine. Cuspidine crystallises at ~1075-1050 °C followed by melilite around 900-850 °C. No minor components could be detected.

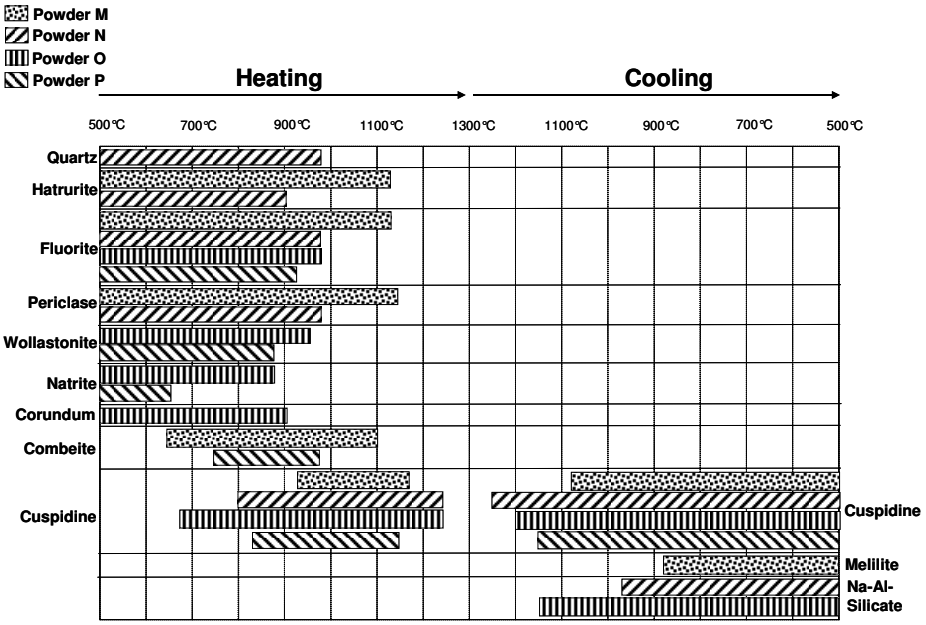

Figure 6.3: *Results of HT-XRD analyses and indications of phase stabilities of major phases within powder M, N, O and P (heating and cooling)*

Mould powders N and O both clearly show crystallisation of cuspidine and Na-Al-Silicate. The start of crystallisation for powder N is around 1250 °C (cuspidine) and 975 °C (Na-Al-Silicate). For mould powder O, these values are 1200 °C and 1150 °C, respectively. Mould powder P shows a lower melting trajectory (natrite, combeite and cuspidine) as well as crystallisation of cuspidine at a temperature between 1150 °C and 1100 °C. No other major phases were detected during cooling.

The amounts of crystals in the post-heated samples after HT-measurements were determined by Rietveld-analysis of final room-temperature XRD-patterns. Results are given in Table 6.7. Note that mould powder P shows a significant amount of Na-Al-silicates which were not detected during HT-XRD. Glass phases are not reflected in the relative amounts.

Table 6.7: *Relative amounts (wt%) of crystalline phases in mould slag*

	M	N	O	P
Major phases				
cuspidine ($Ca_4Si_2O_7F_2$)	60 ± 7	73 ± 3	83 ± 3	80 ± 3
melilite $(Ca,Na)_2(Al,Mg)(Si,Al)_2O_7$	38 ± 6			
Na-Al-Silicates		27 ± 3	17 ± 3	20 ± 3
Minor phases				
fluorite (CaF_2)	1 ± 1			
monticellite ($CaMgSiO_4$)	<1			

The start of solidification or T_{break}, as measured during the viscosity measurements shows some similarity with the start of crystallisation as detected with HT-XRD. An exception is *powder* N which shows a relatively high temperature for the start of crystallisation, Table 6.8 and Figure 6.4.

Table 6.8: *Start of solidification or T_{break} and start of crystallisation) (°C)*

	M	N	O	P
Solidification point (T_{break})	1115	1161	1190	1153
Start of crystallisation (HT-XRD)	1075	1250	1200	1150

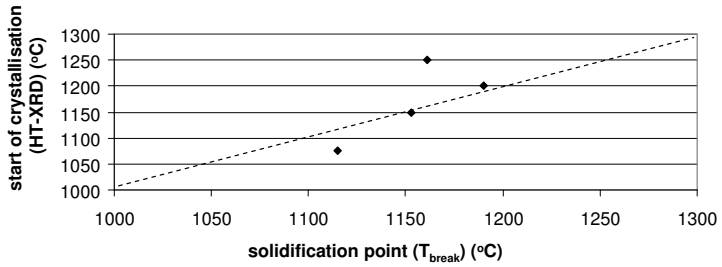

Figure 6.4: *Slag solidification and crystallisation: solidification point or T_{break} (viscosity measurements) versus start of crystallisation (HT-XRD, mould powder M-P) (°C)*

For all materials, the crystal cuspidine is formed first, predominantly followed by a second main crystalline phase (melilite or Na-Al-Silicate).

6.3.3 Cooling rate

Based on the procedure described in Chapter 5, the cooling rate of mould powder P was measured at TU Bergakademie Freiberg, Germany, using the single hot thermocouple method (SHTT). Results were compared with results of the cooling rate of the standard mould powder A. Based on the measurements, a TTT curve was constructed. Subsequently, the nose temperature (T_{nose}) and nose time (t_{nose}) were estimated. For these calculations, the melting trajectory of mould powder P was measured using a hot stage microscope (DIN 51730). Results of the melting trajectory are given in Table 6.9; the TTT curve of mould powder P is illustrated in Figure 6.5.

Table 6.9: *Melting trajectory (mould powder P)*

	P	*A*
Softening temperature (°C)	1057	*1066*
Melting temperature (°C)	1103	*1088*
Fluidity temperature (°C)	1134	*1112*

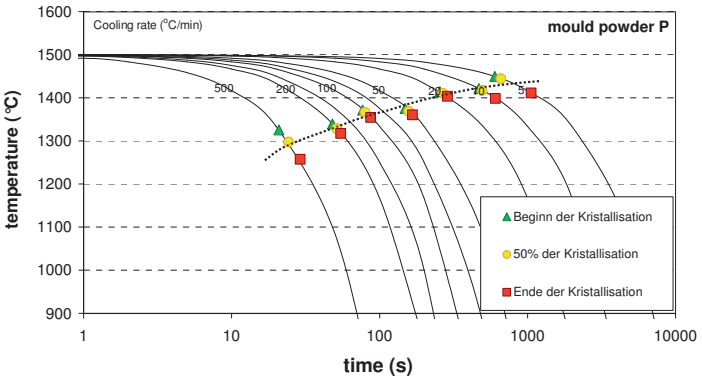

Figure 6.5: *Time-temperature-transformation diagram of a mild cooling mould powder - Mould powder P*

Compared with the standard mould powder A, the mild cooling mould powder P exhibited bigger crystals during the experiments. Furthermore, the higher temperatures and the very small temperature variations between start and end of crystallisation, as found for all cooling rates (up to 500 °C/min) emphasize the increased and stronger crystallisation tendency of mould powder P.
From the results with mould powder P, it is estimated that the nose time (t_{nose}) is between 3 and 10 s. Based on Equations 5.1 and 5.2 and the given melting point of 1103 °C, the nose temperature and the critical cooling rate for mould powder P can roughly be estimated:

nose temperature: $T_{nose} = 0.86T_{liq} \approx 949$ °C

critical cooling rate: $R_c = \Delta T/t_{nose} \approx 30$ °C/s ± 15 °C/s

Compared with the standard mould powder A, an increased surface roughness i.e. increased interfacial thermal resistance can be expected when using mould powder P [13]. The value of the critical cooing rate r_c is higher and an estimation of the normalised cooling rate r_n will be around unity.

6.4 Trials at the pilot caster

The pilot caster of Sumitomo is of a vertical type with a casting length of 3.7 m. The ladle capacity is 2.4 tonnes. The mould dimensions are 800 mm×100 mm, the mould level control is based on an eddy-current system. The caster uses a hydraulic oscillator. The maximum casting speed is 3 m/min.

6.4.1 Caster data

Trials have been done with mould powders M, N, O and with the reference powder A, all using a low-carbon steel grade (C ~ 0.05%) at casting speeds up to 2 m/min and a casting time around 4 minutes. Evaluation of the caster data concentrated on the mould heat transfer including the mould thermocouple temperatures, strand friction, mould level fluctuations and the melting behaviour of the mould powder.
All casting trials were successful. Based on the local heat transfer, 35 mm below the meniscus, powders N and O (mild cooling criteria) showed a decreased heat transfer and some increase in mould level fluctuations. A summary of the caster data is given in Table 6.10. Immediately after a trial, it was tried to collect slag film samples at the meniscus area and under the mould.

Table 6.10: *Local heat flux and mould level fluctuations at the pilot caster*

	M	N	O	*A*
Local heat flux, 35 mm below the meniscus (MW/m^2)	2.3	1.7	1.8	*1.9*
Mould level fluctuations (eddy-current) (mm)	1.9	2.9	3.0	*2.7*

6.4.2 Slag films

The main functions of mould powder i.e. strand lubrication and mould heat transfer are realised by slag films. Understanding the slag films is considered key to a better understanding of the mould powder functions. It will guide mould powder design [14]. The films were characterised with SEM/EDS-techniques. Characterisation concentrated on the structure and composition. Additionally, XRD techniques were used.
All slag films are broken in the transverse direction. In general, the films show a flat and sometimes a wavy surface. Most likely the flat surface corresponds to the mould side. An illustration is given in Figure 6.6.

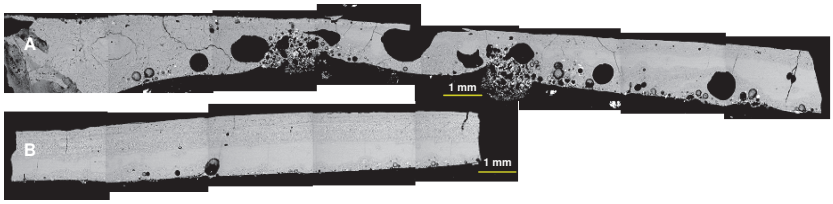

Figure 6.6: *Slag films obtained after the casting trial (under the mould) - Mould powder N, pilot caster*

Mould powder M

Slag films were sampled under the mould. The films show a glass phase, fine crystals (monticellite, melilite and cuspidine) and some unreacted and partly reacted raw materials (periclase, fluorite and Ca_3SiO_5 – hatrurite, a Portland Cement) – these materials adhere to the surface of the films. Note that monticellite is an intermediate (secondary) phase formed during powder melting. This indicates that melting of the mould powder was not completely finished. The film thickness varies between approximately 1 and 2 mm, the

thicker part can possibly be seen as the end of a slag rim. In the glass phase, some (very) small droplets of Fe can be seen.

Mould powder N

After the trial with powder N, slag films were sampled from the meniscus area (adhering to a slag rim) as well as under the mould. In this study, characterisation of slag films obtained under the mould is described. An illustration of the films is given in Figure 6.6 and Figure 6.7. The average thickness of the slag films is 1.5 mm. The films show a glass phase and a crystalline phase. In general, the crystalline phases can be detected in the outside parts of the films (both mould and strand side), the inner parts of the films mainly consist of a glass phase.

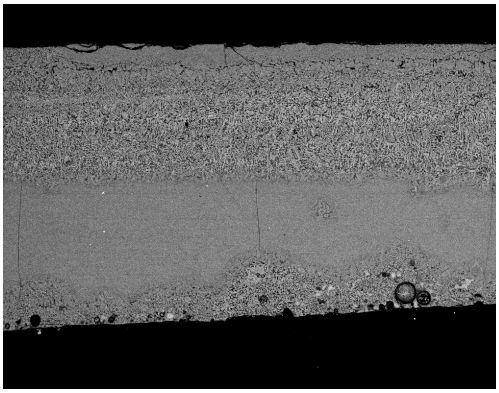

Figure 6.7: *Detail of slag film, obtained after the casting trial (under the mould) showing glass and crystalline phases - Mould powder N, pilot caster*

Detailed analyses of the slag films showed that the crystalline phases mainly consist of large cuspidine crystals (dendrites), together with fine Na-Al-silicate crystals in a glass matrix. All slag films show bubbles and small Fe-droplets. Furthermore, remnants of mould powder raw materials as well as intermediate phases are present, adhering to the surface of the film.

Mould powder A

The films corresponding to mould powder A, sampled under the mould show one area containing glass only and another area containing cuspidine and glass. The thickness is between 0.4 and 1 mm and again Fe (droplets) can be observed here. Some remnants of powder can be seen adhering to the surface; no intermediate phases have been detected.

In general, results of the slag film analyses confirm results obtained with HT-XRD during cooling experiments.

6.5 Trials at the thin slab caster

Evaluation of the mould powder trials at the thin slab caster is based on slag formation (liquid pool depth and rim formation), powder consumption, strand lubrication and mould heat transfer followed by inspection of the slab surface. The desired minimum liquid pool depth during casting is 5 mm. The liquid pool depth is measured by immersing a stainless steel sheet in combination with a copper strip into the mould. The operators observe the formation of rims. The maximum thickness of slag rims is approximately 10 mm; excessive rim formation should be avoided for reasons of process stability [15]. The powder consumption should not be lower than the current average value of 0.05 kg/m^2.
Homogeneous and controlled heat transfer and controlled strand lubrication are desired within the given operational windows of the caster. Mould heat transfer is calculated using mould cooling water temperatures and flow; additional data is obtained via the mould thermocouples. Strand friction is obtained from the hydraulic oscillating system of the mould. Trials were done with mould powders M, O and P. During the trials, it was nearly impossible to collect slag films. Characterisation focussed on slag rims, sampled during trials with powder M and on a slag film which adhered to a small slag rim, obtained after a trial with powder P.

6.5.1 Caster data

Mould powder M
Several plant trials have been done with mould powder M at casting speeds up to 5.0 m/min while casting low carbon steel grades (C ~ 0.045%). The casting speed varied during the trials.
The powder showed good mild cooling properties but significant rim formation during casting. Investigations of the rims indicated sintering behaviour of mould powder M as well as mould level fluctuations, both causing the formation of rims. The sintering behaviour can probably be related to the chemical composition and raw material choice, more specifically the use of MgO (periclase, high melting trajectory) and the relatively high melting temperatures of the raw materials in mould powder M. Furthermore, the use of coke particles as one of the free carbon sources (see rim analysis) will *enhance* the formation of a sinter layer and affect rim growth as well. Coke particles have a different (improved) wetting performance – compared to the more effective carbon black - due to the presence of some inorganic components (oxides) [16]. The presence of monticellite - an intermediate crystalline phase - was also observed [17]. This may indicate incomplete melting.

Figure 6.8: *Slag rim, extracted from the mould - Mould powder M, thin slab caster. Right: mould side*

The liquid pool depth was between 3 and 4 mm; the standard powder only showed a thickness of 2 mm at the same casting speed. The average mould heat transfer during the trial decreased by 5–10%; the friction forces increased by 8% and the torque (withdrawal force) also increased. The friction force is also affected by the taper settings. At the same time, the slab surface temperature, measured at the end of the caster increased

by approximately 15 °C (pyrometer measurements). The trials were stopped because of the rim formation during casting. During and after the trials, several rims have been collected. A more detailed description, based on microscopic analyses is given below; an illustration of a rim is given in Figure 6.8.

Mould powder O

First plant trials with mould powder O have been done on a low carbon steel grade (C ~ 0.045%) with a mould width of 1250 mm and a maximum casting speed of 5.0 m/min, because of the high solidification point of 1187 °C and consequently the expected increased values on strand friction.

The powder shows stable slag pool formation with values between 4-6 mm (reference 4 mm). No slag rims were detected. Comparing to the standard mould powder, the upper rows of thermocouples of the wide faces show a more stable and decreased mould heat transfer (20-30% lower) whereas the lower part of the mould shows an increased mould heat transfer. The average mould heat transfer of the wide faces (based on mould cooling water data) and hence the shell thickness remained the same for both powders.

During continuous casting, the mould heat transfer in horizontal direction reaches its maximum just under the meniscus (20-50 mm). This area can be considered as the most critical part in the casting process with respect to the formation of surface cracks in the just formed shell and the occurrence of thermal wear of the mould copper plates [18].

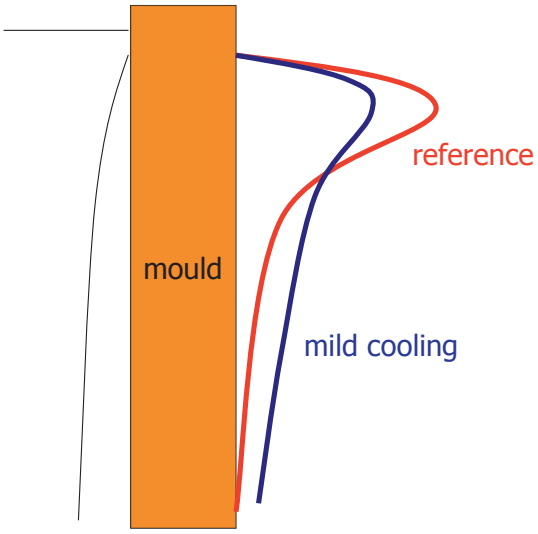

Figure 6.9: *Redistribution of local mould heat transfer during casting as found during plant trials at the thin slab caster - Mould powder powders O and P*

The findings with powder O indicate that the shell thickness is *similar* for both powders, but that the *distribution* of mould heat transfer changes in a very favourable way. A schematic illustration of mould heat transfer during casting is given in Figure 6.9.

The narrow faces show a decrease of the average mould heat transfer by 20-30%. The friction and mould level fluctuations increased during the trial by maximum 15% and 50% respectively. These values are also affected by the taper settings and secondary cooling water during the trial. However, the operational windows were not exceeded. An increase in strand friction can be understood by considering the solidification and crystallisation properties - and consequently the decreased lubrication performance - of mild cooling mould powders. The powder consumption of powder O was roughly the same with values of around 0.06 kg/m^2.

The slab surface temperature, measured at the end of the caster increased; an increase of 30-40 °C was reported (pyrometer measurements). Consequently, the gas consumption in the first segments of the tunnel furnace decreased by approximately 17%. This phenomenon is not fully understood yet. Inspection of the slab surface showed no surface cracks. It has been suggested that the effectiveness of the secondary cooling is significantly affected by the presence of oxidation layers or scale built up on the slab surface [18]. The oxidation layers can be a result of the interaction between the steel surface and the mould slag. The presence of fayalite ($2FeO{\cdot}SiO_2$ or Fe_2SiO_4), formed during this interaction, will enhance scale formation [19,20]. Previous work at the thin slab caster showed effects of mould powder on scale formation and scale build-up; the role of fayalite was clearly indicated [21].
During these trials, comparable effects based on steel slag interaction and the presence of oxidation layers can play a role, resulting in an increased slab surface temperature. Due to priorities within this project and at the DSP caster, this theme was not further investigated. Trials were continued with mould powder P showing a solidification point according to the specifications as given in Table 6.2.

Mould powder P
Various plant trials were performed on low carbon (LC) and high strength low alloyed (HSLA) steel grades at casting speeds up to 5.8 m/min. Based on the condition of the DSP caster and the stability of the casting process, increased casting speeds i.e. >6.0 m/min were not possible.
Compared with the standard practice based on powder A, the melting performance showed a comparable slag pool thickness with no intermediate (sinter) layers and a comparable or even less rim formation. These results are almost similar to the previous results with powder O. The powder consumption increased to around 0.07 kg/m^2 and even 0.08 kg/m^2 at casting speeds between 5.2 and 5.6 m/min. The increased consumption can be understood by the decreased slag viscosity of mould powder P:

$$Q_s = 0.30 / \eta^{0.5} v_c$$

Based on a casting speed of 5.4 m/min and the viscosity data given in Table 6.6, the consumption (Q_s) of mould powder O can be calculated to be Q_s = 0.06 kg/m^2. For mould powder P, the calculated consumption is Q_s = 0.07 kg/m^2. These values are in accordance with the measured values during the plant trials.
The mould level fluctuations slightly increased by 10% or less and were found to be affected by the taper settings and the strand friction during casting as well as the condition of the casting machine and tunnel furnace. In particular the alignment of the segments (caster) and rolls (caster and furnace) are considered to be important subjects.

As before, the trials clearly showed the mild cooling properties i.e. *redistribution* of mould heat transfer as described above: a reduced mould heat transfer in the critical upper part of the mould was found together with an increased mould heat transfer in the lower part of the mould. The total mould heat transfer and hence the shell thickness being roughly the same. In general, the stability of the thermocouples in the upper part of the mould (first two rows) increased. During most trials, the stability of the lower thermocouples decreased and indicated breaking of the solidified slag film. The redistribution of local mould heat transfer as found during the trials is very favourable for continuous casting, in particular for demanding casting processes like thin slab casting at increased casting speeds. Detailed experiences on the mild cooling performance during thin slab casting are given in Chapter 7.

The strand friction increased by maximal 15% when applying powder P. As before, this can be understood by the increased crystallisation tendency and consequently the reduced lubrication properties of the slag film. The current operational window of strand friction at the DSP - *based on mould powder A* - was sometimes exceeded but no operational problems related to strand friction and casting stability were reported. It should be noted that the strand friction, as observed during all the trials, is also affected by the taper settings, the intensity of the cooling water (secondary cooling) at the caster and the condition of the continuous casting machine (alignment of segments).
The slab surface temperature increased by values up to approximately 25 °C. The slab surface showed a good quality with no surface cracks or other defects. The oscillation marks were shallow and straight.

It can be concluded that the effects of mild cooling, in particular with respect to the mould level fluctuations and strand lubrication are less severe when applying mould powder P. This can be explained by the value of the solidification point which is around 40 °C lower than the solidification point of mould powder O. Consequently, mould powder P shows a better lubrication performance than powder O, whilst still showing a redistribution of mould heat transfer.

Surprisingly, it was also found that the effects on mould heat transfer (redistribution), strand friction (increase) and consequently mould level fluctuations are *reduced* by the use of a *previous* mould powder with a reduced basicity and reduced crystallisation tendency. When the sequence starts with mould powder A, followed by mould powder O or P, the values obtained on mould heat transfer, strand lubrication and mould level fluctuations are less characteristic but are still significant. These effects are more profound when a sequence starts with a mild cooling powder like powder O or P.
It is suggested that a previous mould powder or remnants of a previous powder forms an intermediate layer in the slag film, located between the mould copper plates and the slag film, as formed by the mild cooling mould powder. The intermediate layer will act as a coating.

It has been demonstrated that the slag films have a very long residence time and that the transport of the solid part of the slag film i.e. the part adhering to the mould is very slow. Previous analyses of slag films of powder A, obtained at the DSP caster, showed very long residence times and confirm findings reported by other researchers [14].
More details on the redistribution of mould heat transfer, breaking of the slag films and the use of a previous mould powder will be given in Chapter 7.

It can be concluded that a further increase in casting speed is possible and realistic when applying mould powder P. However, the operational windows and casting instructions, in particular on the taper settings, strand lubrication and secondary cooling water should be adapted when applying mild cooling powders at casting speeds up to 8 m/min.
It should also be noted that the actual operational windows and casting practice at the DSP caster are fully based on the experiences with mould powder A and maximum casting speeds between 5 and 6 m/min. Furthermore, the condition of the casting machine and the tunnel furnace are very important subjects for high speed casting, with special requirements on the alignment of the segments and the rolls.

6.5.2 Slag rims and slag films

Mould powder M
A rim was extracted approximately 45 minutes after changing from the standard powder A to powder M. The rim is illustrated in Figure 6.10. The presence of cuspidine, melilite and monticellite indicates that the mould *slag* in the rim predominantly originates from powder M.
The slag contains a significant amount of coarse coke particles which is a raw material, used as a source of free carbon. This observation makes the effectiveness of coke during melting of this powder questionable. The powder particles in the rim originate both from powder M and from the previous powder, powder A. This indicates a long residence time of powder A after the mould powder change and confirms the suggestion of the presence of a previous mould powder.
A part of a slag film adhering to a slag rim was obtained and analysed. The film matches the composition of powder M. The film consists of glass and of the crystals monticellite and cuspidine; the crystals are mostly present at the mould side. Furthermore, porosities were observed, Figure 6.10.
Based on the casting behaviour of powder M, especially rim formation and mould heat transfer, the composition was changed. This resulted in a basicity of 1.2, a solidification point of 1150 °C and a preferred crystallisation of cuspidine. See Table 6.2.

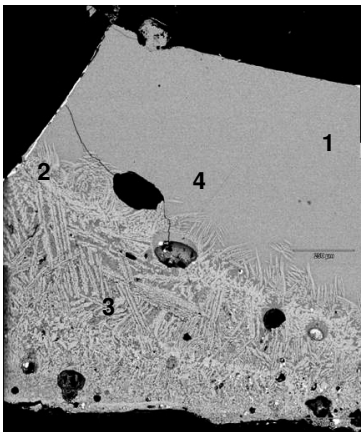

Figure 6.10: *Detail of slag film, adhering to a rim showing glass (1), the crystals cuspidine (2) and monticellite (3) and some porosities (4) - Mould powder M*

Mould powder P
Immediately after casting, a small slag rim including the beginning of a slag film was extracted from a narrow face of the caster (north side). Mould powder P had been used during the last two ladles i.e. around 3 hours of casting. The previous ladles of the sequence were cast with the standard mould powder A. Microscopic investigation concentrated on the slag film, in particular on the presence of the previous mould powder. The chemical composition at various locations in the slag film was analysed and evaluated.
The length of the slag film sample is around 15 mm. The thickness of the slag film decreases from approximately 4 mm at the meniscus area to less than 1 mm at its end. The mould side of the film showed a cuspidine layered structure (cuspidine in a glass matrix), with a total thickness of approximately one third of the thickness of the slag film. Based on the chemical composition within the slag film, in particular the amounts and concentration

profiles of CaO, SiO_2, MgO and Al_2O_3, the presence of the previous mould powder can be reduced. The results indicated a ratio of around 80 wt% powder P and 20 wt% powder A. Based on this analysis, approximately 20 wt% of mould powder A is still present in the slag film. Note that this analysis was done on a small slag film, coming from the upper part of the mould and that other samples are not available. However, the analyses of the slag film seem to confirm the operational findings and proposed mechanism on the effect of a previous mould powder.

6.6 Concluding remarks

Mould powder design for high speed thin slab casting concentrates on mild cooling properties, to be realised by specific values of the basicity (1.2) and the solidification point (1150 °C), promoting the crystallisation of cuspidine. Mild cooling can be considered as a crucial requirement for high speed thin slab casting.

Mild cooling properties at the wide faces will show a reduced mould heat transfer in the critical upper part of the mould, an increased mould heat transfer in the lower part of the mould whilst maintaining a comparable average mould heat transfer and hence shell thickness during casting. These effects are very favourable for continuous casting, in particular for demanding casting processes like thin slab casting. The narrow faces will show a reduced mould heat transfer.
The increased values for strand friction and incidentally, the mould level fluctuations as obtained during the mild cooling practice did not result in any operational restriction.

During this project, it was not possible to apply increased casting speeds >6 m/min due to the condition of the continuous caster and the stability of the casting process. It is recommended, however, to test mould powder P at these increased casting speeds. The operational windows, in particular on strand friction (lubrication), taper settings and secondary cooling water should be adapted and the condition of the continuous caster and tunnel furnace must be appropriate for this casting practice.

As stated before, in-depth characterisation of mould powder, slag rims and slag films, *in combination* with plant trials and operational experiences at the caster proved to be essential for a further understanding of mould powder performance and for a proper mould powder design.

6.7 References

[1] J.A. Kromhout, M. Kawamoto, M. Hanao, Y. Tsukaguchi, E.R. Dekker and R. Boom, Development of mould flux for high speed thin slab casting. Steel Research Int., 80 (2009) 575-581.

[2] T. Kanazawa and M. Kawamoto, Latest technology for QSP process. Proc. Int. Conf. on Continuous Casting - Past, Present & Future, 24-25 October 2005, Jamshedpur, India, The Indian Institute of Metals and TATA Steel Ltd., India, 2005, 227-230.

[3] M. Hara, H. Kikuchi, M. Hanao, M. Kawamoto, T. Murakami and T. Watanabe, High speed continuous casting technologies of peritectic medium thickness steel slabs. La Rev. Métall., 99 (2002) 367-372.

[4] M. Hanao and M. Kawamoto, Mold powder for continuous casting and method of continuous casting using this powder. EP 0 899 041 B1, 2002.
[5] J. A. Kromhout, C. Liebske, S. Melzer, A.A. Kamperman and R. Boom, Mould powder investigations for high speed casting. Ironmaking and Steelmaking, 36 (2009) 291-299.
[6] T. Watanabe, H. Fukuyama and K. Nagata, Stability of cuspidine ($3CaO{\cdot}2SiO_2{\cdot}CaF_2$) and phase relations in the $CaO\text{-}2SiO_2\text{-}CaF_2$ system. ISIJ Int., 42 (2002) 489-497.
[7] M. Hayashi, T. Watanabe, H. Nakada and K. Nagata, Effect of Na_2O on crystallization of mould fluxes for continuous casting of steel. ISIJ Int., 46 (2006) 1805-1809.
[8] M. Hanao, M. Kawamoto and T. Watanabe, Influence of Na_2O on phase relation between mold flux composition and cuspidine. ISIJ Int., 44 (2004) 827-835.
[9] S. Ozawa, M. Susa, T. Goto, R. Endo and K.C. Mills, Lattice and radiation conductivities for mould fluxes from the perspective of degree of crystallinity. ISIJ Int., 46 (2006) 413-419.
[10] S. Sridhar, K.C. Mills, O.D.C. Afrange, H.P. Lörz and R. Carli, Break temperatures of mould fluxes and their relevance to continuous casting. Ironmaking and Steelmaking, 27 (2000) 238-242.
[11] H. Kim, W.H. Kim, J.H. Park and D.J. Min, A study on the effect of Na_2O on the viscosity for ironmaking slags. Steel Research Int., 81 (2010) 17-24.
[12] J.A. Kromhout, A.A. Kamperman, M. Kick and J. Trouw, Mould powder selection for thin slab casting. Ironmaking and Steelmaking, 32 (2005) 127-132.
[13] K. Tsutsumi, T. Nagasaka and M. Hino, Surface roughness of solidified mold flux in continuous casting process. ISIJ Int., 39 (1999) 1150-1159.
[14] P. Hooli, Layers in the slag film between steel shell and mould in continuous casting of stainless steel. Proc. 8th Int. Conf. on Molten Slags, Fluxes and Salts (MOLTEN2009), 18-21 January 2009, Santiago, Chile, GECAMIN Ltd., Santiago, 2009, Chile, 1129-1138.
[15] M. Emi, The mechanisms for sticking type break-outs and new developments in continuous casting mold fluxes. Proc. 74th Steelmaking Conf., 14-17 April 1991, Washington, USA, 1991, Iron and Steel Society, Warrendale, USA, 1991, 623-630.
[16] M. Emi, Nippon Thermochemical Co., Personal communication, 2005.
[17] J.H. Park, D.J. Min, H.S. Song and Y.D. Lee, Influence of CaF_2 on viscosity and structure of molten slags. Proc. 85th Steelmaking Conf., 10-13 March 2002, Nashville, USA, Iron and Steel Society, Warrendale, USA, 2002, 775-786.
[18] M.M. Wolf in 'Metallurgie des Stranggießens, Gießen und Erstarren von Stahl', (Herausgeber K. Schwerdtfeger), Erstarrungsgeschwindigkeid beim Strangguß, Verlag Stahleisen mbH, Düsseldorf, Germany, 1992.
[19] Y. Ito, I. Shimoda, M. Suzuki and Y. Miki, Effect of mould flux on secondary cooling intensity in continuous casting. Proc. 4th Int. Congress on the Science and Technology of Steelmaking (ICS 2008), 6-8 October 2008, Gifu, Japan, The Iron and Steel Institute of Japan, Tokyo, Japan, 2008, 698-701.
[20] H.J. Grabke and M.M. Wolf, in 'Kontaktstudium Metallurgie Teil III: Gießen und Erstarren/Strangießen', Zunderbildung, Entzundern – Verfahrens- und Qualitätsaspekte beim Stranggießen und Warmwalzen, 19-24 October 1997, Goslar-Hahnenklee, Technische Universität Clausthal/VDEh Düsseldorf, Germany, 1997.
[21] M.C.M. Cornelissen, J.A. Kromhout, A.A. Kamperman, M. Kick and F. Mensonides, High productivity and technological developments at Corus DSP thin slab caster. Ironmaking and Steelmaking, 33 (2006) 362-366.

7 Operational experiences

This chapter describes in more detail plant observations from trials with mild cooling powders. Attention is given to mould heat transfer, strand friction and local temperature variations as observed during thin and conventional slab casting. The chapter ends with a general overview on the properties and performance of mould powders for thin slab casting.

7.1 Temperature variations

Plant trials with mild cooling mould powders revealed patterns of temperature variations (mould thermocouples) in the upper part of the mould. Normally, these temperature variations are only observed in the lower part of the mould. A description of this phenomenon with a proposed mechanism is given below.

7.1.1 Introduction

Several investigations on *slab casters* report a cyclic pattern of temperature variations. These are more commonly seen in the lower half of the mould but have occasionally been observed higher in the mould [1,2]. An illustration is given in Figure 7.1.

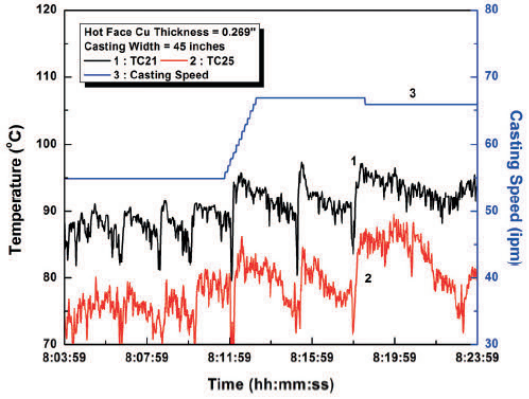

Figure 7.1: *Measurements from broad face thermocouples [2]*

The pattern of saw-tooth like temperature variations is mainly observed when using mould powders with an increased basicity (CaO/SiO_2 = 1.6) and results sometimes in a crossover of the sticker breakout detection thermocouple signals. In general, false sticker alarms are generated but occasionally sticking and breakouts can actually occur. It is suggested that the temperature variations can be associated with the breaking of the solid crystalline slag film during casting. The crystalline nature of the slag film, which includes the presence of pores and small cracks, is an important condition for breaking. Furthermore, relations with the thickness of the mould wall are reported as well; a thinner mould wall will show a decreased hot face temperature and an increased local heat transfer which effects crystallisation. Finally, this will result in more temperature variations. A proposed

mechanism for breaking of slag films is illustrated in Figure 7.2. Up to now, no direct evidence such as slag film samples has been reported in support of the proposed mechanism.

Evaluations at a medium thin slab caster (low carbon and stainless steels) revealed thermal fluctuations, associated with mould level fluctuations, and incidentally, with fracturing and shearing of the solid slag film in the lower half of the mould. As before, the properties of the crystalline slag film are suggested to play an important role but actual mould powder properties are not mentioned [3].
Evaluation of plant data obtained at a thin slab caster at Trico (QSP) showed an incidental pattern of regular oscillations of the thermocouples at the narrow faces, 360 mm from the top of the mould. Although such oscillations were not observed at a higher position, it was concluded that the oscillations were related to mould fluid flow, probably caused by misalignment of the SEN [4]. Within the knowledge of this study, it can be concluded that *breaking* of the slag film can be the origin of the observed temperature variations. Previous evaluation of mould data at this plant, however, indicated incidental breaking of the slag film followed by refilling at locations around 490 mm from top of the mould. No detailed information on slag properties and casting conditions has been given [5].

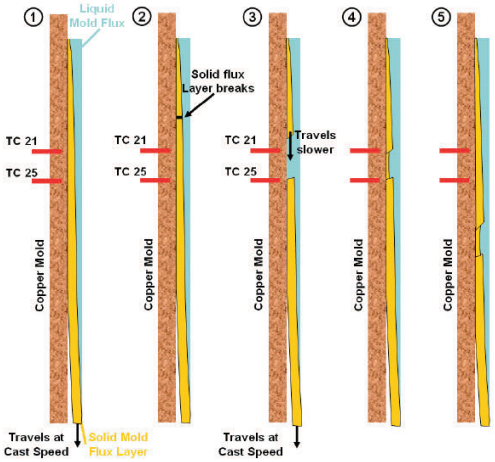

Figure 7.2: *Proposed mechanism for breaking of slag films. Blue = liquid slag, yellow = solid slag [2]*

The authoritative work of Hooli, based on stainless steel continuous casting, describes slag films which consist of several sub layers, voids and pores [6]. Very long residence times (several hours) for the slag films are reported. The slag film (or at least a part of it) adheres or even sticks to the mould wall. Furthermore, the process of *devitrification* is described as an important mechanism for slag crystallisation. Crystallisation of the slag film results in decreased values for mould temperatures and mould heat transfer. Based on thermocouple signals and some slag film samples, evidence of incidental fracturing of the films was reported.

The rupture strength (or elongation stress) of slag films was measured using laboratory scale equipment at 1200 °C [7,8]. The slag films were based on three commercial mould

powders and were prepared in the laboratory. For these “synthetic” film samples, it was concluded that the elongation stress increases with increasing thickness of the slag film, with decreasing temperature and with decreasing NBO/T ratio (a measure of the depolymerisation of the silicate network) i.e. as the slag film becomes more glassy and less crystalline. Like other parameters, attempts were made to relate the elongation stress to the structure of the slag (network), assuming that there will be a correlation between the thermo physical properties and the slag structure [9].

7.1.2 Plant observations: reference situation with standard mould powder

When casting with the standard mould powder A at the DSP, a pattern of temperature fluctuations (between 20 °C and 30 °C) can be observed in the lower part of the mould, around row 7 and 8 of the thermocouples (650-750 mm under the steel meniscus). Most likely, these fluctuations are related to breaking of the slag film. At this location in the mould, the slag films are assumed to be completely solid with a distinct crystalline structure. An illustration of the position of the thermocouples in the DSP mould is given in Figure 7.3 and Figure 7.4.

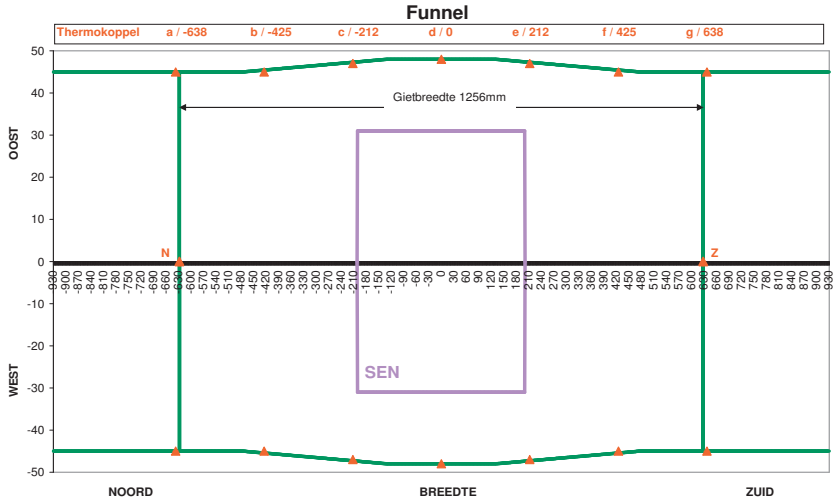

Figure 7.3: *Schematic illustration of DSP mould, wide faces. Thermocouple positions (columns).”Gietbreedte” = casting width*

As described in the previous chapter, slag films sampled under the mould of the DSP (standard mould powder) showed breaking of the slag films in transverse and in longitudinal direction. Breaking in transverse direction can happen in the lower part of the mould or just under the mould. Breaking in longitudinal direction occurred along a line of bubbles, as present in the slag film and is expected to happen in the mould during casting. If the slag film fractures in longitudinal direction, the proposed mechanism is *sheeting* [2,10].

Due to the phenomena described, the mould temperatures observed per *column* of thermocouples (casting direction) deviate from the “ideal” situation.

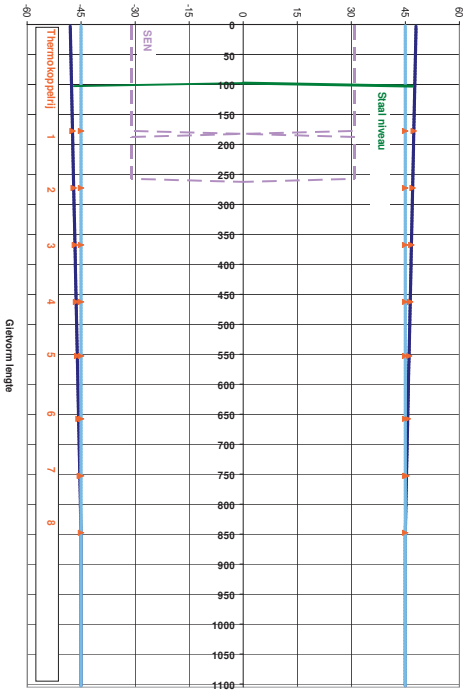

Figure 7.4: *Schematic illustration of DSP mould, narrow face. Thermocouple positions (rows). Green line indicates steel level*

Given this configuration with eight rows of thermocouples, the ideal situation during casting will show a gradual decrease in temperature per row. This can be described as:

t1>t2>t3>t4>t5>t6>t7>t8

The standard practice using powder A was evaluated. For this reference situation, the observed temperature distribution per column thermocouples was found to be like:

parallel	t1>t2>t8>t3>t4>t5>t6>t7
funnel area	t1>t2>t3>t4>t8>t5>t6>t7
parallel	t1>t2>t3>t4>t5>t6>t8>t7

All data were obtained during the same trial at 5.7 m/min. The variations are probably due to disruptions or breaking of the slag film around row 8, resulting in an increased temperature at this position, followed by a gradual temperature decrease. When no breaking occurred, there was a gradual, standard decrease in mould temperatures in the vertical (casting) direction.

7.1.3 Plant observations: mild cooling practice

Plant trials with mild cooling mould powders resulted in a redistribution of local mould heat transfer and in increased friction during casting. Both phenomena can be related to the solidification and crystallisation properties of the mould slag. During the trials,

temperature variations (with sometimes large variations of 20 °C and incidentally up to 50 °C) were present around row 2 and row 3 (>200 mm under the meniscus) or in row 4 (>350 mm under the meniscus). The variations around rows 7 and 8 (650-750 mm under the meniscus) were present as well.

For the mild cooling practice, the temperatures observed per *column* (thermocouples) show significant deviations. The temperature distribution at a casting speed of 5.7 m/min can now be given as:

parallel	t1>t8>t4/t5>t2>t3>t6/t7
funnel area	t1>t2>t3/t4>t5/t6>t8>t7
parallel:	t1/t4>t5>t2/t3>t6>t8>t7

Breaking of the slag film occurred in the upper part (row 4) and lower part (row 8) and resulted in an increased temperature at these positions, followed by a gradual temperature decrease. Breaking of the slag film always occurred, at least at one position. In many cases, casting using mild cooling mould powders resulted in *an extra set* of temperature variations, present in the upper part of the mould.
During all mild cooling mould powder trials, no stickers or break outs occurred, no extra wear or deterioration of the mould plates was seen and slab surface quality was found to be good.

Previous trials with high basicity mould powders (CaO/SiO_2 = 1.3) as described in Chapter 4, revealed patterns of comparable, or even wider, and more “grassy” temperature variations in the lower part of the mould.

During the plant trials with mild cooling mould powders the temperature variations, in particular the variations in the upper part of the mould were found to be influenced by the following variables:

- **Previous mould powder** (standard)

Use of the standard mould powder (mould powder A) i.e. a powder with a lower crystallisation tendency *before* using a mild cooling mould powder, resulted in less, or even no, temperature variations in the upper part of the mould.

- **Position in the mould** (parallel, transition to funnel, funnel)

The parallel part of the mould showed the most stable thermocouple signals, followed by the funnel area. The transition area between the parallel part of the mould and the funnel area showed more temperature variations.

- **Casting speed**

An increased casting speed sometimes resulted in temperature variations at a lower position in the mould.

- **Meniscus fluctuations**

The temperature variations in the upper part of the mould can sometimes be associated with severe meniscus variations due to bulging, waves etc. as detected by the mould level control system.

Figure 7.5 gives an overview of the mould signals during casting at 5.7 m/min, measured at the transition area between the parallel part of the mould and the funnel, and showing very severe disturbances. The saw-tooth pattern (pink) is located at row 2, around 200 mm under the meniscus. As will be described in Section 7.1.5 a decrease in temperature can

probably be related to crystallisation of the slag film and a temperature increase to fracturing. In general, the temperature signals for all columns show that the lowest point of a temperature cycle is “transported” downward within approximately 10 seconds, which can be related to the casting speed. It can be concluded that the film breaks around row 2, 3 or 4 and is transported together with the moving strand.

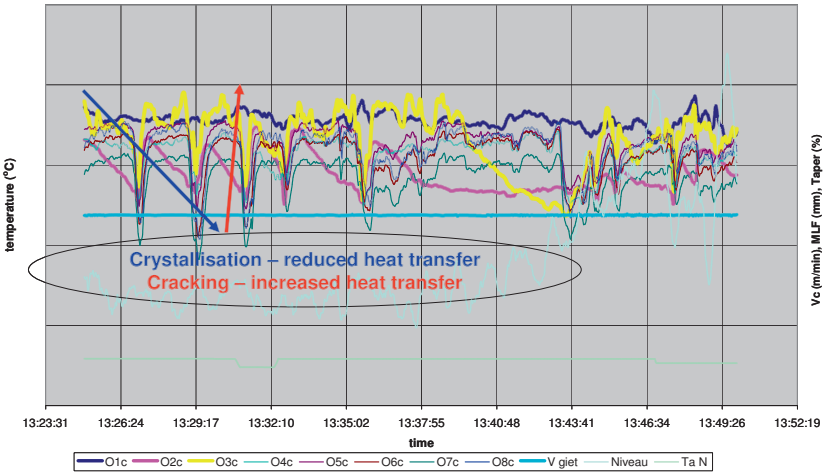

Figure 7.5: *Thermocouple signals from DSP caster (parallel/funnel area), v_c = 5.7 m/min. Left axis: temperature (°C); horizontal axis: time; right axis: casting speed (m/min), mould level fluctuations (mm) and taper (%)*

7.1.4 Analysis of slag films

Inside the mould, DSP

As described in Chapter 5, slag films from the standard powder A were sampled from inside the mould at the DSP caster, immediately after casting.

The films were located around 50 cm below the steel meniscus; the thickness of the films is between 200 and 300 µm. Almost all films show a dominant layer of cuspidine crystals ($3CaO{\cdot}2SiO_2{\cdot}CaF_2$ or $Ca_4Si_2O_7F_2$) in a glass matrix and an amorphous layer. The crystalline layer is located at the mould side; the amorphous layer is present at the strand side and is probably formed from the liquid phase, immediately after casting.

Surprisingly, several samples of the standard powder clearly showed the crystalline layer present in the middle of the slag films and surrounded by two layers of amorphous material. One amorphous layer located between the crystalline layer and the strand and one layer between the crystalline layer and the mould side. An illustration is given in Figure 7.6A; in this figure, the crystalline layer is denoted as II. This crystalline layer appeared to be fully comparable with crystalline layers located at the mould side, as observed in the other slag films. Furthermore, the samples with the crystalline layer in the middle of the film, showed the start of crystallisation in the amorphous layer (devitrification) as present between the crystalline layer and the mould, Figure 7.6B, layer I. It is suggested that the solid part of the slag film fractured and came loose from the copper mould. Subsequently, fresh liquid slag entered the gap between the crystalline film and the copper mould and solidified as amorphous material. After some time,

crystallisation of the newly formed amorphous layer at the mould side started. It is obvious that this process will result in variations in temperature and local mould heat transfer.

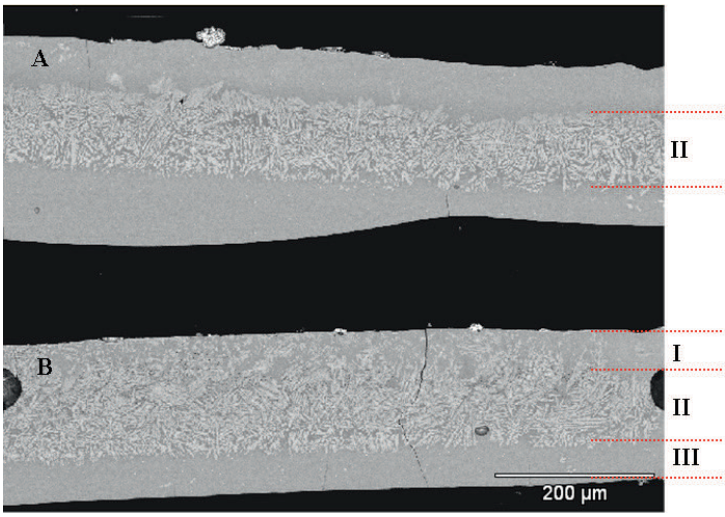

Figure 7.6: *Slag films, sampled from inside the mould, showing a crystalline layer in the middle of the film (A II) and start of crystallisation at the mould side (B I)*

Inside the mould, round billet caster

Further evidence of slag fracture can be found from the analyses of a slag film obtained from a round billet caster. With respect to mould powder requirements, round billet casting can be compared with thin slab casting [11]. During operation, the casting speed was 2.5 m/min with a mould diameter of 250 mm. The basicity (CaO/SiO_2) of the mould powder is 1.0 and the *calculated* solidification point (T_{break}, Sridhar) is 1150 °C.

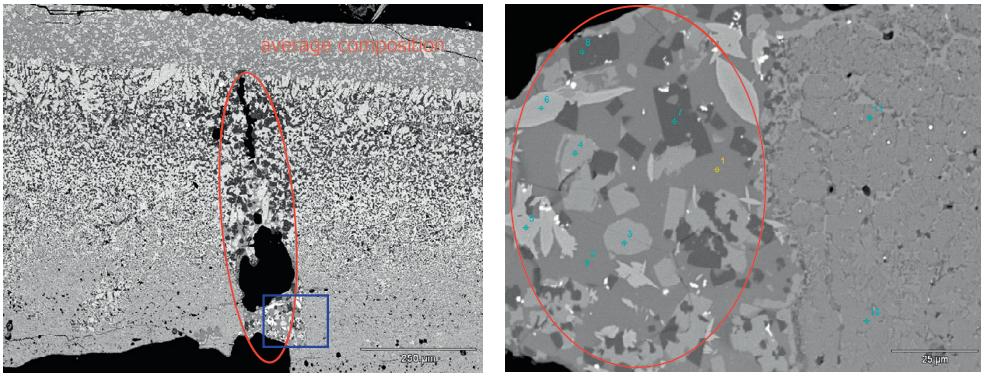

Figure 7.7: *Slag film obtained at a round billet caster showing cracks refilled with slag in the left-hand picture; a detail of the refilled crack is given in the right-hand picture. The upper part of the slag film is the strand side.*

The average film thickness is between 0.7 and 1 mm. The film contains crystals and glass, small metal droplets near the mould and some bubbles. Within the slag film several crystal

layers can be detected as well as a lot of cracks and even a repetition of cracks in transverse direction. The cracks are refilled with liquid slag and show longer crystallisation times (slow growth crystals), Figure 7.7.
The occurrence of cracks followed by refilling and crystallisation will result in variations in local heat transfer. Two mechanisms for refilling are proposed:

1. Partial remelting of the solidified slag film.
2. Filling with fresh mould slag, coming from the liquid part of the slag film.

Based on the microscopic analyses, it is concluded that after breaking, the gap is filled with liquid slag.

Under the mould, DSP
Slag films sampled under the mould of the DSP showed breaking and sheeting of the slag films in transverse and in longitudinal direction. Sheeting in longitudinal direction occurred along a line of bubbles and is expected to happen during casting [10].

7.1.5 Summary of findings, hypothesis and proposed mechanism

It is obvious that the temperature variations associated with breaking and sheeting of the solid slag film are enhanced by the solidification properties of the mould slag. An increased solidification point and an increased crystallisation tendency will result in variations at higher positions in the mould. Deformation of the solid and crystalline slag film due to the shape of the mould (parallel – funnel) further enhances these variations.
There is some similarity with previous work on the formation of star cracks. It is proposed that decreased liquid lubrication i.e. running out of liquid in the slag film enhances the formation of surface cracks and may result in fracturing of the solid slag film in the lower half of the mould [12].

The cyclic temperature variations in the upper part of the mould can be controlled and suppressed by using a previous mould powder with a lower crystallisation tendency. Both the findings of Hooli and those recorded in this work revealed that the residence time of the slag film or at least the part of the film in contact with the mould, is very long (up to 10 hours or more). It is suggested that the slag film formed by a previous mould powder acts as a coating layer with a very long residence time. This coating diminishes the temperature variations resulting from fracturing of the neighbouring slag film. An increased casting speed (within the actual operational window of 5.8 m/min at most) will only result in breaking of the slag film at a somewhat lower position in the upper half of the mould. This can be understood by the increased mould heat transfer at increased casting speeds and consequently by the delayed solidification and crystallisation of the slag film.

Surprisingly, *no operational problems* related to fracturing of mould slag and no surface cracks have been reported during all trials. This indicates that the *first 200 mm* under the steel meniscus are essential for initial solidification and for the formation of a homogenous steel shell, more precisely the top shell. This can be clarified by considering the thickness of the solidified shell in the upper part of the mould i.e. at a casting length of 200 mm.

A general approach to calculate the shell thickness during casting is given in equation 2.35:

$$d_{shell} = k\sqrt{t}$$

The actual value of the solidification coefficient *k* at the DSP caster is around 25 mm/min$^{0.5}$. Given a casting length of 200 mm and an average casting speed of 5.4 m/min, the resulting shell thickness d_{shell} at this location is approximately 5 mm. This value can be compared with the minimum shell thickness as mentioned by Bernard and co workers [13] and is roughly similar to the shell thickness at *mould exit* when applying very high casting speeds, for instance 10 m/min at the QSP pilot caster [14].

After the breaking of the slag film in the upper part of the mould, two underlying mechanisms will happen simultaneously:

1. The hole in the slag film will be refilled with fresh mould slag. This slag solidifies, resulting in amorphous material and hence in increased local mould heat transfer. Subsequently, the slag film crystallises and will break again.
2. The broken part of the film moves downwards with the strand.

A schematic illustration of the temperature variations in the upper part of the mould is given in Figure 7.8 and Figure 7.9.

- At stage A the slag film breaks or shears; resulting in a sharp increase in the mould temperature and the local mould heat flux. Next, the gap is refilled with liquid slag.
- At stage B, the gap is filled with fresh mould slag and after quenching, followed by crystallisation of the amorphous slag (devitrification).
- At stage C, crystallisation of the slag film results in a gradual decrease in temperature and mould heat flux. Pores will be formed due to crystallisation; furthermore the shear force between the solid slag film and the moving strand will result in the formation of stresses and probably cracks in the crystalline material. The presence of pores and cracks will result in a further sharp decrease of the temperature and mould heat flux.

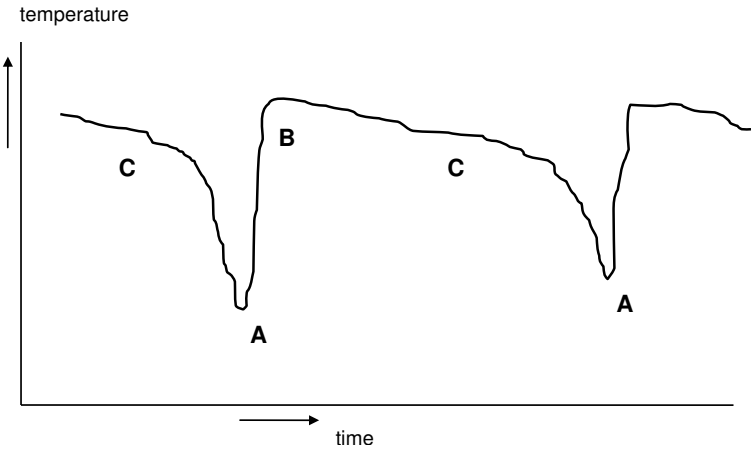

Figure 7.8: *Schematic illustration of mould temperature variations (upper part) - the time between points A is two minutes or more*

The temperature signals in almost all columns show that stage A is “transported” downwards within 10 seconds.

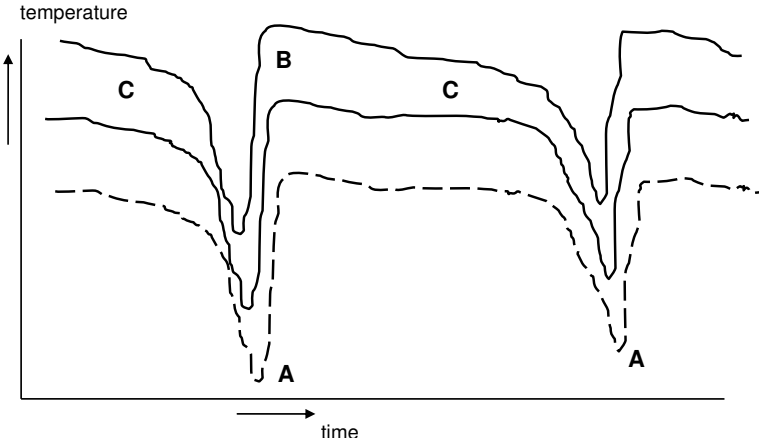

Figure 7.9: *Schematic illustration of mould temperature variations (upper part), followed by the lower thermocouples (dashed curve)*

7.1.6 Next steps

The mild cooling mould powder was initially designed for a maximum casting speed of 8 m/min. During this project, the maximum operational casting speed was 5.8 m/min. Although no operational problems related to the temperature variations and associated with shearing of slag films were reported, it was proposed to decrease or suppress these variations for reasons of operational stability. A decreased crystallisation tendency of the mild cooling mould powders will result in a less rigid slag film and in decreased or no cyclic temperature variations in the upper part of the mould. For plant operations with casting speeds up to 6.0 m/min, a slight decrease in basicity or the solidification point was suggested, whilst keeping all other variables constant. Based on literature findings, the knowledge gained within this project and the experience of the industrial partners, the solidification point was decreased by 20 °C to 1130 °C resulting in mould powder Q [15,16]. An overview of the mould powders is given in Table 7.1.

Table 7.1: *Summary of mould powders for thin slab casting*

Mould powder type/ slag property	Standard **A**	Mild cooling ≤8.0 m/min **P**	Mild cooling ≤6.0 m/min **Q**
CaO/SiO_2	1.0	1.2	1.2
Solidification point (T_{break}) (°C)	1170	1150	1130

The 20 °C decrease in solidification point was realised by adding a small amount of B_2O_3 (0.4 wt%) to the original mild cooling mould powder. After full characterisation and plant trials, next steps on mould powder design can be defined.

It is proposed to measure the rupture strength or elongation stress of slag films for thin slab casting at increased temperatures, using the method described [8]. Slag films from

inside the mould are preferred; however the measurements can start with slag films prepared at the laboratory. It is highly recommended to relate the physical properties (like elongation stress) to the structure of the mould slag.

7.2 On the heat flux ratio during thin slab casting

7.2.1 Introduction

Wünnenberg reviewed various aspects of mould heat transfer during continuous casting [17]. One subject is the *interaction* between the mould heat transfer at the wide faces and the narrow faces, observed at a thin slab caster. It was concluded that an increased mould heat transfer at the *wide faces* will be followed by shrinkage of the shell, which will lead to an increased thermal resistance and finally a decreased mould heat transfer at the *narrow faces*. Based on this mechanism, a decreased mould heat transfer at the *wide faces* will result in an increased mould heat transfer at the *narrow faces*. The work underlines the importance of *adequate taper settings* and mould slag design i.e. the slag film properties in order to achieve a controlled mould heat transfer during casting. In addition, the copper wall thickness and the amount and speed of the mould cooling water are considered to be less important parameters.
Pleschiutschnigg and co workers developed the concept of the Auto-Pilot for automatic taper control and regulation of the casting speed at CSP plants [18,19]. Based on the heat flux for both wide and narrow faces, the taper settings during casting are controlled with the aim to keep the casting process within a window of preferred or ideal casting conditions. A main focus within this concept is the reduction of longitudinal facial cracks. Furthermore, the casting speed is controlled via the steel temperature in the tundish. For the taper settings, the *heat flux ratio* was introduced which is defined as:

heat flux ratio = mould heat transfer narrow face/average mould heat transfer wide faces

where mould heat transfer is given in MW/m^2, based on mould cooling water data.

Previous work on conventional slab casting showed that the optimum range for the heat flux ratio is between 0.8 and 0.9. Within this range, the incidence of longitudinal facial cracks was found to be at minimum. These findings were applied and adapted for high speed thin slab casting. It was advised that the optimum range of the heat flux ratio is between 0.6 and 0.8 for casting speeds up to 10 m/min. However, no detailed information on mould slag properties and other casting parameters has been given.
For all casting applications, the heat flux ratio is tuned by setting and adjusting the narrow face tapers. Figure 7.10 illustrates the course of mould heat transfer for the wide and narrow faces after the start of casting, together with the corresponding heat flux ratios.

7.2.2 Plant observations

The heat transfer properties of mild cooling mould powders, as observed during plant trials at the DSP, were investigated by evaluating the average mould heat transfer of the wide and narrow faces based on mould cooling water data and local thermocouple data.

As described before, casting trials with mild cooling powders (powders O and P) resulted in a *redistribution* of local mould heat transfer at the wide faces. During casting, the upper rows of thermocouples show a more stable and decreased mould heat transfer whereas the lower part of the mould shows an increased mould heat transfer with more temperature

variations. The average mould heat transfer at the wide faces remains roughly the same or shows some increase, comparing to the reference situation (powder A). These findings indicate that the shell thickness at the wide faces is very similar for both casting practices but that the distribution of mould heat transfer changes in a very favourable way.

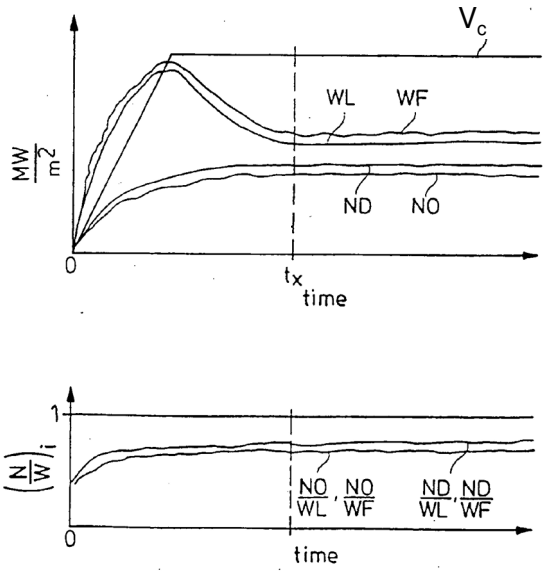

Figure 7.10: *Mould heat transfer at wide (WL, WF) and narrow (ND, NO) faces with the corresponding heat flux ratios $(N/W)_i$ [18]*

For the narrow faces, it was found that the mould heat transfer (based on mould cooling water data) shows a significant *decrease* with lower and more stable local temperatures. A decreased mould heat transfer at the narrow faces will result in a thinner shell, compared to the wide faces of the mould.

A general overview of the average heat transfer for all mould faces during a plant trial with a mild cooling powder (powder P) is given in Figure 7.11. During the sequence, the mould powder was changed from the reference material (powder A) to the mild cooling practice. The trial was performed at a casting speed of 5.4 m/min.
The findings on mould heat transfer can be understood since the mild cooling properties produce a thinner shell in the upper part of the mould. Referring to the wide faces, the contact between the thinner solidified shell and the mould improves, which finally results in an increased mould heat transfer and shell thickness in the lower part. Consequently, shrinkage of the shell will occur which leads to a decreased contact between the shell and the mould at both narrow faces. A decreased contact results in an increased heat resistance and in lower values for mould heat transfer and shell thickness at the narrow faces.

The heat flux ratio decreases from around 0.8 to values around 0.6, as a result of the mild cooling practice. This phenomenon can be explained by the significant decrease in mould heat transfer at the narrow faces, compared to that at the wide faces.

As a consequence, the mild cooling practice, as applied during thin slab casting requires *increased* taper settings at the narrow faces of the mould. By doing so, the contact between the strand and the narrow faces will improve, the mould heat transfer at the narrow faces will increase (less thermal resistance) and the thickness of the as solidified shell will increase as well. Consequently, the overall heat transfer and the *overall shell thickness* of the slab will be more uniform which is very advantageous to the reduction of longitudinal facial cracks in the corner areas of the wide faces.

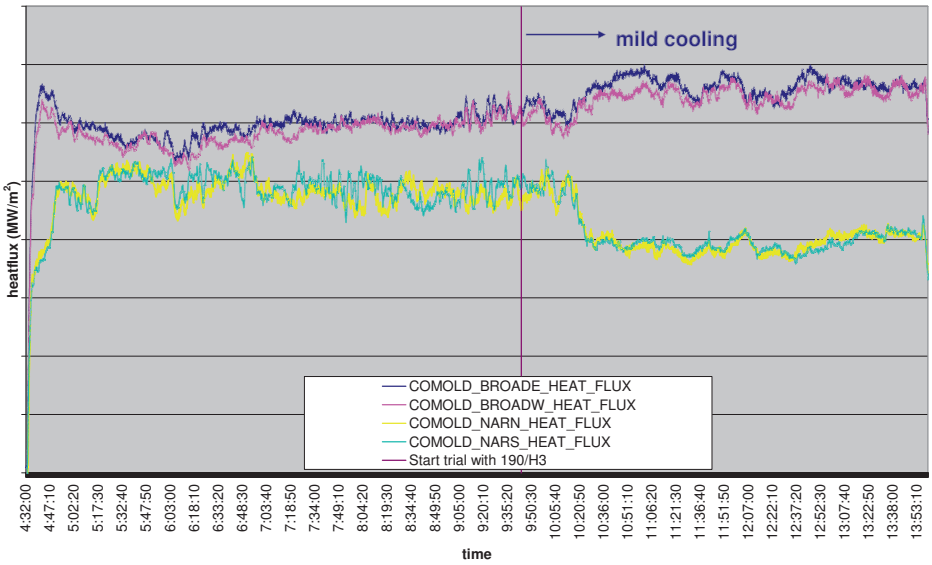

Figure 7.11: *Average mould heat transfer (mould cooling water) during mould powder trial, DSP caster, v_c = 5.4 m/min*

Plant trials with mild cooling mould powders were carried out using increased taper settings at casting speeds up to 5.7 m/min. The taper settings were increased from 1.1 ~ 1.2% to 1.4%. An additional tool for evaluation of these trials is the shape of the narrow faces during casting, as observed at the end of the caster. The caster data showed increased values of the heat flux ratio and a comparable shape for the narrow faces of the slab, indicating an increased uniformity of mould heat transfer and shell thickness around the perimeter of the slab. Longitudinal facial cracks were not observed. Increased taper settings for mould powders with mild cooling properties are now standard practice at the DSP caster.

It should be noted that almost all previous plant trials with high basicity powders as described in Chapter 4 showed a decreased heat flux ratio, compared to the standard practice with the reference powder. Up to now, there has been no satisfactory explanation for this phenomenon. It can be concluded that the mechanism described above, can be applied to these plant observations.

7.3 The next step: mould powders for slab casting

7.3.1 Introduction

As described in Chapter 2, mould powders for thin slab casting were initially based on successful slab casting powders with emphasis on slag viscosity and slag solidification. During this study, powder melting, slag crystallisation and in particular the formation of slag rims during casting were addressed as additional major requirements for thin slab casting mould powders. Comparing to conventional slab casting, the operational windows for thin slab casting are more restricted and critical, resulting from the more demanding process conditions at increased casting speeds.

Previous work focussing on mould powder properties for slab casting and thin slab casting has been published elsewhere [20]. This work was based on a survey of mould powders, powder characterisation and plant trials and revealed that the main properties needed to describe mould powders for slab casting are viscosity, melting point, basicity (CaO/SiO_2) and the free carbon content. Given the variety of data obtained and the very few production rules, it was concluded that wider ranges of physical properties for slab casting mould powders are possible and realistic. For thin slab casting powders, the properties and requirements were more restricted but were found to lie within the operational windows of slab casting mould powders.

It can be stated that mould powders for conventional slab casting cannot be used for the more demanding process of high speed thin slab casting without adaptations. However, it is proposed that mould powders for thin slab casting can be applied to conventional slab casting, in particular when the control of mould heat transfer is an important requirement (for instance for crack sensitive steel grades). During implementation of a thin slab casting mould powder at a conventional slab caster, some minor changes are required, which are related to the specific operational conditions.

An overview on the physical properties of mould powder A is given in Table 7.2. Based on these properties and on the knowledge obtained on free carbon additions, powder melting and slag solidification, plant trials at the conventional slab casters of Tata Steel IJmuiden were performed.

Table 7.2: *Key properties, mould powder A*

	A
Viscosity at 1300 °C (Pa·s)	0.13
Break point (solidification point) (°C)	1167
Melting point (°C)	1088
Basicity (CaO/SiO_2)	1.0
C_{free} (wt%)	3.5

7.3.2 Plant trials

At first, plant trials with mould powder A were done on low carbon steels and HSLA-grades ($0.01 < [C] < 0.06$ wt%) at all operational casting speeds. In general, the trials showed improved thermocouple stability. Furthermore, decreased mould heat transfer and increased strand friction within the operational windows were reported. The trials were

followed by peritectic steel grades (for instance [C] = 0.11 wt%) at all operational casting speeds i.e. up to 1.65 m/min. These trials were successful as well, showing less rim formation and in general, comparable or even improved results related to strand lubrication and mould heat transfer. In general, trials with mould powder A revealed both a well controlled mould heat transfer as well as sufficient lubrication during casting. The *balance* between the two main mould powder functions proved to be sufficient for all operational casting speeds.
As a next step, powder A was adopted for casting almost all steel grades at the IJmuiden plant. Detailed information on mould data and product quality are not given, but it was concluded that almost all trials with this standard thin slab casting mould powder showed the possibility that such a powder could be applied to conventional slab casters. For special steel grades like TRIP steels and very crack-sensitive steels, a more specific mould powder is required. Mould thermal monitoring played an important role during the evaluation of all plant trials at these slab casters. An overview of this work, including examples of mould powder evaluation was presented in 2010 [21].

7.3.3 Slag film characterisation

Slag films, adhering to a slag rim and present around 5 ~ 10 cm under the meniscus were characterised using microscopic techniques. The slag films are composed of a glassy part, which originally was in contact with the hot steel side and a crystalline region, previously located on the mould side. As with thin slab casting the dominant phase in the crystalline region is cuspidine. Furthermore, bubbles are present. An illustration of a typical slag film is given in Figure 7.12.

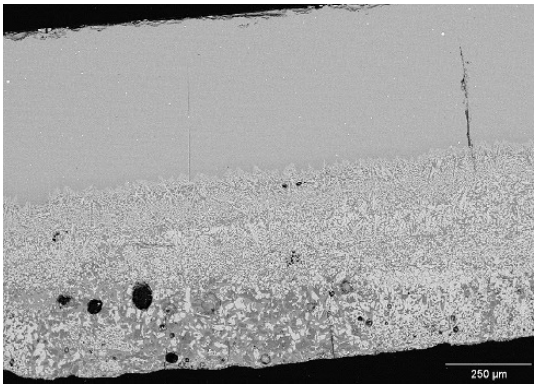

Figure 7.12: *Slag film, obtained after slab casting – Mould powder A*

The thickness of this slag film is around 1 mm or more. Based on Equation 25 in Chapter 2 and the corresponding calculations demonstrated in Chapter 5, the powder consumption during the slab casting trial is estimated to be around 0.30 kg/m^2 or more.
Contrarily to thin slab casting, the composition of these slag films show evidence of Al_2O_3 pick-up (around 3-4 wt%). The crystalline regions can sometimes be subdivided into distinct layers. As described in Chapter 5, the origin of these layers and their formation may reflect severe mould level fluctuations i.e. instabilities at the meniscus area during casting. The crystalline layer closest to the mould sometimes shows some larger grain sizes, indicating a slower local cooling trajectory. It is not clear if this can be related to

fracturing of the slag film during casting, followed by refilling with liquid slag and devitrification as described in section 7.1.

7.4 An overview of mould powders for thin slab casting

An overview on the various process steps and main requirements of mould powders for thin slab casting is given in Figure 7.13. All stages, starting with the supply of fresh mould powders and ending with the formation of a solid slag film are determined by the properties of the mould powder or mould slag (free carbon content, slag viscosity etc.) and the process conditions during casting (EMBR settings, casting speed etc.).

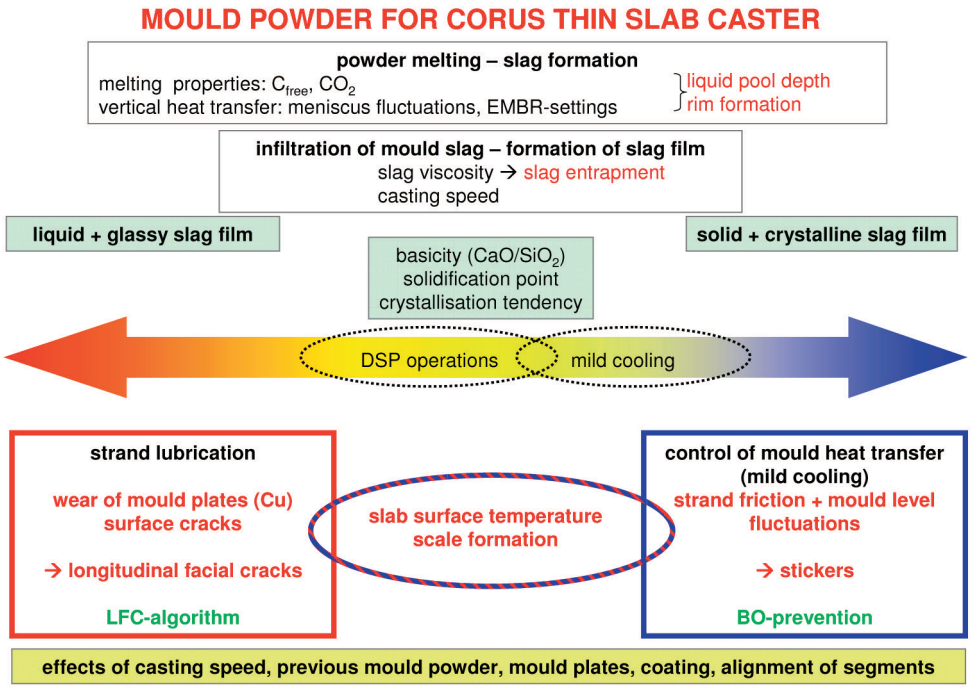

Figure 7.13: *Schematic diagram showing functions of mould powders for thin slab casting*

After melting of the mould powder and infiltration of mould slag, a slag film is formed which dictates the main functions strand lubrication and mould heat transfer. Mould powders with mild cooling properties (i.e. crystalline slag film) are required in order to control the horizontal heat transfer during casting, resulting in less thermal wear of the mould plates and suppression of surface cracks. The increased values of strand friction and incidentally mould level fluctuations have not resulted in any operational restriction. Stickers have not been reported during the introduction and use of mild cooling mould powders at the thin slab caster. It should be noted that the break out (BO) prevention system based on the mould thermocouples can be applied, if desired.

For some specific applications, an increased mould heat transfer (i.e. glassy slag film) is required. This practice shows excellent strand lubrication properties and in general less mould level fluctuations. Special attention should be given to the formation of longitudinal facial cracks (LFC) due to the increased heat load. If needed, the LFC detection system, based on mould thermocouples and corresponding algorithms can be used.

The main mould powder functions are found to be influenced by the casting speed, the presence of a previously applied mould powder, the properties of the mould plates (thickness, coating) and the alignments of the segments. Attention should be given to effects of mould powder on the slab surface temperature and on the formation of scale at the slab surface.

7.5 Concluding remarks

It can be concluded that there is no complete breaking of the slag film in the upper part of the mould but partial *sheeting* of the solid slag film which can occur and is associated with the crystalline nature of the slag film. The part of the slag film in contact with the moving strand fractures and is transported in the casting direction. The remaining hole in the slag film will be refilled by slag, followed by solidification and crystallisation. A critical level of a property of the slag film (e.g. crystallisation) or the casting speed at which fracture occurs cannot be given at this point. However, a programme of measurements of the elongation stress of slag films at increased temperatures in relation to both a parameter providing a measure of the structure of the slag and the performance during casting is recommended.
The trials with mild cooling powders indicated that that the *first 200 mm* under the steel meniscus are essential for initial solidification and for the formation of a homogenous steel shell (top shell).

Mild cooling powders, as applied in thin slab casting, require *increased* taper settings due to the solidification behaviour at the wide and narrow faces. As a consequence, the overall mould heat transfer and hence the shell thickness of the slab will be more uniform which is advantageous in order to suppress the formation of longitudinal facial cracks in the corner area of the wide faces.

Standard mould powders for high speed thin slab casting can be applied for conventional slab casting on various steel grades (low carbons, peritectics), in particular to obtain an improved control of mould heat transfer during casting.

7.6 References

[1] M.R. Ozgu and B. Kocatulum, Thermal analysis of the Burns Harbour No.2 slab caster mold. Proc. 76th Steelmaking Conf., 28-31 March 1993, Dallas, USA, Iron and Steel Society, Warrendale, USA, 1993, 301-308.

[2] I. Sohn, T.J. Piccone, T.T. Natarajan and W.K. Schlichting, Initial study on the effect of mold copper thickness on sticker, flux entrapment and bleeder events at U.S. Steel. Proc. AISTech 2009, 4-7 May 2009, St. Louis, USA, Iron and Steel Society, Warrendale, USA, 2009, 1217-1224.

[3] R.J. O'Malley, Observations of various steady state and dynamic thermal behaviors in a continuous casting mold. Proc. 82nd Steelmaking Conf., 21-24 March 1999, Illinois, USA, Iron and Steel Society, Warrendale, USA, 1999, 13-33.
[4] A. S. Normanton, P. N. Hewitt, N. S. Hunter, D. Scoones and B. Harris, Mould thermal monitoring: a window on the mould. Ironmaking and Steelmaking, 31 (2004) 357-363.
[5] P.N. Hewitt, G.B. Caygill, N.S. Hunter, E. Nixon, J.D. Madill, A.S. Normanton, I. Ellis, D. Jackson and M. Furukawa, Mould thermal monitoring during thin slab casting. Millenium Steel, (2001) 240-244.
[6] P. Hooli, Study on the layers in the film originating from the casting powder between steel shell and mould and associated phenomena in continuous casting of stainless steel, Doctoral Thesis, Helsinki University of Technology, Helsinki, Finland, 2007.
[7] A. Yamauchi, Heat transfer phenomena and mold flux lubrication in continuous casting of steel, Doctoral Thesis, Royal Institute of Technology, Stockholm, Sweden, 2001.
[8] T. Matsushita, Y. Umezawa and S. Seetharaman, Rupture strength of some mould flux slag films relevant to Swedish continuous casting practice. Steel Research Int., 79 (2008) 835-838.
[9] K.C. Mills, The influence of structure on the physico-chemical properties of slags. ISIJ Int., 33 (1993) 148-155.
[10] J.A. Kromhout, S. Melzer, E.W. Zinngrebe, A.A. Kamperman and R. Boom, Mould powder requirements for high-speed casting. Steel Research Int., 79 (2008) 143-148.
[11] M. Kawamoto, Y. Tsukaguchi, N. Nishida, T. Kanazawa and S. Hiraki, Improvement of the initial stage of solidification by using mild cooling mold powder. ISIJ Int., 37 (1997) 134-139.
[12] T.J.H. Billany, A.S. Normanton, K.C. Mills and P. Grieveson, Surface cracking in continuously cast products. Ironmaking and Steelmaking, 18 (1991) 403-410.
[13] C. Bernard, H. Hiebler and M.M. Wolf, How fast can we cast? Ironmaking and Steelmaking, 27 (2000) 450-454.
[14] M. Kawamoto, M. Hanao, H. Kikuchi, T. Murakami and M. Oka, Method for continuous casting of steel. EP 1 059 132 B1, 2002.
[15] M. Kawamoto and M. Hanao, Sumitomo Metal Industries, Personal communication, 2008.
[16] K. Lerch, Metallurgica, Personal communication, 2008.
[17] K. Wünnenberg, Möglichkeiten und Grenzen der Wärmeübertragung in Stranggießkokillen. Stahl u. Eisen, 120 (2000) No.7, 29-35.
[18] F-P. Pleschiutschnigg, S. Feldhaus, L. Parschat, M. Vonderbank, T. Ulke, R.V. Kowalewski and R-P. Heidemann, Automation of a high-speed continuous casting plant. US Patent 6793006 B1, 2004.
[19] F-P. Pleschiutschnigg, SMS Demag, Autopilot für automatische Konizitäts- und Gießgeschwindigkeitsregelungen in CSP-Anlagen, Personal communication, 2005.
[20] J.A. Kromhout, V. Ludlow, S. McKay, A.S. Normanton, M. Thalhammer, F. Ors and T. Cimarelli, Physical properties of mould powders for slab casting. Ironmaking and Steelmaking, 29 (2002) 191-193.
[21] S.P. Carless, A.E. Westendorp, A.A. Kamperman and J.P.T.M. Brockhoff, Optimization of surface quality through mold thermal monitoring. Proc. AISTech 2010, 3-6 May 2010, Pittsburgh, USA, Iron and Steel Society, Warrendale, USA, 2010, Volume 2, 105-113.

8 Conclusions and recommendations

Design of mould powders
In addition to conventional characterisation methods, mineralogical characterisation can provide essential information on the mould powder behaviour and mould powder functions. However, a good understanding of the casting process is a prerequisite for reliable interpretation of these data.

A mould powder can have many components or a complex composition where the motivation of such a composition is not always clear or is even absent. Within the operational windows of the casting process, a simplification of the chemical composition and raw material choice is desired.
This can be illustrated by mould powders for thin slab casting. Only a few families of mould powders are widely used for this relatively new but more complex and demanding casting process. Several mould powders for thin slab casting are universal for various plants. Traditional slab and bloom casting show an enormous variety of mould powders and various adaptations.

The casting process itself is complex and depends on a multitude of variables. Processes in the mould are not fully understood and essential material properties of the solidifying steel are mostly unknown. It is difficult and sometimes nearly impossible to measure the process conditions in the mould and to characterise the various material properties at casting temperatures. As a consequence, essential data on the casting process and the material properties, especially at high temperatures, are often lacking but are needed to evaluate the process and to develop more reliable models. In many cases the input variables of the models are assumptions or results from other models. It is very important to break out of this cycle.

In addition, reliable input data are essential for the successful development and application of thermodynamic models for mould slag. Up to now, important material properties and knowledge on the interactions of various components within the slag, for instance the role of fluorine and sodium at high temperatures, are not or only partially available. Experimental work is crucial for a further understanding of these slag systems as well as for reliable calculations.

Successful casting is a consequence of the choice of optimum casting conditions and mould powder properties. However, given the lack of knowledge, what is optimum?
Over the years mould powders have been expected to be forgiving or flexible in order to overcome the fact that the casting conditions are sometimes not correct. This approach can finally result in a situation where no new developments can be started.

For all these reasons, fundamental research on mould powders and the casting process is essential in order to increase knowledge, to improve the casting process and to be able to cast novel steel grades. A close collaboration between the steel industry, the suppliers and the academic world is essential in order to make significant steps forward.

Melting of mould powders
The raw material choice of a mould powder and the individual material properties at increased temperatures are very important to understand the processes leading to powder melting. However, the process conditions in the mould such as the steel flow in the meniscus area and the vertical heat transfer play an essential role as well.

The free carbon source of a mould powder and a homogeneous carbon distribution within the granules are essential to guarantee stable slag formation without the formation of powder lumps and excessive slag rims. This can be obtained by using one grade of fine carbon black. A stable casting process and in particular, a well controlled steel meniscus and the vertical heat flux are other important conditions. Consequently, the physical properties of mould powders such as the melting point are not as important as widely assumed.

High temperature phase relations of the inorganic raw materials give insights into the processes during powder melting. These include the formation of intermediate phases such as combeite and cuspidine, the formation of phases like tar and sodium which act as binders during rim growth and the formation of Fe-droplets together with graphite.

Both a small liquid pool depth and the very low powder consumption, as found during this work, do not affect the thin slab casting process and the product quality. However, for reasons of operational stability and flexibility as casting speeds increase, a minimum liquid pool depth of 5 mm is desired as well as a minimum powder consumption of 0.05 kg/m^2.

Solidification of mould slag
This study emphasises the need for slag crystallisation in order to control mould heat transfer during casting. However, the mechanism to control mould heat transfer is, as yet, not fully understood. Given the thin slag films as obtained at the thin slab caster and the very low values of the surface roughness, reflection of radiation at the interface of the crystalline slag layer seems to be the plausible mechanism.
The control of mould heat transfer is realised by the slag film properties themselves, the interfacial thermal resistance playing a less dominant role.

The thin slag film layer can be explained by the low values of slag consumption during casting. The very low surface roughness can most likely be related to the relatively low value of the critical cooling rate r_c and hence the relatively high value (>>1) of the normalised cooling rate r_n as well as the ferrostatic pressure during casting. A further improvement of the reflective properties of the slag film, i.e. mild cooling performance, can be obtained by reducing or even leaving out transition metal oxides such as Fe_2O_3.

The break point or break temperature is widely used as an important parameter for mould powder design. Equilibrium melting experiments on four mould powders revealed that the break point (T_{break}) corresponds to the temperature at which 12 ± 3 wt% crystallisation occurs. This value has been found to be independent of its absolute temperature and of the chemical composition of the mould powder.

Crystallisation of mould slag is a function of the composition and the cooling rate. However, in common literature and reports, the cooling rate is rarely addressed and nearly all work on slag crystallisation is only based on the temperature and the slag composition.

This can result in a lack of clarity on crystallisation and crystallisation kinetics. It is recommended to include the cooling rates in all mould powder investigations.

There is no complete breaking of the slag film in the upper part of the mould but partial sheeting of the solid slag film which can occur and is associated with the crystalline nature of the slag film. The part of the slag film in contact with the moving strand fractures and is transported in the casting direction. The remaining hole in the slag film is refilled by slag, followed by solidification and crystallisation. A critical level of a property of the slag film (e.g. crystallisation) or the casting speed at which fracture occurs cannot be given at this point. However, a programme of measurements of the elongation stress of slag films at increased temperatures in relation to both a parameter providing a measure of the structure of the slag and the performance during casting is recommended.

High speed casting
Mould powder design for high speed thin slab casting concentrates on mild cooling properties, which can be realised by specific values of both the basicity (1.2) and the solidification point (1150 °C), promoting the crystallisation of cuspidine.

Mild cooling properties at the wide faces will show a reduced mould heat transfer in the critical upper part of the mould, an increased mould heat transfer in the lower part of the mould whilst maintaining a comparable average mould heat transfer and hence shell thickness during casting. These effects are very favourable for continuous casting, in particular for demanding casting processes like thin slab casting.
The increased values for strand friction and incidentally, the mould level fluctuations as obtained during the mild cooling practice did not result in any operational restriction.

During the study reported in this thesis, it was not possible to apply casting speeds above 6 m/min due to the condition of the continuous caster and the stability of the casting process. However, a further increase in casting speed is possible and realistic when applying the developed mild cooling mould powders. The operational windows, in particular with regard to strand friction, taper settings and secondary cooling water should be adapted and the condition of the continuous caster and tunnel furnace must be appropriate for this casting practice.

The trials with mild cooling powders indicated that the first 200 mm under the steel meniscus are essential for initial solidification and for the formation of a homogeneous steel shell (top shell).

Mild cooling powders, as applied during thin slab casting require increased taper settings due to the solidification behaviour at the wide and narrow faces. As a consequence, the overall mould heat transfer and hence shell thickness of the slab will be more uniform which is advantageous in suppressing the formation of longitudinal facial cracks in the corner area of the wide faces.

Standard mould powders for high speed thin slab casting can be introduced for conventional slab casting of various steel grades, in particular to improve mould heat transfer control during casting.

Fluorine in mould powder – blessing or burden?

A short literature review

The vast majority of mould powders can be described by the CaO – SiO_2 – CaF_2 system. In this system fluorine is an essential component since it has a significant influence on mould powder properties. These are:

- To lower the melting point of mould powder: important for the melting behaviour of mould powder and the lubrication properties of mould slag.
- To decrease the viscosity of mould slag: important for mould powder consumption (slag infiltration) i.e. the formation of a stable slag film.
- Promoting the crystallisation of the slag film: essential in order to control mould heat transfer during casting. As a consequence of the system CaO – SiO_2 – CaF_2, cuspidine crystals ($Ca_4Si_2O_7F_2$) are formed in a glass matrix.

It is obvious that fluorine in mould powder plays a crucial role during the complete process of powder melting, slag infiltration and crystallisation of the slag film. The presence of fluorine is closely related to the two main mould powder functions *strand lubrication* and *the control of mould heat transfer*. From the introduction of mould powders in continuous casting over forty years ago, all important developments related to the casting process and the quality of the as cast product are based on the mould powder system which includes fluorine.

Important disadvantages of fluorine in mould powder are:

- Emission of volatile fluorine components like SiF_4 and NaF. These components are formed due to reactions within the slag.
- Reactions between fluorine components in the mould slag and the cooling water of the caster (secondary cooling), leading to the formation of HF.

The disadvantages of fluorine are the risks for plant personnel and severe corrosion of parts of the continuous caster [1].

The formation of SiF_4 and NaF is important in both cases [2,3]. Some researchers mention the effect of the choice of the fluorine-containing raw materials on this formation. Furthermore, the reactions can be influenced by other constituents in the mould slag [4,5]. The components SiO_2, B_2O_3 en F will promote the formation of SiF_4 whereas components like CaO, MgO, Al_2O_3 and alkaline decrease the formation of SiF_4 [6]. Effects of the presence of carbon and carbonates on the formation of volatile components during powder melting are mentioned as well [7].

It can be concluded that *high temperature phase relations* will result in the formation of volatile components like SiF_4 and NaF. Generally, the reaction temperatures are not specified. Most likely, the high temperature reactions will take place in temperature ranges starting above 1000 °C.

Chemical reactions occurring during powder melting and within the liquid slag are:

$$2CaF_2 + SiO_2 \rightarrow 2CaO + SiF_4$$

$Na_2SiF_6 \rightarrow 2NaF + SiF_4$
$4NaF + SiO_2 \rightarrow 2Na_2O + SiF_4$
$2Na_3AlF_6 + 3SiO_2 \rightarrow 3Na_2O + Al_2O_3 + 3SiF_4$
$CaF_2 + Na_2O \rightarrow CaO + 2NaF$

SiF_4 in the mould slag evaporates during casting but may condense rapidly, possibly in the mould powder layer. The top temperature of the mould powder layer is roughly between 100-200 °C. In the powder layer, the temperature can be up to 500 °C. In the slag film, SiF_4 but also NaF can be transported down the mould via bubbles.

In the secondary cooling zone under the mould, the following reactions can take place:

$SiF_4 + 2H_2O \rightarrow SiO_2 + 4HF$
$SiF_4 + 2HF \rightarrow H_2(SiF_6)$
$2NaF + H_2O \rightarrow Na_2O + 2HF$

Actions aiming at suppressing fluorine emission and formation of HF are:

- The use of pre-molten raw materials. This may result in a decrease of the high-temperature reactions. Fluorine, however, is still present and for financial reasons these materials are rarely used.
- Increase in basicity (CaO/SiO_2) of mould powders or the use of components which will suppress the high temperature reactions. These possibilities are restricted from an operational point of view.
- Decrease the amount of fluorine i.e. use of low-fluorine mould powders. Fluorine is partly replaced but to a lesser degree still present.
- Fluorine-free mould powders. This possibility will be most effective in order to stop fluorine emission and to control machine corrosion. This action will be explained in more detail.

In fluorine-free mould powders, all fluorine components are replaced by other components resulting in equivalent effects on strand lubrication and mould heat transfer. Replacement of fluorine should focus on the melting point, the viscosity and the crystallisation behaviour of the mould flux.

The replacement of fluorine was demonstrated for billet casting and bloom casting (sticker grades). This work focussed on strand lubrication with the melting point and viscosity as main properties. In the period 1996-1997 a lot of work was done by a German mould powder supplier [8]; successful plant trials were reported by Georgsmarienhütte in Germany [9]. Later, other workers on billet casting reported this possibility as well [10,11]. The mould powders contained increased amounts of Na or Li, together with B in order to guarantee a low melting point and a low viscosity. However, at this moment, fluorine free mould powders for billets are not widely used.

Regarding the control of mould heat transfer during casting i.e. the crystallisation of mould slag, the replacement of fluorine is more complicated. Recently it was suggested to use the system $CaO – SiO_2 – TiO_2$ for mould powders where $CaTiO_3$ (perovskite) will be a main crystalline component. This system has been investigated in detail [12,13]. As a next step, mould powders were developed and produced in China. Successful plant trials on peritectic steel grades were done at casting speeds up to 1.5 m/min (slab dimensions 170 mm×1200 mm). This work was reported in the period 2006–2008 [14]. Recently, it has also

been reported that mould powders based on TiO_2, will result in operational disadvantages. These can be related to an increased dependence of the viscosity of the mould flux on changes in the temperature and the chemical composition, a decreased lubrication of the strand and the unwanted formation of the high-melting component TiC. Mould powders which will form the crystalline material $Ca_2Si_3Na_2O_9$ are suggested as alternatives [15].
Researchers in Korea (Posco and a university) mention the use of a large amount of B (around 30 wt% B_2O_3) in mould powders. With this composition, the melting point, the viscosity and the slag crystallisation (formation of CaB_2SiO_7 and $CaAl_4B_2(SiO_4)_8$) were realised sufficiently. Nothing has been reported on B pick-up or SEN erosion due to the presence of B in mould slag [16].
Sumitomo states that fluorine is not necessary in mould powders and mentions the formation of the crystals $CaMgSi_2O_7$ (akermanite) and $CaAl_2Si_2O_7$ (gehlenite) i.e. slag systems based on MgO or Al_2O_3 in order to control mould heat transfer [17].

Concluding remarks

Up to now, nearly all mould powders are still based on systems containing fluorine. The disadvantages of emission and plant corrosion are accepted and considered inevitable by the steel plants.
In the past, fluorine-free mould powders have been developed and successfully used for billets and blooms, focussing on strand lubrication. If the control of mould heat transfer is the second major requirement which is the case for slab casting and thin slab casting, several mould powder developments have been started recently. At this moment, these mould powders are not used as standard materials. The main European mould powder suppliers do not offer fluorine-free mould powders for slab casting; only mould powders with lower fluorine content are commercially available at this moment.
It seems possible to develop and use fluorine-free mould powders for slab casting and thin slab casting. Research on fluorine-free mould powder has to be promoted and plant trials should be organised in order to obtain suitable alternatives for fluorine. This can be realised by collaboration between universities, mould powder suppliers and steel plants.

References

[1] R.E. Hargrave and D.W. Reichgott, Ferrous corrosion in continuous caster spray chambers. Proc. 78th Steelmaking Conf., 2-5 April 1995, Nashville, USA, Iron and Steel Society, Warrendale, USA, 1995, 385-390.
[2] A.I. Zaitsev, A.V. Leites, A. D. Litvina and B. Mogutov, Investigation of the mould powder volatiles during continuous casting. Steel Research Int., 65 (1994) 368-374.
[3] T. Schulz, D. Janke, H-P. Heller und B. Lychatz, Entwicklung umweltfreundlicher Stranggießschlacken. Stahl u. Eisen, 128 (2008) No.4, 65-78.
[4] M. Persson, S. Seetharaman and S. Seetharaman, Kinetic studies of fluoride evaporation from slags. ISIJ Int., 47 (2007) 1711-1717.
[5] K. Shimuzu, T. Suzuki, I. Jimbo and A.W. Cramb, An investigation on the vaporization of fluorides from slag melts. Proc. 79th Steelmaking Conf., 24-27 March 1996, Pittsburgh, USA, Iron and Steel Society, Warrendale, USA, 1996, 723-729.

[6] D.E. Sturgill, The impact of mold flux chemistry on continuous casting secondary cooling water. Proc. 79th Steelmaking Conf., 24-27 March 1996, Pittsburgh, USA, Iron and Steel Society, Warrendale, USA, 1996, 277-283.

[7] A. Shilov and L. Holappa, Mass spectrometric measurements of the gas phase composition over mould powder samples in vacuum conditions at 50-1550°C. Steel Research Int., 77 (2006) 803-808.

[8] H. Heimbach, K. Schulz, J. Markardt und H-J. Ehrenberg, Die Freisetzung von Fluorverbindungen aus Gießschlacken. Stahl u. Eisen, 117 (1997) No.12, 105-110.

[9] H. Abratis, F. Höfer, M. Jünemann, J. Sardemann und H. Stoffel, Einsatz von unterschiedlichen Gießpulvern beim Stranggießen von Vorblöcken und Knüppeln. Stahl u. Eisen, 116 (1996) No.4, 85-91.

[10] A.B. Fox, K.C. Mills, D. Lever, C. Bezerra, C. Valadares, I. Unamuno, J.J. Laraudogoitia and J. Gisby, Development of fluoride-free fluxes for billet casting. ISIJ Int., 45 (2005) 1051-1058.

[11] R. Carli, S. Tintori, G. Marini, A.B. Fox and D. Lever, Development of fluoride-free fluxes for structural steel billet casting. Proc. 5th Eur. Continuous Casting Conf., 20-22 June 2005, Nice, France, La Rev. Métall., Paris, France, 2005, Volume 1, 56-64.

[12] H. Nakada and K. Nagata, Crystallization of CaO-SiO_2-TiO_2 slag as a candidate for fluorine free mold flux. ISIJ Int., 46 (2006) 441-449.

[13] X. Qi, G-H. Wen and P. Tang, Investigation on heat transfer performance of fluoride-free and titanium-bearing mold fluxes. Journal of Non-Crystalline Solids, 354 (2008) 5444-5452.

[14] G. Wen, S. Sridhar, P. Tang, X. Qi and Y. Liu, Development of fluoride-free mold powders for peritectic steel slab casting. ISIJ Int., 47 (2007) 1117-1125.

[15] Q. Wang, S. He and K.C. Mills, Research on decreasing fluorine content from continuous casting mould fluxes. Proc. 4th Int. Conf. On Continuous Casting of Steel in Developing Countries (CCC'08), 4-7 November 2008, Beijing, China, The Chinese Society for Metals, Beijing, China, 2008, 715-720.

[16] S-Y. Choi, D-H. Lee, D-W. Shin, S-Y. Choi, J-W. Cho and J-M. Park, Properties of F-free glass system as a mold flux: viscosity, thermal conductivity and crystallisation behaviour. Journal of Non-Crystalline Solids, 345&346 (2004) 157-160.

[17] M. Hanao, Y. Tsukaguchi, M. Kawamoto, Development of Crystallization-controlled Mold Flux. Proc. 4th Int. Congress on the Science and Technology of Steelmaking (ICS2008), 6-8 October 2008, Gifu, Japan, The Iron and Steel Institute of Japan, Tokyo, Japan, 2008, 694-697.

Summary

Mould powders for high speed continuous casting of steel

Mould powders are essential for the stability of the continuous casting process of steel at all casting speeds. Almost all mould powders are mixtures of several mineralogical components and carbon. The main functions of mould powders are to provide strand lubrication and to control the mould heat transfer in the horizontal direction between the developing steel shell and the water cooled copper mould. At higher casting speeds associated with thin slab casting, the role of mould powder is even more important. During casting, the powder melts on the steel surface, forming a layer of liquid mould slag. Subsequently, the mould slag infiltrates between the steel shell and the oscillating mould, creating a thin slag film which solidifies into glassy and crystalline phases. The properties of the slag film dictate the main functions of strand lubrication and mould heat transfer.
The thin slab caster at Tata Steel IJmuiden (Direct Sheet Plant, DSP) started production in 2000. The caster has one strand and is equipped with a funnel shaped mould, a specially designed submerged entry nozzle (SEN) and an adjustable multiple pole electromagnetic brake (EMBr). The mould level is measured using a radiometric system. Liquid core reduction decreases the slab thickness from 90 mm to 70 mm. The designed production level is 1.3 Mt/y of coils and the maximum casting speed is 6.0 m/min.
It has been decided to increase the production of the thin slab caster of Tata Steel to a level of 1.8 Mt/y using one caster strand. By doing this, extension with a second strand and a second tunnel furnace can be avoided. To meet this demand, the steel in mould time has to be increased to approximately 85% and the maximum casting speed to 8.0 m/min.
A project was started within the framework of the Materials innovation institute M2i - Delft University of Technology with the aim to develop mould powders suitable for high speed thin slab casting with a maximum casting speed up to 8 m/min. For this work, a fundamental understanding and quantification of the melting and solidification behaviour of mould slag as well as the mould powder functions are required. To obtain these, the chemical and mineralogical compositions of mould powders need to be related to the physical properties of mould slag and to the operational performance during casting. Characterisation, plant trials and powder developments are important themes in this study.

Characterisation of mould powder and mould slag focussed on the chemical composition, the mineralogy and the physical properties and was done at room temperature and at elevated temperatures. Main topics are chemical analyses, X-ray diffraction (XRD) including high-temperature XRD (HT-XRD) and Rietveld analysis (quantitative XRD), electron microscopy (SEM-EDS), optical microscopy, hot-stage microscopy and viscosity measurements. High-temperature XRD and Rietveld analyses on mould powders were introduced and optimised as part of this project. Changes in mineralogy of the major phases of mould powders during heating and cooling i.e during powder melting and slag solidification can be observed *in situ* using HT-XRD with supplementary XRD and microscopic techniques.
Additional laboratory scale experiments were done aiming to reveal mechanisms on powder melting and slag solidification. Some of these measurements were done at TU Bergakademie, Freiberg, Germany and at Tokyo Institute of Technology, Japan.

A next step was the evaluation of process data of the casting process such as slag formation, lubrication and mould heat transfer. Various plant trials were performed, both at the pilot caster of Sumitomo Metal Industries, Japan and at the thin slab caster of Tata Steel IJmuiden. This part of the project was completed by the characterisation of mould slag, slag rims and slag films obtained from the casters.
Combination of the chemical and mineralogical composition, the physical properties and the operational performance during casting resulted in an understanding of the working and functions of mould powders at casting speeds up to approximately 6.0 m/min. As a next step, design proposals were made for mould powders suited for high speed casting.

It was found that the selection of raw materials for mould powder and the individual material properties at increased temperatures are very important to understand the processes leading to powder melting. The free carbon source of a mould powder and a homogeneous carbon distribution within the granules are essential to guarantee stable slag formation without the formation of powder lumps and excessive slag rims. This can be obtained by using one grade of fine carbon black. A stable casting process and in particular, a well controlled steel meniscus and the vertical heat transfer are other important conditions. Consequently, the physical properties of mould powders such as the melting point are not as important as widely assumed.
High temperature phase relations of the inorganic raw materials give insight into the processes during powder melting. These include the formation of intermediate phases such as combeite and cuspidine, the formation of phases like tar and sodium which act as binders during rim growth and the formation of Fe-droplets together with graphite.
Both a small liquid pool depth and the very low powder consumption, as found during this work, do not affect the thin slab casting process and the product quality.

This study emphasises the need for slag crystallisation in order to control mould heat transfer during casting. The control of mould heat transfer is realised by the slag film properties themselves, the interfacial thermal resistance playing a less dominant role. Reflection of radiation at the interface of the crystalline slag layer seems to be the plausible mechanism to control mould heat transfer during casting.
Slag films as obtained at the thin slab caster showed a relatively low thickness and surface roughness. These phenomena can be understood by considering the low values of slag consumption during casting as well as the critical cooling rate r_c and the ferrostatic pressure during casting.
Crystallisation of mould slag is a function of the composition and the cooling rate. However, in common literature and reports, the cooling rate is rarely addressed and nearly all work on slag crystallisation is only based on the temperature and the slag composition. This can result in a lack of clarity on crystallisation and crystallisation kinetics.

Mould powder design for high speed thin slab casting concentrates on mild cooling properties, which can be realised by specific values of both the basicity (1.2) and the solidification point (1150 °C), promoting the crystallisation of cuspidine.
Full scale plant trials at the thin slab caster revealed that mild cooling properties at the wide faces will show a reduced mould heat transfer in the critical upper part of the mould, an increased mould heat transfer in the lower part of the mould whilst maintaining a comparable average mould heat transfer and hence shell thickness during casting. These

effects are very favourable for continuous casting, in particular for demanding casting processes like thin slab casting.
It was found that no complete fracture of the slag film will occur in the upper part of the mould but rather partial sheeting which is associated with the crystalline nature of the slag film. The part of the slag film in contact with the moving strand fractures and is transported into the casting direction. The remaining hole in the slag film is refilled by slag, followed by solidification and crystallisation. As a consequence, trials with mild cooling powders indicated that the first 200 mm under the steel meniscus are essential for initial solidification and for the formation of a homogeneous steel shell (top shell).
Furthermore, it was concluded that mild cooling powders, as applied during thin slab casting, require increased taper settings due to the solidification behaviour at the wide and narrow faces. Therefore, the overall mould heat transfer and hence shell thickness of the slab will be more uniform which is advantageous in suppressing the formation of longitudinal facial cracks in the corner area of the wide faces.
The increased values for strand friction and incidentally, the mould level fluctuations as obtained during the mild cooling practice, did not result in any operational restriction.

During the study reported in this thesis, it was not possible to apply casting speeds above 6 m/min due to the condition of the continuous caster at Tata Steel IJmuiden and the stability of the casting process. However, a further increase in casting speed is possible and realistic when applying the developed mild cooling mould powders.
Finally, it was demonstrated that the knowledge gained on mould powders for high speed thin slab casting, i.e. the principles on powder melting, slag solidification and powder design, can also be applied to conventional slab casting of various steel grades.

Samenvatting

Gietpoeders voor het gieten van staal met hoge snelheden

Gietpoeder speelt een belangrijke rol in de stabiliteit van het proces van continue gieten van staal. Vrijwel alle gietpoeders zijn mengsels van mineralogische grondstoffen en koolstof. De belangrijkste functies van gietpoeders zijn het smeren van de gevormde stolhuid en het beheersen van de warmteoverdracht tussen de stolhuid en de koperen gietvorm. Bij het toepassen van hogere gietsnelheden, zoals bij dunne-plakgieten het geval is, wordt de rol van gietpoeder nog belangrijker. Tijdens het gieten smelt het gietpoeder op het staaloppervlak; hierbij ontstaat vloeibare gietslak. Vervolgens infiltreert gietslak tussen de stolhuid en de oscillerende gietvorm. Tijdens dit proces wordt een dunne slakfilm gevormd die vervolgens stolt als glasachting en kristallijn materiaal. De eigenschappen van de slakfilm bepalen de belangrijke gietpoederfuncties smering en warmteoverdracht.
Dungieten bij Tata Steel IJmuiden vindt plaats bij de Direct Sheet Plant (DSP) of gietwalsinstallatie. Deze installatie is in het jaar 2000 in gebruik genomen. De gietmachine die bij deze installatie hoort, bevat één streng en is onder meer uitgerust met een trechtervormige gietvorm, een speciaal ontworpen dompelpijp en een electromagnetische rem. Het staalniveau in de gietvorm wordt gemeten met behulp van een radioactieve methode. Direct onder de gietvorm wordt de dikte van de gegoten plak gereduceerd van 90 naar 70 mm. De installatie is ontworpen voor een jaarlijkse productie van 1.3 miljoen ton gewalst staal (rollen) en een maximale gietsnelheid van 6.0 m/min.
Er is besloten de productie van de dungietinstallatie te verhogen naar een niveau van 1.8 miljoen ton rollen per jaar waarbij gebruik gemaakt wordt van één streng. Hierdoor kan uitbreiding met een tweede streng en de bijbehorende tunneloven voorkomen worden. Om deze doelstelling te behalen moet de tijd dat er zich staal in de gietvorm bevindt (steel in mould time) verhoogd worden naar 85% en dient de maximale gietsnelheid verhoogd te worden naar 8.0 m/min.
Binnen het onderzoekskader van het Materials innovation institute M2i, Technische Unversiteit Delft is een project gestart met als doel het ontwikkelen van gietpoeders die geschikt zijn voor gebruik bij deze hoge gietsnelheden. Hiervoor is een meer fundamenteel begrip van het smelten van gietpoeder en het stollen van gietslak een vereiste. Om dit te realiseren wordt de chemische- en mineralogische samenstelling van gietpoeders gerelateerd aan de fysische eigenschappen van gietslak en aan de operationele gegevens die verkregen worden tijdens het gietproces. Karakterisering, fabrieksproeven en gietpoederontwikkelingen zijn belangrijke onderdelen in dit onderzoek.

De karakterisering van gietpoeder en gietslak heeft zich gericht op het bepalen van de chemische en mineralogische samenstelling en op de fysische eigenschappen bij zowel kamertemperatuur als bij verhoogde temperaturen. Belangrijke onderdelen hierbij zijn kwalitatieve röntgendiffractieanalyse bij kamertemperatuur (XRD) en bij hogere temperaturen (HT-XRD), kwantitative röntgendiffractie (Rietveld analyse), elektronen microscopie (REM-EDS), optische microscopie, verhittingsmicroscopie en viscositeitsbepalingen. Het gebruik van de technieken hoge-temperatuur röntgendiffractie en Rietveld analyses voor de karakterisering van gietpoeder is als onderdeel van dit project geintroduceerd. Veranderingen in de mineralogische samenstelling van gietpoeder en

gietslak tijdens opwarmen en afkoelen kunnen met behulp van HT-XRD en de bijbehorende microscopische technieken in beeld gebracht worden. Als aanvulling zijn experimenten op laboratoriumschaal uitgevoerd, gericht op processen die spelen tijdens het smelten van gietpoeder en het stollen van gietslak. Enkele van deze experimenten zijn uitgevoerd bij TU Bergakademie Freiberg in Duitsland en het Tokyo Institute of Technology in Japan.
Een volgende stap betrof de evaluatie van procesgegevens, afkomstig van fabrieksproeven. De gegevens houden verband met de onderwerpen slakvorming, smering en warmteoverdracht. De fabrieksproeven zijn bij de proefinstallatie van Sumitomo Metal Industries in Japan en de dungietinstallatie in IJmuiden uitgevoerd. Deze fase is afgerond met de karakterisering van gietslak, slakrimmen en slakfilm, verkregen tijdens de proeven. Het combineren van gegevens over de chemische- en mineralogische samenstelling, de fysische eigenschappen en de operationele prestaties tijdens de fabrieksproeven resulteerde in een beter begrip van de werking en functies van gietpoeder bij gietsnelheden tot 6.0 m/min. Een volgende stap betrof het definiëren van gietpoeder dat bij hogere gietsnelheden toegepast kan worden.

Aangetoond is dat de grondstoffenkeuze en de bijbehorende materiaaleigenschappen bij verhoogde temperatuur een zeer belangrijke rol spelen tijdens het smelten van gietpoeder. De keuze voor koolstof (vrije koolstof) in gietpoeder en een gelijkmatige verdeling van koolstof in het gietpoeder zijn van essentieel belang voor een ongestoorde slakvorming. Hierdoor blijft de ongewenste vorming van klonten en slakrimmen tot een minimum beperkt. Het gebruik van roet als enige bron voor koolstof is hierbij een vereiste. Verder zijn een stabiel gietproces en in het bijzonder een beheerst badoppervlakte (staal) eveneens bepalend voor het ongestoord smelten van gietpoeder. Een gevolg is dat de fysische eigenschappen van gietpoeder zoals het smeltpunt, van minder belang zijn dan algemeen wordt verondersteld.
Het smelten van gietpoeder is ook in beeld gebracht door het volgen van de veranderingen in de samenstelling die optreden tijdens het verhitten. De vorming van zogenaamde tussenfasen zoals combeite en cuspidine is hierbij waargenomen, evenals de vorming van teer- en natriumverbindingen en de vorming van ijzerdruppels in combinatie met grafiet. De gevormde teer- en natriumverbindingen kunnen als bindmiddel optreden tijdens de vorming en groei van slakrimmen.
Noch een dunne slaklaagdikte, noch een lage poederconsumptie zoals waargenomen tijdens de gietexperimenten, blijken het gietproces en de kwaliteit van het gegoten product te beïnvloeden.

Uit dit onderzoek volgt dat de beheersing van de warmteoverdracht tijdens het gieten gerealiseerd wordt door de eigenschappen van de gevormde slakfilm. Het belang van kristallisatie van gietslak wordt hierbij onderstreept; de oppervlakteruwheid van de slakfilm speelt een minder belangrijke rol. Reflectie van straling aan de oppervlakte van de kristallaag in de slakfilm kan worden gezien als het meest aannemelijke mechanisme voor de beheersing van de warmteoverdracht.
Slakfilms die verkregen zijn bij de dungietinstallatie vertonen relatief lage waarden voor de dikte en de oppervlakteruwheid. Dit kan verklaard worden door de geringe waarden voor slakconsumptie tijdens het gieten, de waarden voor de kritieke koelsnelheid r_c en de ferrostatische druk die heerst in de gietvorm.
Kristallisatie van gietslak is een functie van de samenstelling en de koelsnelheid. Het effect van de koelsnelheid wordt in de literatuur weinig genoemd en vrijwel al het

onderzoek rond kristallisatie van gietslak is gericht op effecten van de temperatuur en de samenstelling. Deze aanpak kan resulteren in onduidelijkheid over kristallisatie en de bijbehorende kinetiek.

Het beheersen van de warmteoverdracht tijdens het gieten (mild cooling) is het uitgangspunt bij het ontwerp van gietpoeder voor hoge gietsnelheden. Dit kan gerealiseerd worden door een keuze voor specifieke waarden voor de basiciteit (CaO/SiO_2 = 1.2) en het stolpunt (1150 °C), waarbij de vorming van cuspidine bevorderd wordt.
Fabrieksproeven met "mild cooling" gietpoeders laten een herverdeling in locale warmteoverdracht zien: een verlaagde warmteoverdracht in het kritieke bovenste deel van de gietvorm in combinatie met een verhoogde warmteoverdracht in het lagere deel van de gietvorm. De totale warmteoverdracht en als gevolg de dikte van de gevormde stolhuid blijft hierbij vergelijkbaar met de referentiepraktijk. De gevonden herverdeling in warmteoverdracht is bijzonder gunstig voor het continu gieten, in het bijzonder voor meer kritieke processen zoals het gieten bij hogere snelheden.
Verder blijkt dat in het bovenste gedeelte van de gietvorm de slakfilm niet volledig breekt maar gedeeltelijk afschuift; dit proces kan gerelateerd worden aan de mate van kristallisatie van de slakfilm. Het deel van de slakfilm dat in contact staat met de stolhuid breekt en beweegt met deze stolhuid mee (afschuiven). De gevormde ruimte wordt opgevuld met vloeibare slak die vervolgens stolt en kristalliseert, waarna dit proces zich kan herhalen. Het gedeelte van de slakfilm dat zich aan de zijde van de koperen gietvorm bevindt, is veel meer statisch van karakter. Verder volgt uit dit onderzoek dat een lengte van ongeveer 200 mm onder het staalniveau bepalend is voor de eerste stolling en voor de vorming van de stolhuid.
Gietpoeders met "mild cooling" eigenschappen vereisen een verhoogde instelling van de gietvormtaper. Een gevolg hiervan is dat de warmteoverdracht en dus de dikte van de gevormde stolhuid meer gelijkmatig is; dit is zeer gunstig voor het onderdrukken van de vorming van oppervlaktescheuren in het staal (langsscheuren). De gevonden hogere waarden voor de wrijving van de stolhuid en (incidenteel) de variaties in het badniveau tijden het gebruik van "mild cooling" gietpoeders resulteren niet in operationele beperkingen tijdens het gietproces.

Vanwege de conditie van de dungietinstallatie en de stabiliteit van het gietproces bleek het tijdens dit onderzoek niet mogelijk fabrieksproeven uit te voeren bij gietsnelheden hoger dan 6 m/min. Een verhoging van de gietsnelheid met gebruik van de ontwikkelde "mild cooling" gietpoeders wordt echter als mogelijk en realistisch beschouwd.
Tenslotte is aangetoond dat de verworven kennis over gietpoeders voor hoge snelheden, dat wil zeggen de uitgangspunten rond het smelten van gietpoeder, het stollen van gietslak en het ontwerp van gietpoeders, toegepast kan worden bij het conventioneel plakgieten van diverse staalkwaliteiten.

Terugblik en dankwoord

In de loop van het jaar 2004 begon ik na te denken over het doen van meer diepgaand onderzoek, resulterend in een wetenschappelijke promotie. Dit op aangeven van Marc Cornelissen en Sieger van der Laan met wie ik veel samenwerkte. In die tijd was ik projectleider “DSP Casting Technology”. Het was een groot project, er kwam veel uit en er werd ook gepubliceerd. Toch werd het routinematig en kreeg ik regelmatig het gevoel stil te staan. Het waren deze twee collega’s die me wezen op een nieuwe stap; mijn “oude” specialiteit gietpoeder zou zich goed lenen voor een promotieonderzoek.

In 2004 werd ook de ambitie uitgesproken de jaarlijkse productie van de dungietinstallatie DSP te verhogen van 1.3 naar 1.8 miljoen ton gewalste rollen per jaar, gebaseerd op gebruik van de bestaande streng. Zowel het rendement van de gietmachine moest omhoog als de maximaal te behalen gietsnelheid. In dit klimaat werd meer diepgaand onderzoek als vanzelfsprekend gezien.

Toen ik dit overzag waren er een onderwerp – gietpoeder voor hoge gietsnelheden – een groot project en de business unit DSP die alle steun verleende. Bovenal was er een beoogd promotor, professor Rob Boom die vanaf het allereerste begin zeer enthousiast was over mijn ambitie. Deze steun heb ik erg op prijs gesteld.

Het toenmalige hoofd van de afdeling Steelmaking & Continuous Casting (SCC), wijlen Adrian Normanton heeft vanaf het begin achter dit onderzoek gestaan. Na het overdragen van mijn project kon ik medio 2005 aan de slag. Tata Steel Research Development & Technology gaf vanuit het Seedcorn budget mogelijkheden extra onderzoek uit te voeren. René Duursma speelde hierbij een belangrijke en stimulerende rol. Direct bij aanvang is professor Ken Mills, Imperial College, Londen betrokken bij het onderzoek. Hiermee was een goed begin verzekerd, wat zich mede vertaald heeft in dit werk.

Onderzoek aan gietpoeder kon vlekkeloos ingebracht worden in de samenwerking tussen Tata Steel en Sumitomo. Dit heeft zeer veel kennis en inzicht opgeleverd op het gebied van gietpoeder, gieten en stollen. De contacten met Sumitomo Metals in Hasaki, Kashima en Wakayama, Japan waren verrijkend en plezierig. Masayuki Kawamoto, Masahito Hanao en Yuichi Tsukaguchi hebben hier veel aan bijgedragen.

Het onderzoek had een vliegende start door de voortreffelijke medewerking van Darja Benne, Frank van der Does, Jaap Koster, Sieger van der Laan, Stefan Melzer en Enno Zinngrebe, werkzaam bij het Ceramics Research Centre (CRC) in IJmuiden. Later is dit aangevuld met vakkundig werk van Max Koolwijk, Christian Liebske en James Small. Jan Trouw, tot 2003 werkzaam bij het CRC, heeft aan de basis gestaan van veel karakteriseringswerk aan gietpoeder.
Bij het GeoForschungsZentrum gevestigd te Potsdam, is een aantal belangrijke metingen uitgevoerd op het gebied van kwantitatieve röntgendiffractie.

Het werk in de DSP en in het bijzonder de fabrieksproeven zijn mogelijk gemaakt door de medewerking van Edward Dekker, Ruud Honig, Arnoud Kamperman, Lisette Sierevogel en zeer belangrijk, de ploegen werkzaam bij de gietmachine. In de afgelopen jaren bleek Edward Dekker een enorme steun en een constante bron van informatie.

Het was verheugend te zien dat resultaten van dit onderzoek een weg vonden naar de gietinstallaties van de nabijgelegen Oxystaalfabriek 2. Stephen Carless heeft dit geweldig opgepakt.

In mijn afdeling SCC heb ik met diverse mensen samengewerkt. De proeven met Bastiaan de Bruijn en Frank Grimberg verliepen plezierig en hebben veel informatie opgeleverd. De besprekingen in het toenmalige 1.8 miljoen ton project zijn het werk ten goede gekomen, ik denk hierbij onder meer aan Arie Hamoen en Raimond Koldewijn. Neil Jones heeft een goede start gemaakt met thermodynamische berekeningen aan gietslak.

De eigen bibliotheek van Tata Steel Research, Development & Technology, Ina van Egmond en collega's zorgden snel voor de vele documenten en waren altijd in staat de meest onmogelijke referenties te vinden.

Met Tokyo Institute of Technology, professor Masahiro Susa en professor Kazuhiro Nagata is kennis uitgewisseld, wat het onderzoek duidelijk verder heeft geholpen. Hetzelfde geldt voor Technische Universität Bergakademie Freiberg, professor Piotr Scheller. Aan beide instituten zijn tevens metingen uitgevoerd waarvan de resultaten in dit proefschrift verwerkt zijn. Verder had ik het voorrecht mijn onderzoek te bespreken bij professor Toshihiro Tanaka, Osaka University.
De firma Metallurgica GmbH heeft regelmatig metingen verricht en op aangeven vanuit dit onderzoek gietpoeders ontwikkeld en beschikbaar gesteld. De medewerking van Kurt Lerch was hierbij essentieel.

De bijeenkomsten en congressen waren mijlpalen gedurende dit project. Er werden resultaten gepresenteerd en er kwam veel informatie voor terug. Met plezier denk ik terug aan de bijeenkomsten van de VDEh in Völklingen, Düsseldorf en Münster en aan de congressen TSCR2006 in Guangzhou, ECCC2008 in Riccione en MOLTEN2009 in Santiago.

Het was voor mij inspirerend met zoveel verschillende mensen aan dit onderwerp te werken. Dank aan allen die dit mogelijk gemaakt hebben. Dank aan Tata Steel die me de kans gegeven heeft dit onderzoek op te pakken en uit te voeren.
Verder een woord van dank aan diegenen die bij de afronding van dit onderzoek een rol gespeeld hebben; ik denk hierbij zeker aan de goede bijdragen van Dick Hamels.

Mijn gezin was nauw betrokken bij het wel en wee van dit onderzoek. Marijke, Steven, Emil en Philip: heel veel dank voor de betrokkenheid, het geduld en de stimulerende sfeer.

Jan Kromhout

Publications

Novelty destroying prior art

1. A method of continuous casting, 1999, HO 836 TN.

Conference contributions

1. J.A. Kromhout, Drying behaviour of water based shell materials and thermal behaviour of colloidal silica. Proc. 7th Int. Symposium on Investment Casting (PRECAST 93), 17-20 May 1993, Brno, Czech Republic, SPL, Brno, Czech Republic, 1993, 216 (poster presentation).

2. J.A. Kromhout, V. Ludlow, S. McKay, A.S. Normanton, M. Thalhammer, F. Ors and T. Cimarelli, Physical properties of mould powders for slab casting. Proc. 6th Int. Conf. on Molten Slags, Fluxes and Salts, 12-17 June 2000, Stockholm/Helsinki, KTH, Stockholm, Sweden, 2000, pdf 097.

3. J. A. Kromhout and D.W. van der Plas, The melting speed of mould powders: determination and application in casting practice. Proc. 6th Int. Conf. on Molten Slags, Fluxes and Salts, 12-17 June 2000, Stockholm/Helsinki, KTH, Stockholm, Sweden, 2000, pdf 151.

4. A.S. Normanton, V. Ludlow, S. McKay, T. Cimarelli, A. Spaccarotella, J.A. Kromhout, F. Ors, J.J. Laraudogoitia, K.C. Mills and M. Thalhammer, Developments of mould powders and an expert system for their selection at higher casting speeds. Proc. 8th Continuous Casting Conf. (CCC 2000), 5-7 June 2000, Linz, Austria, Voest-Alpine Industrieanlagenbau, Linz, Austria, 2000, paper no. 11.

5. J.A. Kromhout, A.A. Kamperman, M.Kick and J. Trouw, Mould powder selection for thin slab casting. Proc. 7th Int. Conf. on Molten Slags, Fluxes and Salts, 25-28 January 2004, Cape Town, South Africa, The South African Institute of Mining and Metallurgy, Johannesburg, South Africa, 2004, 731-736.

6. M.C.M Cornelissen, J.A. Kromhout, A.A. Kamperman, M. Kick and F. Mensonides, High productivity and technological developments at the Corus DSP thin slab caster. Proc. 5th Eur. Continuous Casting Conf., 20-22 June 2005, Nice, France, La Rev. Métall., Paris, France, 2005, Volume 1, 322-328.

7. T.W.J. Peeters, R. Koldewijn, J.A. Kromhout and A.A. Kamperman, Optimisation of an EMBr for a thin-slab caster. Proc. 5th Eur. Continuous Casting Conf., 20-22 June 2005, Nice, France, La Rev. Métall., Paris, France, 2005, Volume 2, 516-523.

8. J.A. Kromhout, S. Melzer, E.W. Zinngrebe, A.A. Kamperman and R. Boom, Mould powder requirements for high-speed casting. Proc. 2006 Int. Symposium on Thin Slab Casting and Rolling (TSCR2006), 11-13 April 2006, Guangzhou, China, The Chinese Society for Metals, Beijing, China, 2006, 306-313.

9. K.C. Mills, J.A. Kromhout, A. Hamoen and R. Boom, Selection of mould fluxes for thin slab casting. Proc. AdMet, 27-30 May 2007, Dnipropetrovsk, Ukraine, National Metallurgical Academy of Ukraine, Dnipropetrovsk, 2007, Volume 2, 174-181.

10. J.A. Kromhout, S. Melzer, D. Benne and R. Boom, Mould fluxes for thin slab casting at high speeds. Proc. 2nd CSM – VDEh – Seminar on Metallurgical Fundamentals, 18-19 June 2007, Düsseldorf, Germany, Stahlinstitut VDEh, Düsseldorf, Germany, 2007, 279-288.

11. J.A. Kromhout, C. Liebske, S. Melzer, A.A. Kamperman and R. Boom, Mould powder investigations for high speed casting. Proc. 6th Eur. Conf. on Continuous Casting, 3-6 June 2008, Riccione, Italy, Associazione Italiana di Metallurgia, Milano, Italy, 2008, 76.pdf.

12. J.A. Kromhout, M. Kawamoto, M. Hanao, Y. Tsukaguchi, E.R. Dekker and R. Boom, Development of mould flux for high speed thin slab casting. Proc. 13th VDEh – ISIJ – Seminar, 19-20 November 2008, Münster, Germany, Stahlinstitut VDEh, Düsseldorf, Germany, 2008, 203-210.

13. J.A.Kromhout, M. Kawamoto, M. Hanao and R. Boom, Development of mould flux for high speed thin slab casting. Proc. 8th Int. Conf. on Molten Slags, Fluxes and Salts (MOLTEN2009), 18-21 January 2009, Santiago, Chile, GECAMIN Ltd., Santiago, Chile, 2009, 1041-1052.

14. J.A. Kromhout, M. Kawamoto, M. Hanao, Y. Tsukaguchi, E.R. Dekker and R. Boom, Development of mould flux for high speed thin slab casting: the control of mould heat transfer. Proc. 8th Int. Conf. on Molten Slags, Fluxes and Salts (MOLTEN2009), 18-21 January 2009, Santiago, Chile, GECAMIN Ltd., Santiago, Chile, 2009, (poster presentation).

Journal papers

1. J.A. Kromhout, V. Ludlow, S. McKay, A.S. Normanton, M. Thalhammer, F. Ors and T. Cimarelli, Physical properties of mould powders for slab casting. Ironmaking and Steelmaking, 29 (2002) 191-193.

2. J.A. Kromhout and D.W. van der Plas, The melting speed of mould powders, determination and application in casting practice. Ironmaking and Steelmaking, 29 (2002) 303-307.

3. J.A. Kromhout, A.A. Kamperman, M. Kick and J. Trouw, Mould powder selection for thin slab casting. Ironmaking and Steelmaking, 32 (2005) 127-132.

4. M.C.M. Cornelissen, J.A. Kromhout, A.A. Kamperman, M. Kick and F. Mensonides, High productivity and technological developments at Corus DSP thin slab caster. Ironmaking and Steelmaking, 33 (2006) 362-366.

5. J.A. Kromhout, S. Melzer, E.W. Zinngrebe, A.A. Kamperman and R. Boom, Mould powder requirements for high-speed casting. Steel Research Int., 79 (2008) 143-148.

6. Y. Tsukaguchi, M. Hanao, M. Kawamoto, C. Liebske and J.A. Kromhout, Melilite Crystallization of High Basicity and High Viscosity Mold Flux. CAMP-ISIJ, 21 (2008) 826-829.

7. J.A. Kromhout, C. Liebske, S. Melzer, A.A. Kamperman and R. Boom, Mould powder investigations for high speed casting. Ironmaking and Steelmaking, 36 (2009) 291-299.

8. J.A. Kromhout, M. Kawamoto, M. Hanao, Y. Tsukaguchi, E.R. Dekker and R. Boom, Development of mould flux for high speed thin slab casting. Steel Research Int., 80 (2009) 575-581.

Curriculum Vitae

Jan Kromhout (22 October 1960, Leiden, The Netherlands) graduated in chemical engineering from HTS Den Haag (The Hague Technical College) in 1984 and in business engineering from HTS Dordrecht (Dordrecht Technical College) in 1985. After his military service, he joined Hoogovens Research & Development (now Tata Steel RD&T), IJmuiden, The Netherlands in 1987. He started working in the field of engineering ceramics, followed by investment casting.

In 1993 he joined the group Casting Metallurgy Flat Products, concentrating on the continuous casting process of steel with main topics mould fluid flow and mould heat transfer, argon injection, mould powders and tundish metallurgy. During the period 1996-2000 he represented Hoogovens as project leader in an international ECSC-project on mould powders for slab and billet casting as well as thin slab casting.
From the introduction of the thin slab casting process in IJmuiden in 2000, he was involved in process research and technological developments for this novel casting technique, both as researcher and project leader.

Following the decision to increase the production of the thin slab caster in IJmuiden, he initiated a doctoral research project entitled “Mould powders for high speed continuous casting of steel” in 2005 at TU Delft with Prof.dr. Rob Boom, whilst being a researcher employed by Corus RD&T, now Tata Steel RD&T. This project within the framework of the Materials innovation institute (M2i) aims to develop mould powders suitable for high speed thin slab casting. Main partners are Imperial College London (UK), Sumitomo Metal Industries (Japan), Tokyo Institute of Technology (Japan) and TU Bergakademie Freiberg (Germany).